University of Southampton

Faculty of Engineering and Environment

Application of signal processing to respiratory cycle related EEG change (RCREC) in children

By:

Shayan Motamedi Fakhr

Supervisors:

Dr. Mohamed Torbati

Prof. Martyn Hill

Dr. Catherine Hill

Thesis for the degree Doctor of Philosophy

February 2014

University of Southampton

ABSTRACT

FACULTY OF ENGINEERING AND ENVIRONMENT

Engineering Sciences

Doctor of Philosophy

APPLICATION OF SIGNAL PROCESSING TO RESPIRATORY CYCLE RELATED EEG CHANGE (RCREC) IN CHILDREN

By Shayan Motamedi Fakhr

Sleep is an important part of everyday life. It directly affects daytime cognition and general performance. In children, sleep is a crucial requirement for growth and learning and lack of sleep may manifest itself as a long lasting developmental deficit. Sleep disorders which disrupt the normal continuity of sleep therefore benefit from early identification and treatment. A common cause of sleep disruption is sleep disordered breathing which can be associated with frequent arousals from sleep. Many relevant areas of sleep research continue to generate new and interesting findings utilising biosignals such as EEGs. Respiratory cycle related EEG change (RCREC) is a good example of this. The method for quantification of RCREC relies on the appropriate application of signal processing and the signals involved in the procedure are polysomnographic. Furthermore, RCREC is thought to reflect morbid micro-arousals in sleep and is hence also of clinical importance. Given that the field of RCREC research is a recently established one, there is much room for constructive investigation. The current state of RCREC research is therefore expanded in this thesis. The method for calculation of respiratory cycle related EEG change (RCREC) is replicated and expanded in this project. Shortcomings of the method have been identified and accounted for where appropriate. In particular, the sensitivity of RCREC to airflow signal segmentation is addressed and alternative segmentation approaches are suggested. The general influence of airflow segmentation on RCREC is investigated and a mathematical explanation for RCREC sensitivity is given. Additionally, the ability of RCREC related parameters to predict daytime cognitive functions is assessed. Results suggest that RCREC parameters are capable of predicting quality of episodic memory, power (speed) of attention and internal processing speed.

DECLARATION OF AUTHORSHIP

I, Shayan Motamedi Fakhr

Declare that the thesis entitled:

"Application of signal processing to respiratory cycle related EEG change (RCREC) in children"

And the work presented in the thesis are both my own, and have been generated by me as the result of my own original research. I confirm that:

- this work was done wholly or mainly while in candidature for a research degree at this University;
- where any part of this thesis has previously been submitted for a degree or any other qualification at this University or any other institution, this has been clearly stated;
- where I have consulted the published work of others, this is always clearly attributed;
- where I have quoted from the work of others, the source is always given. With the exception of such quotations, this thesis is entirely my own work;
- I have acknowledged all main sources of help;
- where the thesis is based on work done by myself jointly with others, I have made clear exactly what was done by others and what I have contributed myself;
- none of this work has been published before submission.

Signed:

Date: 27/2/2014

Table of contents

x

Chapter 1

Introduction

Polysomnography (PSG) is the gold standard method in sleep monitoring. It provides a rich data set containing both physiological and diagnostic information. The information contained in PSG data is far more than what is routinely extract from it. Signal processing is a tool which helps to extract further information from any data set. There are a vast number of techniques which can be applied to different sets of data (based on the applications) to learn more about the underlying structure of that data. In sleep analysis, signal processing techniques can be particularly useful as they may reveal diagnostic or physiological information which cannot be detected on standard visual inspection.

The overall aim of this project was to identify, develop, and combine signal processing techniques which can be effectively applied to PSG data sets in order to detect or analyse important events in sleep such as arousals or micro arousals. To this end, a substantial review of the literature focusing on the applications of signal processing in sleep EEG analysis was carried out (see Appendix A). The starting point of the experimental and analytical works outlined in this thesis was the study of an American group led by Dr. Ronald Chervin on respiratory cycle related EEG changes (RCREC) [1]. This phenomenon is characterised by statistically significant changes of EEG power in different stages of respiration. It is hypothesised that RCREC reflects brief but frequent micro-arousals which are capable of producing morbid daytime effects. The relation to arousals combined with the fact that the method for calculation of RCREC was largely dependent on signal processing, encouraged us to further investigate the method, the parameter and the relationship between the parameter and daytime neurobehavioral measures. As a result, this thesis is dedicated to the various analyses of RCREC carried out during the course of research. In particular, dependence of RCREC on respiratory signal segmentation was found to be an area not addressed in the literature previously and since respiratory cycle segmentation is an integral part of RCREC quantification, potential effects of airflow signal segmentation on RCREC were thoroughly investigated. Suggestions for improvement of the original method for calculation of RCREC were also given. In addition, daytime neurocognitive correlates of RCREC parameters were identified in a relatively large sample of paediatric subjects. The latter study

revealed for the first time that RCREC parameters may be capable of predicting quality of episodic memory, power (speed) of attention and quality of internal processing in the brain.

The rest of the thesis is arranged as follows: first, since the subject of research is inherently multidisciplinary, a literature review covering the relevant aspects of sleep and sleep disordered breathing (SDB) is provided (Chapter 2), the data used throughout the project is also described in Chapter 2, this includes the acquisition procedure, notes on post-acquisition scoring, and any personal observations worthy of note during the data acquisition sessions. Respiratory Cycle Related EEG Change (ECREC) is then formally introduced; this includes the review of relevant previous studies on RCREC and touches on the current method to calculate RCREC (Chapter 3), Chapter 3 also describes the methodology which was developed in this project to quantify RCREC; this includes the development of a respiratory cycle detection algorithm, automatic abnormal nasal flow data rejection, pre-processing done on the PSG signals prior to RCREC calculation and statistical analyses required for full RCREC characterisation. Chapter 4 describes the preliminary investigations on RCREC. In this chapter, the work on RCREC was first replicated in a single subject. Two selected experimental case studies with relatively small sample sizes were then carried out. Relationship with apnoea-hypopnoea index (AHI) and effect of airflow segmentation on RCREC were briefly assessed. The results obtained from the initial case studies directed the research to systematically test the hypotheses emerged during the analyses. Hence, chapter 5 includes a thorough investigation (both theoretical and experimental) of the effects of alternative airflow segmentation on RCREC. Chapter 6 examines the ability of RCREC parameters to predict daytime measures of neurocognition. The seventh and the final chapter of the thesis presents a summary of the main findings, conclusions and describes potential future work. The next chapter provides a background for sleep and sleep disordered breathing and details the data used for analytical studies.

Chapter 2

Sleep and sleep disordered breathing (SDB)

This section aims to provide an introduction to sleep and some of the closely related topics such as sleep evaluation, sleep scoring, sleep staging and sleep disordered breathing based on the current literature. It also describes the data used throughout the project for case studies.

2.1 Introduction to Sleep

Sleep put simply is what occurs between goings to bed at night and waking up in the mornings. More accurately, however, sleep experts define it as "a reversible state of perceptual disengagement. A universal behaviour across the animal kingdom" [2]. It is fundamentally driven by the brain state. Sleep is a crucial part of everyday life. It directly affects cognitive performance, learning capabilities, and general physical and emotional wellbeing. While adults spend more than one third of their lives sleeping, children spend about half of their lives in this brain state. During infancy when brain development is rapid, sleep occupies up to 16 hours a day [3, 4]. Sleep is traditionally divided into REM (rapid eye movement) and NREM (non rapid eye movement). NREM sleep is further categorised into four stages with Stage one being the lightest stage of sleep and stage four being the deepest. This will be further described in the sleep staging section. Figure 1 shows a hypnogram (decomposition of sleep into stages) of a paediatric subject.

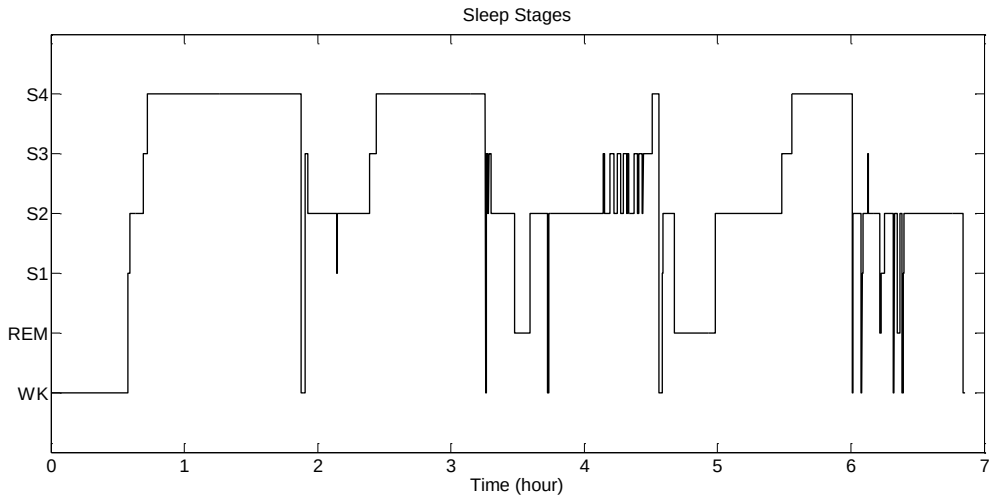

Figure 1. Traditional hypnogram of a single paediatric subject. WK represents wake, an arousal from sleep.

Sleep is the primary activity of the brain in infancy and is thought to promote neural plasticity [5, 6]. Sleep problems in early life may result in lasting neurocognitive deficits [5]. Understanding the role of brain activity in sleep is an exciting frontier of neuroscience. Krueger *et al.* [7] point out that "during sleep one gives up the opportunities to reproduce, eat, drink or socialize and one is subject to predation. Sleep could only have evolved despite these high evolutionary costs if it serves a crucial, primordial function". It also plays an important role in memory consolidation [8]. Sleep clearly serves an important role for the very young.

A more recent theory on sleep function suggests that sleep should no longer be looked at as a whole organism phenomenon controlled by a single central mechanism. It is more likely that sleep is governed by numerous local neuronal assemblies within the brain (a distributed control system) [7]. That is to say at any given time, a part of one's brain can be asleep whilst the rest is awake.

A very common question regarding sleep is: how much sleep is enough to maintain health? As was mentioned above the amount of required sleep varies significantly with age, as infants may need up to 16 hours of sleep a day and adults only need about eight hours. A relatively recent study on 48 healthy adults shows that sleeping less than six hours may ultimately be as harmful as not sleeping for two consecutive nights in terms of cognitive deficits [9]. However, in general there is not a physiologically evidenced number associated with the optimal amount of sleep required.

2.2 Sleep Evaluation

In order to research sleep there must be a means to quantify sleep. Sleep activities are commonly measured using bioelectric signals (e.g. EEG, EMG, ECG, etc). There have also been several methods used extensively for sleep evaluation out of which polysomnography (PSG) is known as the gold standard and is discussed here. The next section gives an introduction to bioelectric signals and then continues to introduce polysomnography in more details.

2.2.1 Introduction to Bioelectric signals

A signal is a way of conveying information. Biomedical signals are signals acquired from living beings. They generally aim to extract information about a specific function. For instance, to examine the response of visual cortex to sudden changes in the luminosity of the surrounding

environment, one can stimulate the eye with a sequence of light flashes and monitor the brain activities in the occipital lobe for consistent changes.

Bioelectric signals are biomedical signals which are electromagnetic in nature. The existence of bioelectric signals is directly related to existence of neurons (nerve cells). That is due to the fact that nerve cells (also muscular cells) function chemically in nature and the chemical reactions induced by these cells, affect the electric and/or magnetic fields of those cells and their neighbouring ones. These changes in electric and/or magnetic fields caused by changes in intracellular and extracellular ion concentration can then be measured using appropriate instruments.

Why is there any change in the electric/magnetic field? The answer to this question lies in the mechanism by which neurons work. A neuron is capable of processing, transferring and acquiring information. Its main parts are the cell body (soma), the dendrites and the axon. A schematic of a neuron is shown in Figure 2.

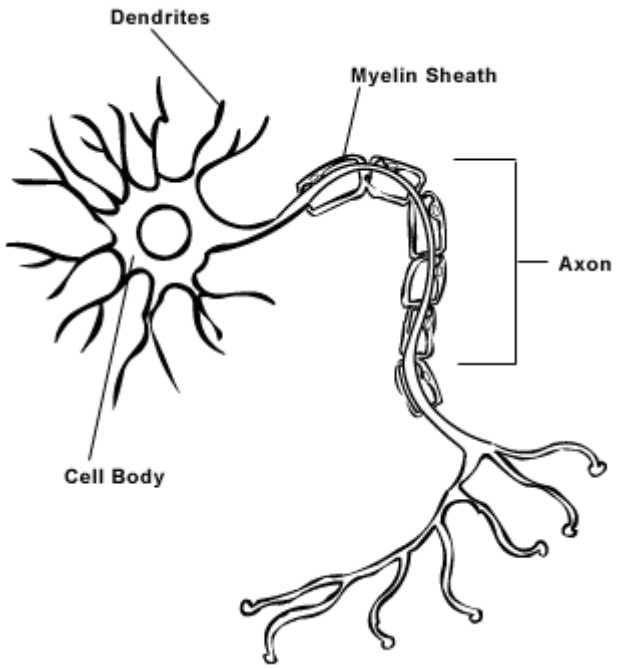

Figure 2. A schematic of a nerve cell. The axon (output of the neuron), the dendrites (connections with other neurons) and the cell body (containing intracellular fluids essential for cell functioning) can be seen.

The cell body is surrounded by an excitable membrane (dendrites are the extensions of the cell membrane). Since the ion concentration in intracellular and extracellular fluids is not the same and the membrane permeability also responds differently to each of the ions, there would always be an electric/magnetic field across the membrane. This base voltage created across the membrane is referred to as the resting potential. Although the resting potential varies in different cells, an approximate value of 80 millivolts (mV) has been given in literature (inside of the cell being negative with respect to the outside environment)[10]. The resting potential can

change dramatically if a cell is stimulated by a chemical or electrical reaction. If a stimulus elevates the voltage across the membrane of a cell up to a certain threshold, that cell will no longer retain its resting potential. Instead, the resting potential will be increased, becomes positive for a short period of time and then declines back to its previous value. This cycle of resting potential – polarisation – depolarisation and resting potential is referred to as an action potential. Action potentials differ in time duration and shape in different cells as for instance, muscle cells have an action potential with a much longer duration than the nerve cells. A typical action potential is shown in Figure 3.

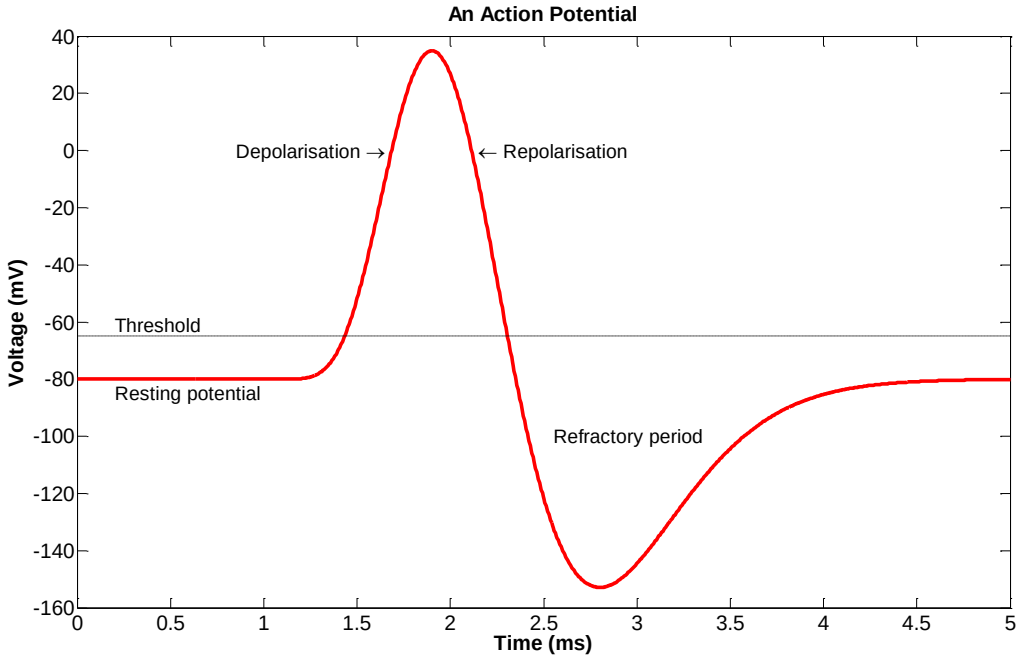

Figure 3. Different phases of an action potential can be seen in the above graph. Action potentials provide a means for information transfer. Action potential above was synthetically generated in Matlab using the first derivative of a gamma probability density function with θ=0.15 and α=10.

Note that although action potentials are discussed for a single cell, they never occur in only one cell alone, as excitation of one cell results in excitation of neighbouring cells (provided that the excitation is strong enough). Hence there will be a propagation of the action potentials. However, this propagation is always in one direction and cannot propagate back as the potential of the exciting membrane will be still too high to be excited again by a neighbouring cell (it can only be excited again if enough time has elapsed and the voltage across the membrane has come back down to its resting potential, this duration is referred to as the "refractory period").

Existence of action potentials is the reason there is a change in electric/magnetic field of cells. It also describes the nature of bioelectric signals. Hence, for example, when measuring an electroencephalography (EEG) signal, what is actually being measured is a superposition of many electric fields in the brain caused by propagation of action potentials. This section was

largely based on the following references [10, 11]. The next section introduces polysomnography.

2.2.2 Polysomnography (PSG)

Polysomnography is an investigative tool which is widely used in sleep analysis. The direct translation of the name is “many sleep writings” and in fact polysomnography is nothing but a large collection of biomedical signals acquired from different body parts of a living being while asleep.
Standard signals acquired during polysomnography include:

1) Electroencephalograms (EEG) which are measured by attaching electrodes to the scalp. The obtained EEG recordings are associated with the brain activities.
2) Electrocardiograms (ECG) which are recorded by attaching electrodes to the chest area anterior to the heart, the so called ‘precordium’. ECGs are associated with heart activities. Other derived parameters like RR (the interval between two successive ventricular systoles) can also be calculated from the ECG signal.
3) Electromyograms (EMG) which are measured by attaching electrodes to certain muscles such as the submentalis chin muscle as it is very sensitive and can reflect wake/sleep status or the anterior tibialis in the lower leg to measure limb movements in sleep.
4) Electrooculograms (EOG) which are measured by connecting one electrode alongside each outer canthus. EOG signals are associated with eye movements.
5) Flow which is measured by thermistors or nasal pressure transducers and is associated with oral/nasal air flow, new standards recommend simultaneous use of both in children.
6) Thoracic and abdominal excursions which are measured by piezoelectric belts or respiratory inductance plethysmography (RIP). The obtained signals from the above two are directly associated with thoracic and abdomenal movements.
7) Oxygen saturation (SpO_2) which is measured by pulse oximetry and represents the oxyhaemoglobin saturation in blood.

EEG, EOG and EMG signals are required to define sleep stages as well as arousal events. Other parameters yield important information about cardiorespiratory activities and in conjunction with the EEGs, enhance interpretation of sleep stages and also open new dimensions as to measure other bodily functions such as autonomic activities (e.g. heart rate variability). Some studies also include CO2 measures and oesophageal manometry. Although the number of

signals in polysomnography can vary greatly, these are the usual combination for a standard study. There are also a number of parameters in each PSG which are not independently measured but are derived from the existing signals, RR interval and pulse transit time (PTT) are examples of those. Figure 4 shows a 30 second epoch of a standard polysomnograph of a child (Alice 5 software, Respironics).

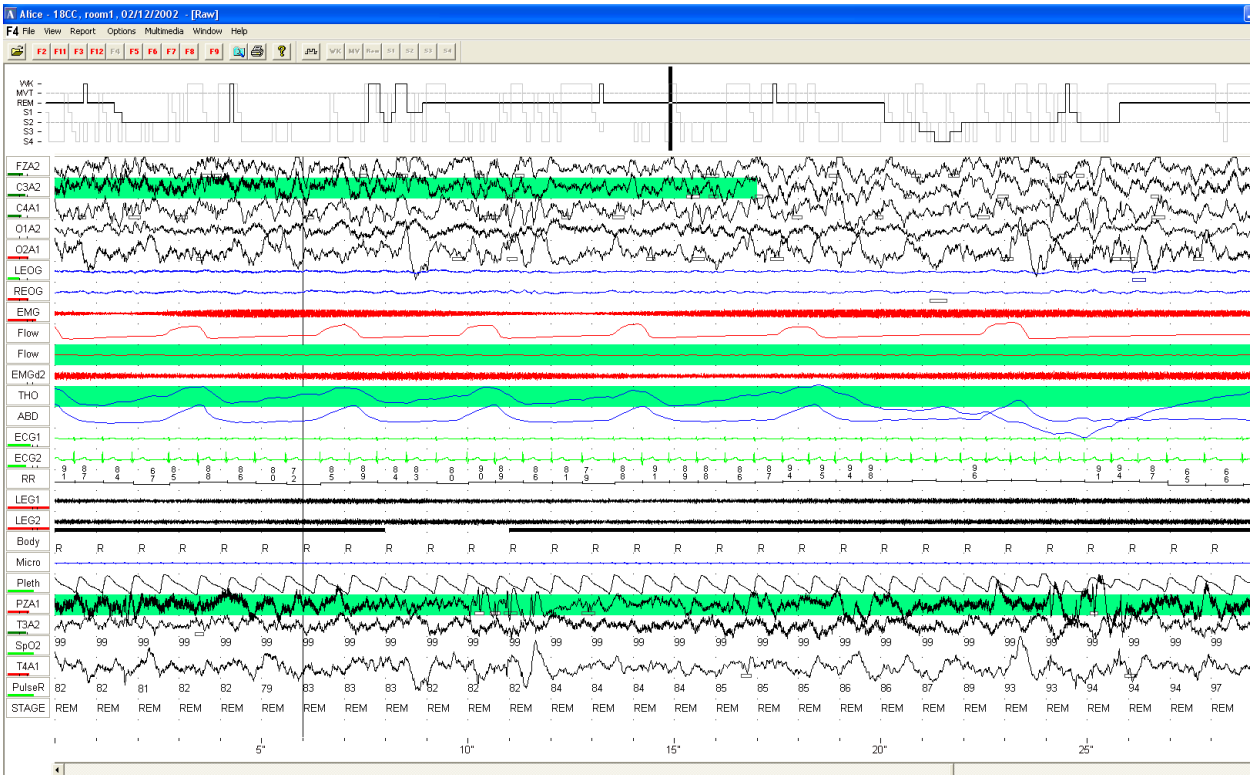

Figure 4. A 30 seconds epoch of a full PSG of a child (obtained from Southampton General Hospital, Welcome Trust Research Facility). FzA2, C3A2, C4A1, O1A2, O2A1, PzA1, T3A2 and T4A1 are the EEG signals obtained from electrodes placed in different scalp locations, LEOG and REOG are the left and right EOG signals, THO and ABD are the thoracic and abdominal movements respectively and SpO_2 is the oxygen saturation level in percent.

In order to have a clearer understanding of the EEG signals, it is essential to know how the electrodes are placed on the scalp to measure different bioelectric brain signals. EEG electrodes are currently placed according to the 10-20 international electrode placement system [12]. This system suggests placing the electrodes in 10 and 20 percent deviation from the 4 anatomical brain landmarks, those are the nasal bridge, the occipital protuberance and left and right depression points in front of each ear [4]. Furthermore, as can be seen in Figure 4, in each PSG, EEG signals can be distinguished from one another using their names. The starting letter in each name indicates the general scalp region (F for frontal, C for central, O for occipital and T for temporal) and the following number specifies the exact electrode positioning. Electrodes placed on the left side of the brain are assigned odd numbers and electrodes on the right are associated with even numbers. Electrodes in the middle are indexed as “z”. For instance, C3A2 is referred

to the electrode placed on the left-central side of the brain. A1 and A2 refer to left and right earlobes respectively, they are used as references since they have little to no EEG activity [4]. Figure 5 shows a schematic of the 10-20 electrode placement system [12].

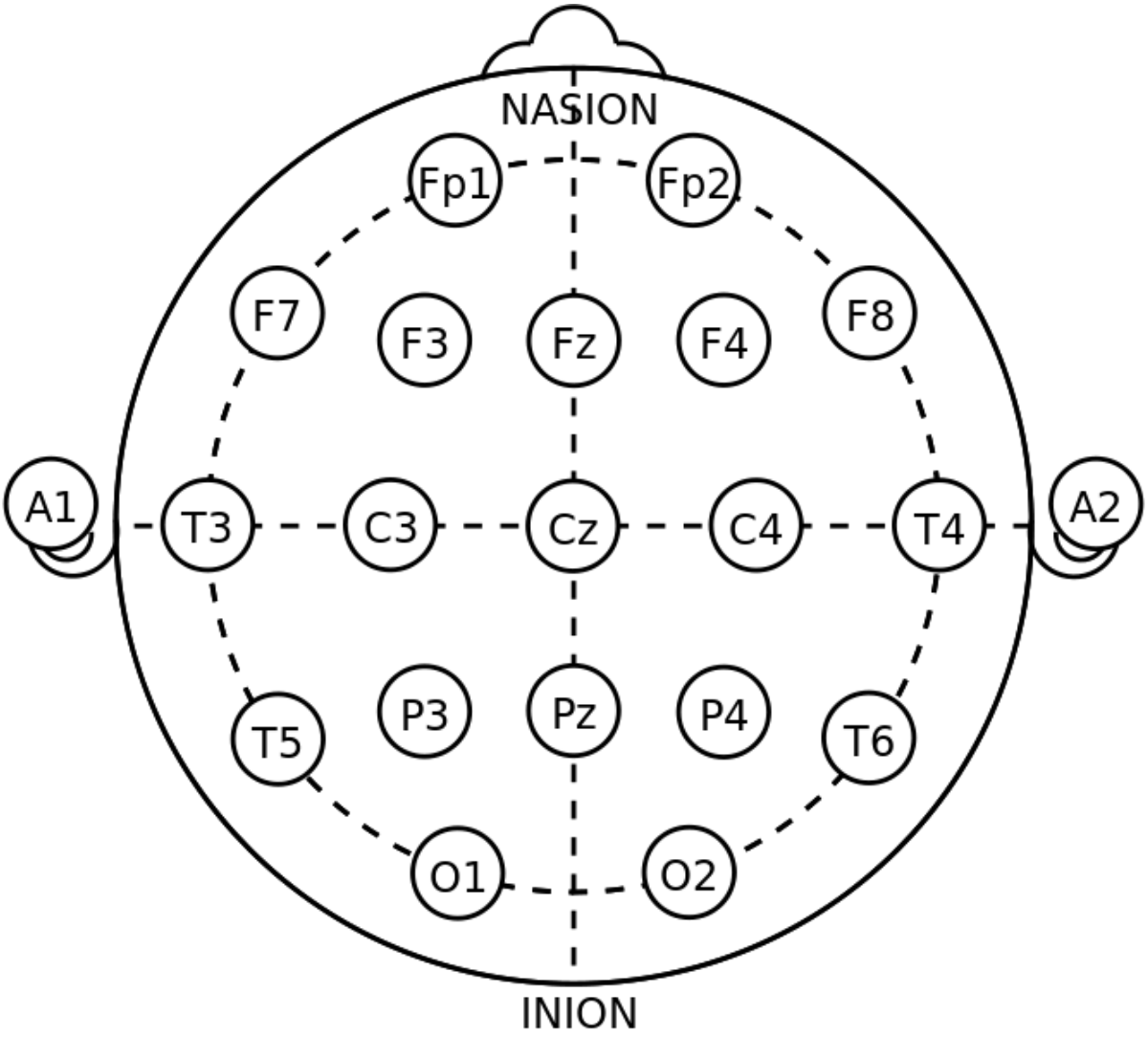

Figure 5. EEG electrode placement according to the international 10-20 electrode placement system (no permission required, public domain material).

PSGs are extensively used in sleep analysis and diagnosis of certain sleep disorders and can be performed on infants and children of any age given that experienced technicians are available [3].

2.3 Sleep scoring and sleep staging

Sleep staging is the process of dividing sleep into several distinct and physiologically meaningful intervals based in the information gathered from polysomnography. Sleep scoring is the process

of recognising/identifying certain signal patterns in polysomnography, and is the basis upon which sleep staging is formed.

Sleep is traditionally divided into REM and Non-REM (NREM) sleep (Active and Quiet sleep in infants [2-4]). NREM Sleep is then divided into four stages referred to as stages 1 to 4, however, due to physiological similarities between stage 3 and stage 4, these two were more recently merged to create a single sleep stage referred to as stage 3 or slow wave sleep (SWS) [4]. Each of the above stages is associated with certain EEG patterns and unique physiological interpretations. More recently, the American Academy of sleep medicine (AASM) has re-defined and re-categorised the conventional sleep stages (Stages 1 to 4) into three new categories namely N1, N2 and N3 with N1 corresponding to Stage1, N2 to stage 2 and N3 to SWS. This new classification aims to update the conventional standards by Rechtschaffan and Kales [13] which had been in place for more than 40 years. Although the newly introduced standards seem to have had a positive impact on sleep scoring and sleep staging overall [14], the Rechtschaffen and Kales manual is still in use to date and complete transition from the old standards to the AASM is likely to take few more years. The next section describes some of the sleep EEG patterns which are commonly used in sleep staging and scoring.

2.3.1 Introduction to well-known EEG patterns

EEG signals are made up of a range of frequencies (0 to 30 Hz). These frequencies are conventionally divided into five groups, each having a unique name. In the literature, these frequency bands are referred to as delta (0.5-4 Hz), theta (5-7 Hz), alpha (8-12 Hz), sigma (13-15 Hz) and beta (16 to 30 Hz) [15, 16]. Slightly different categorisation may be found in the literature [17]. The frequency bands introduced above are routinely used in describing different EEG patterns and the spectral contents of different sleep stages.

Sleep Spindles:

According to Rechtschaffen and Kales [13], Sleep Spindles are transient waves of 12-14 Hz frequency (distinct from the background) which last for more than 0.5 seconds (in adults). More recently, it was found that Sleep Spindles in children could occur independently at two frequency intervals of 11 to 12.75 Hz and 13 to 14.75 Hz over frontal and Centro parietal electrodes respectively. Furthermore, Sleep Spindles are known markers of sleep stage 2 [4]. A typical sleep spindle is shown in figure 6 (taken from [18]).

K-complexes:

A K-complex is a bi/triphasic pattern which starts with a rapid negative component, followed by a slower positive one and could last from 0.5 to 2 seconds; they occur in the delta frequency band and have higher amplitude than the background EEG activity (the amplitude is often >200 μV) [4, 15, 18, 19]. A K-complex is shown in Figure 6 (taken from [18]).

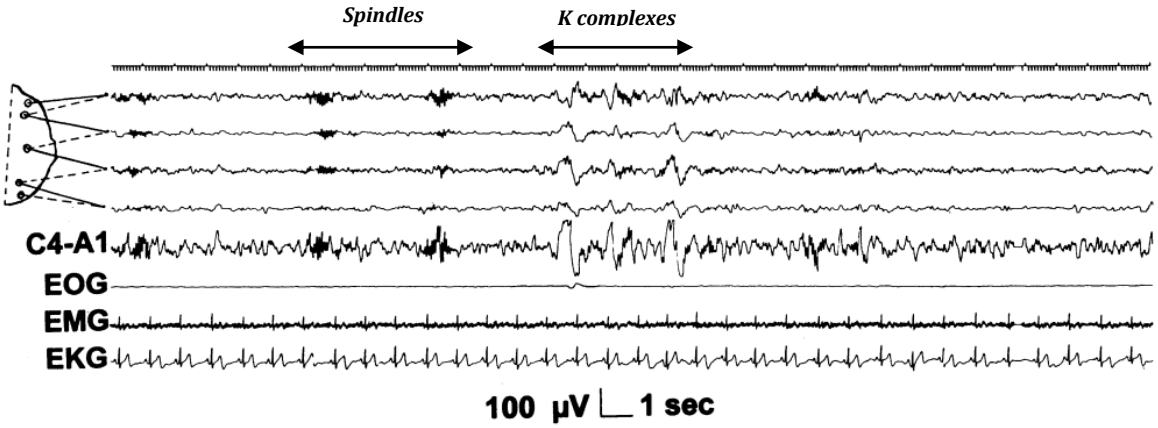

Figure 6. *Sleep Spindles* followed by a sequence of *K complexes*. As can be seen spindles are more pronounced in the central area rather than the occipital region (compare C4A1 with the rest of the EEG patterns) [18].

Vertex Sharp waves:

A vertex sharp wave is composed of a very rapid negative component followed by a sharp positive component. Vertex sharp waves last from 50 to 200 msecs and are particularly present in the transient between stage 1 and stage 2 of sleep [4, 18]. Figure 7 (taken from [18]) shows a sequence of vertex sharp waves.

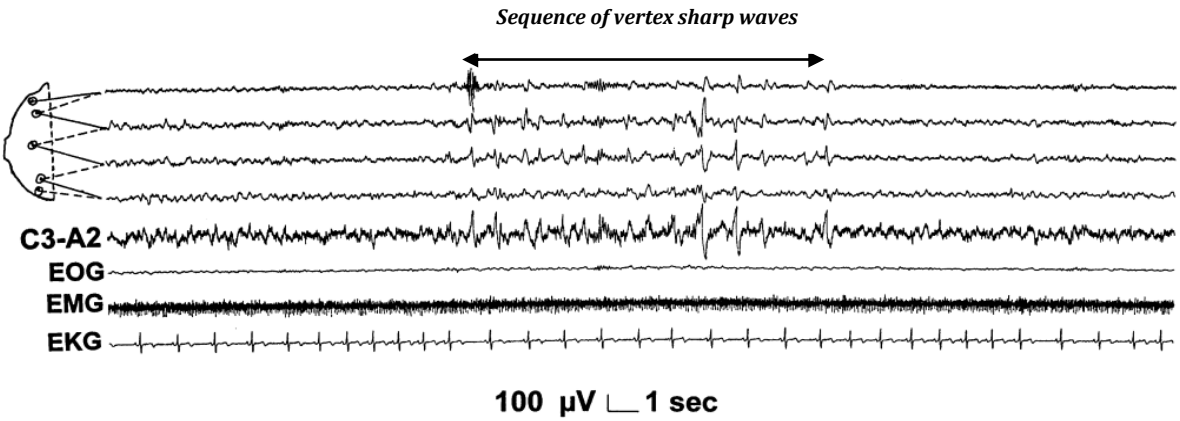

Figure 7. A sequence of *vertex sharp waves* in transient between stage1 and stage2 of sleep [18].

Delta bursts:

Delta bursts are described as waves with at least two cycles of delta frequency activity (0.5 to 4 Hz) with amplitudes 1/3 (or more) greater than the background activity. They are most prominently seen in the slow wave sleep (SWS) with a lower frequency than the Posterior rhythm. Figure 8 shows a typical delta burst (taken from [18]).

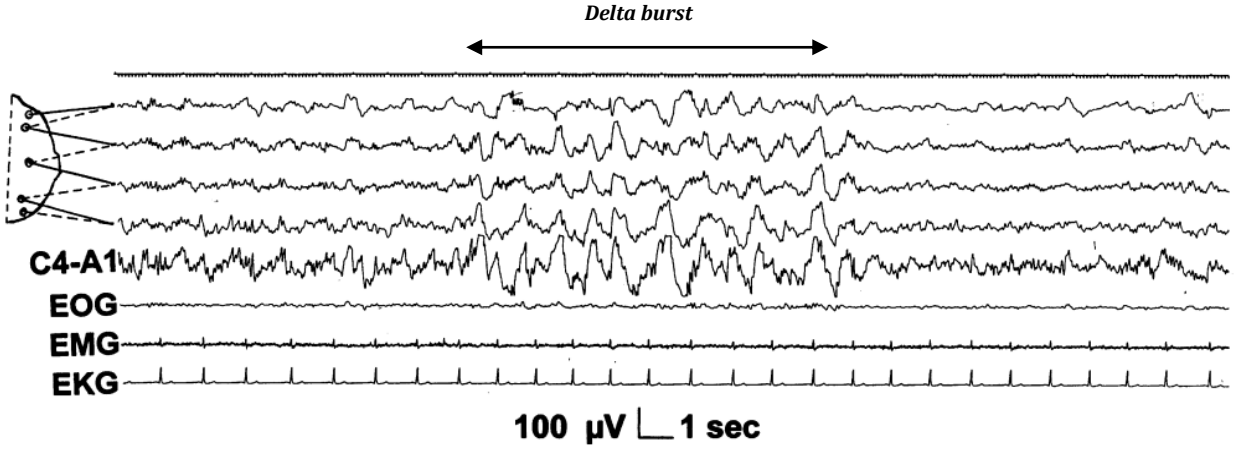

Figure 8. A Typical *delta burst* in slow wave sleep [18].

Polyphasic bursts:

Polyphasic bursts are groups of high amplitude delta waves accompanied (or mixed) by theta, alpha or beta rhythms. They are mostly seen in sleep stage 2 and especially before REM onset. A polyphasic burst is shown in Figure 9 (taken from [18]).

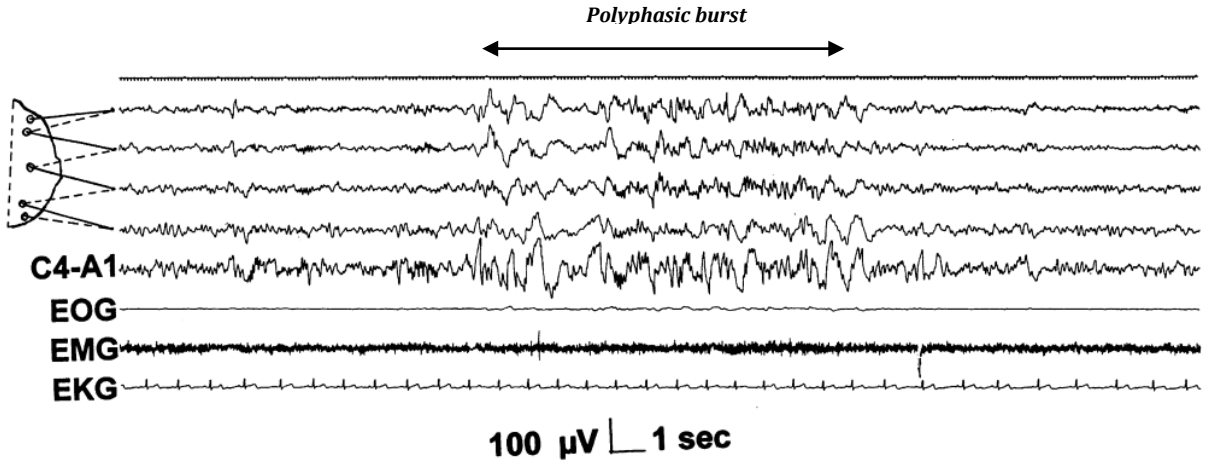

Figure 9. A Typical *polyphasic burst* in sleep stage 2 [18].

EEG arousals (or cortical arousals):

An EEG arousal is described as an abrupt change in the EEG frequency towards higher frequencies including theta, alpha and beta but not spindles. For an arousal to be scored, it should be preceded by at least 10 seconds of sleep and last for 3 seconds (Mograss *et al.* [20] argue that one second of EEG frequency shift is adequate to score an arousal in paediatric subjects). EEG arousals are thought to fragment sleep and have deleterious effects if they occur frequently [18, 21]. Figure 10 depicts an EEG arousal (taken from [18]). EEG arousal is the last EEG pattern touched on here. The next section describes the conventional sleep stages and their physiological properties.

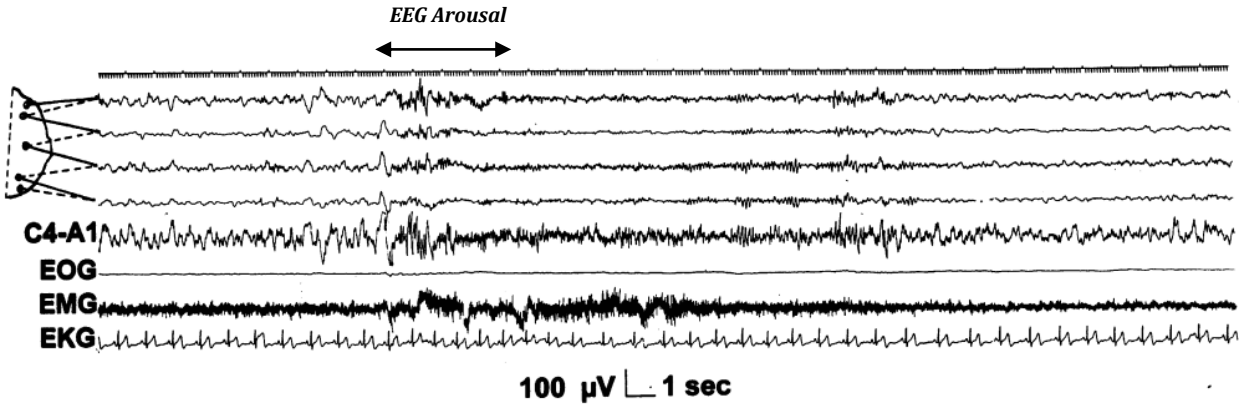

Figure 10. An *EEG arousal* preceded and followed by sleep [18].

2.3.2 REM (rapid eye movement) sleep

The term rapid eye movement (REM) was first used in 1953 [2, 18]. REM sleep is a sleep state which is closely associated with rapid eye movements (as verified by the EOG signals) and low amplitude mixed frequency EEG activity. REM sleep is the most relaxed stage of sleep in terms of muscle activities even though the brain signals closely resemble those of wakefulness. In infants there is a REM like state called "active sleep (AS)" which has a similar EEG and polysomnographic characteristic as the REM sleep. REM (or AS in infants), is described as an stage with rapid eye movements, irregular respiration and heart rate (higher sympathetic nervous system activation rate), negligible chin EMG (very relaxed muscle tone) and frequent small limb or face movements [4]. REM sleep (or AS) is particularly important in neonates as they spent 2/3 of their total sleep time in this state as opposed to adults which spend only 20-

25% [3]. Figure 11 shows the polysomnographic features of REM sleep (Alice 5 software, Respironics).

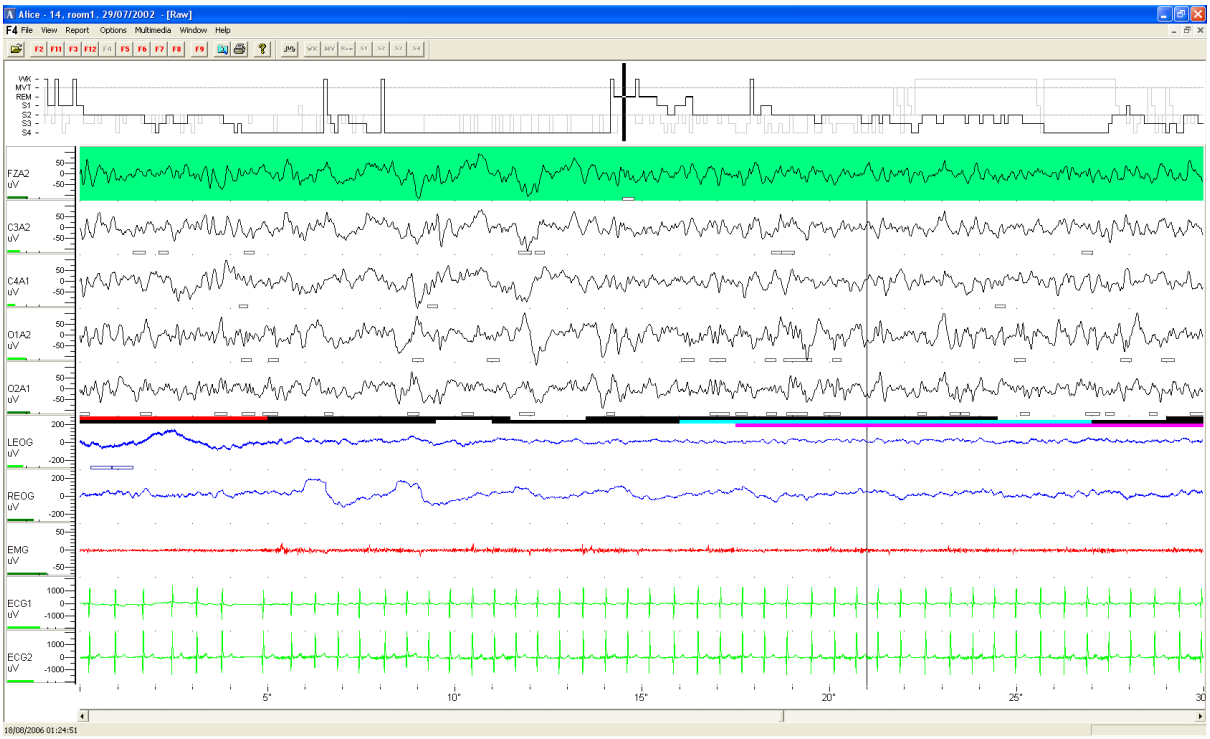

Figure 11. A 30s epoch showing a child in REM sleep. Rapid eye movements are clearly seen (particularly in the 5 – 10s region). The muscle tone is decreased and is at its lowest. High amplitudes of EOG signals confirm the "rapid eye movement" feature of the REM sleep. Furthermore, variations in heart rate (irregularities seen in the ECG signal) also confirm the elevated sympathetic activation and hence the REM stage.

2.3.3 Non Rapid Eye Movements (NREM)

All the other sleep stages (i.e. Stage1, Stage2 and SWS) are categorised as NREM. Sleep commonly starts from Stage 1 (NREM1) and then alternates between other NREM and REM stages. NREM stages are explained in more details below.

i. *NREM 1(stage 1)*

NREM1 is generally the first stage of sleep (sleep onset in infants younger than 3 month is REM sleep). It starts with drowsiness (slower eye movements, spontaneous eye closure, reduced muscle tone) followed by a decrease in the background EEG frequency with respect to the age specific wakefulness EEG activity. An epoch of NREM sleep would be scored as NREM 1 if it has

no spindles, K-complexes or Slow Wave activities (SWA)[4]. Note that vertex sharp waves may also be present in NREM1 especially in transient between NREM1 to NREM 2 [18]. NREM1 is usually quite short in duration and is immediately followed by NREM2. A 30 seconds epoch showing a paediatric subject transitioning into NREM1 is shown in Figure 12 (Alice 5 software, Respironics).

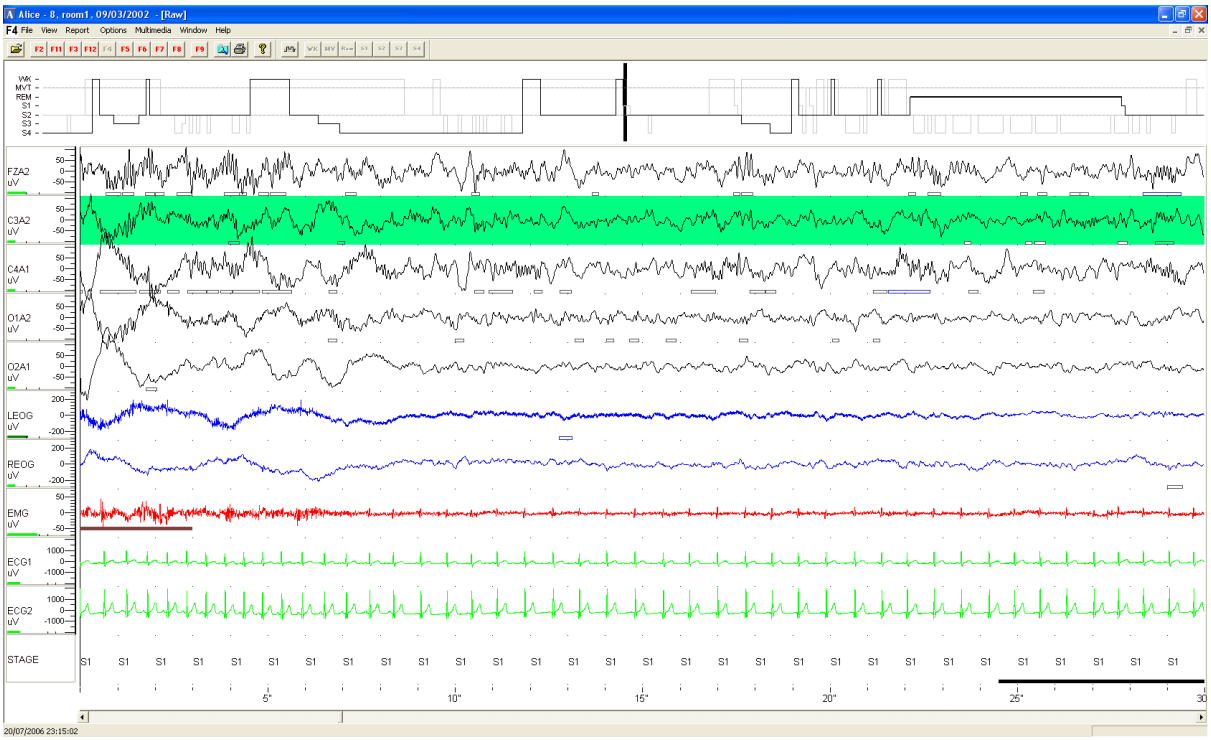

Figure 12. An epoch of a standard paediatric polysomnograph of a child transitioning into NREM1 stage (NREM1 starts at about 10 seconds in). Slower eye movements and decreased EEG frequency can be clearly seen in epoch shown.

ii. *NREM 2(stage 2)*

NREM2 generally follows after NREM1 at sleep onset. Sleep spindles are characteristic of this stage and in fact are the best polysomnographic markers for this stage. Another feature of NREM 2 is the presence of K-complexes; if a thirty second epoch contains either sleep spindles or K-complexes and <20% of slow wave activity (delta activity) it is scored as NREM 2. Muscle tone in NREM2 is reduced relative to NREM1 and little to no eye movement is expected [18, 19]. In adolescents and adults, NREM2 is the most prevalent stage. A study on 6 to 11 year old children showed that on average 51% of sleep time was spent in stage 2 [2]). Figure 13 shows a thirty second epoch of NREM2 stage (Alice 5 software, Respironics).

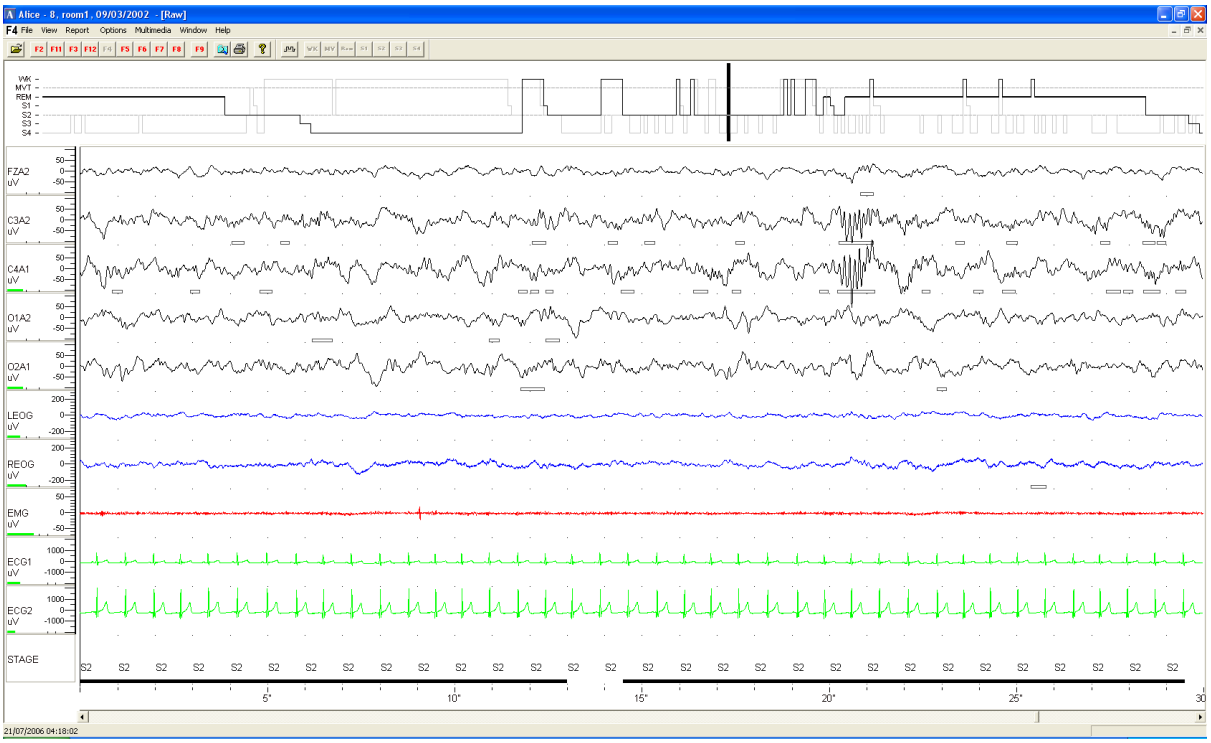

Figure 13. A 30 second epoch of full PSG of a child in NREM2 stage (30 seconds event). Little to no eye movements can be spotted. A spindle like activity is visible around the 21 second mark.

iii. *Slow Wave Sleep (NREM 3)*

Slow wave sleep (SWS) is the deepest stage of sleep when one is least arousable. It is thought that this stage is important for growth (especially in infants and pre-pubertal children) as growth hormone is uniquely secreted at this time. A thirty second epoch would be scored as NREM3 if >20% of the epoch contains slow wave activity (i.e. 0.5-2 Hz EEG waves with high amplitudes of usually > 75 μV). It is worth mentioning that scoring criteria for SWS remains the same in both children and adults [4]. Figure 14 shows an example of SWS (Alice 5 software, Respironics).

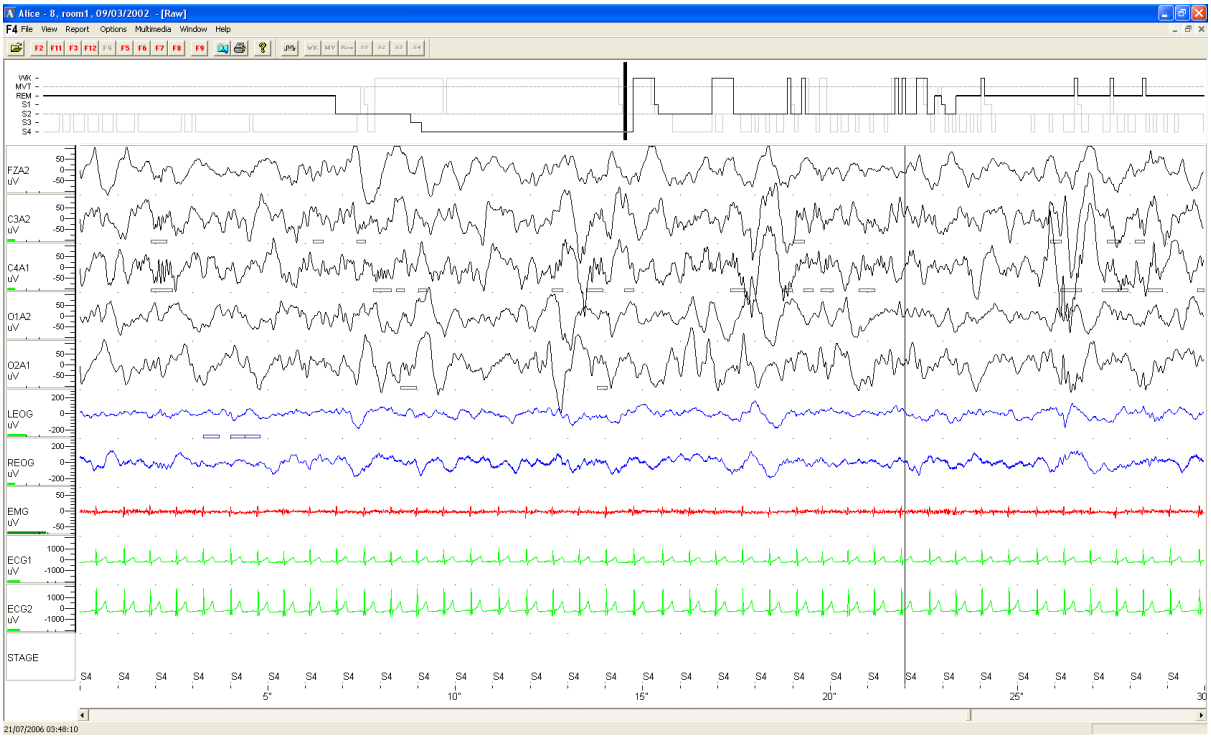

Figure 14. An epoch of a full PSG of a child in SWS sleep (30 seconds event). The slow wave activity and high amplitudes of the EEG signals are clearly seen.

2.4 Introduction to SDB

SDB is a term encompassing any respiratory difficulty associated with sleep. The most common in children is obstructive sleep disordered breathing which describes a spectrum of upper airway problems in sleep ranging from snoring to upper airway resistance, to obstructive sleep apnoea.

Obstructive sleep apnoea (OSA) is formally defined as a "disorder of breathing during sleep characterized by prolonged partial upper airway obstruction and/or intermittent complete obstruction that disrupts normal ventilation during sleep" [22]. It may be caused by adenotonsillar hypertrophy (enlargement of adenoid and tonsil tissues) in healthy typically developing children (particularly in 2 to 8 year olds) and it has been shown that it can be treated in these children by surgically removing the enlarged tissues [23]. Other factors in OSA include but are not limited to age, obesity and craniofacial anatomy.

Upper Airway Resistance Syndrome (UARS) is referred to as increased respiratory effort during sleep with no obstructive apnoea, arousal or abnormal gas exchange [3]. Diagnosis of UARS is done by direct measurement of breathing effort using an oesophageal pressure manometer (Pes) [3].

Snoring is the most common clinical manifestation of SDB [24]. It is important to note that the prevalence rate of obstructive sleep apnoea is from 0.9% to 4.3%. Furthermore, it is reported that primary snoring, that is snoring without apnoea, hypoventilation or excessive arousals from sleep [25] occurs in 10% of pre-school children [2].

SDB and in particular OSA in children is associated with consequences such as day time sleepiness, behavioural problems such as conduct difficulties, hyperactivity and impaired academic achievement. OSA is also known to affect executive function and neurocognitive performance in children [16, 17, 22, 26-28].

Obstructive SDB manifests itself as apnoeic or hypopnoeic events (apnoea-hypopnoea). Apnoea and hypopnoea are known to disturb sleep architecture (e.g. unwanted arousal from sleep). The next section will consider apnoea and hypopnoea in more detail.

2.4.1 Apnoea-Hypopnoea

Apnoea is defined as a cessation of breathing (nasal and oral airflow) for a certain amount of time. In children this time is defined as anything greater than two breath cycles, that is, an apnoeic event would be scored if there is no airflow for > 2 breaths cycle duration [15, 17]. In adults, an apnoea is defined as cessation of breathing for more than 10 seconds [29]. This is mainly due to the underlying change of respiratory rate with development. Figure 15 shows a PSG epoch with normal respiration.

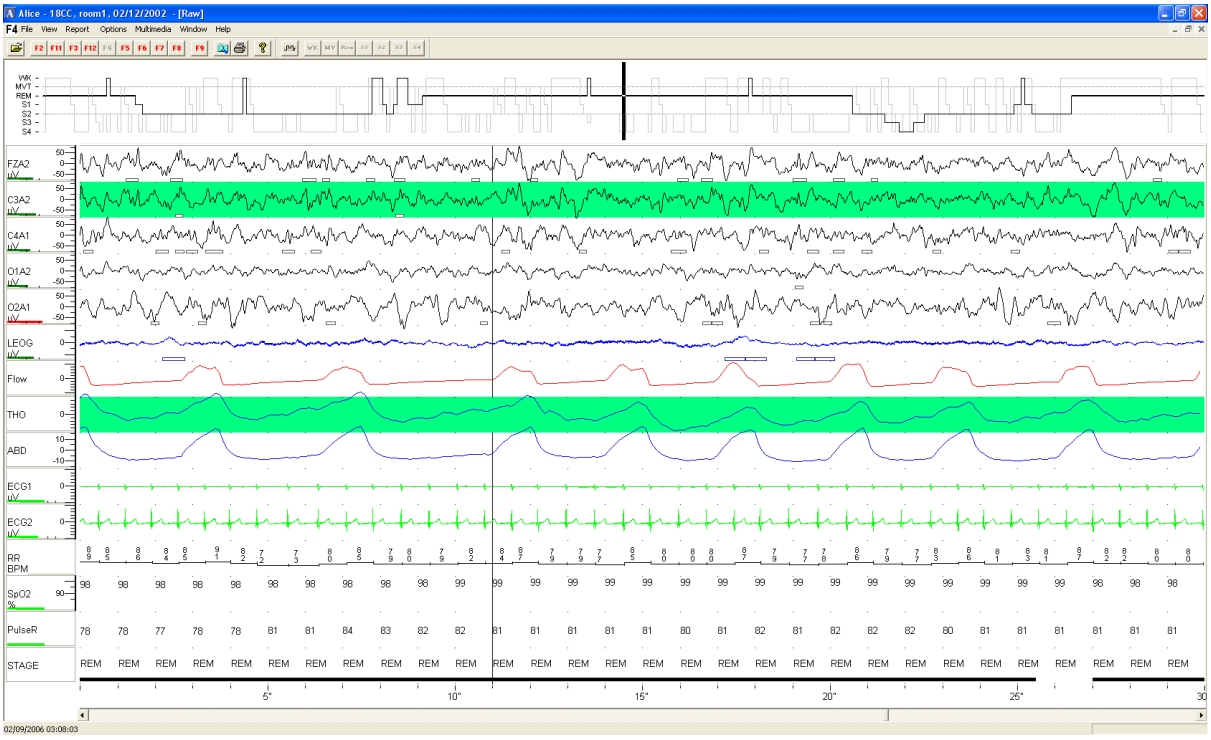

Figure 15. Parameters THO and ABD (thoracic and abdominal movements) clearly are in-phase. Flow parameters also show a clear airflow at the nose.

Apnoeas in general fall into three categories:

Obstructive Apnoea:

Obstructive apnoea is defined as cessation of nasal and oral air flow in presence of continued chest and abdominal movements for > 2 breaths cycles [17, 28]. Obstructive apnoeas occur when thoracic and abdominal movements are out of phase due to upper airway obstruction. Normally, in the inspiration phase, both thorax and abdomen move outward and in the expiration phase both of them come back down to the normal level. However, in obstructive apnoea thoracic and abdominal movement will be out of phase. This phenomenon is also referred to as paradoxical breathing. Figure 16 shows an example of paradoxical breathing (Alice 5 software, Respironics).

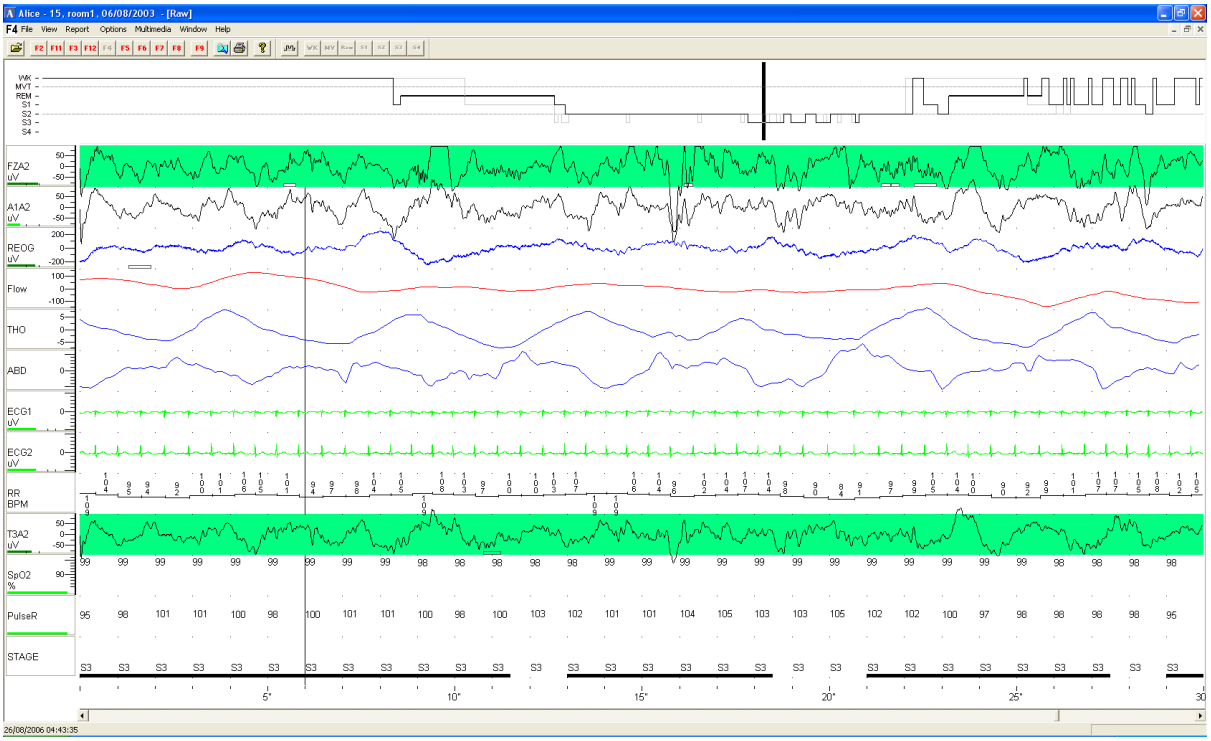

Figure 16. Parameters THO and ABD (thoracic and abdominal movements) clearly show out of phase movements which result in a diminished airflow.

Central Apnoea:

Central apnoea is defined as cessation of airflow due to absence of chest and abdominal movements for at least two breaths cycle duration. Central apnoeas are frequently seen in infants and children, particularly during REM sleep [3]. Figure 17 shows an example of a central apnoea (Alice 5 software, Respironics).

Mixed Apnoea:

Mixed apnoea is the mixture of obstructive and central apnoeas and as all apnoeas, it results in full or partial cessation of breathing for greater than 2 breaths cycle duration in children (or 10 seconds in adults). Figure 18 shows an occurrence of a mixed apnoeic event (Alice 5 software, Respironics).

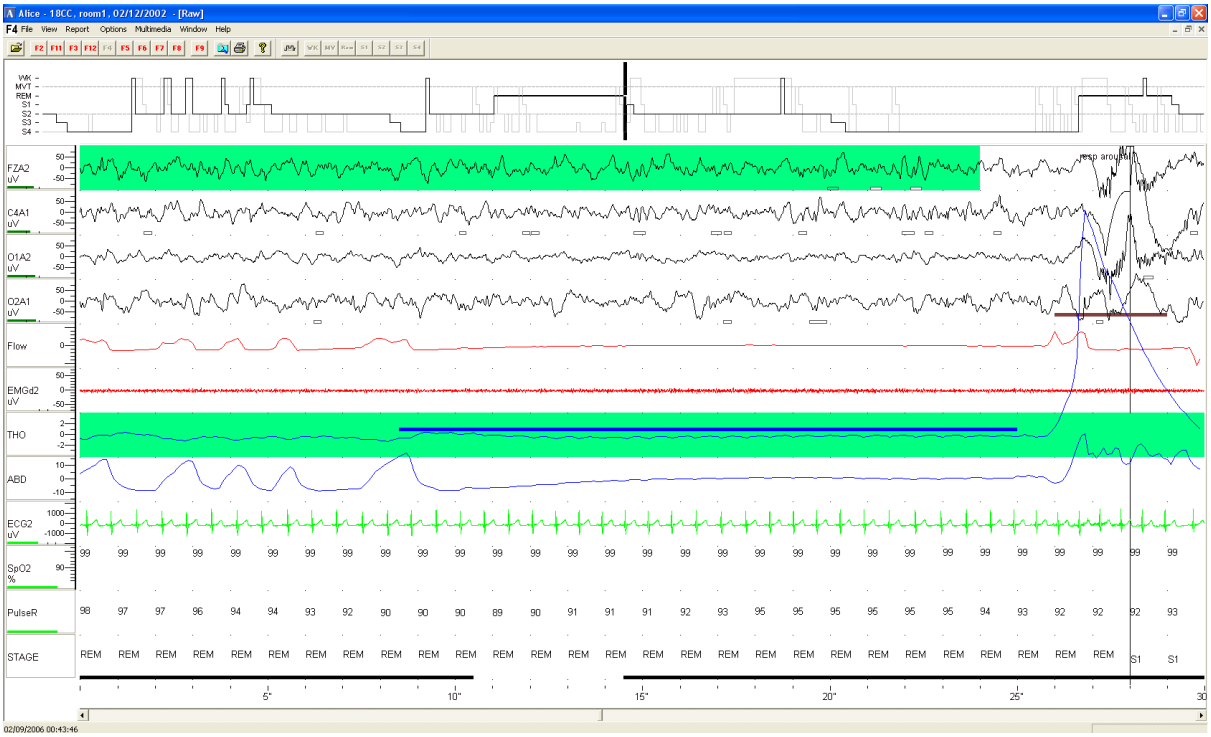

Figure 17. It is clear that there are no thoracic or abdominal movements for a period of about 15 seconds. This event which results in cessation of air flow is referred to as a central apnoea and may be followed by an arousal.

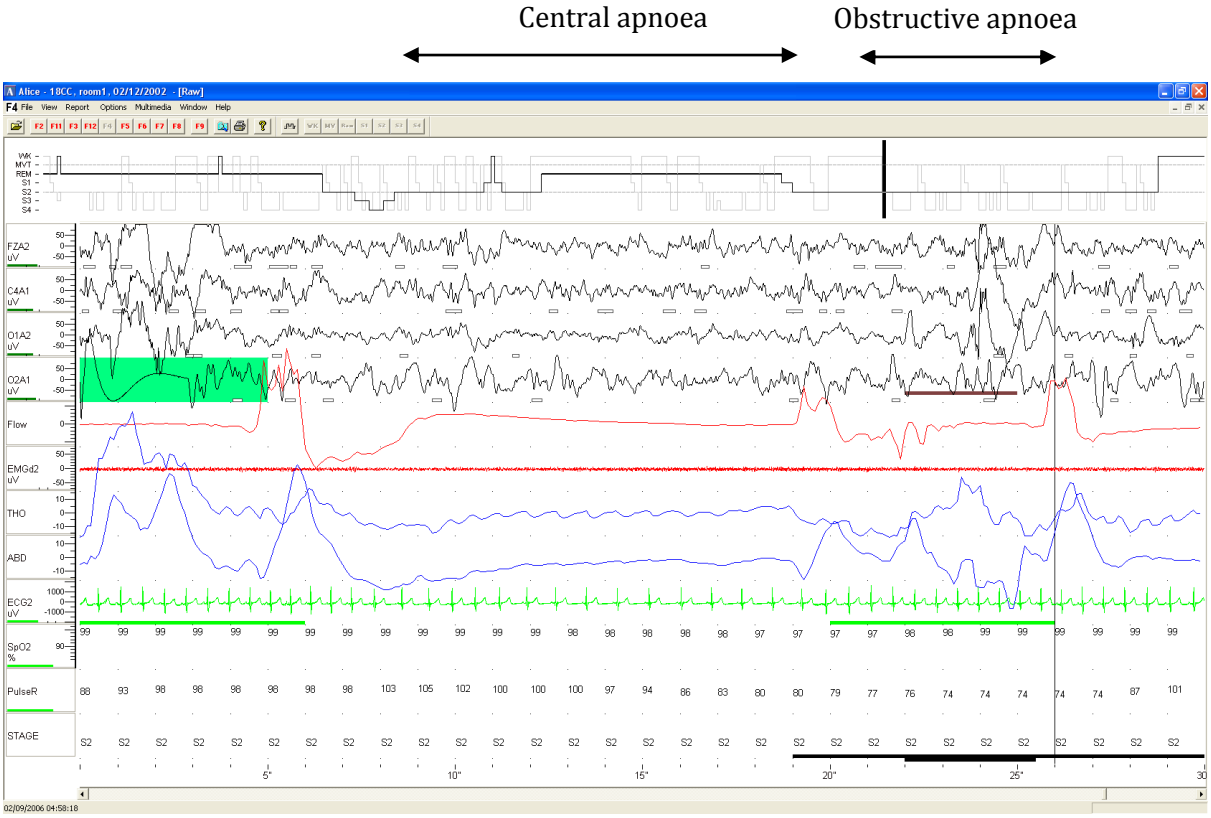

Figure 18. A mixed apnoeic episode is shown in the figure above. Observe the flow parameter.

Hypopnoea:

Hypopnoea is defined as a decrease in oral and nasal air flow by >50% accompanied by oxygen de-saturation of > 4% (or 3% in children) and/or an arousal [17].

The Average number of apnoeas and hypopnoeas per hour of sleep is referred to as the apnoea-hypopnoea Index (AHI). AHI is the standard measure used in the diagnosis of OSA.

Apnoeas may be but are not necessarily followed by arousals (waking up from sleep for a short period of time or going to lighter stages of sleep) or oxygen de-saturation [15]. Arousals are known to disturb the normal sleep structure. The next section is dedicated to arousals, and their influence on normal sleep.

2.4.2 Arousals

Arousals are important defence mechanisms. Human beings respond to changes in their surrounding environment even in sleep. For example, they may wake up from sleep if someone turns on a light or shouts (i.e. visual and auditory stimuli). Arousals also protect against the cardio respiratory sequelae of SDB as one breathe better awake than asleep [3]. In children and infants, the arousal threshold is higher than adults, meaning that arousals are less frequent in children. It is thought that sleep in infants and children is of significant importance to neurodevelopment and since frequent arousals in infants could be harmful to that, they tend to have a higher arousal threshold [4]. It is also important to note that although cortical arousals in children are less frequent, there may be sub-cortical arousals present which do not reach the cortex and will not be detected by the EEG electrodes; but may be identifiable from the other polysomnographic signals such as the pulse transit time (PTT) or heart rate, hence it is worthwhile to closely monitor other signals included in the PSG in a suspected arousal event.

i. *Definition and importance of Arousals*

An arousal is defined as a transient intrusion of wakefulness into sleep. If wakefulness lasts for more than 15 seconds or behavioural components such as crying of eye opening are seen, then the term arousal should be replaced with awakening [21]. A more practical definition of arousal (often referred to as an EEG arousal or cortical arousal) is given by the American Academy of sleep medicine (AASM). EEG arousal is an abrupt shift in frequency towards higher frequencies, theta, alpha or beta but not spindles. The definition is valid if at least 10 seconds of sleep is observed before scoring an arousal [18, 21]. There are 3 types of arousals:

Spontaneous arousal:

Spontaneous arousals are present in the normal structure of sleep. It is believed that they do not disturb the natural process of sleep as they are spontaneous and not caused by an external stimulus [21].

Respiratory related arousals:

Respiratory related arousals occur immediately after a respiratory event such as an obstructive apnoea or hypopnoea. These arousals are both protective and harmful. they are protective when apnoeic events occur by minimising exposure to hypoxia but harmful when they happen too frequently and result in sleep fragmentation which may cause daytime symptoms such as sleepiness and behavioural deficits [21]. In children and infants, since arousal threshold is higher, respiratory related arousals are less frequent and hence they are less likely to suffer from fragmented sleep [4].

Non-respiratory related arousals:

Arousals which are due to environmental stimuli are referred to as non-respiratory arousals as they are neither respiratory related nor spontaneous.

2.4.3 Influence of SDB on the Autonomic Nervous System (ANS)

This section aims at briefly describing some of the potential deficits which are thought to arise from the influence of SDBs on the autonomic nervous system (ANS) such as various cardiovascular abnormalities including heart failure, elevated blood pressure, ischaemic heart disease, etc. It will also briefly mention why SDB can play a very important role in long term development of such problems.

i. *Brief introduction to Autonomic Nervous System (ANS)*

The ANS is part of the human nervous system which works without conscious control. It governs glands, cardiac muscle, and smooth muscles (i.e. muscles with no voluntary control) such as those of the digestive system, respiratory system, and the skin. The ANS is traditionally divided into the two subsystems, the sympathetic nervous system (SNS) and the parasympathetic nervous system (PNS) [30]. The SNS is the branch of the ANS which is generally activated to prepare organs for facing a threatening situation. This response has also been loosely referred to as a “fight or flight” response. Physiological alterations observed in these situations can be summarised as:

- Increased Heart Rate (HR)
- Increased Blood Pressure (BP)
- Redirection of blood flow to skeletal muscles from other organs such as skin or spleen
- Pupillary dilation and bronchiolar airway dilation
- Mobilization of energy stored in fat cells

It can be intuitively seen that the above changes are advantageous in a threat like situation.

The PNS on the other hand, is mainly responsible for restorative functions and it normally activates when an organ is at rest. This process has been loosely referred to as "rest and digest" response. Physiological changes upon activation of PNS can be summarised as follows:

- Reduction in cardiovascular activity (reduced HR and BP)
- Facilitation of digestion
- Absorption of nutrients and excretion of waste materials

Heart rate regulation through the vagus nerve is probably the most significant function of the PNS as it can increase the heart rate in situations which require high vigilance without a need for SNS activation. This is achieved by simply switching off the inhibition of the Ventral Vagal Complex located in nucleus ambiguus.

Having control over cardiac and smooth muscles, ANS is responsible for regulating parameters such as blood pressure, arterial wall stiffness and respiratory sinus arrhythmia (respiratory induced heart rate variability).

ii. *Consequences of SDB on Autonomic Nervous System*

SDB has been associated with ANS dysfunctions in adults. For instance, it is well documented in the literature that arousals in sleep activate the SNS with a resulting pressor response (i.e. rise in blood pressure) [31]. Furthermore OSA in adults is associated with cardiovascular abnormalities such as hypertension, ischaemic heart disease, arrhythmia and heart failure [32]. O'Brien and Gozal studied such associations in children. They reported that SDB in young children is associated with persistent waking associated autonomic nervous system dysfunction [31, 33]. Although it had been previously shown by Baharav *et al.* [34] that children with OSA have enhanced sympathetic activity, the study was not based on direct measurements such as pulse arterial tonometry (used by O'Brien and Gozal) but based on spectral analysis of the heart rate signal. Importantly in children the development of the human nervous system (SNS in particular) does not terminate at birth but continues throughout the life. This suggests that SDB in young children could have the potential to manifest as a cardiovascular disease years later.

Note that analogous to the SNS, maturation of the brain in response to stimulation (sometimes termed neuroplasticity) also continues in the postnatal life. This maturation process characterized by remodelling of the brain via using/disusing a particular neural networks, apoptosis (or programmed cell death), dendritic arborisation, myelination, etc. can also be affected by sleep and SDB [35]. Therefore, it is apparent that sleep disorders in children can adversely affect both the ANS and the CNS (central nervous system) and give rise to developmental deficits.

It is clear from the argument above that early diagnosis of OSA (or in general SDB) is of essence and should be given extra attention to.

2.4.4 Potential predictors of SDB outcomes

As was mentioned above, frequent arousals from sleep may have deleterious effects on quality of sleep. In children this is of particular importance as sleep fragmentation may cause long term developmental deficits. Therefore, even though infants and children have fewer cortical arousals [4] there may be sub-cortical arousals present in the sleep and this may cause health issues similar to that of sleep fragmentation. Hence, there is a need to detect such harmful events and identify their originating sources.

As was previously discussed, SDBs have potentially morbid consequences. Some of the known consequences or outcomes are thought to be predictable using certain analytical techniques. Respiratory cycle related EEG changes (RCREC) is for instance, a derived parameter from PSG which is capable of predicting next day sleepiness in adults [16]. Cyclic alternating pattern (CAP) is another polysomnographic feature which can be used to improve the correlation between PSG parameters and day time consequences. CAP can be interpreted as a measure of sleep instability. Arousals from sleep are the main driver of sleep instability. Unstable sleep is caused by frequent arousals and can result in sleep fragmentation (CAP) [18]. These two parameters essentially define two distinct ways of interpreting the same signal or in other words looking at different features of the same signal. The above two parameters are briefly introduced below.

i. *Respiratory Cycle Related EEG Changes (RCREC)*

For the first time, in 2003, Chervin *et al.* [15] developed a computerized signal analysis algorithm to observe whether cortical activities change from breath-to-breath cycles. It was later on shown that RCREC could predict next day sleepiness (in adults) [16]. The current hypothesis states that RCREC may be a manifest of short duration but numerous micro arousals [15].

This technique, divides a breath cycle into four segments based on expiratory and inspiratory peaks and their middle points. Figure 19 shows a typical example of this segmentation (taken from [15]). As can be seen the respiratory cycle is divided into four segments, namely, early expiration, late expiration, early inspiration and late inspiration respectively.

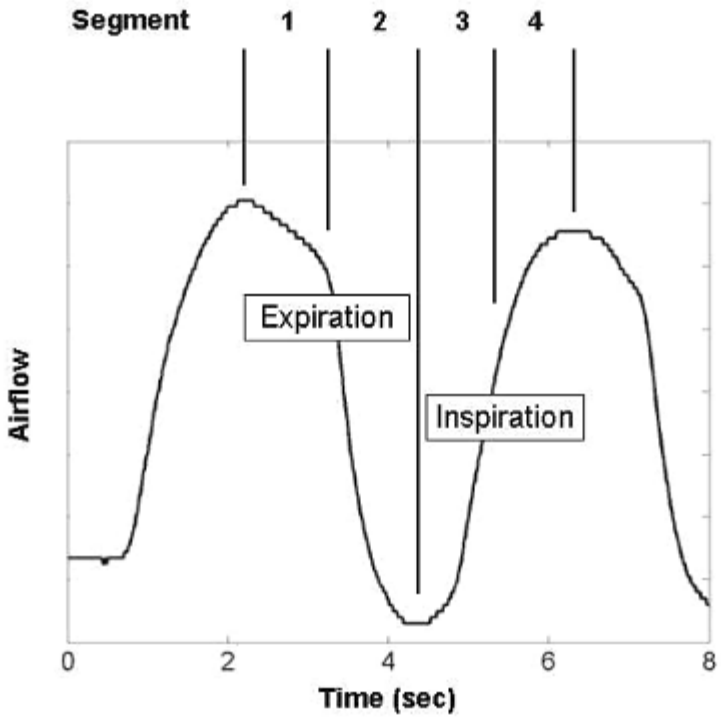

Figure 19. Segmentation of a respiratory cycle in RCREC algorithm. Note that the segmentation is performed by calculating the peak points and then the middle points, i.e. the points placed in the middle of two consecutive local peaks [15].

The aim is to calculate the EEG power in each segment (e.g. EEG power in early inspiration portion) and divide it by the total EEG power of the respiratory cycle to obtain relative powers. In the original work, EEG power was calculated using Short Time Fourier Transform (STFT) with a one second sliding window. The signal processing methods mentioned here as well as the method for quantification of RCREC will be addressed more thoroughly in the subsequent chapters.

Average change of relative EEG power from one respiratory cycle segment to another was then used as the predictive parameter. For instance RCREC in the sigma (13-15 Hz) band has been shown to predict next day sleepiness as measured by multiple sleep latency tests.

ii. *Cyclic Alternating Pattern (CAP)*

CAP is another sleep analysis parameter which uses the polysomnographic data and looks at patterns which can be associated with sleep instability. Frequent arousals for instance can be interpreted as a form of sleep instability as they distort the natural process of sleep. It is speculated that some types of CAP sequences may be associated with brain attempts to preserve sleep by blocking arousals [18].

CAPs are defined as periodic EEG activities in Non-REM sleep which are distinct from the background activities and recur at least, every 1 minute, they consist of an A-phase followed by a B-phase each lasting 2 to 60 seconds. An A-phase could be any of the wave forms introduced in 2.3.1 and a B-phase is just the background activity which separates two A-phase components. Figure 20 shows a good example of a CAP sequence (taken from [18]).

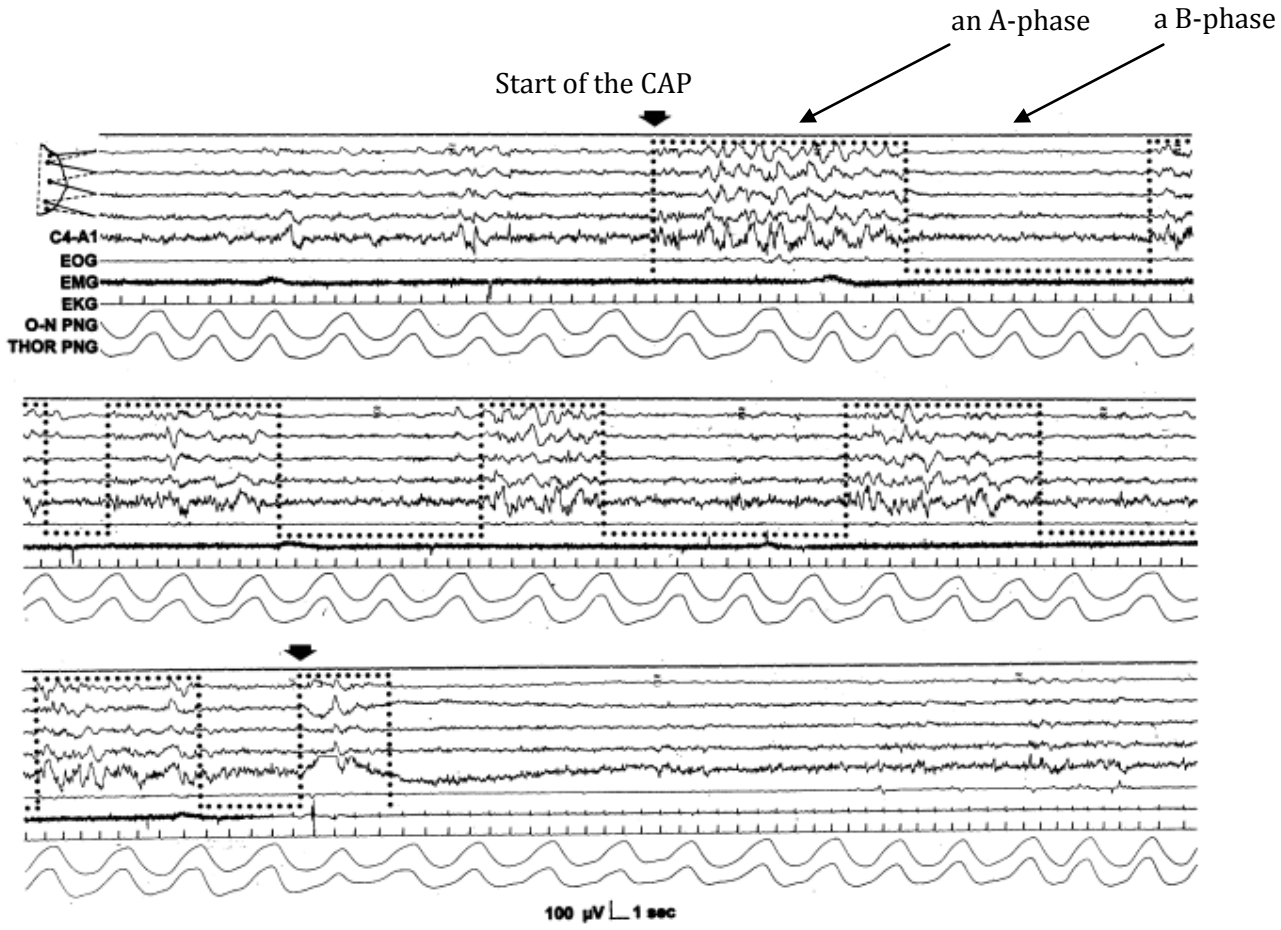

Figure 20. A typical CAP sequence is shown between the two black arrows. As can be seen, the final A-phase is not followed by a B-phase and another A-phase and hence the black arrow shows the end of the sequence [18].

An A-phase is divided into three categories based on the synchrony level of EEG wave forms. In A1, de-synchrony of neurons firing is less than 20% (slow wave) and hence A1 can be easier to

score as it contains high amplitude, slow wave activity which are distinct from the background. In A2, de-synchrony is greater than 20% but less than 50% and finally in A3, de-synchrony is higher than 50% making scoring more difficult [18]. Figure 21 shows an example of the three A-phases (taken from [18]).

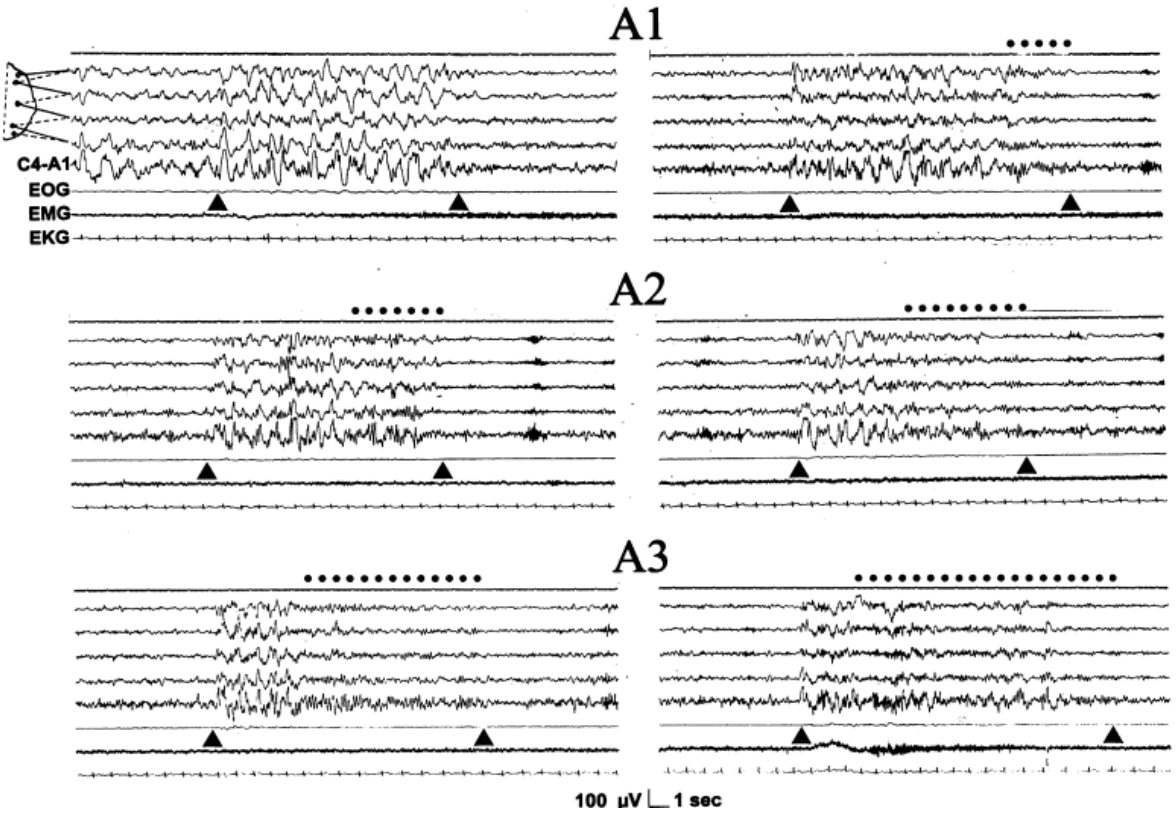

Figure 21. Sub-types of A-phase. A-phases are shown between the black arrows. Black dots show the extent of de-synchrony and as can be seen, de-synchrony in A3>A2>A1 [18].

A recent study by Kheirandish-Gozal *et al.* [28] suggests that children with SDB have reduced CAP rate and also reduced CAP entropy, this may suggest non-restorative sleep in these children. It has also been suggested that CAP may correlate better with certain outcomes of SDB than the conventional parameters however.

2.5 Data

Data is an important part of every biomedical research and as such needs to be described in details; therefore, this section is dedicated to the data that has been used during the course of this project. In particular, two sources of data were made available to us, the first was through the Wellcome Trust Clinical Research Facility (WTCRF) in the Southampton General Hospital and the second was the data gathered by Dr. Catherine Hill's group when studying the chronic effects of altitude on sleep architecture of Bolivian children (henceforth will be referred to as the Bolivian data). Each data set is described below in details.

2.5.1 Wellcome Trust Clinical Research Facility (WTCRF) data

The WTCRF within Southampton General Hospital (SGH) is an established centre for biomedical research. Research conducted in the centre ranges from cancer related research to nutritional care to sleep and respiratory related researches. The WTCRF also benefits from a fully equipped paediatric research section which includes a sleep laboratory and offers full night PSG and bronchoscopy services. Full night PSGs of paediatric subjects generated in the WTCRF were the only data available at the early stages of the project. Data acquisition procedure, data acquisition software/hardware, signals obtained, equipments used and PSG scoring are expanded on below.

i. ***WTCRF data acquisition procedure***

Children suspected with OSA accompanied with parent(s) with prior appointment for a full night sleep test show up in the WTCRF sleep laboratory between 6:00 to 8:00 PM and are greeted by the friendly staff of WTCRF, they are then guided to their room (prepared in advance for the sleep test). It is not uncommon for parent(s) to stay with their child throughout the night and therefore additional beds are provided when needed. An experienced sleep technician will then prepare the subject for the PSG. This generally involves attaching the appropriate electrodes to the appropriate parts of the body of the subject and has to be done with care as the quality of the later obtained data will directly depend on the electrode attachment, this process is fully non-invasive. Data collection starts shortly after; the subject and the real-time signals will be monitored throughout the night by the sleep technician to first ensure the safe progression of the test and second, to avoid losing signals due to excessive movement of the subject. If a signal happens to be lost duo to movement, the technician will re-attach the corresponding electrode and resume the sleep test. Once the test finishes (i.e. when the child wakes up in morning) the data is stored and readied for subsequent scoring. Note that since the

WTCRF data is collected on an ongoing basis and occasionally includes non-OSA patients (e.g. cystic fibrosis patients), selection of any population for further analysis will depend on the analysis to be done and therefore, providing demographic information is avoided here. For the purpose of RCREC analysis however, demographics are be given in the subsequent chapters.

ii. *Data acquisition software/hardware*

WTCRF data is obtained using Alice 5 diagnostic sleep system (Respironics, Philips). Alice 5 includes both the hardware and the software necessary to acquire a full night polysomnographs. The hardware includes a PC like base station and a head-box. The head-box serves as the interface between the base station and the electrodes connected to a subject. The base station includes the necessary electronics to receive, slightly process (analogue to digital conversion) and store the data. Further information about the Alice system can be found on their website[1].

iii. *Signals and equipments*

As mentioned, the data from WTCRF is collected on an ongoing basis and therefore, minor inconsistencies between the instruments used and the signals obtained are not uncommon. However, in general, the following signals are present in the WTCRF data:

EEG: Four EEG channels (C3/M2, C4/M1, O1/M2 and O2/M1) with electrode placement according to the international 10-20 system [12] commonly exist in the WTCRF data. In some cases these four channels are complemented with another four (Fz/M2, Pz/M1, T3/M2 and T4/M1). The letter "M" indicates a mastoid reference. EEG signals in the WTCRF are acquired using standard electrodes, sampled at 100 Hz and quantised using a 10 bit Analogue to digital convertor.

ECG: A single channel of ECG is commonly present in the WTCRF data. ECG signal is acquired using standard ECG electrodes, is sampled at 200 Hz and quantised using a 12 bit A to D convertor. A standard three lead placement system is commonly used in WTCRF to acquire ECG signals.

EOG: Two EOG channels marked as LEOG and REOG (left and right EOG) are present in the WTCRF data. The EOG signals are sampled at 100 Hz and quantised using an 8 but A to D convertor.

[1] http://www.healthcare.philips.com/main/homehealth/sleep/alice5/default.wpd

EMG: Three EMG channels (submentalis chin, right leg and left leg) are commonly included in the WTCRF data. The EMG signals are acquired using standard EMG electrodes and are sampled at 200 Hz and quantised with an 8 bit A to D convertor.

Flow: A single channel of flow signal is present in most WTCRF data. This flow signal is either measured using a nasal pressure transducer cannula or a nasal thermistor. Pressure transducer based flow measurement instruments are more responsive to changes in the nasal flow but less bearable for most children, therefore, it is not uncommon for the flow signal to disappear (subject removing the sensor) and re-appear (technician re-installing the sensor or replacing it with a flow thermistor). Flow signal in the WTCRF is sampled at 10 Hz and quantised using a 16 bit A to D convertor.

Thoracic and abdominal excursions: Thoracic and abdominal excursion are acquired using piezoelectric belts in the WTCRF data. Similar to the flow signal, the excursions are sampled at 10 Hz and quantised using a 16 bit A to D convertor.

Blood oxygen saturation: Oxyhaemoglobin saturation in blood measured using a pulse oximeter is also included in the WTCRF data. This data is sampled at 1 Hz and quantised using a 10 bit A to D convertor.

Plethysmograph: A single channel of plethysmography (marked as pleth) is often present in the WTCRF data. This signal is sampled at 100 Hz and quantised with 10 bits.

Secondary parameters such as RR interval (time interval between two successive ECG-R peaks) and pulse transit time (PTT) which can be calculated from the above signals are also included in the WTCRF data.

iv. *WTCRF Polysomnography scoring*

Following a successful data acquisition, each PSG is scored by an expert sleep technician based on the AASM criteria on paediatric sleep staging and sleep scoring. These criteria are discussed in the previous sections are therefore not repeated here.

2.5.2 Bolivian data

As part of a larger study (Development and Sleep at Altitude - DeSAt) investigating the effects of altitude on sleep disordered breathing and neurocognitive performance, 62 children and adolescents from Santa Cruz, 500 m above sea-level (n_L=33) and La Paz, 3700m above sea-level

(n_H=29), Bolivia underwent a single night of attended polysomnography and completed a series of neurocognitive measurement tests. Subjects were aged from 7 to 17.15 years, (35M:27F), had been born at term, had no chronic health conditions and had been born and lived at their respective altitudes for at least five years prior to participation. The study was approved by the institutional ethics committees of the University of Western Australia and the Universidad Privada de Santa Cruz de la Sierra, Bolivia.

i. ***Bolivian data, acquisition procedure***

Recruited children showed up in the place of experiment with their parent(s) between 6:00 to 9:00 PM. Having completed a set of neurocognitive measurement tests, each subject was prepared for polysomnography (similar to the WTCRF data). Attended polysomnography was carried out in an established sleep laboratory setting (Santa Cruz) and temporary adapted facility (La Paz) using computerised ambulatory systems (Compumedics PS2 system, Melbourne, Australia) according to accepted guidelines [36]. All studies were performed by an experienced polysomnographic technologist.

ii. ***Bolivian data acquisition software/hardware***

Software and hardware for the experiments were provided by Compumedics Ltd. ProFusion PSG 2 software was used to extract the raw data (stored as EDF files). Further information regarding compumedics sleep solutions can be found on their website[2]. Biosig toolbox for Octave and Matlab version 2.49 was used to import the EDF files into Matlab.

iii. ***Signals and equipments***

Although the equipments used at high altitude were part of an ambulatory system, the signals obtained from all PSGs are identical. All PSGs include the following signals:

EEG: Two channels of EEG (C3/A2 and C4/A1) are available in the Bolivian data. Standard EEG electrodes have been used in the data acquisition. EEG signals are sampled at 256 Hz using an 8 bit A to D convertor. Generally speaking, quality of the EEG signals in the Bolivian data is higher than those from the WTCRF data.

[2] http://www.compumedics.com/products.asp?p=39

ECG: A single ECG channel accompanies the Bolivian data. The ECG signal is acquired using a standard three lead placement and is sampled at 64 Hz using an 8 bit A to D convertor. The sampling rate of the ECG signal is rather low, but most ECG related analyses can get away by interpolating the signal. Sampling rate of 200 Hz or above is usually recommended for ECG data acquisition.

EOG: Two EOG channels are present in the Bolivian data (marked as EOG/L and EOG/R). The EOG signals are sampled at 128 Hz with an 8 bit A to D convertor.

EMG: A single EMG channel is present in the Bolivian data. The EMG signal is sampled at 128 Hz with an 8 bit A to D convertor. There are also two leg movement indicators (LEG/L and LEG/R) which record (crudely) if there was a leg movement. The later two signals are sampled at 32 Hz and quantised using an 8 bit A to D convertor (the sampling rate is not nearly enough for accurate recording of leg muscle EMG).

Flow: A single flow channel (nasal thermistor) is provided in the Bolivian data. The flow signal is sampled at 16 Hz using an 8 bit A to D convertor.

Thoracic and abdominal excursions: Two separate signals are provided for thoracic and abdominal excursion (Thor and Abdo). Both signals are acquired using RIP (respiratory inductance plethysmography) bands, sampled at 16 Hz using and quantised with an 8 bit A to D convertor.

Sound: sound is also recorded for potential detection of snoring. The sound data is sampled at 16 Hz using a 6 bit A to D convertor. This is not to be confused with an audio signal as the sampling and quantisation rates are far too low for a meaningful audio. It can instead be thought of as a simple indicator for audible snoring.

Blood oxygen saturation: A single SaO_2 channel indicating the saturation of oxyhaemoglobin in blood is present in the Bolivian data. SaO_2 signal is sampled at 1 Hz.

Similar to the WTCRF data, secondary parameters such as pulse rate are also present in the Bolivian data. Lack of a plethysmograph however, means that no PTT measure can be provided.

iv. *Bolivian data scoring*

Polysomnographs were scored based on the established sleep staging [13] and respiratory [37] criteria for paediatrics and all studies were peer reviewed. Obstructive apnoea was defined as

chest or abdominal wall movement in the absence or decrease of airflow by > 90% of the preceding breath for two or more breaths. Hypopnoeas were classified as for apnoeas but where the reduction in flow was 50-90% of the previous breath and only if accompanied by either oxyhaemoglobin (SpO2) desaturation ≥ 3% or arousal within 2 breaths of event termination. Central apnoeas were scored if there was a reduction in airflow amplitude by >90%, in the absence of respiratory effort, and if they were associated with either an arousal, an awakening or a >3% oxyhaemoglobin desaturation. The Apnoea-Hypopnoea Index (AHI) was defined as the number of obstructive apnoeas, hypopnoeas and mixed apnoeas per hour of total sleep time.

2.6 Summary

This chapter was dedicated to sleep, sleep disordered breathing and sleep data. Sleep was initially defined as a reversible state of perceptual disengagement however, it was pointed out the more recent theories on sleep suggest that sleep should no longer be looked at as an event occurring at a whole organism level but it may be a property of brain's neuronal assemblies [7]. Quantification of sleep (sleep evaluation) was discussed, polysomnography was introduced and criteria for sleep staging and scoring were described. Sleep disordered breathing was then touched upon and in particular OSA (obstructive sleep apnoea), its definition, its polysomnographic traits and its morbid effects on daytime neurocognitive functions were explained. Two potential predictors of SDB outcomes, namely, RCREC and the CAP sequences were also introduced. Last but not least, the polysomnographic data sets used in the project were described in details. The next chapter is dedicated to RCREC introduction and its quantification.

Chapter 3

RCREC

3.1 Introduction to RCREC

In the previous chapter, the concept behind Respiratory Cycles Related EEG Change (RCREC) was briefly introduced [15]. RCREC is a phenomenon characterised by a statistically significant change in relative EEG power during different stages of respiration. It was first reported by Chervin *et al.* [15] in 2003 when investigating whether individual non-apnoeic respiratory cycles in children with sleep disordered breathing (SDB) are associated with brief changes in cortical activity. In their first study on a single child with sleep disordered breathing, quantifiable differences in delta, theta and sigma power between different stages of the respiratory cycle (early expiration, late expiration, early inspiration and late inspiration) were observed. Interestingly, these differences demonstrated change following adenotonsillectomy leading the authors to hypothesise that RCREC may represent brief microarousals and could offer a more sensitive measure of sleep disruption than standard EEG arousal scoring. This hypothesis was later strengthened when they found evidence suggesting that micro arousals may get more intense with increased breathing effort [38]. In a second study they further tested this theory in nine paediatric subjects before, and a year after, adenotonsillectomy [1]. While this was a small sample and only five of the children had obstructive sleep apnoea, RCREC changes, but not changes in apnoea/hypopnoea indices (AHIs), predicted changes in Multiple Sleep Latency tests (MSLT) across the time points. It was also noted that RCREC existed in both OSA patients and controls. More extensive studies in adult patients supported these data indicating that RCERC can predict objective sleepiness measured by MSLT in adults [16]. The relationship between RCREC parameters and neurobehavioral measures associated with OSA is also noted in the patent describing the system and the algorithm for RCREC quantification. In short, it is reported that RCREC parameters are more likely to be correlated with neurobehavioral measures such as IQ, children's memory scale (CMS) attention/concentration score, and Wechsler individual achievement test (WIAT)-mathematical reasoning score than are conventional polysomnographic variables such as AHI, EEG arousal index or minimum oxygen saturation [39]. RCREC is therefore a promising parameter which can help to predict neurobehavioral outcomes of SDB in paediatrics and adults and as such it is of significant

clinical importance. The physiology driving RCREC is not yet fully understood however, the working hypothesis is that it represents numerous subtle inspiratory related microarousals [40, 41]. The method for calculation of RCREC as detailed in [15] is described below.

3.1.1 Method for calculation of RCREC in the literature

The method for calculation of RCREC can be divided into two parts, first is the detection and segmentation of the airflow signal into the four respiratory cycle segments (see Figure 19), and second, is the calculation of the frequency band specific relative EEG power for each respiratory cycle segment. Description for each part follows.

i. ***Respiratory cycle detection/segmentation***

The first three hours of sleep is selected for the analysis in the original work. This is justified by stating that the first three hours of sleep is more likely to have long streams of slow wave sleep. Respiratory cycles below the 5^{th} or the above the 95^{th} percentile in amplitude and duration were removed to ensure regular respiratory cycle detection. For clipped peaks, the mid point was used as an estimate of where the true peak lies. Chervin then suffices to stating that a computerised algorithm divided each respiratory cycle into four segments based on inspratory and expiratory peaks/troughs and their mid points. No further detail about the respiratory cycle detection/segmentation algorithm and its performance is provided. A new respiratory cycle detection/segmentation algorithm is hence developed here which will be discussed further in the subsequent sections.

ii. ***Relative EEG power calculation in a single respiratory cycle***

Upon successful detection and segmentation of respiratory cycles, relative EEG power in each of the conventional frequency bands (1-4 Hz delta, 5- 7 Hz theta, 8- 12 Hz alpha, 13- 15 Hz sigma and 16- 30 Hz beta) and in each respiratory cycle segment is calculated. This is done by first band-pass filtering the EEG signal into the conventional bands and then dividing the frequency band specific EEG power corresponding to each respiratory cycle segment by the frequency band specific EEG power corresponding to the entire respiratory cycle. Note that only one EEG channel (C3/A2) is used in the original study. Short time Fourier transform (STFT) with one second windows (Hanning weighted and detrended) and 98% overlap was used to calculate the filtered EEG power. The formula below clarifies the above mathematically.

$$C_i = \frac{\frac{1}{T_i}\int_F\int_{T_i}|S(f,t)|^2 dfdt}{\frac{1}{T}\int_F\int_T|S(f,t)|^2 dfdt} - 1 \quad (1)$$

Where S is the STFT of the signal, F is the frequency band (e.g. delta), T_i is the time duration of the respiratory cycle segment of interest (e.g. early expiration) and T is the time duration of the whole respiratory cycle.

The index C_i reflects the difference between frequency band specific EEG power of a sub-segment and frequency band specific EEG power of the whole respiratory cycle that the sub-segment belongs to. If the two quantities in the numerator and the denominator are almost equal, the ratio approaches unity and C_i approaches zero which means there is no difference between the respiratory cycle average EEG power and respiratory cycle sub-segment average EEG power. If C_i is greater than 1, it implies that the average EEG power of respiratory cycle sub-segment is greater than that of the whole respiratory cycle and if C_i is smaller than 1 the average EEG power of the respiratory cycle is greater than that of the respiratory cycle sub-segment.

In a more recent work, STFT is replaced with simple digital filtering for EEG power calculation as there is really no need to use STFT to calculate EEG power [16](this can be simply done by squaring the EEG signal samples and summing them in the time domain).

3.1.2 Definition of RCREC

Repeating the procedure described above for all the selected respiratory cycles will give an ensemble of frequency band and respiratory cycle segment specific relative EEG powers averaging over which gives what is referred to as mean relative EEG power (MREP) which is also frequency and respiratory cycle segment specific. RCREC in each frequency band is then defined as the maximum MREP in that frequency band minus the minimum MREP in that frequency band. Figure 22 shows an example of how RCREC (magnitude) is calculated from MREPs. As can be seen RCREC is a range parameter measuring how EEG power varies between respiratory cycle segments. MREPs have been shown to be statistically significantly different between respiratory cycle segments in most subjects and this difference was actually the spark which brought about RCREC as a measure of neurocognition.

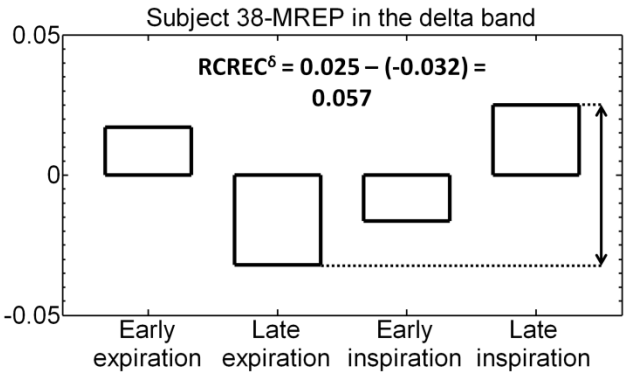

Figure 22. An example showing how RCREC magnitude is calculated from MREPs

The next section elaborates on how RCREC is quantified.

3.2 Quantification of RCREC

In order to understand RCREC, there must be a means to quantify it. This section is therefore dedicated to details on quantification of RCREC. The algorithm for calculation of RCREC although explained in the original work is not fully reproducible without making a few assumptions on the flow signal segmentation algorithm. It is thus attempted to give a complete algorithm for flow signal segmentation and also validate it. Processing of the EEG signal and statistical methods used in calculation of RCREC are also discussed. First however, the algorithm for calculation of RCREC is explained in a step by step manner.

3.2.1 RCREC quantification: overall algorithm

Although explained in 3.1, it is helpful to give an overall structure to the steps needed to calculate RCREC. The algorithm utilised can be summarised in the following steps:

1) Nasal air flow signal was segmented into individual respiratory cycles using the peaks and the troughs present in the signal.
2) Individual respiratory cycles were divided into 4 sub-segments namely: early expiration, late expiration, early inspiration and late inspiration. This is after removing portions of the data which may have been abnormal; this includes apnoea, hypopnoea or any other respiratory disturbances that cause significant deviation from a normal (semi-sinusoidal) respiratory pattern. Figure 23 shows how the typical segmentation is done.

3) Corresponding EEG powers (C3/A2) in delta, theta, alpha, sigma and beta bands were quantified for each and every respiratory segment. This is done by band-pass filtering the EEG signal to generate frequency band specific EEG (e.g. delta EEG) and then calculating the power of the filtered signal in the time domain. Note that respiratory and EEG signals are time locked.

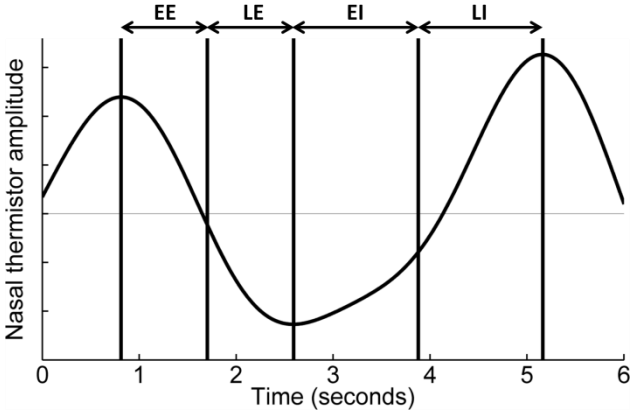

Figure 23. Conventional segmentation of a single respiratory cycle. The thermistor generated flow signal is divided into four segments based on its local maximum, minimum and the mid points. EE stands for early expiration, LE for late expiration, EI for early inspiration and LI for late inspiration.

4) Frequency band specific powers of each sub-segment were normalised (divided by the frequency band specific power of the whole respiratory segment) to generate frequency band and respiratory cycle segment specific relative EEG power. This can be mathematically shown as:

$$S_j^f = \frac{\frac{1}{N_j}\sum_{i=n_j}^{n_j+N_j-1}\left|X_i^f\right|^2}{\frac{1}{N}\sum_{i=n_1}^{n_1+N-1}\left|X_i^f\right|^2} - 1 \qquad (2)$$

Where N_j is the length of the *jth* respiratory cycle segment (*j=1,2,3,4* where 1 corresponds to early expiration, 2 to late expiration, 3 to early inspiration and 4 to late inspiration), N is the length of the respiratory cycle in samples, n_j is the starting sample of the jth respiratory cycle segment, n_1 is the starting sample of the respiratory cycle and X_i^f is the *ith* element in the frequency band specific EEG signal. The parameter S_j^f is the segment and frequency specific relative EEG power. Note that the above formula relates to a single respiratory cycle only.

5) Taking into account all respiratory cycles leads to formation of the frequency band specific matrix Q^f from the calculated S_j^f values:

$$Q^f = \begin{bmatrix} S^f_{1,1} & \cdots & S^f_{1,4} \\ \vdots & \ddots & \vdots \\ S^f_{M,1} & \cdots & S^f_{M,4} \end{bmatrix} \quad (3)$$

Where M is the total number of regular respiratory cycles.

6) The significance of the difference between the four columns of Q^f (i.e. the relative EEG powers in different respiratory cycle segments) is assessed using the one way analysis of variance (ANOVA) test. Fisher's F values are produced as a measure of this significance. Further information about one way ANOVA can be found in [42].

7) Averaging over the columns of Q^f, a frequency band specific RCREC parameter is defined as

$$RCREC^f = \max(\overline{Q^f}) - \min(\overline{Q^f}) \quad (4)$$

Where

$$\overline{Q^f} = \left[\overline{S^f_1}, \overline{S^f_2}, \overline{S^f_3}, \overline{S^f_4} \right] \quad (5)$$

And

$$\overline{S^f_j} = \frac{1}{M} \sum_{i=1}^{M} S^f_{i,j} \quad (6)$$

$\overline{S^f_j}$ is the frequency band and respiratory cycle segment specific mean relative EEG powers (MREP).

All the steps above were implemented using Matlab (Mathworks). The overall algorithm is explained in details in the subsequent sections, details of the airflow segmentation algorithm and the spectral analysis routine are in particular discussed.

3.2.2 RCREC quantification: airflow signal segmentation

The airflow signal – being from a nasal pressure transducer of a thermistor – generally follows a sinusoidal like morphology. Peaks and troughs in the signal indicate the beginning of expiration or beginning of inspiration. In order to segment the airflow signal, peaks and troughs should be

carefully identified. As with all biomedical signals, the airflow signal also suffers from various artefacts such as multichannel interference, movement and displacement of the measuring instrument. These challenges particularly complicate the automatic detection of peaks and troughs when large streams of data are to be analysed.

A simple and fast algorithm is therefore developed which can automatically segment the airflow signal into individual respiratory cycles and exclude the spurious flow data. This algorithm uses a derivative based maxima/minima detector at its core and utilises thresholds (constant and adaptive) to detect abnormalities. It is fast since operations performed on the data are not sequential but global meaning that the data points are not analysed one after another but as a whole, which significantly enhances the execution speed of the algorithm even when analysing long streams of data. The rest of this section illustrates the algorithm in a step by step manner.

Detecting the peaks and troughs:

1. Initial maxima/minima detection: first order derivative of the signal was used to detect all the existing local maxima and minima in the flow signal. Due to existence of artefacts, peaks and troughs of interest are not the only local maxima and minima detected. Figure 24 shows an example of the initial detection; troughs are highlighted with red circles. Note that for presentation purpose, the focus is on detection of the troughs only but the actual detection procedure is almost identical for both the peaks and the troughs.

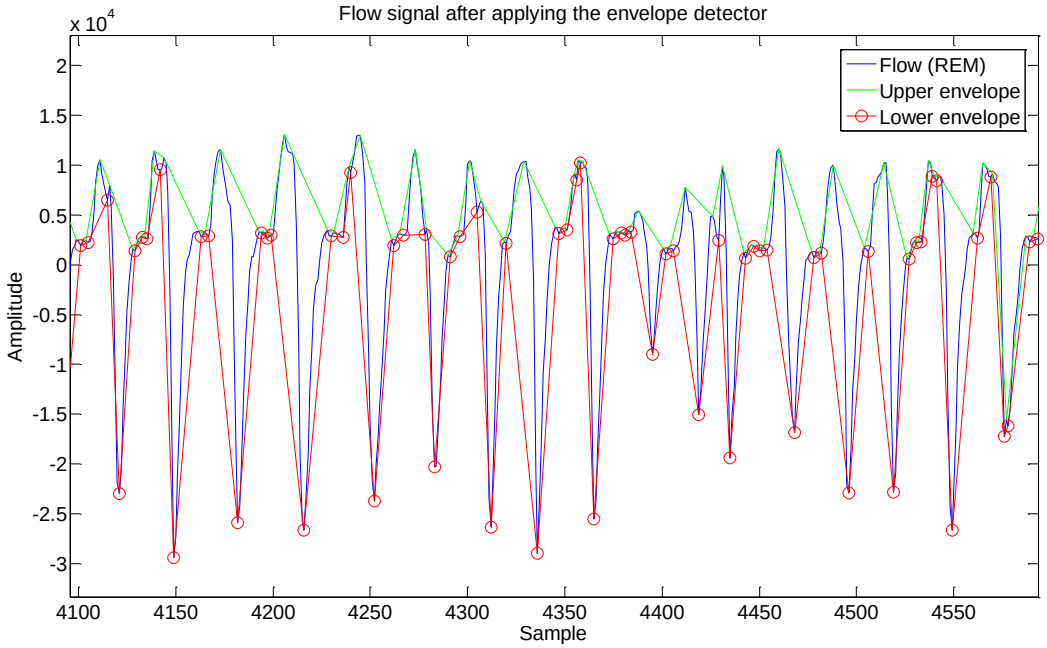

Figure 24. Flow signal after applying the maxima/minima detector. Red circles show the positions of the detected minima. As can be seen, not all the minima correspond to the notches in the flow signal. That is due to small fluctuations in the signal caused by different sources of errors (e.g. high frequency electrical noise or interference), and hence, we must differentiate between the "true minima", i.e. those which correspond to the notches in the flow signal, and "false minima". An amplitude threshold can be applied to remove some of the erroneous minima.

2. Amplitude thresholding: an amplitude threshold was applied to the lower envelope to remove the false minima. This threshold removes troughs with positive amplitude (similarly to detect peaks, there is a threshold which removes peak with negative amplitude). Since airflow signal amplitude can differ from one data set to another, the flow signal is de-trended prior to peak detection. Figure 25 shows the remaining troughs after applying the amplitude threshold.

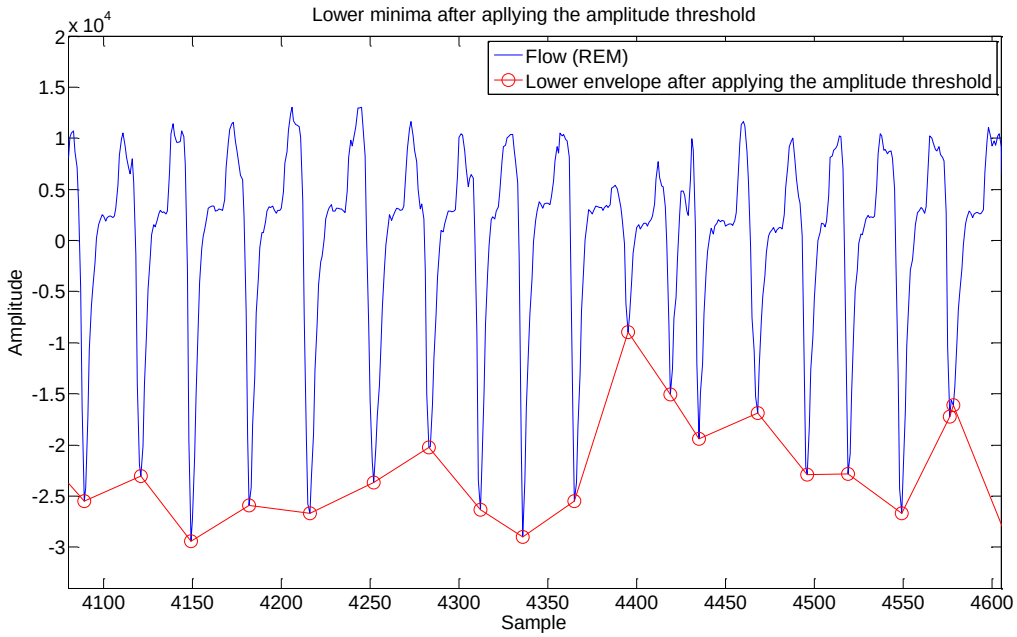

Figure 25. As can be seen most of the false minima are removed. Applying an amplitude threshold is also useful in identifying spurious events in sleep and can be used to remove abnormal data.

3. Duration thresholding: Immediately after applying the amplitude thresholds, a duration threshold was applied to remove samples which are too close to each other (see the two samples between 4550 and 4600 in figure 25) the threshold was set to 1.5 second. Figure 26 shows the typical result after applying the duration threshold.

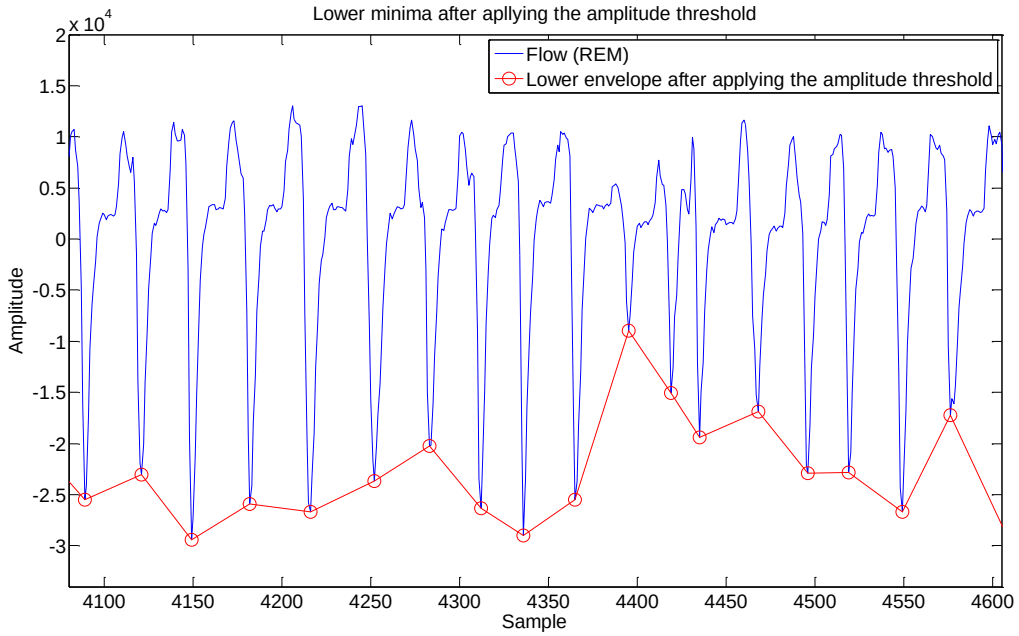

Figure 26. Note that the false minimum between the samples 4550 and 4600 is removed.

4. Abnormal data removal: an additional duration threshold was applied to differentiate between normal and abnormal data parts based on the separation between two consecutive troughs. For instance, if separation of two consecutive troughs is greater than 6 seconds – which is longer than an average breath cycle – it becomes evident that the interval between the two detected troughs contains abnormal data (previously removed by the amplitude threshold or two consecutive troughs with separation of greater than 6 seconds). Figure 27 illustrates how abnormal data is removed using the algorithm.

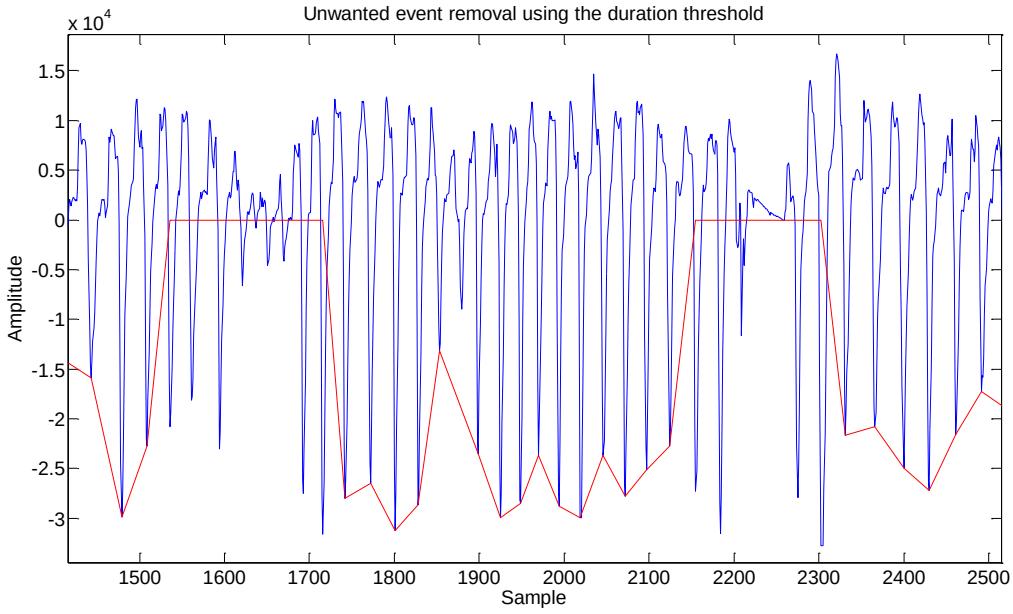

Figure 27. Unwanted values are replaced with "Pi" (a unique number) for presentation purposes. Once the duration between two consecutive samples is greater than the adjusted duration threshold, those samples in addition to their adjacent ones are identified as abnormal and are removed.

The same procedure was carried out to detect the peaks in the flow signal. Union of the excluded (abnormal) regions from both the peak and the trough detection routines was calculated and excluded from further analysis. Note that in case of poor signal quality, the abdominal (or thoracic) excursion signal can be used to either estimate the peak positions in the airflow signal, or replace the flow signal entirely, however, the produced results may be arguable. Figure 28 shows the airflow signal plotted together with the abdominal excursion.

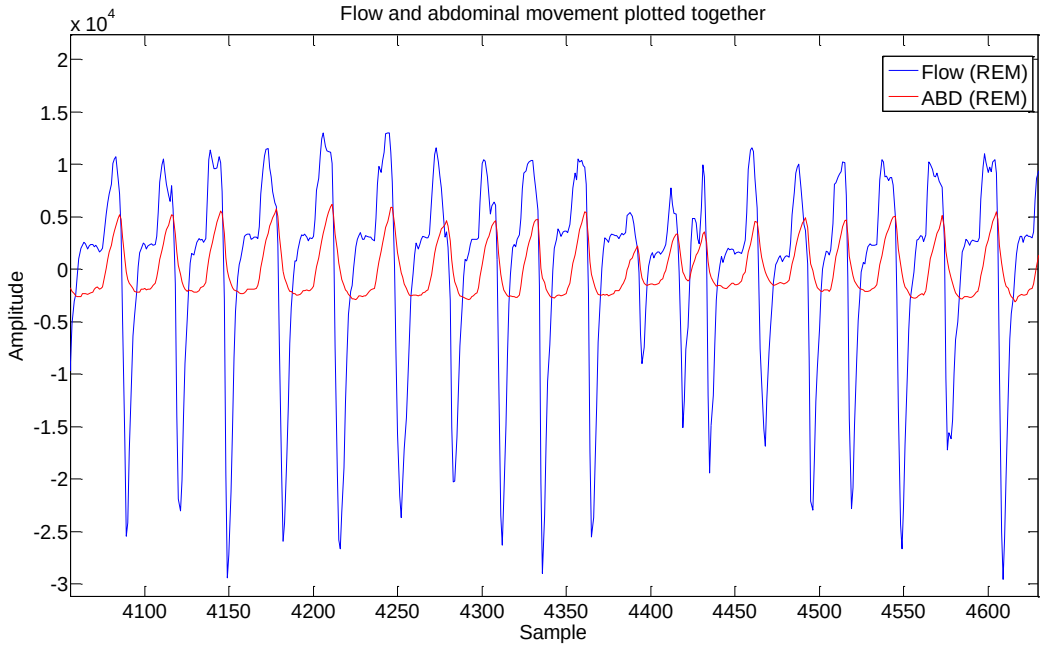

Figure 28. Flow and abdominal movement plotted together.

5. Refinements: Upon detection of abnormal data, four preceding and processing respiratory cycles were rejected to ensure physiologically regular respiratory cycle detection, additionally, a minimum continuous data requirement was added to the algorithm which rejected any streams of data smaller than 12 consecutive respiratory cycles, this will ensure a low false positive detection rate for respiratory cycles which is essential for RCREC quantification. Implementation of a routine which ensures that each respiratory cycle starts with an early expiration (i.e. a local maximum) and calculation of the mid points were the final refinements of the algorithm. Figure 29 shows an example output of the completed algorithm.

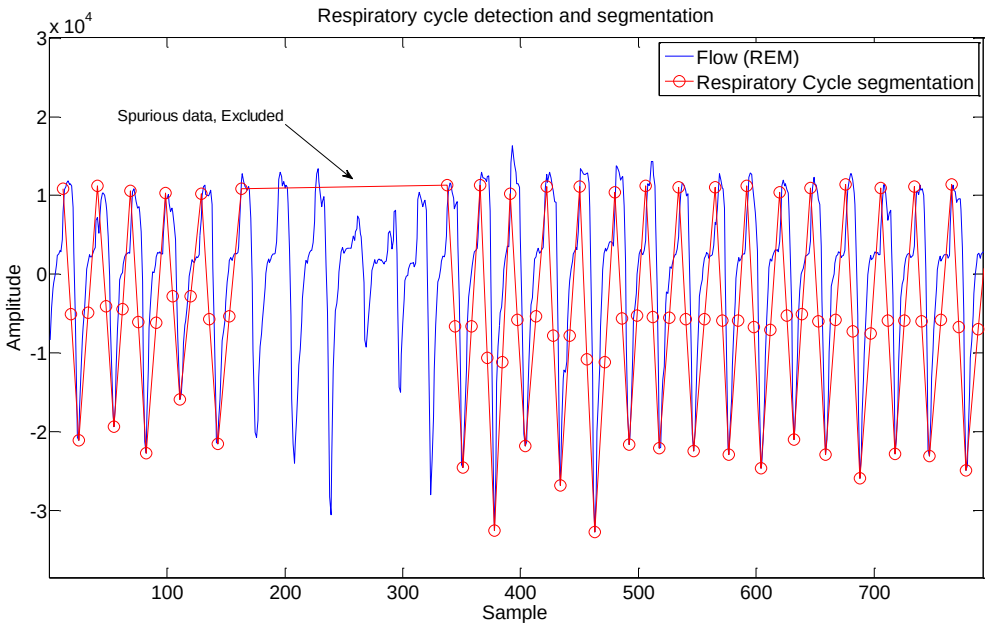

Figure 29. Respiratory cycle detection and segmentation. Starting from the beginning of the graph, the first red circle is the starts of an early expiration and the 5th red circle is the end of the late inspiration of that cycle (or the start of the next early expiration). Due to poor signal quality, abdominal excursion is used for peak position estimation.

The above five steps describe the segmentation algorithm developed for the purpose of RCREC quantification. Note that the flow signal can be low-pass filtered prior to segmentation for smoothing purpose; however, the cut-off frequency should not be set very low. Filtering with a very low cut-off frequency can change the peak and trough positions significantly and may mask the actual physiology of respiration reflected by the airflow signal. Figures 30 and 31 show the output of the algorithm when applied to 3 hours of PSG data. Note that the flow signal is low-pass filtered with cut-off frequency of 0.5 Hz in the subsequent figures (this cut-off frequency although quite low, is chosen to conform to the previous work on the RCREC).

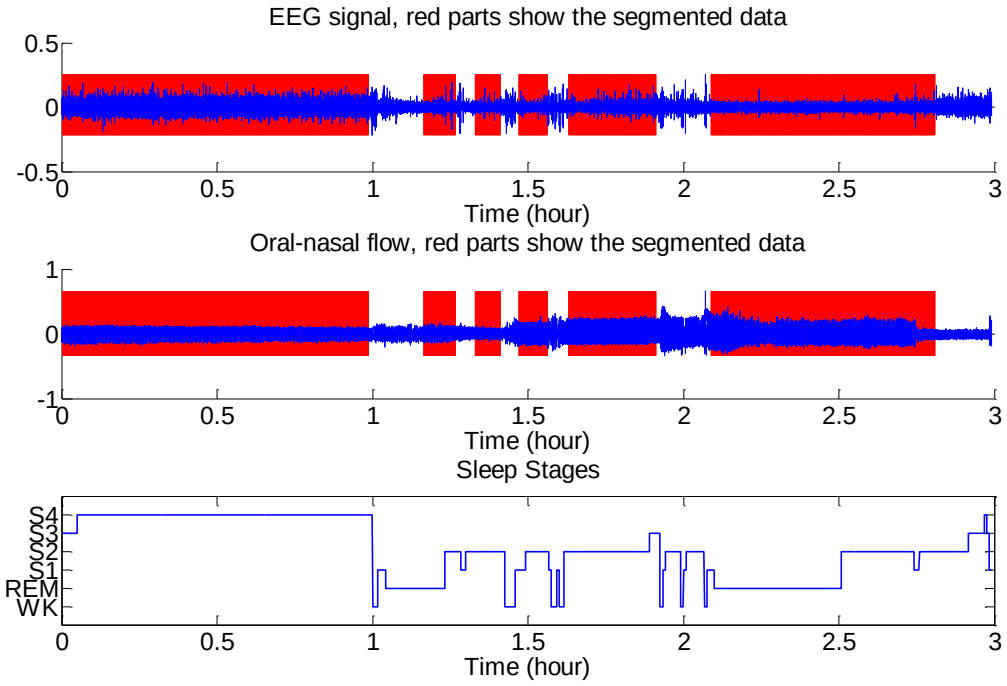

Figure 30. First 3 hours of sleep EEG and Flow signals. Dense vertical red lines show the segmented regions. The rest of the signal is automatically detected as abnormal. Figure 31 shows a zoomed in version of this figure.

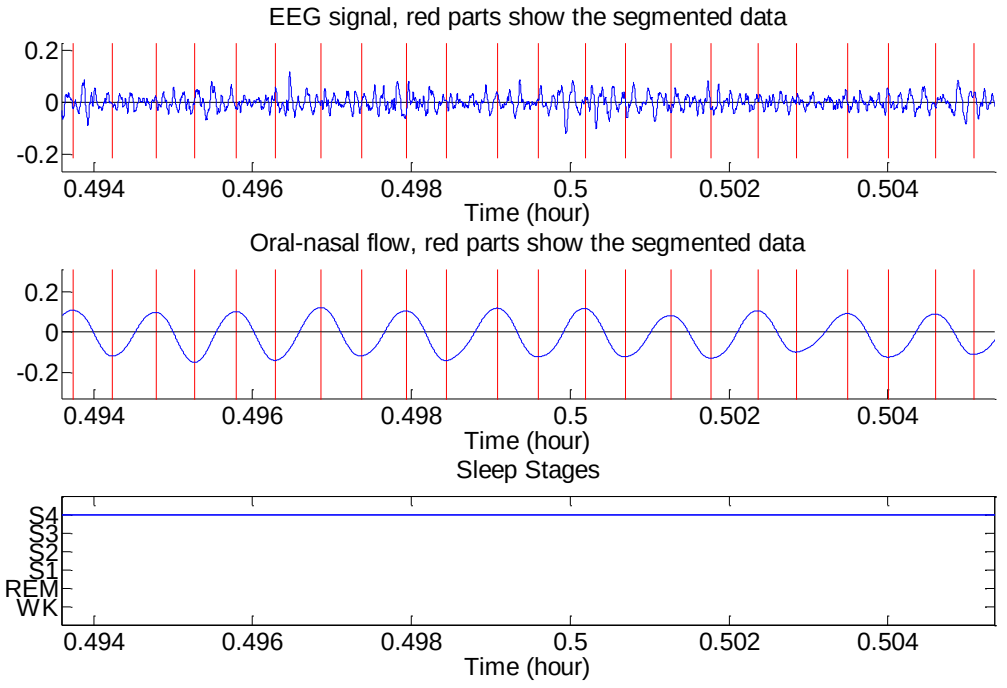

Figure 31. Zoomed in version of figure 30. Maxima and minima are detected and shown by red vertical lines. Note that this graph does not show the mid points.

Finally, several other features such as manual exclusion of data, successive envelope detection for higher reliability and sleep stage specific airflow segmentation (using the scored sleep stage signal) were also added to the algorithm to complement the package. The next section shows the validation procedure for the developed flow segmentation algorithm using a representative sample of the available flow signal.

3.2.3 Airflow segmentation algorithm validation

Now that the development of the algorithm is finished, it is essential to test and quantify its performance. As a result, an algorithm validation procedure was developed to test the capabilities of the algorithm in real life tests. The section below describes this procedure.

i. *Validation procedure*

The Bolivian PSG data was used as the test data for the validation process. Ten random subjects were selected for the analysis (using a uniform random number generator for subject selection). For each subject a continuous stream of 100 respiratory cycles was selected. This selection was also randomised; a uniform random number generator was used to generate a random starting epoch for each subject, 100 respiratory cycles were then counted from the starting epoch. Each stream of 100 respiratory cycles was scored manually for abnormalities, that is, any significant deviation from the background nasal flow signal. Flow signals were low-pass filtered with cut-off frequency at 0.5 Hz.

The developed nasal airflow signal detection/segmentation algorithm was applied to the selected flow data for each subject. In order to quantify the performance of the algorithm, each automatically scored flow signal was compared to its corresponding manually scored flow signal. True positive, false positive, true negative and false negative detection rates were then computed to quantify the performance of the algorithm through sensitivity and specificity figures. Assuming that the manual scoring represents the gold standard, a true positive detection indicates that a regular (normal) respiratory cycle is detected as such. A false positive detection however indicates that an abnormal respiratory cycle is falsely detected as a normal respiratory cycle. A true negative detection shows successful rejection of abnormal respiratory cycles and a false negative detection shows false rejection of a true respiratory cycle. Using the four parameters above one can calculate the sensitivity and specificity of the algorithm. Sensitivity here measures the ability of the algorithm to detect true normal respiratory and specificity measures how well the algorithm rejects abnormal respiratory cycles. Results of the validation follow.

ii. ***Validation results***

Table 1 shows the true positive (TP), false positive (FP), true negative (TN) and false negative (FN) detection rates for the selected subjects. Equations for calculating sensitivity and specificity are given below:

$$Sensitivity = \frac{TP}{TP + FN} \tag{7}$$

$$Specificity = \frac{TN}{TN + FP} \tag{8}$$

Where TP stands for true positive, FN stands for false negative, TN stands for true negative and FP is short for false positive. Table 1 provides the numerical figures corresponding to the performance of the algorithm. Based on the above formulas above and the data in Tabel1, the segmentation algorithm developed here is 92.4% sensitive and 97.4% specific.

Table 1. Nasal airflow signal detection/segmentation algorithm performance

Subject ID	***True positive (TP)***	***False positive (FP)***	***True negative (TN)***	***False negative (FN)***	***Total***
1	*98*	*2*	*0*	*0*	*100*
2	*85*	*0*	*7*	*8*	*100*
3	*94*	*0*	*6*	*0*	*100*
4	*100*	*0*	*0*	*0*	*100*
5	*83*	*0*	*9*	*8*	*100*
6	*84*	*0*	*9*	*7*	*100*
7	*97*	*0*	*0*	*3*	*100*
8	*85*	*0*	*5*	*10*	*100*
9	*70*	*0*	*8*	*22*	*100*
10	*57*	*0*	*31*	*12*	*100*
Total	*853*	*2*	*75*	*70*	*1000*

Sensitivity	$\frac{853}{853+70}=92.4\%$
Specificity	$\frac{75}{75+2}=97.4\%$

iii. ***Validation discussion***

As can be seen, there is a very good agreement (92.3%) between the manually scored flow signal and the automatically scored one. Since the algorithm developed here was designed to be used for polysomnographic RCREC quantification, and RCREC quantification requires regular (normal) airflow signal to be valid, care has been taken to make sure what the algorithm detects as a regular respiratory cycle is in fact a regular respiratory cycle and not an artefact, this is reflected by the very low false positive detection rate in Table 1 (this is at the expense of having a slightly higher false negative detection rate). To conclude, given the sensitivity and specificity figures, it is clear that the developed algorithm for nasal airflow signal detection/segmentation performs well and is particularly well suited to applications where RCREC is to be quantified.

All the Matlab codes and functions for nasal airflow segmentation are available. The next section describes the EEG processing required for RCREC quantification.

3.2.4 RCREC quantification: EEG processing

PSG provides a set of time locked signals and hence by segmenting the respiratory cycles it is possible to directly capture the corresponding EEG segmentation. The next step in quantification of RCREC is to calculate the EEG power for each sub-segment namely: early expiration, late expiration, early inspiration and late inspiration across all the segmented respiratory cycles. This is achieved by filtering the signal into conventional frequency bands (e.g. delta, alpha, etc.) and calculating the power in the time-domain. The EEG signal was notch filtered at 50 Hz with a second order infinite impulse response (iir) filter, then band-pass filtered between 0.4 Hz and 32Hz using a 5^{th} order Butterworth filter and finally de-trended prior to the analysis. Figure 32 clarifies how the procedure is done in practice.

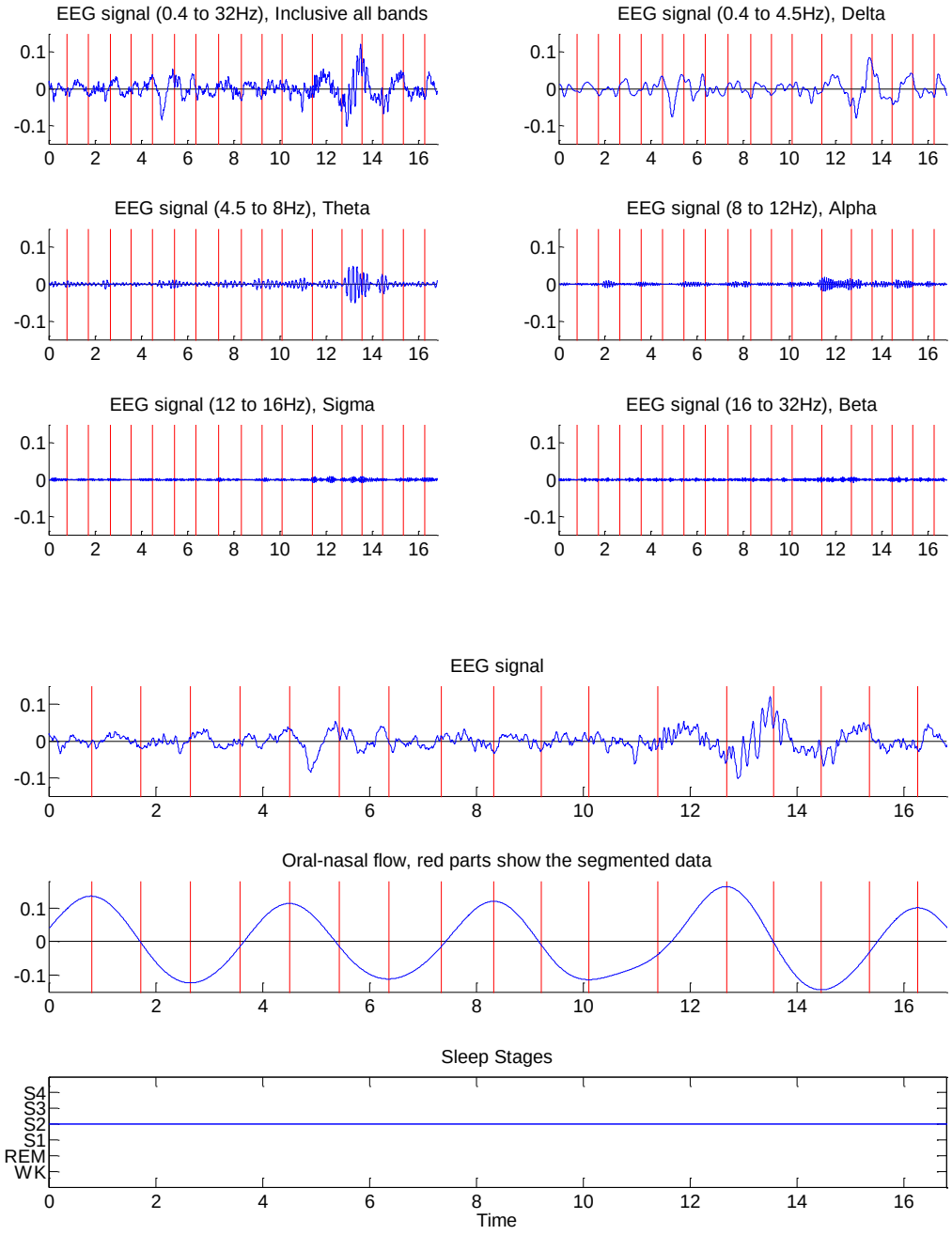

Figure 32. Roughly 16 seconds of EEG data filtered into the conventional frequency bands and segmented into early and late expirations and inspirations.

For each respiratory cycle, EEG power in early expiration was divided by that of the entire respiratory cycle. This was repeated for the other three segments (i.e. late expiration, early inspiration and late inspiration). More formally (as defined in equation two and repeated here for convenience), relative power in each frequency band (e.g. delta) for an individual respiratory cycle was calculated using the following formula:

$$S_j^f = \frac{\frac{1}{N_j}\sum_{i=n_j}^{n_j+L_j-1}\left|X_i^f\right|^2}{\frac{1}{N}\sum_{i=n_1}^{n_1+L-1}\left|X_i^f\right|^2} - 1$$

Where X^f represents the frequency band specific (i.e. filtered) EEG signal, N_j is the length of the *jth* respiratory cycle segment (*j=1,2,3,4* where 1 corresponds to early expiration, 2 to late expiration, 3 to early inspiration and 4 to late inspiration), N is the length of the respiratory cycle in samples, n_j is the starting sample of the jth respiratory cycle segment, n_1 is the starting sample of the respiratory cycle and X_i^f is the *ith* element in the frequency band specific EEG signal.

The parameter S_j^f is the segment and frequency specific relative EEG power (e.g. S_1^δ is the relative EEG power in the delta band and in the early expiration segment). It reflects the difference between frequency band specific EEG power of a segment and frequency band specific EEG power of the whole respiratory cycle. If the two quantities in the numerator and the denominator are almost equal, the ratio approaches unity and S_j^f approaches zero which means there is no difference between the respiratory cycle average EEG power and respiratory cycle segment average EEG power. If S_j^f is greater than zero (positive), it implies that the average EEG power of respiratory cycle segment is greater than that of the whole respiratory cycle and if S_j^f is smaller than zero (negative), the average EEG power of the respiratory cycle is greater than that of the respiratory cycle sub-segment.

Calculating the S_j^f for all respiratory cycles results in formation of the frequency band specific matrix Q^f from the calculated S_j^f values:

$$Q^f = \begin{bmatrix} S_{1,1}^f & \cdots & S_{1,4}^f \\ \vdots & \ddots & \vdots \\ S_{M,1}^f & \cdots & S_{M,4}^f \end{bmatrix}$$

Where M is the total number of regular respiratory cycles (can range from 1000 to 7000 depending on the quality of the data). Averaging across the columns of Q^f gives the segment specific mean relative EEG powers or MREPs for short. Figure 33 shows the distribution of MREPs in the delta band for an arbitrary subject.

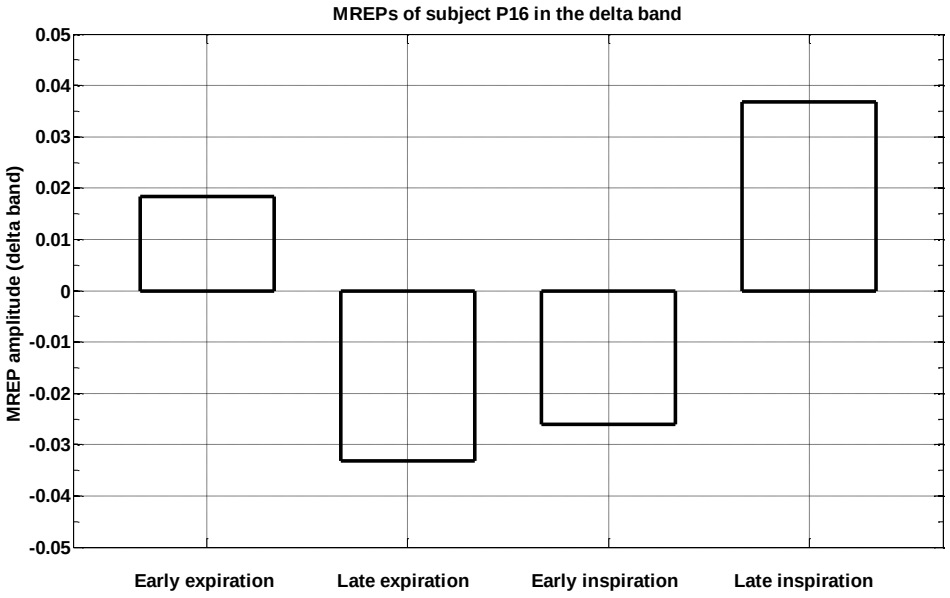

Figure 33. Mean relative EEG power of an arbitrary subject in the delta band. This graph is directly used in calculation of RCREC. In fact, RCREC is the difference between the maximum and the minimum values in the graph above which in this case translates to mean relative EEG power in the late inspiration minus the mean relative EEG power in the late expiraiton. This figure serves as an example only.

Mean relative EEG powers (MREP) are directly used in calculation of RCREC; in fact, frequency band specific RCREC is given as the maximum difference between segment specific MREPs for that frequency (e.g. in the figure above, RCREC is the MREP of late inspiration minus the MREP of late expiration). Note that RCREC magnitude is always positive. MREPs are shown to be statistically significantly different from one another, that is, they are highly unlikely to have emerged from the same statistical population. More information on the statistical tests used to draw such conclusions is given in the subsequent section.

3.2.5 RCREC quantification: statistical analysis

As was mentioned above, what is noteworthy about RCREC is that in majority of subjects, MREPs of the four segments do not come from the same statistical population; what many may intuitively think otherwise. The test used in the original study to highlight this is the one way analysis of variance (ANOVA), however, depending on the analysis, other tests may also be used. This section gives a brief introduction to the statistical tests used in quantification of RCREC. Other statistical tests used throughout the thesis for different analysis purposes are also briefly addressed here.

i. *One way analysis of variance (ANOVA)*

One way analysis of variance is a parametric statistical hypothesis test which determines whether means of two or more groups of observations differ significantly. In its simplest form, it is a generalisation of Student's t-test to more than two groups. One way ANOVA requires the observations to be independent, normally distributed and have the same variance, however, in practice, it has been shown that ANOVA has been particularly robust to violations of the normality assumption [43]. Significance of ANOVA is calculated using the Fisher's F value. Mathematically it is given as:

$$F = \frac{between\ group\ variance}{within\ group\ variance} \tag{9}$$

The F-value can be translated into a P-value based in its numerical value and the degrees of freedom of the numerator and the denominator of equation 9. MANOVA (multivariate ANOVA) is a variant of ANOVA which has been used in Chapter 5. It is essentially, used when there are dependencies between the groups of observations [44]. There are many other variants of ANOVA used in the literature (ANCOVA, ANORVA, etc.) discussing which is outside the scope of this thesis. For further information on ANOVA see [45].

ii. *Kruskal-Wallis test*

Kruskal-Wallis test (sometimes referred to as non-parametric ANOVA or one way ANOVA by ranks) is the non-parametric version of ANOVA test [46]. A non-parametric test may be preferable when the distribution of samples is not normal. Although non-parametric tests in general are less powerful than parametric test, they may be more appropriate if the pre-requisites of the parametric tests are not met. The Kruskal-Wallis test determines if two or more groups of observations with the same distribution shape and scale have the same median. More detailed information on the Kruskal-Wallis test can be found in [46]

iii. *Wilcoxon signed-rank test*

Wilcoxon singed-rank test is a non-parametric paired hypothesis test which determines whether two related groups of observations (e.g. before and after treatment) have the same median. Being a non-parametric test, It however, requires the observations to be independent. The Wilcoxon signed-rank test does not require the populations to be normally distributed. It is

a replacement for paired t-test (or independent sample t-test) when the population cannot e assumed normal.

iv. ***Mann – Whitney – U test***

Mann – Whitney – U test (also known as Wilcoxon rank sum test) is a non-parametric hypothesis test which determines whether two groups of observations come from populations with differing medians. The test requires the groups of observations to be independent. The Mann – Whitney – U test can be used in situations where the number of observations in the two groups is not equal. For more information on the test see [46].

v. ***Shapiro – Wilk test***

Shapiro – Wilk is a test to determine whether a given group of observations come from a normal distribution. The test is simple to compute and can be used for small sample sizes ($n<20$) with considerable sensitivity. Further information regarding the Shapiro – Wilk test can be found in the original paper describing the methodology [47].

vi. ***Lilliefors test***

Lilliefors test is another test of normality, it determines whether a given set of observations (i.e. data, samples) come from a family of normal distribution, that is, mean and variance of the normal distribution need not to be specified.

This concludes the statistical hypothesis tests that have been used in the thesis. The next chapter details the preliminary case studies on RCREC. The statistical analyses in the thesis where done in Matlab and SPSS.

3.3 Summary

This chapter was dedicated to RCRECC, its definition and quantification. The chapter starts by introducing RCREC as described in the literature and follows to include the algorithms which have been developed and used to quantify RCREC. Since the information given in the literature was not sufficient for fully reproducing RCREC studies, this chapter expands on RCREC quantification to provide a step by step description of the airflow signal segmentation algorithm, EEG processing and pre-processing, and finally includes a range of statistical tests which have been used in RCREC quantification.

Chapter 4

Preliminary case studies

The chapters above provide background to sleep, sleep disordered breathing, RCREC and the data used in the course of the project. This chapter provides details on the preliminary investigative works done on polysomnographic RCREC quantification. These preliminary analyses led to more substantial studies which are discussed in Chapter 5.
The case studies here focus on replication of Respiratory Cycle Related EEG Changes (RCREC) in a single paediatric subject and then expand and explore the relationship between RCREC and AHI in a few subjects with an without OSA. Alternative airflow segmentation and its effect on RCREC is also investigated.

4.1 RCREC – replication in one paediatric subject

4.1.1 Introduction

Now that the algorithm for quantification of RCREC is developed and the airflow segmentation algorithm is tested and validated, a complete replication of the original work [15] is attempted. This is to quantify RCREC in a single paediatric subject and compare the results with that of the original work. The procedure and the results follow.

4.1.2 Subject and methods

The methodology follows the approach detailed in the Chapter 3. Quantification of RCREC is attempted in a 4 year old with very mild OSA (apnoea-hypopnoea index of 1.2). The subject is selected from the WTCRF data set. This should be comparable to post-operative data provided by Chervin [15] in the original work. The subject had a standard all-night polysomnography.

4.1.3 Results

Having calculate the RCREC parameters in all the conventional frequency bands it was found that frequency band specific mean relative EEG powers were statistically significantly different

in all the frequency bands. Table 2 shows the results of the analysis done here and that of the original work (post-operative).

Table 2. MREP difference amongst 4 respiratory cycle sub-segments in all frequency bands using ANOVA

	Delta	***Theta***	***Alpha***	***Sigma***	***Beta***
ANOVA P-value	*<0.0001*	*<0.0001*	*<0.0001*	*<0.0001*	*<0.0001*
ANOVA P-value (Chervin [15])	*<0.0001*	*<0.001*	*<0.01*	*<0.01*	*<0.01*

A small P value suggests that the relative EEG powers significantly change between the different stages of respiration. Note that the findings here are very similar to Chervin's in [15] where all frequency bands were statistically significantly different. Since distribution of relative EEG powers were not normal, a non-parametric test hypothesis test was also used to confirm the findings. Although ANOVA is known to be robust to violation of the normality assumption, nevertheless, a non-parametric significance test may be more appropriate. Table 3 shows the results after employing the Kruskal-Wallis test (non-parametric one way ANOVA which employs ranks instead of absolute values).

Table 3. MREP difference amongst 4 respiratory cycle sub-segments in all frequency bands using The Kruskal-Wallis test

	Delta	***Theta***	***Alpha***	***Sigma***	***Beta***
Kruskal-Wallis P Value	*<0.0001*	*<0.0001*	*<0.0001*	*0.089*	*0.0068*

As can be seen in the tables above, relative EEG powers change significantly amongst different stages of respiration. The obtained miniscule P values confirm the existence of RCREC, in other word, the probability that RCREC happen by chance is less than 0.01%.

In order to further ensure that the simulation is comparable with the original work, a graph of mean relative EEG powers in all frequency bands was generated and compared them with those provided by Chervin. Note that since the chosen subject had almost normal AHI index, the MREP results were compared with the postoperative MREPs of Chervin's. Figure 34 shows this comparison (the graph on the left is taken directly from [15]).

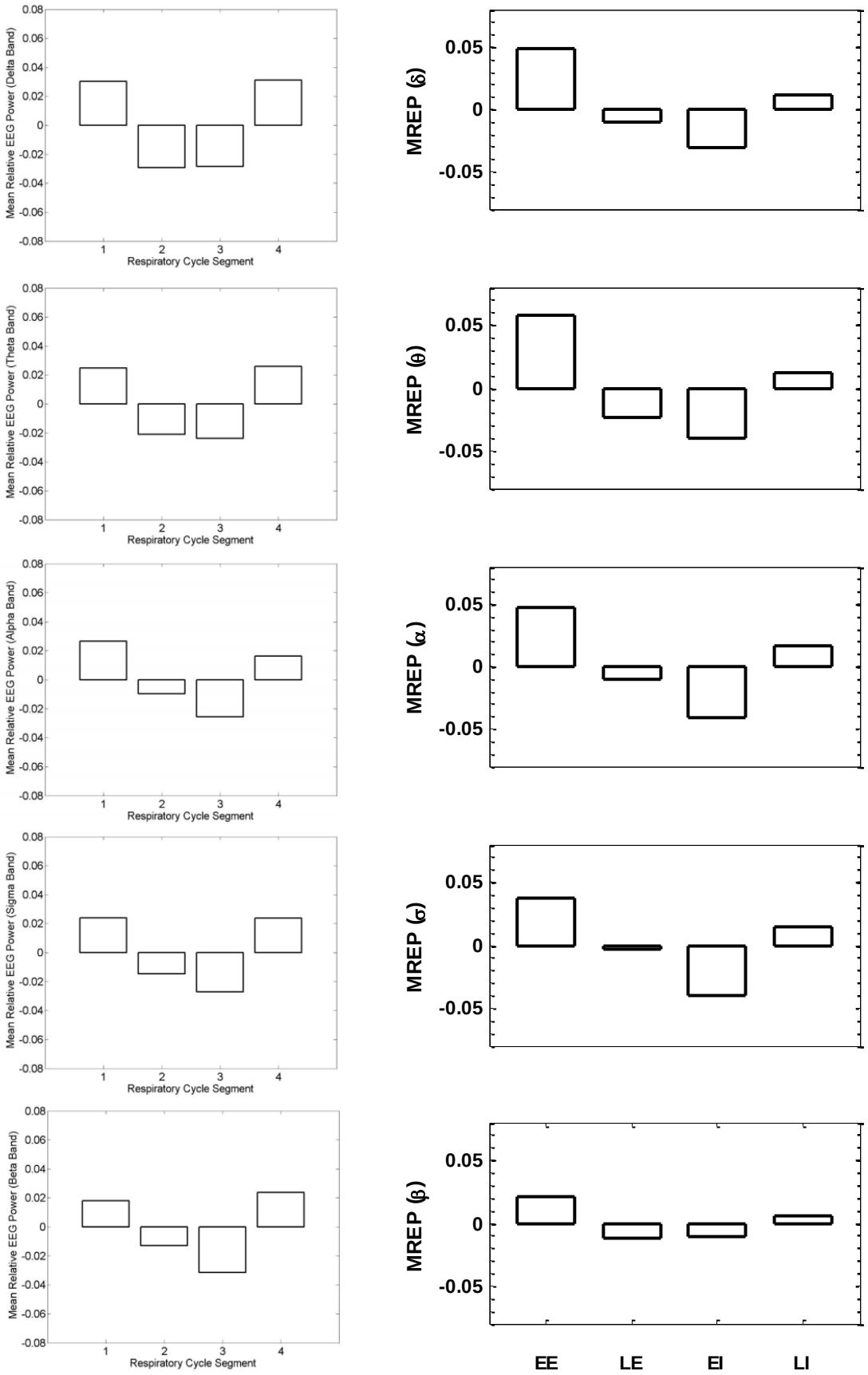

Figure 34. Comparison of mean relative EEG powers of two almost normal (AHI= 0.2 for the left graph and AHI≈1 for the one on the right) paediatric subjects in all frequency bands. As can be seen the magnitude of MREPs in both graphs are similar (range from -0.06 to +0.06) which ensures us that we have correctly replicated Chervin's work. Furthermore, the trends of MREPs in both graphs are alike which further shows that the replication is appropriately done.

As can be seen in Figure 34, both the amplitude values and trends are comparable in the original and the replicated results. Some discrepancies exist as the subjects and naturally the EEG patterns are different. The results suggest that the method for quantification of RCREC is correctly replicated.
During the replication process, some interesting observations emerged which are discussed below.

4.1.4 Discussion and conclusion

The main goal of this case study was to replicate Chervin's original method on quantification of RCREC. As can be seen in the result section this goal has been successfully achieved. Both the statistical analysis and graphs highlighting the mean relative EEG powers are closely comparable with the original results [15].
In the original work, Chervin band-pass filters the EEG signal to divide it into the five conventional frequency bands (e.g. delta, theta, etc) prior to the spectral analysis. This filtering process introduces spectral leakage into other frequency bands which may slightly affect the relative EEG powers. It is possible to avoid this spectral leakage by taking the spectrogram of the original EEG signal and then calculating the average power in the different frequency bands; the frequency resolution of 1Hz (due to use of 1 second windows) is adequate to differentiate between the conventional frequency bands of interest. Further, Chervin low-pass filters the air flow signal prior to segmentation. A low pass filter with sufficiently low cut-off frequency can potentially transform the flow signal into a smooth sinusoidal waveform and greatly ease the peak and trough identification process; however, it also shifts the position of the actual peaks and troughs by up to about half a second. This shift may remove the physiological information contained withinin the original flow signal. Filtering can dramatically affect the morphology of the flow signal and can hence alter the results and their subsequent interpretation. It has been in fact observed that quantification of RCREC can be greatly influenced by the air flow signal segmentation.
Another observation that was made was the high standard deviation of the relative EEG powers in a given band. Figure 35 shows an example relative EEG powers in the delta band.

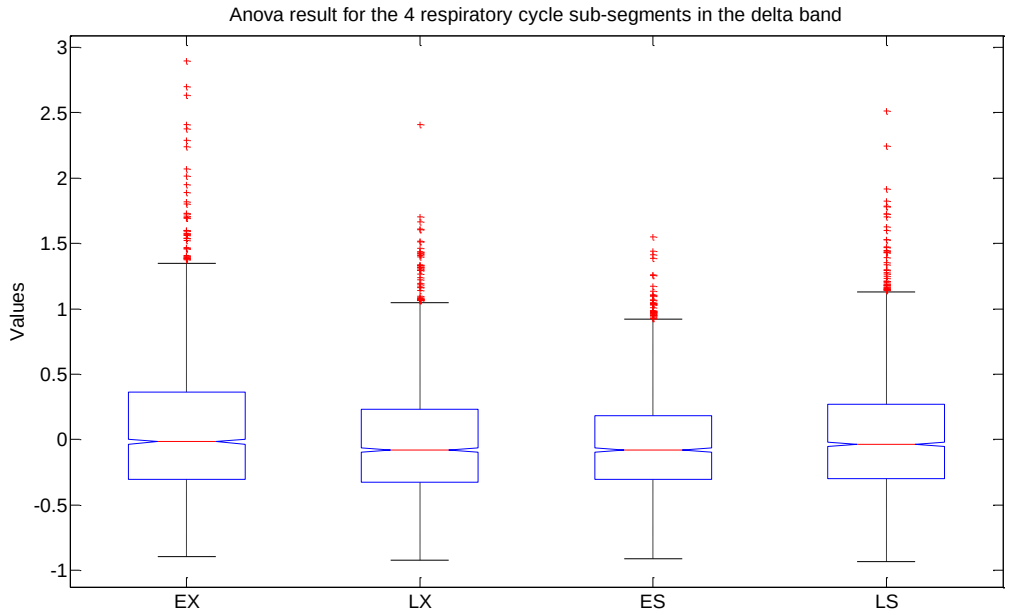

Figure 35. Box and whisker plot ANOVA results for relative EEG powers of the 4 respiratory cycle sub-segments in the delta band. Note that red crosses represent the outliers (i.e. data points outside 1.5 times the inter quartile range) As can be seen, even though there is a statistically significant (p<0.0001) difference amongst the 4 stages, the standard deviation considerably overlap. Hence it is not unlikely to obtain vastly different trends for the mean relative EEG power values.

Figure 35 shows that although there is seemingly a considerable overlap between the standard deviations of the relative EEG powers, it is highly unlikely that they come from the same population (P<0.0001).

Based on the previous works, RCREC is a promising parameter which can help to predict neurobehavioral outcomes of SDB. Chervin's Method for quantification of RCREC has been successfully replicated. Moreover, it has been observed that certain aspects of the algorithm can be improved. This case study helped to better understand the RCREC parameter and opened the way for more critical research questions, some of which will be addressed in the subsequent case studies.

4.2 RCREC – investigation in 7 paediatric subjects with AHIs ranging from 0.2 to 8.2

4.2.1 Introduction and motivation

Diagnosis of OSA is solely performed by calculating the apnoea-hypopnoea index (AHI) which is the number of apnoea and hypopnoea per hour of sleep. A subject is diagnosed with mild OSA if

his/her apnoea-hypopnoea index (AHI) is greater than one but smaller than five, and is diagnosed with severe OSA if the AHI is greater than five. Hence it is clear that AHI is an established and clinically valuable parameter in sleep analysis and the most important parameter in OSA diagnosis.

The study was motivated by the fact that quantification of the AHI is a manual, time consuming and effortful process; should RCREC – which is an automatically derived parameter – be able to predict the AHI well enough, it can potentially remove the need for laborious calculation of the AHI.

Hence, this case study aims to investigate possible relationships between the AHI and frequency band specific RCREC. Graphs of RCREC versus AHI have been inspected for meaningful patterns. Furthermore, duration of slow wave sleep within the first three hours of sleep onset in different subjects is investigated.

4.2.2 Materials and methods

Whole night polysomnograms of seven paediatric subjects with AHIs ranging from 0.2 to 8.2 were selected from the WTCRF data set. All subjects were 4 to 5 years old at the time of data acquisition. As with the previous case study, PSGs included standard sleep montage with EEG leads (C3/A2, O1/A2, C4/A1, O2/A1); nasal air flow (Protech) and thoracic and abdominal excursions.

Magnitude of RCREC in each frequency band and for each subject was. Graphs of AHI indices against frequency band specific RCREC were inspected for patterns. Moreover, RCREC in different frequency bands in all subject were plotted against the amount of slow wave sleep (duration of slow wave sleep within the first three hours of sleep) to check for potential correlations. Pearson linear correlation was employed for the correlation analysis. The results are described below.

4.2.3 Results

Table 4 shows the details of the subjects selected for this study.

Table 4. Subjects selected for the study.

Patient ID	*D.O.B*	*Acquisition*	*Age*	*Sex*	*AHI*
12	*19/06/2002*	*20/07/2006*	*4*	*F*	*0.2*
06	*05/02/2001*	*23/06/2006*	*5*	*M*	*0.7*
18cc	*02/12/2002*	*01/09/2006*	*4*	*M*	*1.2*
11	*31/03/2001*	*21/07/2006*	*5*	*M*	*1.9*
02	*01/06/2001*	*29/06/2006*	*5*	*M*	*4.7*
08	*09/03/2002*	*20/07/2006*	*4*	*M*	*6.3*
28	*29/01/2001*	*10/11/2006*	*5*	*M*	*8.2*

Mean relative EEG powers (MREPs) were calculated in each frequency band and for each patient. The analysis was once carried out for all the data within the first three hours of sleep and again for SWS portions of the data within the first 3 hours of sleep. The amount of slow wave sleep was also calculated. Figures 36 and 37 show an example of segmentation and MREP quantification in one subject (AHI=0.2, all sleep stages).

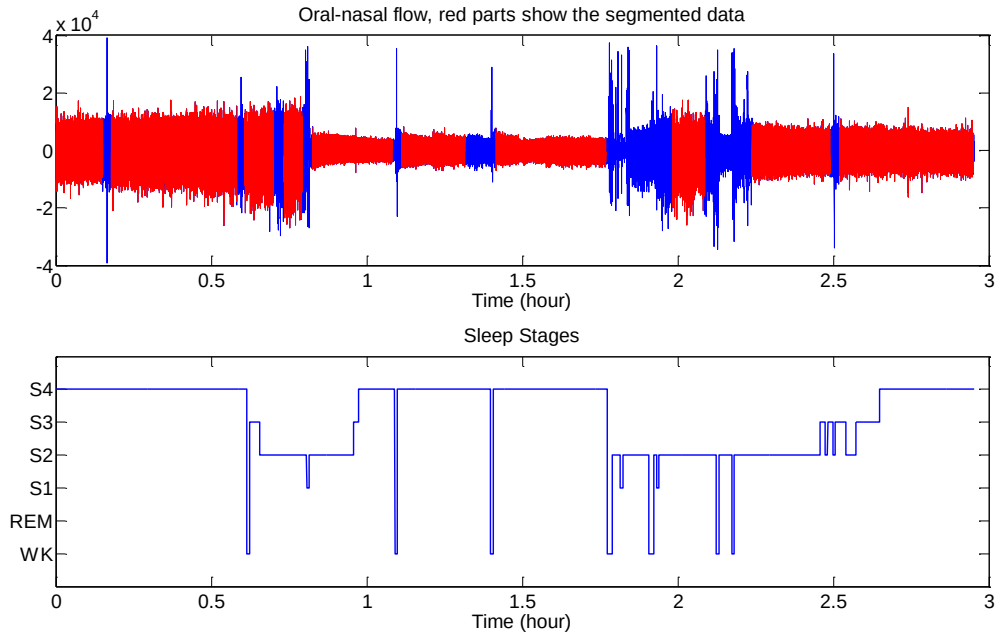

Figure 36. Nasal air flow and sleep stage signals plotted together for patient 12 (AHI=0.2). Note that 74.4% of the segmented data is composed of SWS. Also note that the duration of SWS in the first 3 hours is 1.59 hours.

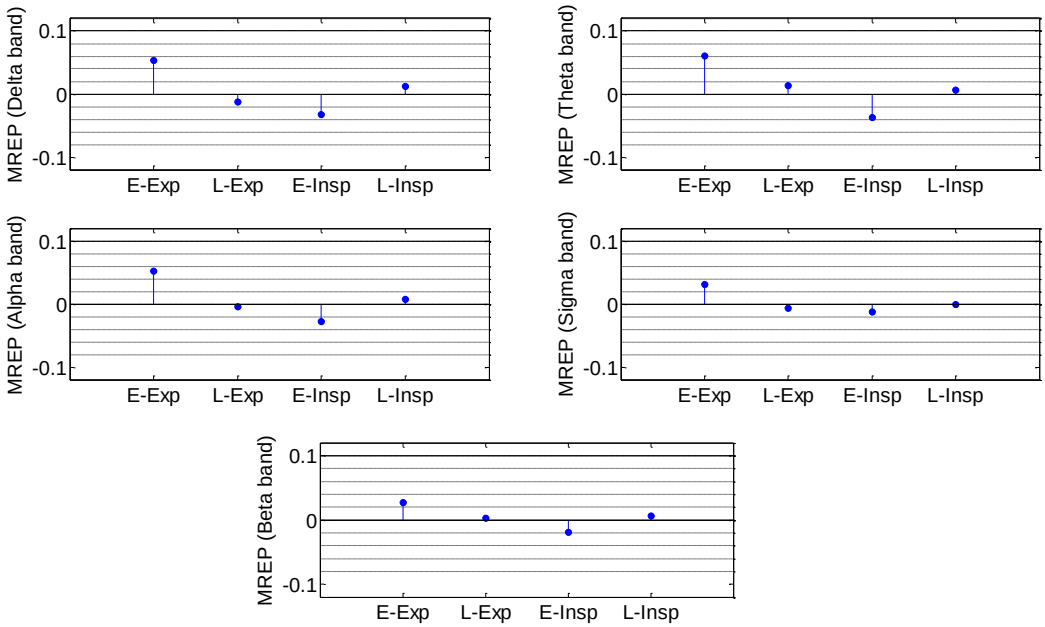

Figure 37. Mean relative EEG power changes in 5 different frequency bands for patient 12 (AHI=0.2, all sleep stages)

The MREP graphs were used to calculate the RCREC magnitude. Figure 38 shows the RCREC against AHI in three hours of sleep data where all stages are analysed (on the left) and where only SWS is analysed within the first three hours of sleep (on the right).

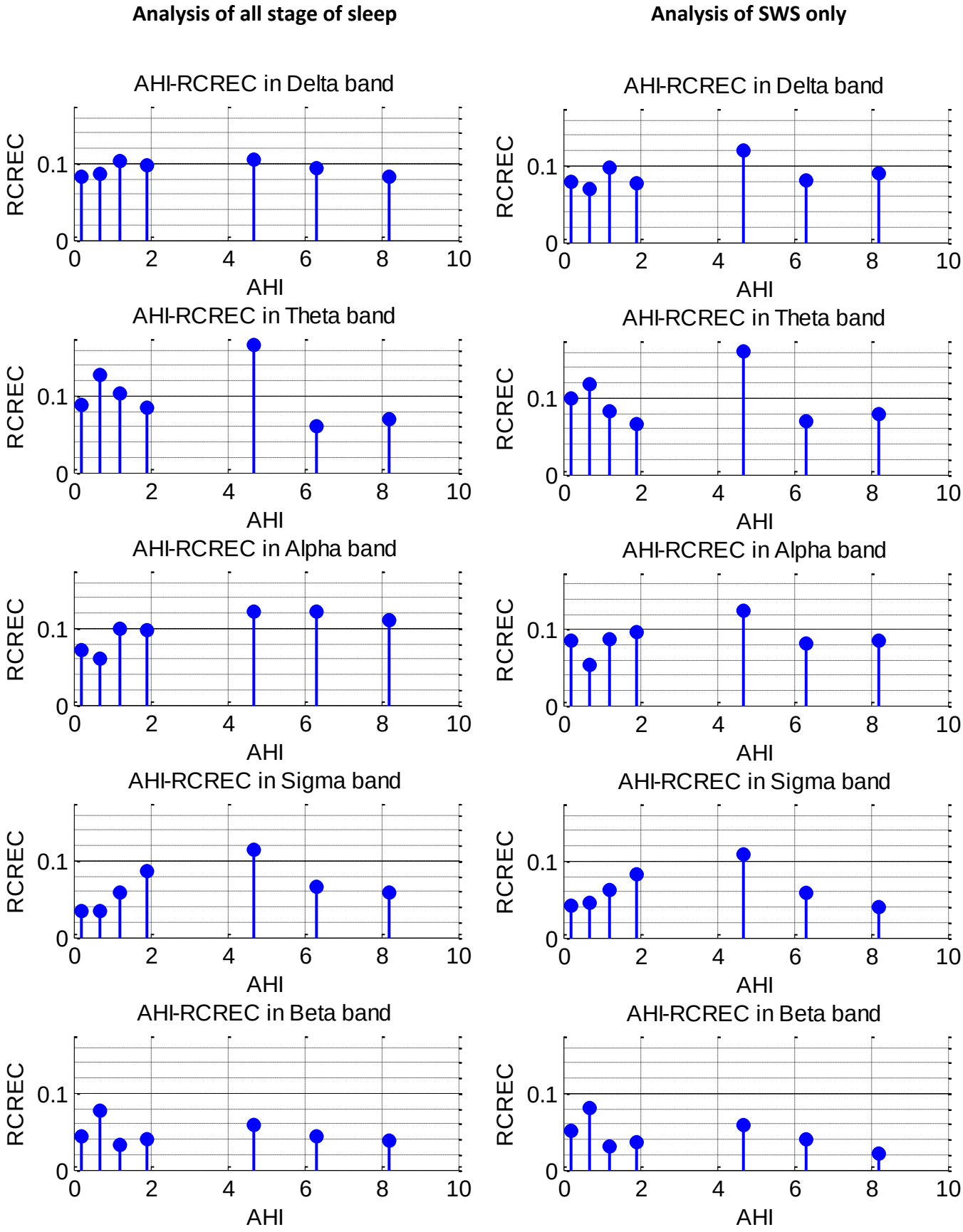

Figure 38. AHI Vs. frequency specific RCREC. The analysis was done on all sleep stages (left) and SWS only (right).

No meaningful patterns were found between the AHI and RCREC. As an extension of the work, frequency band specific RCREC values were checked against SWS portion (percentage of the SWS within the first three hours of the segmented data when taking into account all sleep stages) and SWS duration (duration of SWS only within the first three hours of sleep). It was found that there was a negative correlation between alpha RCREC and SWS portion and a positive correlation between beta RCREC and SWS duration, Figure 39 and 40 clarify this further.

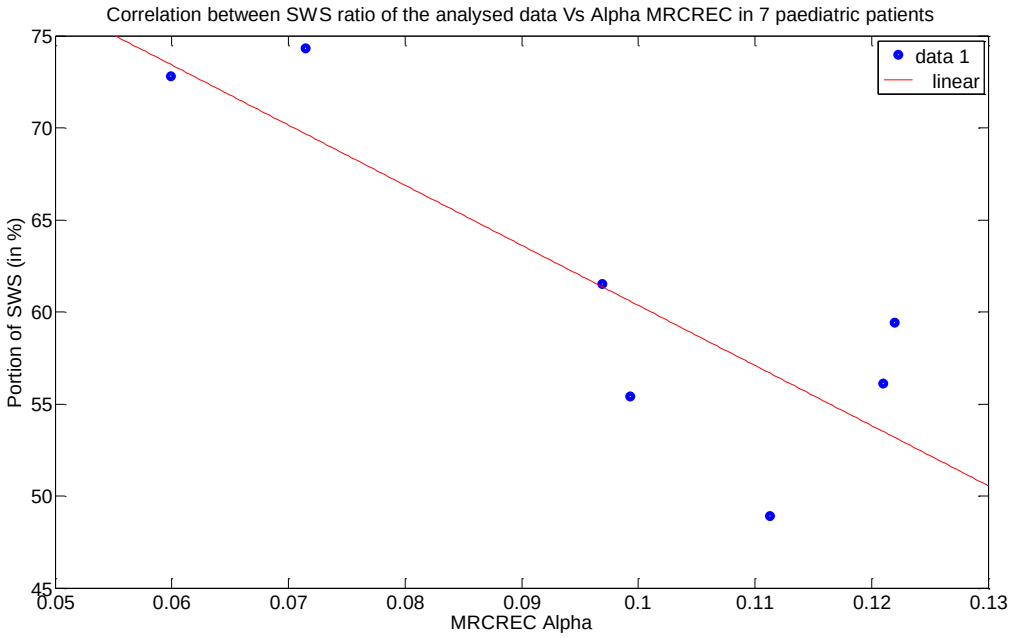

Figure 39. Correlation between SWS portion and alpha RCREC in the 7 subjects (p=0.0185<0.05). Note that the P value is calculated using the Pearson correlation coefficient, the same correlation does not reach significance if Spearman's rho is employed instead (0=0.13)

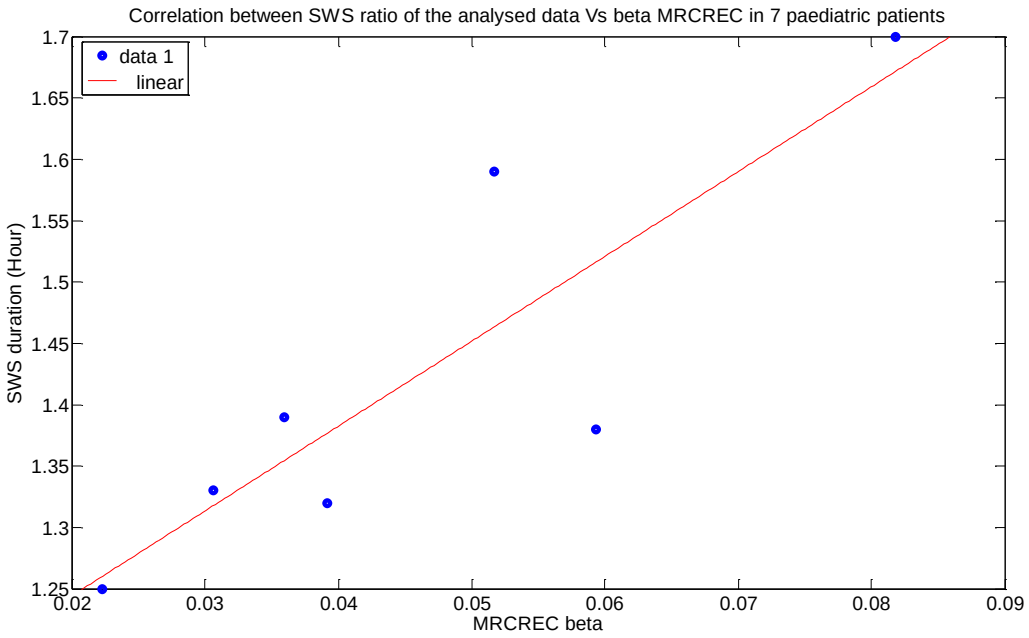

Figure 40. Correlation between SWS duration and beta RCREC in the 7 subjects (P=0.0125). Note that the P value is calculated using the Pearson correlation coefficient, the same correlation does not reach significance if Spearman's rho is employed instead (0=0.06)

Note that no other significant correlations were found in any of the other frequency bands. Discussion of the results and the conclusions are given next.

4.2.4 Discussion and conclusion

The results above show that the airflow segmentation algorithm and automatic abnormal data exclusion work well, it also shows that given a hypnogram, the algorithm can successfully analyse specific sleep stages such as the slow wave sleep. The reason behind choosing to analyse slow wave sleep (or deep sleep) rather than all the other stages such as S1, S2 or REM, is because of its physiological importance. Slow wave sleep is known to have recuperating effects and people suffering from SDB have lesser slow wave activity (SWA) compared to the normal population [48]. Hence it was decided to give special attention to SWS and analyse it in more details.

Figure 38 (AHI vs. RCREC) showed there was little difference between RCREC parameters when calculated from all sleep stages inclusive against SWS only. This is probably due to the fact that most of the segmented data within the first three hours is composed of SWS and hence by removing other sleep stages from the analysis, not a considerable amount is actually removed. therefore, there are no significant trend changes between the two graphs. However, subjects

with higher AHIs do seem to have more varying RCREC which may be caused by the lack of SWS compared to the other subjects.

Correlation analysis revealed that there may be a degree of correlations between frequency specific RCREC and SWS in absolute duration (Figure 40) and, RCREC and SWS percentage (Figure 39). The result in Figure 39 loosely suggests that on average, changes in EEG relative power in alpha band declines with increasing amount of SWS. In other words, alpha activity becomes more regular or stable (less variable) as one experiences more SWS. Similarly, the result depicted in Figure 40 suggests that on average, relative EEG power changes in the beta band increases with increasing SWS duration, meaning that beta activity becomes more variable as one goes through more deep sleep. Assuming that SWS is responsible for restoration of cortical columns and beta activity discharges the restored cells, the latter finding suggests that the more one recuperates through deep sleep, the more fatigued one gets which seems contradictory.

Finally, note that the P values obtained from the correlation analyses are only marginally significant, and if a non-parametric test such as the Spearman's rho is employed, P values do not reach significance. It should also be noted that a sample size of seven is not suitable for drawing solid conclusions out. Hence, repeating the analysis on a bigger population is worthwhile.

4.3 RCREC – Extension, is RCREC sensitive to airflow segmentation?

4.3.1 Introduction and motivation

In a recent work on RCREC it was noted that the authors use the esophageal pressure monitor signal (acquired with an esophageal balloon) and low-pass filter it to produce a respiration signal with reduced artefact [38]. In the previous section, where replicating the method to quantify RCREC, it was noticed that low pass filtering the airflow signal would greatly smooth it and simplifies the peak and trough detection process, however, at the same time it changes the actual peak and trough positions. This can alter the physiological information embedded in the airflow signal and ultimately influence the RCREC values. In order to test whether filtering of the airflow signal can influence the RCREC, two different smoothing methods were compared, first a standard 5^{th} order digital Butterworth filter with cut off at 0.51 Hz was employed and then a 2^{nd} order (or 2^{nd} degree) Savitzky-Golay filter (a polynominal fitting filter). The Savitzky-Golay filter is known for its shape-preserving capability which means it can better preserve the actual peaks and troughs. Note that the airflow signal was originally sampled at 16 Hz and then was interpolated to have the same number of samples as the EEG signal (256 Hz).

Respiratory cycle related EEG power changes as well as changes in four other parameters namely: skew, kurtosis, length of each sub-segment and irregularity index were then quantified. The irregularity index was calculated using the Sample Entropy (SampEn) method; a technique developed for estimating the complexity of time series [49].

The employed parameters provided us with a clearer judgement as to whether RCREC is sensitive to the airflow segmentation process. It was found that RCREC is sensitive to airflow segmentation and different smoothing algorithms can produce differing results.

Looking at the irregularity index was also of particular interest. It was speculated that if the changes in RCREC are caused by numerous micro-arousals, then respiratory cycle related EEG complexity changes may reveal that more clearly. In other words, it was hypothesised that frequent microarousals may manifest themselves as EEG complexity changes; however, difference between the complexity of the EEG signals within the four respiratory cycle sub-segments did not reach significance for any of the subjects.

4.3.2 Materials and Methods

Polysomnograms of ten paediatric subjects (Bolivian data set) from 8 to 15 year old were imported from the Compumedics software to Matlab as EDF files. Biosig toolbox for octave and Matlab[3] was used to read the EDF files in Matlab. Subjects' respiratory disturbance index (RDI) ranged from 0.1 to 3. RDI is a measure almost identical to AHI with the difference that it may also take into account deleterious respiratory events other than apnoea and hypopnoea.

In addition to mean relative EEG powers, three other parameters were computed in a similar way. Skewness, kurtosis and length of each sub-segment of the EEG signal in each and every respiratory cycle sub-segment and each frequency band were calculated for the first three hours of sleep and used as features. The irregularity index was not calculated for each band but for the original EEG signal using standard parameterisation with m=2 and r=0.25 (see Richman [49] for fundamental information on SampEn and Aboy [50] for its synthetic and real applications). Skewness measures the asymmetry of the underlying probability distribution of a real random variable; kurtosis is a measure of how "peaked" the underlying probability distribution is (e.g. a high value of kurtosis means most of the variability in the signal is caused by extreme values). Length of each respiratory cycle sub-segment was also included to inspect if different smoothing routines can significantly change the length of the sub-segments. In this study it was aimed to find out whether the parameters mentioned above change significantly with different smoothing procedures. Results of the study are provided below.

[3] http://biosig.sourceforge.net/download.html

4.3.3 Results

Table 5 shows details of the subjects selected for this study. If only AHI is taken into account, all subjects can be considered controls.

Table 5. Details of the ten paediatric subjects selected for this study.

Patient ID	*Age*	*Sex*	*AHI*	*RDI*
P11	*10*	*M*	*0.1*	*0.1*
P1	*15*	*F*	*0.0*	*0.2*
P3	*15*	*F*	*0.4*	*0.5*
P12	*13*	*F*	*0.0*	*0.5*
P5	*9*	*M*	*0.2*	*0.8*
P18	*8*	*F*	*0.8*	*1.2*
P9	*9*	*M*	*0.6*	*1.4*
P4	*8*	*M*	*0.7*	*2.0*
P10	*9*	*M*	*0.6*	*2.3*
P8	*8*	*M*	*0.6*	*3.0*

RCREC in power, skewness, kurtosis and sub-segment length were calculated for all subjects, once after using a Butterworth filter and another time with the Savitzky-Golay filter and the differences between them were tested using one way ANOVA. Tables 6 and 7 show the resulting P values for subject P1 (with zero AHI) as an example.

Table 6. P1, airflow signal smoothing using the Butterworth low-pass filter.

Patient1	*All bands*	*Delta*	*Theta*	*Alpha*	*Sigma*	*Beta*
Power (2 seg)	*0.01*	*0.03*	*0.22*	*0.09*	*0.0006*	*0.08*
Skew (2 seg)	*0.07*	*0.01*	*0.07*	*0.25*	*0.04*	*0.84*
Kurt (2 seg)	*0.04*	*0.03*	*0.12*	*0.31*	*0.29*	*0.37*
Seg length (2 seg)	*0*	*0*	*0*	*0*	*0*	*0*
Irregularity (2 seg)	*0.27*					
Power (4 seg)	*2.7E-08*	*7.1E-07*	*0.003*	*0.0001*	*0.0003*	*0.0002*
Skew (4 seg)	*0.29*	*0.09*	*0.89*	*0.66*	*0.66*	*0.51*
Kurt (4 seg)	*0.41*	*0.13*	*0.03*	*0.006*	*0.85*	*0.81*
seg Length (4 seg)	*0*	*0*	*0*	*0*	*0*	*0*
Irregularity (4 seg)	*0.34*					

Table 7. P1, airflow signal smoothing the using Savitzky-Golay filter.

Patient1	*All bands*	*Delta*	*Theta*	*Alpha*	*Sigma*	*Beta*
Power (2 seg)	*0.01*	*0.02*	*0.41*	*0.01*	*0.0001*	*0.11*
Skew (2 seg)	*0.12*	*0.06*	*0.81*	*0.19*	*0.01*	*0.005*
Kurt (2 seg)	*0.003*	*0.001*	*0.002*	*0.004*	*0.003*	*0.57*
Seg length (2 seg)	*0*	*0*	*0*	*0*	*0*	*0*
Irregularity (2 seg)	*0.25*					
Power (4 seg)	*1.3E-09*	*8.4E-08*	*0.002*	*9.0E-05*	*4.7E-05*	*4.9E-05*
Skew (4 seg)	*0.07*	*0.03*	*0.37*	*0.12*	*0.13*	*0.84*
Kurt (4 seg)	*0.006*	*6.7E-05*	*2.3E-06*	*9E-06*	*0.02*	*0.79*
seg Length (4 seg)	*0*	*0*	*0*	*0*	*0*	*0*
Irregularity (4 seg)	*0.54*					

The entries in the above two tables are the P values, those highlighted in green indicate $P<0.01$ and those in yellow are for $P<0.05$. Parameters marked with "2 seg" indicate that in the analysis, each respiratory cycle was divided into two segments i.e. expiration and inspiration and "4 seg" indicates that each respiratory cycle is divided into four segments namely: early expiration, late expiration, early inspiration and late inspiration. It is clear from the tables that the number of parameters which reach significance is different when the smoothing procedure changes (in the above example, the number of parameters which reach significance is higher when SG filter is used). The results suggest that although the difference between the smoothing procedures may not seem significant when visually assessing the two versions of the smoothed airflow signal (see Figure 41 for clarification), it can almost substantially influence the results. Table 8 emphasizes the difference between the two smoothing procedures.

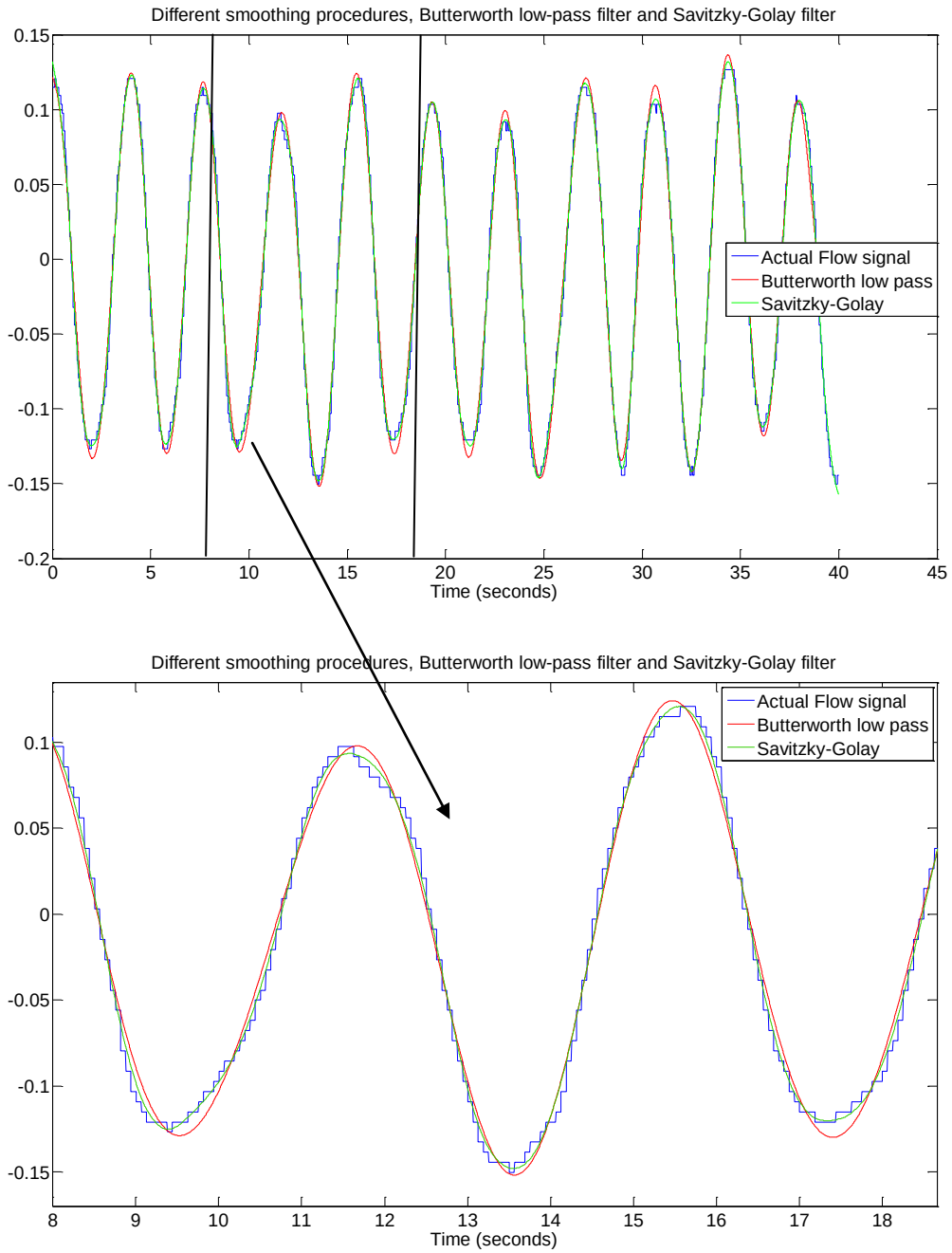

Figure 41. An example comparing Butterworth low pass filter smoothing against the Savitzky-Golay smoothing. Peaks/troughs produced by the two procedures can differ up to 0.5 second in position. Although the difference does not seem significant for the majority of the peaks and troughs, it was shown that it can influence the results.

Table 8. difference in number of parameters reaching significance for the two smoothing procedures (Butterworth vs. Savitzky-Golay)

		Butterworth low-pass filter		***Savitzky-Golay fitting filter***	
Subject ID	***RDI***	*Number of parameters reaching significance at p<0.01*	*Number of parameters reaching significance at p<0.05*	*Number of parameters reaching significance at p<0.01*	*Number of parameters reaching significance at p<0.05*
P11	*0.1*	*20*	*27*	*21*	*29*
P1	*0.2*	*20*	*27*	*29*	*35*
P3	*0.5*	*3*	*6*	*17*	*26*
P12	*0.5*	*6*	*9*	*18*	*24*
P5	*0.8*	*17*	*24*	*28*	*29*
P18	*1.2*	*20*	*25*	*28*	*32*
P9	*1.4*	*2*	*18*	*21*	*27*
P4	*2.0*	*22*	*24*	*20*	*25*
P10	*2.3*	*21*	*26*	*18*	*20*
P8	*3.0*	*22*	*27*	*23*	*27*
Total		*153*	*213*	*223*	*274*

The table above essentially compares the overall number of parameters reaching significance when smoothing with the SG and the Butterworth filter. For instance, the first table for subject P1 (Table 6) has 20 green entries and 7 yellow entries meaning that it has 20 parameter reaching significance at P<0.01 and 27 parameters reaching significance at P<0.05. As can be seen in Table 8, the number of parameters reaching significance is considerably higher in total when SG filter is employed. A further observation was that respiratory cycle related complexity changes (i.e. the irregularity index) did not reach significance in any of the subjects.

4.3.4 Discussion and conclusion

The results provided above suggest that RCREC is sensitive to prior airflow signal segmentation and seemingly small variations in peak/trough position estimation can lead to differing results. During the simulations it was observed that commonly, smoothing the airflow signal using a

standard low pass filter with a relatively low cut off frequency results in a relatively uniform separation of peaks and troughs, however, this uniform separation was artificial and not physiologically plausible. It had also been noticed that the lower the cut off frequency the more uniform the peak/trough separation. The airflow signal smoothed by the low-pass filter therefore had its actual peaks and troughs positions shifted in time (see Figure 41). As a result, it was evident that in order to take full advantage of the physiological information embedded within the airflow signal, there was a need to produce better estimates of the actual peak and trough positions. Hence, a Savitzky-Golay filter, which is known for its shape preserving ability, was chosen as the appropriate smoothing filter. As the results suggest, the SG filter accentuates the differences between the respiratory cycle segments. A direct consequence of use of SG filter is that the peak/trough separation (i.e. length of the respiratory cycle sub-segments) will not be artificially uniform and in fact, will be dramatically different.

One way analysis of variance (ANOVA) was employed despite our prior knowledge of statistical tests such as Wilcoxon rank-sum or Kruskal-wallis which better suit this purpose in this particular case study. The main reason for doing so was to keep the results comparable with the results previously published in the literature.

An interesting observation which came out of this study was that complexity of the EEG signal did not significantly change within the respiratory cycle segments. This observation opens three possibilities, 1) RCREC is not caused by frequent microarousals, 2) frequent microarousals do not manifest themselves as complexity changes and 3) the method used has not been appropriately chosen (or the results have not been interpreted appropriately). SampEn method was chosen because it was a nonlinear method capable of producing complexity estimates without requiring a large number of samples and with a reduced bias compared to the Approximate Entropy method. Other complexity measures usually require a large number of samples to reliably estimate the complexity. In order to quantify the complexity of the EEG signal for a single respiratory cycle sub-segment (about 300 samples), the required method had to be capable of producing reliable complexity measures with a small number of samples and therefore, SampEn method was chosen. Matlab code for calculating sample entropy was employed from the physionet sample entropy toolbox[4]. The question as to whether RCREC is caused by numerous microarousals or whether microasousals manifest themselves as complexity changes is a substantial one which requires dedicated research and is outside the scope of this case study. What can be addressed with certainty here is that RCREC is sensitive to prior segmentation of airflow signal and the RCREC values quantified may not be consistent and hence appropriate pre-processing is of essence.

[4] http://www.physionet.org/physiotools/sampen/.

Another issue which may be influencing RCREC is that the amount of data selected for the analysis in each subject is different from that of others simply because the amount of rejected data (i.e. abnormal, apnoea, hypopnoea) varies from one subject to another due to factors such as different sleeping patterns or different severity degree of the underlying SDB. How data length affects RCREC is something that has not been looked at and may need further investigation.

This concludes the chapter on preliminary case studies. The case studies here helped in better understanding some of the gaps in RCREC research and defined the next steps of the research. The next chapter is dedicated to the substantial investigations on the effects of alternative airflow segmentation on RCREC.

4.4 Summary

In this chapter the preliminary analyses on RCREC were described, it started with successful replication of the original RCREC work on a single paediatric subject and then expanded to explore possible simple relationships between AHI and RCREC in a small sample of seven subjects. No significant relationships or patterns were found between AHI and the RCREC parameters. Effects of alternative airflow signal smoothing was also addressed. It was found that seemingly negligible changes in the airflow smoothing can significantly alter the statistics of respiratory cycle segments.

Chapter 5

Systematic investigation of the effects of alternative airflow segmentation on RCREC

The preliminary case studies provided valuable clues to the direction of RCREC research. In particular, the third case study revealed that seemingly negligible changes in airflow signal segmentation can change the RCREC parameters extracted from PSG. This paved the way for a systematic analysis on the effects of alternative airflow segmentation on RCREC. The rest of this chapter contains the main case study on the effects of alternative airflow segmentation with an emphasis on transition segmentation, an airflow segmentation routine based on inspiratory/expiratory transitions. Different oral/nasal airflow measurement instruments were also looked at and their potential influence on RCREC were investigated. Last but not least, an attempt was made to mathematically explain how a small shift in the airflow signal segmentation points can change RCREC.

5.1 Effects of modified respiratory cycle segmentation on RCREC

RCREC has been demonstrated to predict sleepiness in patients with obstructive sleep apnoea and is hypothesised to represent microarousals. As such RCREC may provide a sensitive marker of respiratory arousals. A key step in quantification of RCREC is respiratory signal segmentation which is conventionally based on local maxima and minima of the nasal flow signal. An alternative respiratory cycle segmentation method based on inspiratory/expiratory transitions is investigated here.

5.1.1 Motivation and data set

As it was revealed in the third preliminary case study, identification and segmentation of respiratory cycles is a crucial step in the quantification of RCREC. Recall that in the original work, after removal of abnormal portions of thermocouple generated flow signal, each respiratory cycle was divided into four segments based on its local maximum, minimum and the mid points between the two. Whilst segmenting the signal directly according to its extrema is intuitive, it may not be optimal. The aim here is therefore to test a novel approach to respiratory cycle segmentation to achieve greater significance in the relative EEG power differences and

hence potentiate the ability of this measure to predict neurocognitive outcomes of sleep disordered breathing.

5.1.2 Methods

i. *Pre-processing*

Bolivian data was selected for the analysis duo its higher overall quality and larger samples size. PSGs with less than one thousand regular respiratory cycles or insufficient quality in either of the EEG or the flow signal were excluded from further analysis. This initial sifting procedure left 47 refined PSGs (24M:23F) to work with. EDF files were imported into Matlab using the Biosig toolbox version 2.49 for Octave and Matlab [51]. The toolbox, by default, inverts the neurophysiological signals (EEG, EOG, EMG, ECG) and zero-order interpolates all polysomnographic signals to match the highest sampling rate in the data set (EEG with 256 Hz in this case). Neurophysiological signals were hence re-inverted and all interpolated signals were decimated to their original sampling rates. They were then re-interpolated by zero padding and low-pass filtering using a symmetric Finite Impulse Response (FIR) filter [52]; this is to avoid artificial discontinuities in the signals introduced by zero-order interpolation. EEG channels were notch filtered at 50 Hz and then band-pass filtered between 0.5 and 32 Hz using a 5^{th} order digital Butterworth filter. The thermistor flow signal was low-pass filtered at 0.5 Hz also using a 5^{th} order Butterworth filter. As a result of filtering, clipped regions of the flow signal were smoothed. Although the 0.5 Hz cut-off is generally too low for filtering the respiratory signal, it does not considerably affect the thermistor generated flow signal as thermocouple based flow monitors are less sensitive to rapid changes in airflow. The 0.5 Hz cut-off was chosen to conform to previous work in the area [38]. Filtering for all signals was executed in forward and reverse directions to avoid unnecessary phase shifts (zero phase filtering). EEG channels and the thermistor flow signal were finally de-trended and readied for subsequent analysis. Since quantification of RCREC is solely dependent on a single EEG channel and a time-locked naso-oral flow signal, pre-processing was limited to the EEG and the thermistor flow signals.

ii. *Transition segmentation*

The respiratory cycle segmentation approach employed here is based on a novel departure from the conventional segmentation. Instead of dividing each respiratory cycle into four segments based on the detected maxima-minima and their mid points the average position of every two consecutive conventional segmentation points (mid points) were used to define respiratory cycle segments. This new segmentation captures the peaks and troughs and essentially looks at

the transitions from expiration to inspiration and vice versa. It is therefore referred to as transition segmentation henceforth; Figure 42 clarifies the transition segmentation.

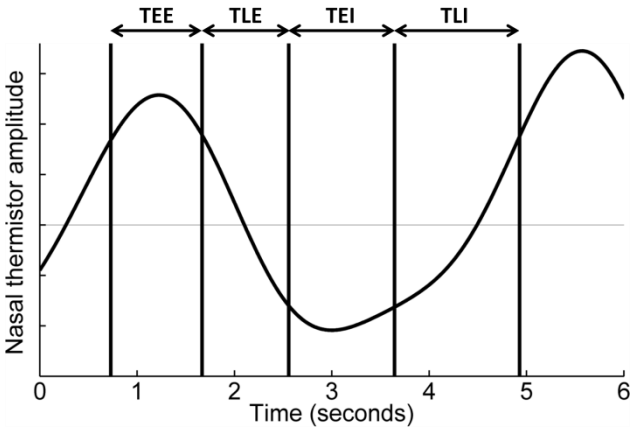

Figure 42. Transition segmentation of the same respiratory cycle shown in Figure 23. The flow signal is divided into four segments based on the mid points of the conventional segmentation points. TEE stands for transition to early expiration, TLE for transition to late expiration, TEI for transition to early inspiration and TLI for transition to late inspiration.

iii. *Statistical analysis*

Demographic data and polysomnoraphic variables were examined for normality using the Shapiro-Wilk test. As most variables were non-parametric in distribution, group differences were evaluated using the Mann Whitney U tests and all data, irrespective of distribution, are presented as medians for clarity. As age was found to differ significantly between the high and low altitude groups, altitude comparisons were co-varied for age but only for measures of sleep architecture and total sleep time which are influenced by age [53].

For each subject and in each frequency band, relative EEG powers in the four respiratory cycle segments were compared using the parametric one way analysis of variance (ANOVA) in accordance with previous work [15]. Note that although ANOVA assumes independence of samples and that is unlikely to be the case here, we have kept it for compatibility with the original studies on RCREC. Inclusion of dependent samples in ANOVA can affect the degrees of freedom of the test and subsequently change the corresponding P values and with that, interpretation of what is and what is not statistically significant. The significance of the difference between relative EEG powers was measured using the Fisher's F value derived from ANOVA. The distributions of the relative EEG powers were not normal, however, ANOVA has been shown to be robust to violations of the normality assumption [43]. F values were calculated once with the conventional segmentation and once with the transition segmentation and were then statistically compared. Given that, arguably, the extracted F values for each

individual were likely to be correlated, and the potential for Type one error due to multiple comparisons (6 frequency bands), repeated measures multivariate analysis of variance (MANOVA) was selected for the comparison of the conventional and the transition RCREC F values across the 6 bands. Assuming a main effect of segmentation method (conventional vs. transition), the univariate tests were inspected to see which frequency bands were driving this effect. Accordingly, no adjustment for multiple comparisons was required. Conventional and transition F values in each band were also compared using the paired non-parametric Wilcoxon signed rank test to confirm the findings. No differences in the results were found, therefore, the results from the univariate tests are reported here. As age did not correlate with the F values in any of the frequency bands, and there were no gender differences, no account was taken of these in the analyses.

5.1.3 Results

Children at high altitude were statistically significantly older than those at low altitude. Analysis of PSG variables that are known to vary with age were therefore controlled for age effects. Key PSG findings of the 47 subjects are summarised in Table 9. Total sleep time, sleep efficiency and REM% were comparable between settings. Children at low altitude had significantly more delta sleep and less stage 2 sleep than those at high altitude after controlling for age effects. As would be predicted, SpO2 variables were significantly lower at high altitude. Obstructive apnoea/hypopnoea indices indicated high rates of sleep disordered breathing at high altitude with significantly more children having an obstructive AHI $\geq$ 1. Children at high altitude experienced more central apnoeas than those at low altitude.

Table 9. Key demographic and polysomnographic variables

	Low altitude (N=26) Median (IQR)	***High altitude (N=21) Median (IQR)***	***P value***
Age in years	*9.7 (4.7)*	*12.1 (5.4)*	*<.05*
Gender	*12 male*	*12 male*	*NS*
Total sleep time in minutes	*405.3 (71.8)*	*378.5 (103.0)*	*NS[a]*
Sleep efficiency	*94.9%*	*92.6%*	*NS[a]*
N2 %	*44.9(7.8)*	*50.7 (11.2)*	*<.05[a]*
N3 %	*31.0 (8.4)*	*25.7 (9.2)*	*<.05[a]*
REM %	*19.8 (5.7)*	*18.3 (7.6)*	*NS[a]*
Mean SpO2%	*97 (2.0)*	*88 (3.0)*	*<.001*
Minimum SpO2	*92 (3.3)*	*81 (7.5)*	*<.001*
Central apnoea index	*0.3 (0.6)*	*0.7 (1.6)*	*<.05*
Obstructive apnoea index	*0.0 (0.0)*	*0.0 (0.0)*	*NS*
Obstructive apnoea/hypopnoea index	*0.6 (1.1)*	*2.0 (3.0)*	*<.01*
No. children with AHI ≥1	*7*	*13*	*<.02*
No. children with AHI ≥5	*0*	*3*	*NS*
Respiratory arousal index	*0.3 (0.4)*	*0.3 (0.7)*	*NS*
Number of respiratory cycles analysed	*3507 (2099)*	*4496 (2184)*	*NS*

[a] Controlling for the effect of age

Multivariate comparison of Fisher's F values across 47 subjects and in all frequency bands revealed that utilising the transition segmentation strongly increases the statistical significance of the difference between the relative EEG powers in the four respiratory cycle segments, $F(6,41)=7.06$, $P<.001$. The main effect size, partial η^2, associated with the segmentation method used, was 0.51 which is interpreted as "large enough to be visible to the naked eye"[54]. Frequency band specific F values were also individually compared (univariate comparison) and the transition F values were found to be significantly higher ($p<.05$) than the conventional ones in all frequency bands except beta, Table 10 contains the details of the comparison. Since in calculation of F values (i.e. between group variability/within group variability), the degrees of

freedom of the denominator, associated with the number of non-apnoeic respiratory cycles throughout sleep, is large, F values are comparable and therefore, statistics such as mean and standard deviation are defined and meaningful. The distribution of the F values for the conventional and the transition RCREC are also graphically shown as box plots in Figure 43. No significant differences were found in the RCREC or transition RCREC parameters between the low and high altitude groups having controlled for age. RCREC and transition RCREC parameters were also compared across the two AHI groups (27 controls vs. 20 mild/severe OSA) using the Mann-Whitney U test and no significant differences were found.

Table 10. Statistical comparison of the conventional and the transition RCREC

	Conventional RCREC F-values Mean± SD	***Transition RCREC F-values Mean± SD***	***Significance***
Whole spectrum (0.5-32 Hz)	*25.8 ± 17.1*	*31± 22.6*	*F(1,46)=8.63 P<.01*
Delta (0.4-4.5 Hz)	*25.7 ± 18.3*	*30± 24.1*	*(1,46)=5.32 P<.05*
Theta (4.5-8 Hz)	*15.1 ± 9.6*	*18.8 ± 11.5*	*F(1,46)=27.3 P<.001*
Alpha (8-12 Hz)	*14.4 ± 10.5*	*19.4 ± 14.5*	*F(1,46)=21.2 P<.001*
Sigma (12-16 Hz)	*12.9 ± 12.3*	*16.3 ± 15.9*	*F(1,46)=9.99 P<.01*
Beta (16-30 Hz)	*13.7±20.5*	*13.6±20.3*	*F(1,46)=.004 P>.5*

Statistical comparison of the conventional and the transition Fisher's F values in 47 subjects using the repeated measures MANOVA. Mean and standard deviation (SD) of the F values associated with each segmentation method are provided.

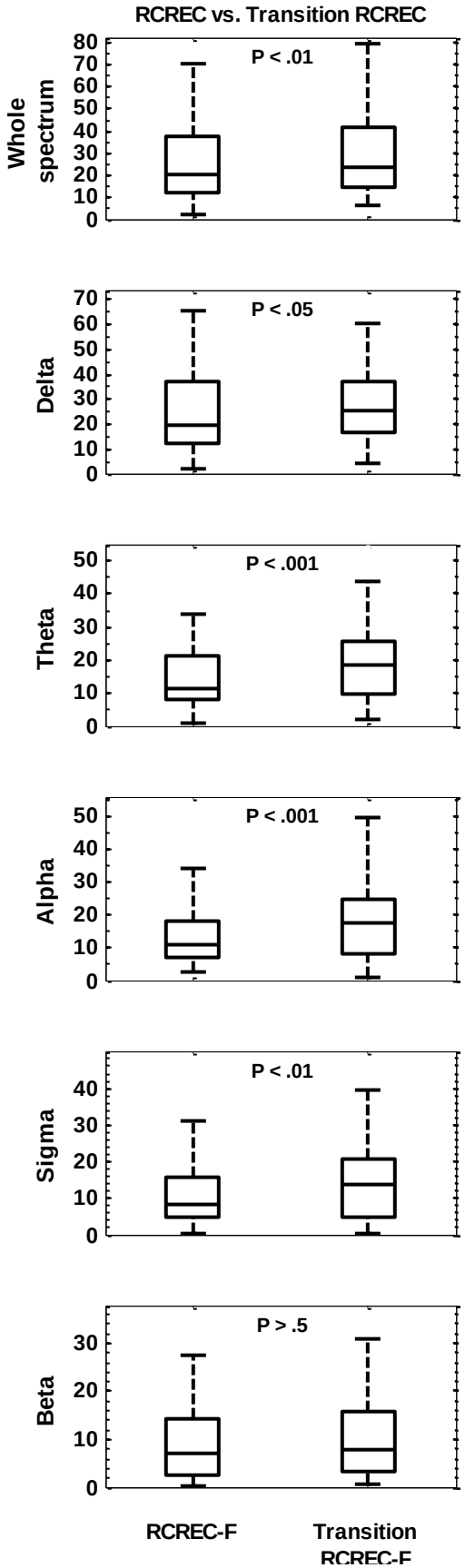

Figure 43. F value distribution of the conventional and the transition RCREC as illustrated by box plots. The top and the bottom lines of the box represent the upper and lower quartile values respectively and the middle line represents the median of the distribution. Maximum whisker length is set at 1.5 × the interquartile range, and all points outside this range (outliers) are removed. P values are the exact counterparts of those shown in Table 1.

i. *Variations of segmentations tested*

To gain further insight into the effects of alternative segmentations on the statistical significance of RCREC, several variations of respiratory cycle segmentation were also tested, details of which are briefly described below.

Backward shift

The conventional segmentation points shown in Figure 23 were all shifted by an arbitrary 50 samples (195 milliseconds) to the left (backward) to generate a new segmentation. Similar to the previous analysis, significance of the difference between respiratory cycle segments were computed for conventional and backward shifted RCREC in 47 subjects. Multivariate comparison of Fisher's F values across the six bands showed a statistically significant increase in the difference between relative EEG powers in the backward shifted segments, $F(6,41)=7.63$, $P<.001$. Note that the F values extracted from the transition segmentation were on average larger than those obtained from the backward shift segmentation in all frequency bands except beta.

Forward shift

Original segmentation points were also shifted forward by 50 samples (195 milliseconds) and the same procedure as above was carried out for the analysis. By contrast, the forward shift significantly decreased the significance of the difference between relative EEG powers in the forward shifted respiratory cycle segments, $F(6,41)=6.47$, $P<.001$.

Long shift

To investigate the criticality of synchronisation between the EEG and nasal flow signals, influence of longer shifts on RCREC were assessed. For simplicity, instead of shifting the segmentation points, the time-locked C3/A2 EEG channel was temporally shifted. The EEG signal was once circularly shifted backwards and once forward by an arbitrary time of one minute. F values for both cases were calculated in the same manner as above and compared with the original RCREC F values. F values for forward and backward long shifts were both significantly ($p<.001$) lower than the conventional F values, $F_{forward}(6,41)=11.36$ and $F_{backward}(6,41)=13.03$. No significant differences were found between the forward and backward long shift F values $F(6,41)=.72$, $P>.5$.

ECG based segmentation

To assess the relationship between cardiac rhythm and RCREC, respiratory cycles were segmented based on time-locked ECG R peaks (detected automatically using a modified Pan-Tompkins algorithm [55]). Segment specific relative EEG powers in respiratory cycles with the most frequent number of R peaks were calculated in 12 subjects. A preliminary comparison of P values associated with the difference between relative EEG powers in the conventional and ECG segmented respiratory cycles showed no significant increment, suggesting that RCREC is unlikely to be influenced by the temporal location of R peaks within respiratory cycles.

5.1.4 Discussion

In this case study, a number of alternative segmentation routines were introduced and their effect on RCREC was investigated. In particular, the transition segmentation was found to increase the significance of the difference between respiratory cycle segment specific relative EEG powers. We speculate that this increment in significance is a result of better isolation of the temporal source(s) driving the RCREC.

The results presented here show that segmenting the thermistor generated respiratory cycles based on transitions from expiration to inspiration and vice versa (Figure 44) noticeably increases the statistical significance of the difference between relative EEG powers in the four respiratory cycle segments. This study is not the first to emphasise the physiological importance associated with transition from expiration to inspiration or vice versa. In an investigation of the effects of respiration on input pulmonary arterial impedance (Z) in dogs, Castiglioni *et al.* [56] reported that Z modulus and phase undergo significant changes in transition from inspiration to expiration. In contrast, in a similar study in humans, where respiration was only classified into inspiration and expiration, no significant differences were found in the overall Z-spectrum between inspiration and expiration [57]. In another study on rats, Ezure *et al.* [58] investigated the firing properties of respiratory centre neurons in the brainstem just before the transition from expiration to inspiration. They concluded that some inspiratory neurons are activated prior to the start of inspiration whilst some are inhibited by strong firing of the augmenting expiratory neurons of the Bötzinger complex; a further insight into the process of brainstem activity in transition from expiration to inspiration.

The results generated from the brief forward and backward shifts suggest that RCREC is sensitive to respiratory cycle segmentation. Whilst slightly shifting the conventional segmentation points backward significantly increases the differences between relative EEG powers, a shift forward, will do the exact opposite. Changes in significance induced by simply shifting the segmentation points back and forth are likely to be related to the temporal location

within the respiratory cycle at which the underlying physiology (or physiologies) driving the RCREC occurs. Hence, in order to gain insight and ideally identify the physiological mechanisms underpinning RCREC, instrumental delays must be taken into account. Whilst there is virtually no delay in EEG signal acquisition, the thermocouple based flow signal monitors are associated with relatively large delays. Xiong *et al.* [59] report an average of 370 milliseconds delay (ranging from 120 to 720 milliseconds) for nasal flow thermistors compared to oesophageal pressure fluctuations and emphasise that only a small portion of this delay is due to the physiology of the respiratory system. A pilot experiment was also designed to assess potential phase differences between a thermistor and a pressure transducer nasal cannula which follows after this case study. Although in general these delays can be neglected in most sleep scoring and sleep event identification criteria, it has been shown that they have a profound effect on RCREC and hence should be taken into account when investigating the physiological basis of the technique. The increase in the statistical significance of RCREC seen after briefly shifting the conventional segmentation points backward is likely to therefore represent temporal alignment of the airflow and EEG signals. Filtering the flow signal may also introduce artificial shifts (see Chervin *et al.* [38] for an example), particularly when the cut-off frequency is very low with respect to the major spectral content of the signal, and should hence generally be avoided as it may affect the resulting RCREC.

Long shifts revealed that circularly shifting the EEG signal by one minute dramatically reduces the differences between the relative EEG powers in the respiratory cycle segments, suggesting that synchronisation between the EEG and the respiration signal plays an important role in RCREC and is crucial for its detection and understanding. Furthermore, there were no significant differences between the forward and backward F values after the long shift, implying that the systematic pattern brought out by the small forward and backward shifts only holds when the EEG and the flow signal are relatively well synchronised.

ECG based segmentation failed to increase the significance of the difference between respiratory cycle segments when compared to the conventional segmentation routine. This suggests that temporal locations of R peaks within respiratory cycles are unlikely candidates to explain the regulation of RCREC.

In this study only three subjects were diagnosed with moderate-severe OSA (AHIs of 7.2, 7.2 and 40.6) out of which only one had an obstructive apnoea index of greater than one. Given that RCREC were consistently present in most frequency bands (number of significant RCREC in delta: 46, theta: 43, alpha: 44, sigma: 38 and beta: 32 out of 47 participants) and that there were no significant differences between the RCREC parameters between the two AHI groups led to

the speculation that although RCREC may be related to inspiratory microarousals and respiratory effort [38, 40], it might not be dominantly derived from them.

Another speculation into the origin of RCREC can be made based on its consistent presence in different populations. RCREC exists in children as well as adults and in controls as well as OSA patients; consequently, RCREC could be a manifestation of the respiratory regulatory system. One hypothesis, noted by Chervin *et al.* [15], is the possible relationship between respiratory related evoked potentials [60] (RREP) and RCREC. It is possible that inspiring against a fully or partially obstructed airway is analogous to common stimuli used in RREP studies (e.g. inspiratory occlusion or the use of resistive loads), and hence, coherently averaging the EEG signals (time-locked to the start of inspiration) across a few hundred respiratory cycles gives a consistent pattern. This hypothesis was briefly assessed from a technical stand point using a bootstrapping method developed for objective detection of evoked potentials [61] (see Appendix B). A single control subject with very significant respiratory cycle related EEG changes in all bands was selected for this analysis. The PSG was divided into eight large segments, each having more than 250 respiratory cycles and a significant RCREC ($P<0.01$) when looking at the whole spectrum of the EEG signal. The coherently averaged EEG signals: 1) produced different patterns across the eight segments and 2) the generated patterns were not significantly different from randomly generated ones in seven out of eight segments, suggesting that there is little evidence to support a causal relationship between RREP and RCREC, however, reaching a firm conclusion will need further investigation.

In summary RCREC is sensitive to respiratory cycle segmentation and as a result, experimental designs regarding RCREC should carefully account for factors which may alter the morphology of the respiratory signal as well as ensuring optimal synchrony between respiratory and EEG signals. The introduced respiratory cycle segmentation technique based on inspiratory and expiratory transitions strengthens the statistical significance of the respiratory cycle related EEG changes when compared to previously published segmentation techniques. The transition segmentation approach may thus provide a better synchronisation with the underlying RCREC driving physiology and increase the ability of this measure to predict neurocognitive outcomes in sleep disordered breathing.

5.2 Comparison of two nasal airflow measurement instruments: pressure transducer nasal cannula vs. nasal thermistor

5.2.1 Motivation

The previous case study showed that if the segmented airflow signal is shifted slightly to the left (by 0.2 – 1 second), it is highly likely that the corresponding EEG power changes between the respiratory cycle sub-segments will increase. Similar shifts to the right yielded the opposite effect. This was puzzling and therefore, it was argued that since the selection of the inspiratory/expiratory peaks as the basis for segmentation have been somewhat arbitrary, it could be that the transition points from expiration to inspiration and vice versa, hold greater physiological importance. However, it was also important to account for delays imposed by various airflow measurement instruments [59], hence it was speculated that this shift can be related to the existing delays in the airflow measurement instruments. Since the RCREC research subjects had their flow measured using thermistors, the findings about shifting the flow signal were, strictly speaking, limited to the airflow signals acquired using thermistors. It was naturally presumed that the flow signal measured by different but commonly used instruments should more or less result in similar general signal structure, and the expiration and inspiration peak positions should be partially preserved. Based on that assumption, a simple experiment was designed to reveal those presumably fine differences between two of the most commonly used nasal flow measurement instruments in sleep research. The experiment was to simultaneously measure the signal generated from both a nasal thermistor and a pressure transducer nasal cannula and characterise their relative delays. In contrast to the assumption made, results revealed that the signals generated from the two instruments are considerably different. The expiratory and inspiratory peak positions particularly, are not well preserved. This can be crucially important in applications where flow signal morphology and the inspiratory/expiratory peak positions are core to the analysis, an example of such application, is quantification of RCREC.

5.2.2 Materials

Simultaneous nasal airflow signal was acquired from a single healthy adult subject using a pressure transducer nasal cannula and a nasal thermistor in sitting position. A nasal/oral thermistor was used but the oral sensor was deliberately covered with blue tack. Both instruments were provided by pro-tech (component number P1259 and P1274 from the Pro-Tech diagnostic sensor catalogue) and Alice 5 diagnostic sleep system[5] was used as the data

[5] http://www.healthcare.philips.com/gb_en/homehealth/sleep/alice5/default.wpd

acquisition platform. The sampling rate was set to 200Hz to ensure accurate delay profile estimation and 16 bits were used for quantization. In total, 11 minutes of data was acquired and in order to avoid excessive artefacts, the subject was instructed to breathe calmly and regularly through his nose. Figure 44 shows a snap shot of the subject (with his consent) after the setup and an example of the acquired normalised raw signals.

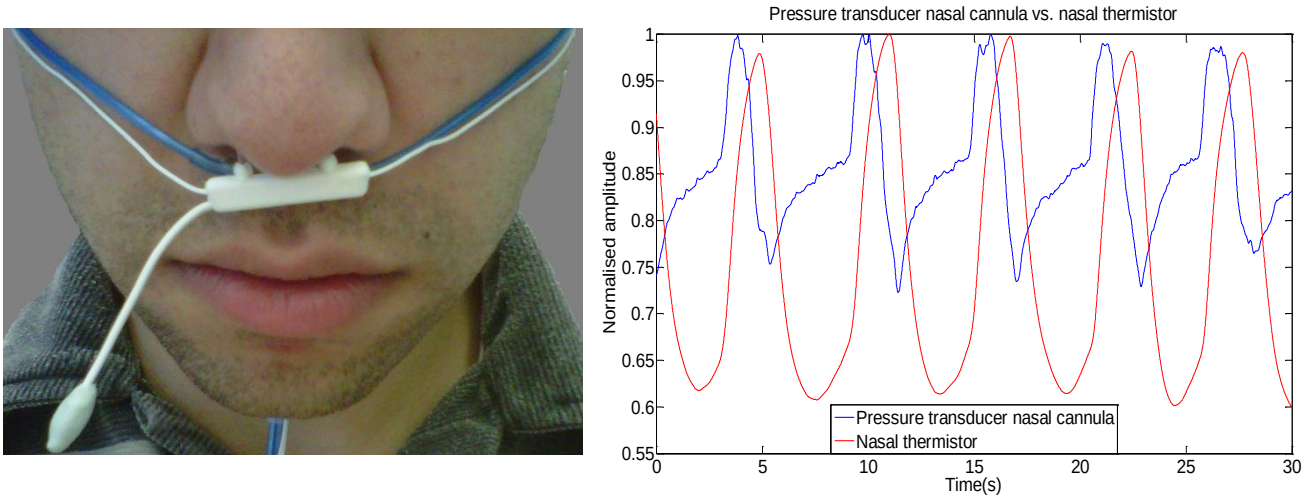

Figure 44. Left) Snap shot of the subject after setup, the blue tube is the nasal cannula and the white rectangular box with two heat sensitive nasal sensors is the thermistor. Note that the oral sensor is blocked with blue tack and moved away from the mouth. Right) An example highlighting both signals in raw form.

5.2.3 Methods

Signals acquired from the Alice 5 platform were imported into Matlab. The first few respiratory cycles (approximately 32 seconds) were removed from the analysis; this is to allow the thermistor to heat up and reach its steady state. Both signals were zero phase filtered (forward and backward filtering) with a 5th order digital low-pass Butterworth filter with cut off at 1 Hz. As can be seen in Figure 44, the fundamental frequency is approximately 1/6 Hz (5 cycles in 30 seconds) which means the chosen cut-off frequency allows up to five harmonics to reconstruct the signal whilst removing any higher spectral components; this is desirable as the information of interest largely lies within the low frequency region. Both signals were then de-trended. Figure 45 shows an example of the resulting waveforms; the graph shown is the same as the one in Figure 44, pre-processed but not normalised.

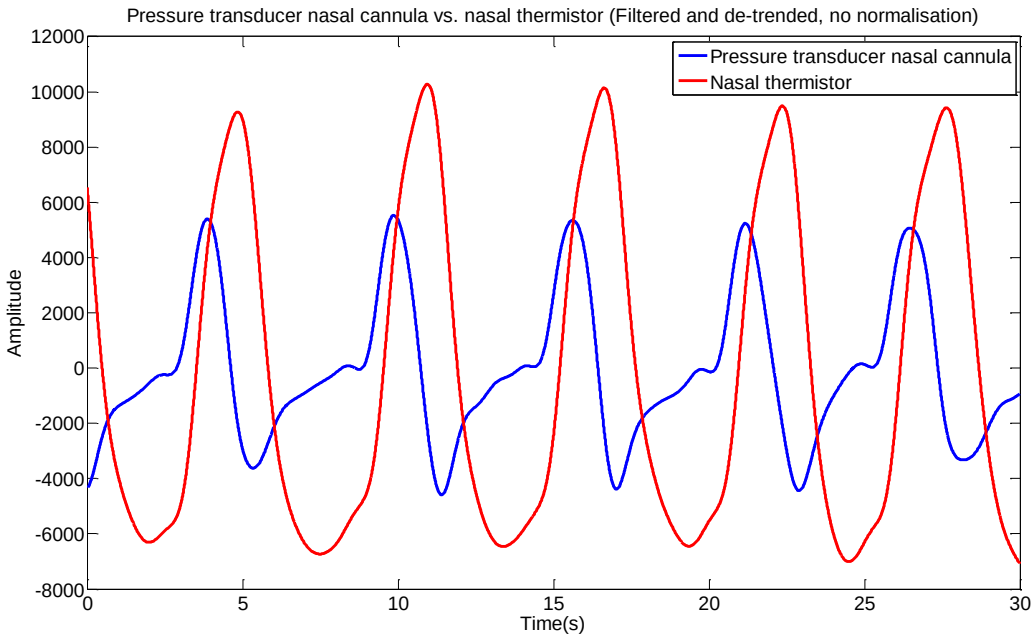

Figure 45. Pre-processed nasal airflow signals. Removal of high frequency components is apparent.

Next, peaks and troughs of both signals were detected using amplitude and duration thresholds. All the detected extrema were visually inspected to ensure that the number of peaks and troughs in both signals are equal. The difference between peak positions of the two signals gives a direct indication of the delay between them; similar statement can be made about the troughs.

5.2.4 Results

A total of 111 peaks and 111 troughs were extracted from each signal. The difference between the extrema of the two signals was calculated as follows:

$$Peak\ delay\ vector = \overrightarrow{PP_T} - \overrightarrow{PP_C}$$

$$Trough\ delay\ vector = \overrightarrow{TP_T} - \overrightarrow{TP_C}$$

Where $\overrightarrow{PP_T}$ is the peak position vector generated by the thermistor and $\overrightarrow{PP_C}$ is the peak position vector generated by the cannula. Similarly, $\overrightarrow{TP_T}$ and $\overrightarrow{TP_C}$ are trough position vectors generated from the thermistor and the cannula respectively. Mean and standard deviation of both $Peak\ delay\ vector$ and $Trough\ delay\ vector$ are shown in Table 11.

Table 11. Standard statistics of peak and trough delay vectors

	Mean (seconds)	***Standard deviation (seconds)***
Peak delay vector	*1.035*	*0.164*
Trough delay vector	*2.054*	*0.265*

Underlying distribution of the delay vectors were assessed using histograms and norm plots. Figure 46 and 47 illustrate the results for peak and trough delay vectors.

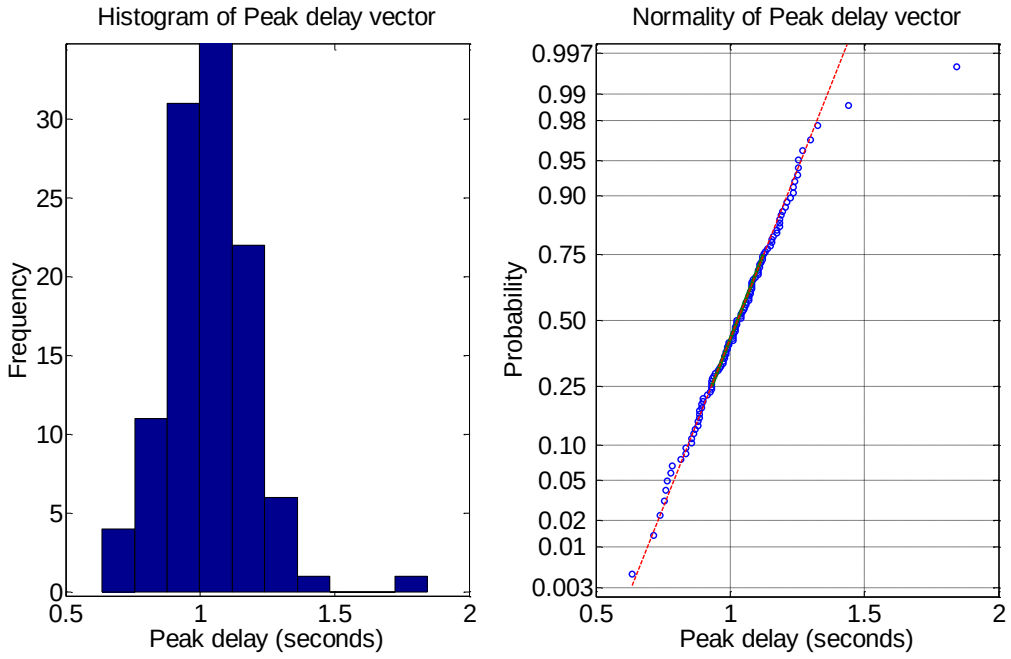

Figure 46. Histogram and norm plot of peak delay vector. The histogram appears to be following a near normal distribution and the almost straight line on the norm plot (deviation of data points from a normal distribution, curvature in the data points is a marker of non-normal distribution) confirms this. Lilliefors test of normality also confirms that the data can be assumed to be normally distributed (P>0.5). As can be seen there are clear outliers in the data which can influence the characterisation of the distribution and for that reason they were removed from the data.

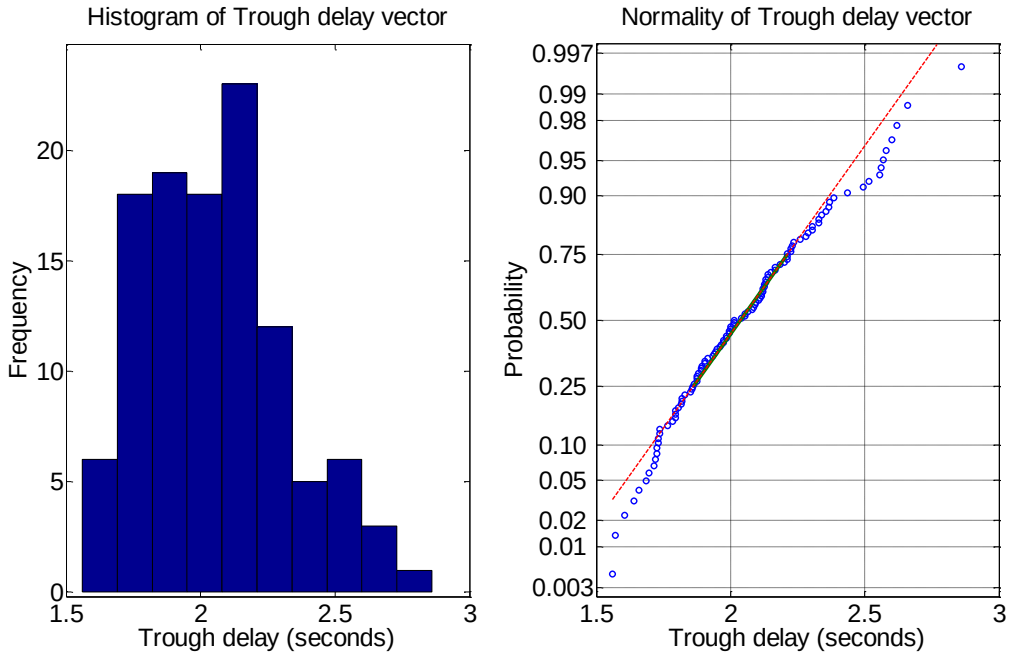

Figure 47. Histogram and norm plot of trough delay vector. This histogram also can be modelled with a normal distribution although the data points on the norm plot are not a clear straight line. A Lilliefors test of normality revealed that the data can be assumed to be normally distributed (P=0.32, null hypothesis stating that the data comes from a normal distribution is not rejected). After outlier removal the P value increased to more than 0.5.

As can be seen, both histograms and norm plots suggest that delay vectors can be assumed to be normally distributed. Lilliefors test of normality was also applied to both the peak delay vector and the trough delay vector to test the assumption. In both cases the test failed to reject the null hypothesis (P>0.5 for the peak delay data and P>0.3 for trough delay data) indicating that the normal distribution assumption for the delay data is reasonable.

To parameterise the distribution, the outliers (defined by any data value which lies outside "$mean \pm 2 \times standard\ deviation$" of the data vector) were removed and normal distribution parameters (i.e. mean and standard deviation) were calculated using the maximum likelihood estimation method. Table 12 shows the estimated parameters and their 95% confidence intervals.

Table 12. Distribution parameterisation of the peak and the trough delay vectors

	$\mathcal{N}(\mu, \sigma)$	$\mu_l < \mu < \mu_u$	$\sigma_l < \sigma < \sigma_u$
Peak delay vector distribution	$\mathcal{N}(1.0275, 0.1362)$	$1.0014 < \mu < 1.0537$	$0.1207 < \sigma < 0.1580$
Trough delay vector distribution	$\mathcal{N}(2.0309, 0.2383)$	$1.9850 < \mu < 2.0768$	$0.2111 < \sigma < 0.2766$

Where $\boldsymbol{\mu}$ is the mean and $\boldsymbol{\sigma}$ is the standard deviation of the normal distribution; $\boldsymbol{\mu_l}$ and $\boldsymbol{\mu_u}$ are the lower and upper bounds of the 95% confidence interval for the mean $\boldsymbol{\mu}$ and $\boldsymbol{\sigma_l}$ and $\boldsymbol{\sigma_u}$ are the lower and upper bounds of the standard deviation $\boldsymbol{\sigma}$.

5.2.5 Discussion and conclusion

The above results suggest that there are profound differences between the two measures of nasal airflow. It is visibly clear that the morphology of the two signals is different. Whilst the thermistor produces a regular sinusoidal-like waveform, the signal generated from the pressure transducer nasal cannula is more complex. The signal from the nasal cannula is more responsive and sensitive to small changes in breathing patterns, whereas, the thersmistor is slow to respond and considerably less sensitive to small physiological changes. This is not the first study to promote the use of nasal cannulae; Trang *et al.* [62] have shown that nasal cannulae outperform thermistors in detection of respiratory events, in particular, obstructive apnoea and obstructive hypopnoea; similar findings have been reported by Budhiraja *et al.* [63]. Furthermore, sensitivity of nasal cannulae offers an extra advantage in detecting UARS (upper airway resistance syndrome) [64].

Here, the relative responsiveness of the thermistor is quantified with respect to the pressure transducer nasal cannula. The results indicate that under normal (healthy, calm and regular) breathing condition, the thermistor is on average approximately one second lagging behind the pressure transducer nasal cannula and the delay profile follows a normal distribution. Furthermore, assuming that the valleys present in both signals mark the start of inspiration (end of expiration), it has been shown that inspiration starting time in each respiratory cycle measured by the thermistor is on average delayed by about two seconds (normal delay profile) relative to the inspiration starting point measured by the nasal cannula (these delays are also apparent in Figure 45). Whilst a delay of one second between the peaks can be explained by the slow response of the thermistor to thermal changes, a delay of two seconds between the troughs cannot; that is where the signal morphology and inherit differences between the methods come in to play. Each peak in the pressure transducer cannula signal is often followed by a sharp transient to a trough whereas, the same transition for the thermistor is considerably slower. Therefore, it is not clear where the actual inspiration points are located. Moreover, during the experiment, it was noticed that the inspiration to expiration duration ratio for nasal cannula was on average, 2.25 times greater than that of the thermistor (2.8 compared to 1.2). Neither of these values support what is considered a normal inspiration to expiration (I:E) ratio. A normal I:E ratio setting for mechanical ventilators mimicking normal respiration physiology can ranges from 1:1.5 to 1:4 (that is 0.67 to 0.25) [65, 66]. It is evident that both values (2.8 and 1.2) obtained in the experiment significantly exceed normal I:E ratios; this is another indication that

the true inspiration point locations may not be well defined in thermistor and nasal cannula generated signals. This is most likely an artefact of the simplistic definition of inspiration, although it is not uncommon to define inspiration as the interval between a local minimum and its successive local maximum on flow signals [15].

In short, it is concluded that the inherit difference between the two instruments can have a notable effect on the resulting RCREC parameters and should hence be accounted for.

5.3 Shifting the segmentation points - a mathematical point of view

The first study in this chapter showed that a small phase shift (≈200 msec) in the airflow signal segmentation points can noticeably affect the statistical significance of RCREC. The second study emphasised that phase shifts of this magnitude are quite common between different flow monitors. Filtering the flow signal as noted in the preliminary studies can also cause similar shifts. Given that time shifts can influence RCREC and the fact that relative time shifts between different measures of respiration are common, it was attempted to mathematically investigate the conditions under which a small shift in airflow segmentation points results in an increment of RCREC significance.

5.3.1 Why does a small shift accentuates the significance of RCREC

In order to answer this question, a subject whose relative EEG power differences were significantly increased after a small shift was selected. Table 13 shows how the statistical significance values change after shifting the segmentation points 50 samples backward in a single subject.

Table 13. RCREC significance as indicated with Fisher's F value in a single subject

	All bands	***Delta***	***Theta***	***Alpha***	***Sigma***	***Beta***
P16 F-values	*18.75*	*18.09*	*11.43*	*32.63*	*33.16*	*2.63*
P16 F-values 50 samples Backward shift	*25.85*	*22.95*	*15.95*	*37.26*	*36.42*	*5.65*

MREPs (mean relative EEG powers) of the whole spectrum (denoted as “All bands” above) for both segmentations are now considered.

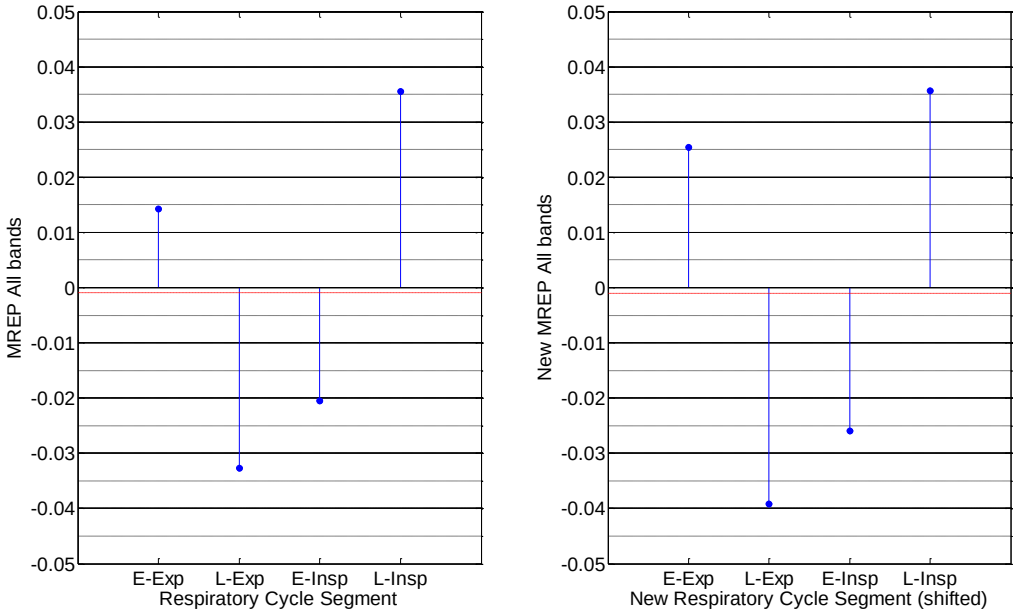

Figure 48. Mean relative EEG powers (whole spectrum) of a single subject. Left figure shows the MREPs after conventional segmentation and the right figure shows the MREPs after a small backward shift is applied to all the conventional segmentation points.

Observe that magnitudes of MREPs are noticeably increased after applying the shift, this increment is most pronounced in early expiration. In ANOVA, the F statistic is essentially defined as:

$$F = \frac{Between\ group\ variance}{Within\ group\ variance}$$

In the above subject, as it is in most, it was the "$Between\ group\ variance$" which changed after applying the shift. The "$Within\ group\ variance$" remained almost identical. Hence, the increase in the significance of RCREC can be explained by the increased between-group variability and the increase in this variability is due to the induced change in the magnitude of MREPs. In the subject above, MREP in early expiration has the most increase and therefore contributes most to the increased between group variability. This also holds for the majority of the other subjects, that is, the increased between group variability after the shift is mostly due to contribution from a single MREP. It is therefore possible to refine the original question to how does a small shift increase the mean relative EEG power? Or decrease it when the MREP is negative to begin with.

5.3.2 Condition for increment of an MREP after a phase shift

A single respiratory cycle is considered (Figure 49).

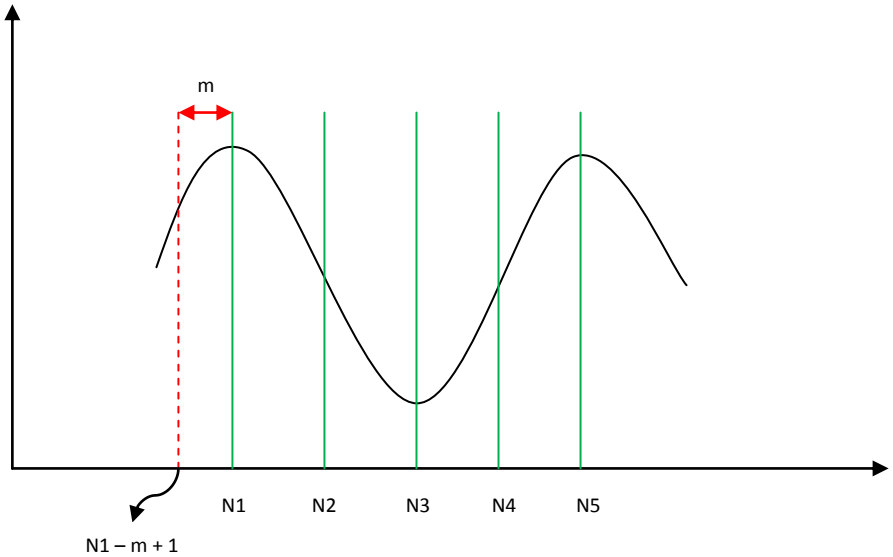

Figure 49. A single respiratory cycle. The dotted red line indicates an arbitrary "m" samples backward shift

Relative EEG power in early expiration according to the above figure is defined as:

$$S_{ee} = \frac{\frac{1}{N_2 - N_1 + 1}\sum_{i=N_1}^{N_2}|X_i|^2}{\frac{1}{N_5 - N_1 + 1}\sum_{i=N_1}^{N_5}|X_i|^2} - 1 \tag{10}$$

Where X is the "all band" EEG and S_{ee} is the relative EEG power in early expiration. N_1 to N_5 are the conventional segmentation points shown in Figure 49. All the segmentation points are then shifted by m samples to the left to define the new relative power in early expiration. This will yield:

$$S'_{ee} = \frac{\frac{1}{N_2 - N_1 + 1}\sum_{i=N_1-m+1}^{N_2-m+1}|X_i|^2}{\frac{1}{N_5 - N_1 + 1}\sum_{i=N_1-m+1}^{N_5-m+1}|X_i|^2} - 1 \tag{11}$$

Where S'_{ee} is the shifted early expiration relative EEG power. Now re-write S'_{ee} as:

$$S'_{ee} = \frac{\frac{1}{N_2 - N1 + 1}\left(\sum_{i=N_1-m+1}^{N_1-1}|X_i|^2 + \sum_{i=N_1}^{N_2}|X_i|^2 - \sum_{i=N_2-m+2}^{N_2}|X_i|^2\right)}{\frac{1}{N_5 - N_1 + 1}\sum_{i=N_1-m+1}^{N_5-m+1}|X_i|^2} - 1 \quad (12)$$

For readability define:

$$\alpha = \frac{1}{N_2 - N_1 + 1} \quad (13) \qquad \beta = \frac{1}{N_5 - N_1 + 1} \quad (14)$$

$$E_1 = \sum_{i=N_1}^{N_2}|X_i|^2 \quad (15) \qquad E_{rc} = \sum_{i=N_1}^{N_5}|X_i|^2 \quad (16)$$

$$E'_{rc} = \sum_{i=N_1-m+1}^{N_5-m+1}|X_i|^2 \quad (17) \qquad Y_1 = \sum_{i=N_1-m+1}^{N_1-1}|X_i|^2 \quad (18)$$

$$Y_2 = \sum_{i=N_2-m+2}^{N_2}|X_i|^2 \quad (19) \qquad Y_5 = \sum_{i=N_5-m+2}^{N_5}|X_i|^2 \quad (20)$$

$$Z_{ee} = S_{ee} + 1 \quad (21) \qquad Z'_{ee} = S'_{ee} + 1 \quad (22)$$

Where α is the number of samples in early expiration, β is the number of samples in entire whole respiratory cycle, E_1 is the EEG signal energy in early expiration, E_{rc} is the EEG signal energy in the whole respiratory cycle, E'_{rc} is the EEG signal energy associated with the shifted respiratory cycle, Y_1 is the EEG signal energy corresponding to the initial m samples of the shifted respiratory cycle, Y_2 is the EEG signal energy corresponding to the m samples preceding late expiration, Y_5 is the EEG signal energy corresponding to the latter m samples of the shifted respiratory cycle and, Z_{ee} and Z'_{ee} are simple transformations of the original EEG relative power equations as follows:

$$Z_{ee} = \frac{\alpha E_1}{\beta E_{rc}} \tag{23}$$

$$Z'_{ee} = \frac{\alpha(Y_1 - Y_2) + \alpha E_1}{\beta E'_{rc}} \tag{24}$$

This is done by substituting the parameters above into Equations 10 and 12. For MREP in early expiration after the shift to be greater than that before the shift, the following must be true:

$$E\{Z'_{ee} - Z_{ee}\} > 0 \tag{25}$$

Where E is the expected value operator. Equation 25 is in essence the mean difference between relative EEG powers of early expiration after and before the shift is applied. Note that from this point on, the whole ensemble of respiratory cycles are considered and therefore all the parameters are treated as random variables. Substituting for Z'_{ee} and Z_{ee} we will have:

$$E\left\{\frac{\alpha(Y_1 - Y_2) + \alpha E_1}{\beta E'_{rc}} - \frac{\alpha E_1}{\beta E_{rc}}\right\} > 0 \tag{26}$$

Rearranging the equation above, will yield:

$$E\left\{\frac{\alpha}{\beta E'_{rc}}\left[(Y_1 - Y_2) + E_1\frac{(E_{rc} - E'_{rc})}{E_{rc}}\right]\right\} > 0 \tag{27}$$

Denoting $\frac{\alpha}{\beta E'_{rc}}$ as A and $\left[(Y_1 - Y_2) + E_1\frac{(E_{rc} - E'_{rc})}{E_{rc}}\right]$ as B results in:

$$E\{AB\} > 0 \tag{28}$$

Using the covariance of AB will give:

$$C_{AB} = E\{AB\} - E\{A\}E\{B\} \tag{29}$$

$$C_{AB} + E\{A\}E\{B\} > 0 \tag{30}$$

Where C_{AB} is the covariance of A and B. Note here that $E\{A\}$ is a positive quantity and therefore inequality 30 can be written as follows:

$$E\{B\} > \frac{-C_{AB}}{E\{A\}} \tag{31}$$

Therefore, for MREP in early expiration after the shift to be greater than that before the shift, inequality 31 should hold. If the covariance of A and B is positive the right hand side of inequality 31 will be negative and consequently, inequality 31 will satisfy the condition stated in inequality 25.

$$E\{B\} > 0 \tag{32}$$

$$E\left\{\left[(Y_1 - Y_2) + \frac{E_1}{E_{rc}}(E_{rc} - E'_{rc})\right]\right\} > 0 \tag{33}$$

Therefore, a sufficient condition for MREP to increase in early expiration is that the covariance of A and B be positive. For the particular subject here C_{AB} was 0.06.

With a simple substitution and an approximation (assuming that $\frac{E_1}{E_{rc}}$ and $E_{rc} - E'_{rc}$ are uncorrelated) we can further infer that:

$$E\{(Y_1 - Y_2)\} > E\{\frac{E_1}{E_{rc}}\} \tag{34}$$

Replacing $E\{\frac{E_1}{E_{rc}}\}$ with an approximate value of 0.25, inequality 35 will emerge as:

$$E\{(Y_1 - Y_2)\} > \frac{1}{4}E\{(Y_1 - Y_5)\} \tag{35}$$

Inequality 35 states that the MREP in early expiration after the shift will be increased if the difference between Y_1 and Y_2 is on average, greater than approximately 25% of the average difference between Y_1 and Y_5. Figure below attempts to graphically clarify inequality 35. Note that the Figure only displays a single respiratory cycle and is solely provided to make the concept more tangible. Note that the above was specifically focused on an increment of MREP in

early expiration, however, the calculations can be very similarly extended to include any of the other respiratory stages.

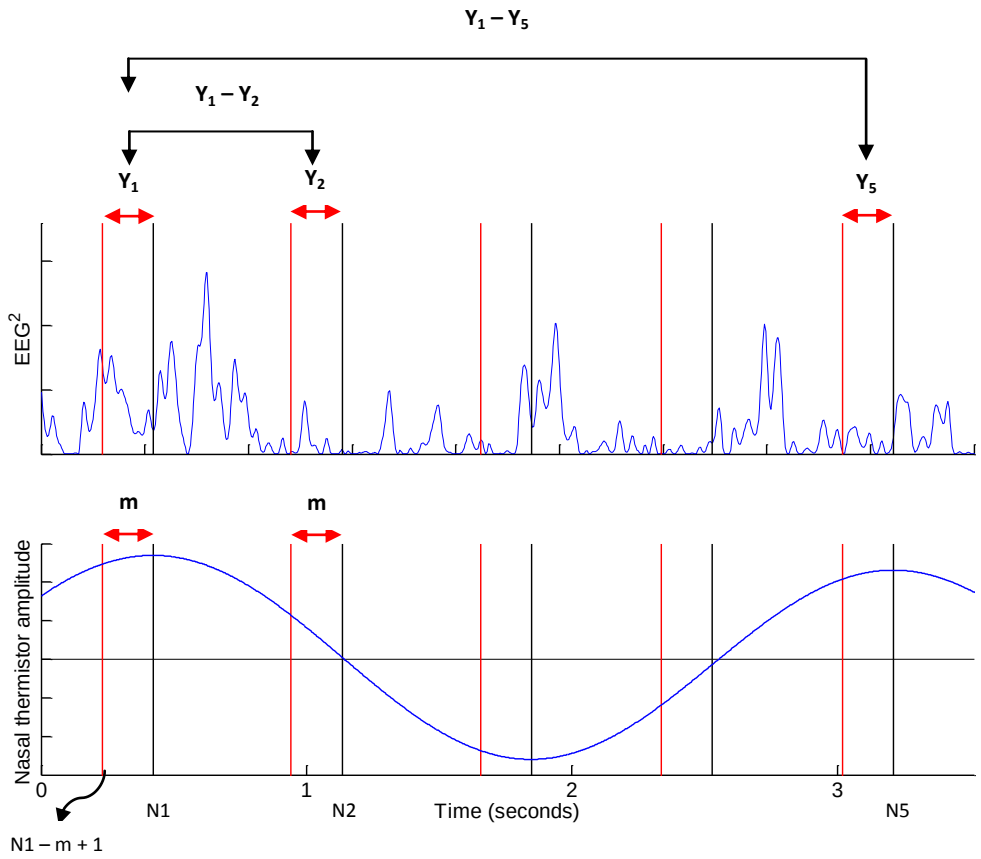

Figure 50. EEG signal energy (EEG^2) plotted together with the time-locked respiration signal. In this figure, the relationship Y1 - Y2 > 0.25(Y1 - Y5) is almost visually identifiable. Note however that this is only a single respiratory cycle and inequality 35 requires the average of all Y1 – Y2 to be greater than the average of all 0.25(Y1 – Y5). The figure is only to provide visual clarification. Also note that Y_1, Y_2 and Y_5 are those defind in Equations 18 – 20.

5.3.3 Conclusion

Here it is shown mathematically how an arbitrary shift in airflow segmentation points may increase the statistical significance of RCREC. Although the final inequality given is an approximation, it may yet provide valuable information on the mechanism of RCREC. Based on inequality 35, an increment in early expiration MREP is elicited if the difference between the energy of the initial m samples and the m samples just before the start of late expiration (N2) is greater than roughly a quarter of the difference between the energy of the initial and the latter m samples. If $Y_1 - Y_2$ was negative, and $Y_1 - Y_5$ was positive, the inequality would obviously not hold. If both the left and the right hand sides of the inequality were negative, it would still not be very likely for the inequality to hold as a quarter of $Y_1 - Y_5$ will make the right hand side

fourfold larger. If however $Y_1 - Y_2$ is positive, it is more likely for the inequality to hold as now, even where $Y_1 - Y_5$ is positive, the approximate 0.25 scaling factor works in favour of holding the inequality and decreases the right hand side. Therefore, when $E\{Y_1\} > E\{Y_2\}$, it is probable that an increment in early expiration MREP is seen. This might have a few physiological implications. In its simplest form, it can be argue that the MREP in early expiration is increased since the EEG signal energy in the initial m samples after the shift is greater than energy content of the EEG signal in the portion removed from early expiration MREP after the shift. Since the shift also accentuates the RCREC significance, it can be argued that the physiology driving RCREC is better aligned with the shifted segmentation than the conventional one. A speculation may be that the shifted segmentation accounts for most of the delay present in thermistor generated nasal flow signal and is hence more responsive to changes in respiration. This is however, assuming that respiration itself is evoking RCREC which may not be the case and hence it is left as a speculation. A worthwhile suggestion for future work may be to use a more sensitive respiratory monitor device such as the pressure transducer cannnulae for experiments.

5.4 Summary

In this chapter, effects of alternative airflow signal segmentation were assessed in details, in particular, a new segmentation routine (transition segmentation) was introduced and it was shown that the new segmentation accentuates the difference between MREPs of different respiratory cycle stages. It was further highlighted that shifting the conventional segmentation points slightly forward or backward results in a considerable change of RCREC significance. Given that a small shift in airflow signal segmentation points can produce varying RCREC parameters, it was noticed that airflow measurement instruments can introduce delays when compared to each other. As a result, relative delay profiles of the two of the most commonly used nasal flow measurement instruments were inspected. Significant differences were found between the relative delay profiles of the nasal pressure transducer cannula and the thermistor highlighting the point that use of different measurement instruments can result in differing RCREC parameters. Finally, a mathematical analysis of RCREC was carried out to determine why a shift in flow signal segmentation points can increase or decrease the significance of RCREC. As the result of this work, a mathematical condition (inequality) was derived which if satisfied, guarantees that a shift in airflow signal segmentation points results in an increment in RCREC significance. The next chapter discusses the neurobehavioral implications of RCREC.

Chapter 6

Day time neurocognitive correlates of RCREC

In the previous chapter it was revealed that alternative airflow segmentations can affect the significance of RCREC. In particular, small backward shift and transition segmentation considerably increased the significance of RCREC. Whilst that is an improvement in itself and is a step towards identification of the physiology underpinning RCREC, it does not guarantee a stronger correlation between RCREC parameters and day time neurocognition. Arguably, the most important finding to date regarding RCREC is that it can predict next day sleepiness (as measured with multiple sleep latency tests) in adults with sleep disordered breathing [16]. It was unfortunately not possible to objectively test whether the alternative segmentations improve the predictive power of RCREC as the available PSG data sets did not contain next day multiple sleep latency (MSLT) data, however, the Bolivian data described in Chapter 2 was accompanied by a number of neurocognitive measures including but not limited to: accuracy of attention, power of attention, speed of memory retrieval, quality of working and episodic memories, Wechsler intelligence scale for children (WISC) processing speed index and Ravens progressive matrices. This offered an opportunity to investigate the relationship between RCREC and day time neurocognitive functions. Furthermore, it was now possible to assess whether different airflow segmentations potentiate RCREC to better correlate with neurocognitive measures. Hence this chapter is dedicated to investigation of day time neurocognitive correlates of RCREC. It is worth re-emphasising that the information in the previous chapter empirically justified that the statistical significance of RCREC (as measured using Fisher's F value), increases when employing the small backward shift (henceforth will be referred to as "shifted segmentation") or the transition segmentation. An increment in the significance of RCREC however, may not necessarily change the magnitude of RCREC parameters. In the literature, in all the previous work involving RCREC as a predictive measure, it is the magnitude of RCREC parameters that correlate with or predict the neurocognitive measures and not their statistical significance (F values). If the increment in the statistical significance of RCREC does not at least moderately change the magnitude of RCREC parameters, then there will be little point in investigating whether RCREC calculated with our alternative flow segmentation routines can better relate to the neurobehavioral measures. Therefore, the effect of increased RCREC significance on RCREC magnitude is first briefly examined. Exploring

the potential relationship between RCREC and day time neurocognitive performance then follows.

6.1 Does Shifted/transition segmentation change RCREC magnitude?

To answer this question, the Bolivian data set described in Chapter 2 was once again employed for the analysis. PSGs with less than one thousand regular respiratory cycles or insufficient quality in either of the EEG or the flow signal were excluded from further analysis. In total, 47 subjects were selected for the subsequent analysis. RCREC parameters (magnitudes) in all the five conventional bands were calculated once using the conventional segmentation, then using the transition segmentation and finally using the shifted segmentation routines. The difference between RCREC magnitudes and transition and shifted RCREC magnitudes were statistically assessed using the paired sample t-test. The results are tabulated below. Note that we denote transition RCREC as TRCREC and shifted RCREC as SRCREC. We also use the absolute value operator notation to indicate magnitude.

Table 14. Magnitude difference between RCREC and TRCREC in a cohort of 47 subjects.

	Mean difference	***t-statistic***	***Significance (P value)***
$\|\boldsymbol{RCREC}(\boldsymbol{\delta})\| - \|\boldsymbol{TRCREC}(\boldsymbol{\delta})\|$	*-.0033*	*-1.09*	*.280*
$\|\boldsymbol{RCREC}(\boldsymbol{\theta})\| - \|\boldsymbol{TRCREC}(\boldsymbol{\theta})\|$	*-.0035*	*-1.75*	*.085*
$\|\boldsymbol{RCREC}(\boldsymbol{\alpha})\| - \|\boldsymbol{TRCREC}(\boldsymbol{\alpha})\|$	*-.0055*	*-2.36*	*.022**
$\|\boldsymbol{RCREC}(\boldsymbol{\sigma})\| - \|\boldsymbol{TRCREC}(\boldsymbol{\sigma})\|$	*-.0065*	*-2.20*	*.032**
$\|\boldsymbol{RCREC}(\boldsymbol{\beta})\| - \|\boldsymbol{TRCREC}(\boldsymbol{\beta})\|$	*.0000*	*.023*	*.981*

As can be seen in the table above, magnitude of RCREC is on average, consistently lower than that of TRCREC. Furthermore, this difference is statistically significant in the alpha and sigma bands, and is close to significance in the theta band.

Table 15. Magnitude difference between RCREC and SRCREC in a cohort of 47 subjects.

	Mean difference	***t-statistic***	***Significance (P value)***
$\|\boldsymbol{RCREC}(\boldsymbol{\delta})\| - \|\boldsymbol{SRCREC}(\boldsymbol{\delta})\|$	*-.0015*	*-.92*	*.362*
$\|\boldsymbol{RCREC}(\boldsymbol{\theta})\| - \|\boldsymbol{SRCREC}(\boldsymbol{\theta})\|$	*-.0046*	*-3.51*	*.001**
$\|\boldsymbol{RCREC}(\boldsymbol{\alpha})\| - \|\boldsymbol{SRCREC}(\boldsymbol{\alpha})\|$	*-.0063*	*-4.08*	*.000**
$\|\boldsymbol{RCREC}(\boldsymbol{\sigma})\| - \|\boldsymbol{SRCREC}(\boldsymbol{\sigma})\|$	*-.0036*	*-2.24*	*.030**
$\|\boldsymbol{RCREC}(\boldsymbol{\beta})\| - \|\boldsymbol{SRCREC}(\boldsymbol{\beta})\|$	*-.0012*	*-.88*	*.382*

Similarly, it is shown that shifted RCREC magnitudes are consistently larger than those of RCREC. Moreover, this difference is significant in three of the five conventional frequency bands. Since the distribution of RCREC/TRCREC/SRCREC magnitudes in few of the frequency bands could not be assumed to be normal (as tested using the Lilliefors test of normality [67]), the above comparisons were repeated using the paired non-parametric Wilcoxon sign rank test; the results remained largely the same, that is, the difference between RCREC and TRCREC magnitudes were significant in the alpha and sigma bands and the difference between RCREC and SRCREC magnitudes reached significance in the theta, alpha and the sigma bands.

6.1.1 Conclusion

Given that the magnitude of RCREC parameters were significantly different than those of TRCREC and SRCREC in almost three of the five conventional bands, it is sensible to include TRCREC and SRCREC parameters in predictive models of neurocognition as they may provide additional information not reflected by the RCREC parameters alone. For completeness sake, all the parameters obtained from TRCREC and SRCREC (even those not significantly different from the RCREC parameters) are included in the subsequent analysis. Also note that the magnitudes of TRCREC and SRCREC parameters are on average consistently higher than those of RCREC which is what is expected given that the statistical significance of TRCREC and SRCREC are higher than RCREC. The next logical step is to investigate any potential relationships between RCREC/TRCREC/SRCREC and day time neurocognition.

6.2 Neurcognitive correlates of RCREC, TRCREC and SRCREC

6.2.1 Motivation

The notable fact regarding RCREC is that it is one of few automatically driven measures extracted from PSG which has been shown to predict a day time consequence of SDB (sleepiness) and correlate with few neurocognitive functions [1, 16, 39]. Given the unique opportunity provided by a large matched data-set of neurocognitive and PSG data, it was possible to assess the relationship between RCREC and neurocognitive function. It was anticipated that this work would add to the existing body of literature on RCREC and may lead to discovery of new associations between RCREC and cognitive functions. Neurocognitive measures selected for this analysis are accuracy and power of attention, quality of episodic and working memories, speed of memory retrieval, WISC processing speed index and Raven progressive matrices. This selection was made based on personal communication with cognitive neuropsychologist Professor Romola S. Bucks (School of psychology, University of Western Australia). Additionally, the relationship between RCREC parameters and AHI was also revisited here. An exploratory correlation analysis was conducted on the measures above and the RCREC/TRCREC/SRCREC parameters. Pairs with significant correlation were then selected and further analysed using multiple linear regression to observe whether of RCREC parameters are capable of predicting neurocognitive functions. Confounding factors such as age and gender were also controlled for in the analysis. The rest of section two will first briefly describe the neurocognitive measures employed and give details of their acquisition procedure; it then describes the methods used in the analysis in further detail and finally presents the results of the study and attempts to discuss the implications of the obtained results.

6.2.2 Neurocognitive measures

The neurocognitive measures used in this study can be divided into two separate categories, CDR (cognitive drug research) based or non-CDR based. CDR is a computerised cognitive function assessment tool developed by Professor Keith Wenes in 1970 and has since been consistently used in clinical trials aiming to quantify cognitive deficit/improvement [68]. Accuracy and power of attention, quality of episodic and working memories and speed of memory retrieval are the CDR based neurocognitive measures used in our study and the WISC processing speed index and Ravens progressive matrices are the non-CDR based parameters. A brief description for each of the above measures is given below.

i. *CDR based neurocognitive measures*

Accuracy of attention:

Accuracy or continuity of attention reflects the ability of a subject to sustain his/her attention over a prolonged period of time. Accuracy of attention is a combined measure calculated from digit vigilance detection accuracy, choice reaction time accuracy, digit vigilance false alarms and tracking error.

Power of attention:

Power or speed of attention reflects the ability of a subject to dedicate his/her attention (focus) to a particular task for a short period of time. It is a combined measure of three independent tests namely, simple reaction time, choice reaction time and digit vigilance detection speed.

Quality of episodic memory:

Ability of a subject to encode, hold, and retrieve information. Quality of episodic memory is a combined measure calculated from immediate and delayed word recall accuracies, word recognition accuracy and picture recognition accuracy.

Quality of working memory:

Quality of working memory reflects the ability of a subject to temporarily hold numeric and spatial information. It is another combined measure quantified from the numeric working memory accuracy and spatial working memory accuracy. It is also a component of executive function.

Speed of memory retrieval:

Speed of memory retrieval reflects the speed at which a subject can decide whether something specific is stored within the working or the episodic memory. It is a combined measure calculated from picture recognition speed, word recognition speed, numerical working memory speed and spatial working memory speed.

Further information regarding the individual tests included in the CDR package can be found in [68].

ii. ***Non-CDR based neurocognitive measures***

WISC processing speed index:

Wechsler intelligence scale for children (WISC- III) processing speed index measures the ability of children (aged 6 – 16) in understanding and organising visual information. It is a combined measure taking into account motor control as well as mental processing speed and accuracy [69].

Ravens progressive matrices:

Raven's progressive matrices score (RPM) is a measure of general non-verbal intelligence. It consists of a series of multiple choice questions each asking the subject to choose a (visual) pattern which completes a bigger picture. The questions are sorted based on their difficulty and aim to quantify one's "reasoning" capability [70].

6.2.3 Neurocognitive testing procedure

Neurocognitive data collection took place within universities UPSA (Santa Cruz, 500m) and Universdad de La Salle (La Paz, 3700m). All participants were informed and had contested to take part in the study (parents contested for children). Participants attended either a morning or an afternoon session of neurocognitive data collection which included the CDR battery, Raven's progressive matrices (questionaire) and the WISC (III). All sessions were supervised by Masters of Psychology students. Participants were given a small gift for their participation.

6.2.4 Methods

The Bolivian data described previously was employed for the analysis. PSGs with less than one thousand regular respiratory cycles or insufficient quality in either of the EEG or the flow signal were excluded from further analysis. This initial sifting procedure left 47 PSGs (24M:23F) for the subsequent analysis. Since the neurocognitive data was provided as an SPSS file, RCREC related parameters were prepared and then imported into SPSS. The statistical analyses done

on the data were henceforth carried out within the SPSS software package. Details of the analyses performed on the data are described below.

i. ***Correlation analysis***

Having grouped the neurocognitive measures as well as RCREC, TRCREC and SRCREC parameters including their magnitude and significance (Fisher's F values) under a single SPSS file, an exploratory correlation analysis was conducted including all the measures to identify potential significant correlations. Since the majority of the parameters were not normally distributed, the non-parametric Spearman's Rho was used as the correlation measure. We were aware of the potential risk of type one error in our correlation analysis, however, since RCREC research is a relatively new field and there have not been many studies on day time neurobehavioral correlates of RCREC, hypothesis driven analysis of the data would not have been very practical. This study may instead serve as a pilot to discover and establish relationships between RCREC and neurocognition. Note that existence of a strong correlation between two parameters does not necessarily guarantee a relationship as it may be caused by a confounding factor. The aim of the correlation analysis is to provide an initial "guess" on what may be a correlate of RCREC. It is possible to then examine that guess further using linear regression and controlling for common confounding factors.

ii. ***Linear regression***

Having identified the potential correlates of RCREC through the correlation analysis, it is essential to ensure that the obtained results are in fact genuine. This was carried out by employing linear regression and controlling for confounding factors. Each of the neurocognitive measures found to correlate with any of the RCREC parameters was checked for common confounds including age, gender and altitude. Group differences between the neurocognitive measures for gender and altitude were assessed using the non-parametric independent samples Mann-Whitney U test. Upon finding a significant group difference, the grouping parameter (gender or altitude) was added to the regression model as an independent variable. As for age, since it correlated very significantly with almost all the neurocognitive measures (except the WISC processing index as it by definition is adjusted for age), it was included as an independent variable in almost all the regression models. Having controlled for the appropriate confounding factor, if the correlate of a particular neurocognitive measure still adds significantly to the regression model, an underlying relationship between the two parameters is assumed. Also

note that since the predictive power of regression models lower with increasing number of independent variables, the number of additional independent variables is kept minimal.

6.2.5 Results

i. *Correlation analysis*

Inclusion of the entire correlation table here is not feasible due to its sheer size, however, significant observations are reported below. Accuracy of attention correlated positively with RCREC magnitude in the delta band (rho=-.29, P=.048) and SRCREC magnitude in the same band (rho=-.33, P=.022). Quality of episodic memory correlated positively with RCREC magnitude in the theta band (rho=.32, P=.025) and TRCREC magnitude in the delta band (rho=.30, P=.036). Including the significance of RCREC as separate parameters in the correlation table also yielded some interesting results. Power of attention was found to correlate with RCREC F value in the theta, alpha and sigma bands (rho=.29, P=.043, rho=.38, P=.008 and rho=.42, P=.003 respectively). TRCREC and SRCREC F values were also found to correlate strongly with power of attention in the alpha and sigma bands, the correlation coefficient for TRCREC alpha was rho=.39, P=.006 and for sigma was rho=.37, P=.01, whilst that for SRCREC alpha was rho=.4, P=.005 and for sigma was rho=.46, P=.001. Speed of memory retrieval correlated positively with RCREC F values in the alpha band (rho=.3, P=.04) and finally, WISC processing index was found to correlate with RCREC F value in the theta band (rho=.29, P=.041). Note that all the P values provided are two sided. The tables below summarise the results obtained from the correlation analysis. Each entry in the table is a pair of correlation coefficient (Spearman's rho) and its associated statistical significance (P value). Note that none of the correlations between RCREC, TRCREC and SRCREC parameters correlated with AHI which suggests the poor ability of RCREC to reflect AHI.

Table 16. Neurocognitive measures correlating with the magnitude of RCREC, TRCREC and SRCREC parameters. Each entry is pair of correlation coefficient and its associated statistical significance (rho, P).

	Magnitude of			
	RCREC		***TRCREC***	***SRCREC***
	(δ)	**(θ)**	**(δ)**	**(δ)**
Accuracy of attention	*(.29, .048)*			*(.33, .022)*
Quality of episodic memory		*(.32, .025)*	*(.30, .036)*	

Table 17. Neurocognitive measures correlating with the significance of RCREC/TRCREC/SRCREC parameters. Each entry is pair of correlation coefficient and its associated statistical significance (rho, P).

	Significance (Fisher's F value) of							
	RCREC			***TRCREC***			***SRCREC***	
	(θ)	**(α)**	**(σ)**	**(δ)**	**(α)**	**(σ)**	**(α)**	**(σ)**
Power of attention	*(.29, .043)*	*(.38, .008)*	*(.42, .003)*		*(.39, .006)*	*(.37, .010)*	*(.40, .005)*	*(.45, .001)*
Speed of memory retrieval		*(.30, .040)*						
WISC processing speed index				*(.30, .041)*				

ii. *Regression analysis*

The results obtained above revealed significant correlations between RCREC, TRCREC and SRCREC parameters and day time neurocognitive measures. It was interesting that employing the significance of RCREC parameters as a correlate resulted in more frequent and more significant correlations. However, many of the resulting correlations may be spurious. To assess this, each of the neurocognitive measures included in Tables 16 and 17 was tested for potential

confounds. Table 18 shows the extent to which age, gender and altitude influence the neurocognitive measures.

Table 18. Potential confounds of neurocognitive measures.

	Correlation (Spearman's rho)	**Group differences (Mann-Whitney U test)**	
	Age (rho, P value)	***Gender (P value)***	***Altitude (P value)***
Accuracy of attention	*(.66, .000)**	*.004**	*.129*
Power of attention	*(-.82, .000)**	*.444*	*.716*
Quality of episodic memory	*(.54, .000)**	*.617*	*.493*
Speed of memory retrieval	*(-.80, .000)**	*.067*	*.168*
WISC processing speed index	*(-.10, .474)*	*.034**	*.018**

*Statistical significance reached

As can be seen, age correlates very strongly with all the neurocognitive measures except the WISC processing speed index which is age adjusted by definition. This implies that the subsequent regression models for accuracy and power of attention, quality of episodic memory and speed of memory retrieval must include age as an independent variable. Note that the correlation between age and the neurocognitive measures is not unexpected given the age range of our subjects (7-17 year olds). Given the strong correlation between age and the neurocognitive data, it is quite likely that the correlations found previously (Table 16 and 17) in fact reflect age. Gender and altitude can play a similar role; accuracy of attention and WISC processing speed index are shown to be significantly different between the two genders with females scoring on average higher than males in the both categories. WISC processing speed index is also significantly different between the children from low and high altitudes. Accounting for the influence of age, gender and altitude on a neurocognitive measure, if an RCREC/TRCREC/SRCREC parameter still adds significantly to the variance explained by the regression model, it may be possible to assume an underlying relationship between the two parameters.

iii. ***Significant observations:***

Having controlled for age, RCREC magnitude in the theta band was found to predict quality of episodic memory. Inclusion of theta RCREC magnitude in the regression model predicting

quality of episodic memory significantly added to the variance already explained by age (R^2 change = .350 - .256 = 9.4%, P=.015). The rest of RCREC/TRCREC/SRCREC magnitude measures did not hold a statistically significant predictive power.

Significance of RCREC, TRCREC and SRCREC parameters as measured using Fisher's F values, added significantly to the model predicting power of attention, (after controlling for age). WISC processing speed index was not affected by age but by gender and altitude. Inclusion of delta TRCREC F values in the model predicting the WISC processing index score still added significantly to the variance explained by the model even after controlling for gender and altitude. Speed of memory retrieval on the other hand, was not found to relate significantly to any of the RCREC related parameters. Table 19 summarises the significant results obtained from the regression analyses. For readability, the absolute value operator is used to denote the magnitude of an RCREC parameter and the norm operator is employed to indicate the significance of an RCREC parameter.

Table 19. Summary of the significant observations obtained from the regression analyses

	Controlled for	***Parameter added to the regression model***	***Increase in the variance explained by the model (R^2 change)***	***Significance of R^2 change (P value)***
Quality of episodic memory	*Age*	$\lvert RCREC(\theta)\rvert$	*.350 – .256 = .094*	*F=6.3, P=.015*
Power of attention	*Age*	$\lVert RCREC(\alpha)\rVert$	*.721 – .646 = .075*	*F=11.7, P=.001*
		$\lVert RCREC(\sigma)\rVert$	*.689 – .646 = .043*	*F=5.9, P=.019*
		$\lVert TRCREC(\alpha)\rVert$	*.690 – .646 = .044*	*F=6.1, P=.017*
		$\lVert TRCREC(\sigma)\rVert$	*.679 – .646 = .033*	*F=4.5, P=.039*
		$\lVert SRCREC(\alpha)\rVert$	*.716 – .646 = .070*	*F=10.7, P=.002*
		$\lVert SRCREC(\sigma)\rVert$	*.695 – .646 = .049*	*F=7.0, P=.011*
WISC processing speed index	*Gender, altitude*	$\lVert TRCREC(\delta)\rVert$	*.325 – .216 = .109*	*F=6.8, P=.012*

6.2.6 Discussion

Results presented above revealed that RCREC parameters may potentially predict certain neurocognitive functions. When looking at the magnitude of RCREC/TRCREC/SRCREC (as defined by maximum difference between frequency band specific MREPs), quality of episodic memory is the only neurocognitive measure which relates significantly to an RCREC parameter (RCREC magnitude in the theta band). When looking at the significance of RCREC/TRCREC/SRCREC (as measured using Fisher's F value generated from one way ANOVA) however, two more neurocognitive measures come into play. Magnitude of RCREC is essentially a change parameter. It measures the range between frequency bad specific MREPs across early and late expiration and inspiration. The significance of RCREC is however, a somewhat more complicated measure. It measures the relative variability of MREPs. Whilst both measures are similar in that they indicate the amount of average EEG power change over the four respiratory intervals and that are generally proportional (the higher the range, the higher the variability), they reflect different qualities. RCREC magnitude reflects the maximum change in mean relative EEG power from early expiration to late inspiration, whereas, RCERC significance, broadly speaking, reflects the variability of mean relative EEG powers between the respiratory cycle segments. RCREC magnitude is a measure essentially calculated from two of the four MREPs (i.e. maximum MREP – minimum MREP) whilst RCREC significance takes into account all the four MREPs. It is therefore not unreasonable to include the significance of RCREC parameters as predictive measures.

Power of attention was found to relate to RCREC, TRCREC and SRCREC significance in the alpha and sigma bands. It is worth noting that magnitudes and significance of RCREC, TRCREC and SRCREC parameters are often considerably inter-correlated and it therefore is not unexpected to obtain results such as those we have found and tabulated in Table 19 (where significance of RCREC, TRCREC and SRCREC in the alpha and sigma bands are all significant predictors of power of attention).

The quality of episodic memory was predicted by the magnitude of theta RCREC after controlling for age (P=.015). Episodic memory is a subset of the working memory system which deals with encoding of temporal-spatial information, that is to say, when and where something happened [71]. The relationship between theta band EEG synchronisation (an increment in EEG power when compared to a baseline) and episodic memory is well documented in the literature, in short, theta band EEG is associated with encoding of new information into episodic memory [72]. Note that the method for calculation of RCREC is in fact very similar to that used in event related synchronisation/de-synchronisation analyses [73]. In event related synchronisation

(ERS) studies, relative EEG signal power in a specific frequency band is measured before and after a particular event, this is repeated several times. Then, if the EEG power in that band is on average significantly larger after the event has occurred, we have a case of event related synchronisation; otherwise, it is an event related de-synchronisation. RCREC is different from ERS in two major aspects, 1) in RCREC analysis there is no predefined event aiming to measure a particular cognitive function and 2) whilst ERS/D analyses are performed in awake human subjects, RCREC is calculated solely from PSGs, that is, sleeping human subjects. Yet it is shown that there may be a link connecting respiratory related change of EEG power in the theta band to quality of episodic memory in sleep. Whether episodic memory and respiration are directly connected remains unknown and there is little that the literature can offer on this specific topic. However it is known that respiration (breathing) can influence the brain function. A manifest of this influence is the effect of respiration on patients with epilepsy (a brain disorder characterised by unpredictable disruptions of normal brain function [74]) where for instance slow breathing reduces the rate of epileptic seizures [75] or most people with idiopathic epilepsy are also associated with moderate to severe hyperventilation [76]. The relationship between sleep and memory consolidation is well-established, with most studies suggesting that different aspects of memory (semantic, episodic and procedural) are enhanced after an episode of sleep [8, 77]. An opposing view by Fosse *et al.* [78] suggests that episodic memory consolidation is not sleep related at all, however, the focus of that study is generally around reported recollection of dreams and not the analysis of polysomnographs and it hence is not directly comparable with the study here. Based on the above, that is, given that EEG power changes in the theta band reflect episodic memory activity in awake human subjects and that respiration can affect cognitive function and the fact that sleep plays a crucial role in memory consolidation (including episodic memory consolidation) it is not unreasonable to speculate that theta RCREC reflects to an extent the quality of encoding new information into episodic memory or shows the degree to which the recent memory traces in the episodic memory are consolidated in children.

The significance of RCREC, TRCREC and SRCREC in the alpha and sigma bands were all found to predict power of attention. As was mentioned, this is probably due to inter-correlation between these parameters. The significance of Alpha RCREC was the strongest predictor of power of attention ($F = 11.7$, $P=.001$). To ensure that the rest of the parameters indeed appear due to inter-correlation, the regression model for power of attention was expanded to include an additional independent variable. Whilst the significance of alpha RCREC was kept as the second independent variable (after age), an additional predictor of power of attention was added it to the model as the third independent variable, this procedure was repeated for all five

parameters. This is done to observe whether the different predictors add independently to the variance explained by the regression model. The overall variance explained by the multiple regression model was not significantly increased by any of the five parameters. Looking at the standardised coefficients of the models to assess the effect of each independent variable on the dependent (power of attention) would not be advised as the inter-correlated nature of the independent variables (regressors) impose a classic case of multicollinearity and therefore inaccurate model coefficient estimation [79]. A potential treatment for multicollinearity is having a-priori knowledge about the problem. Fortunately, the literature can help with providing such information in this case. Alpha band EEG power de-synchronisation is known to occur as a response to attentional demands [80-83]. These studies, as a whole, suggest that there is an established link between alpha band EEG power changes and attention. Although the details of these studies are different from the study here in various aspects such as awake vs. sleeping subjects, or slightly different definitions for the alpha band (e.g. dividing the alpha band into lower alpha, higher alpha and/or individually adjusted alpha bands) nevertheless, they are all congruent in that activity in the alpha band is related to attention. It is shown here that respiratory related changes in alpha band EEG power in normal sleeping children is a strong predictor of their general power of attention. Whilst age is negatively correlated with power of attention, that is, older children have a lower reaction time (faster response), RCREC significance in the alpha band is correlated positively with power of attention. Assuming that a higher RCREC significance reflects a larger EEG change and a lower RCREC significance reflects a lower EEG power change (stability), one may conclude that subjects with more stable breath-to-breath EEG change in the alpha band score higher in power of attention related subtests (e.g. simple reaction time, choice reaction time, etc.). Implications of this may be significant as this is the first study to show the influence of RCREC on neurocognition in a relatively large sample of normal children. This will however remain as a hypothesis which requires further research.

The potential relationship between WISC processing speed index and the significance of TRCREC in the delta band is a difficult one to interpret. This is mainly due to the relatively broad spectrum that WISC processing speed parameter covers. WISC processing speed index does not measure a single cognitive function but a combination of few. A high processing speed score requires concentration (an attentional demand) and a strong integration between subsets of the working memory. Furthermore, the measure itself can be sensitive to motivation and adaptation to work under pressure [84]. There are also no previous findings on the relationship between WISC processing speed index and delta EEG activity. If however, we interpret the WISC processing speed as an attentional demand requiring internal processing and concentration, it may be possible to justify the relationship between TRCREC delta and the WISC processing

speed. Harmony *et al.* [85], observed an increment in the delta band EEG activity during the progress of a mental task. They hypothesised that the increase in the delta band activity is an indication of attention to internal processing. A more recent study has attributed the delta band EEG activity to load on working memory (a factor in the WISC processing speed index) [86]. Whether delta TRCREC significance is truly related to WISC processing speed index remains unknown, however, the two studies mentioned above in addition to our result here, may suggest a potential link between sleep and respiratory related regulation of processing speed in the brain.

AHI and RCREC, TRCREC and SRCREC parameters were not found to significantly correlate suggesting that RCREC is not a correlate of AHI. Although it had previously been suggested that RCREC changes may be related to changes in AHI [1], the results here suggest otherwise.

6.3 Summary

In the first study done in this chapter, it was shown that transition and shifted segmentations not only increase the significance of RCREC but also increase its magnitude and hence it is sensible to use transition and shifted RCREC parameters in subsequent statistical analyses to link RCREC and neurocognition. The second study, bringing together all the previous RCREC parameters (conventional, transition and shifted) suggests that RCREC parameters may predict neurocognitive functions in normal children. The quality of episodic memory was predicted by the magnitude of RCREC in the theta band. Magnitude of theta RCREC may therefore be associated with sleep related encoding of new information into the episodic memory. Power of attention was predicted by the significance of RCREC in the alpha band. It is speculated that a low alpha RCREC significance reflects a stable breath-to-breath alpha EEG activity throughout the night and that plays a role in the general ability of children to focus their attention. In short, the more stable the alpha EEG activity in sleep, the shorter the reaction time of the children (faster response time). Transition RCREC significance in the delta band was also found to predict WISC processing speed index. The latter result is not directly supported by the literature however, important factors in brain processing speed (load on the working memory, attention to internal processing) have been reported to be correlated with delta EEG activity and hence the relation between TRCREC delta and WISC processing speed may be genuine. Last but not least, the alternative segmentations used for quantification of RCREC (i.e. TRCREC and SRCREC) helped in revealing an additional link between RCREC and neurocognition (WISC processing speed and TRCREC delta) and therefore, are advised to be kept as predictive measures in relevant future studies. No significant correlations were found between AHI and RCREC parameters.

Chapter 7

Summary and conclusions

The work done in this thesis is the collection of investigations on respiratory cycle related EEG changes (RCREC). The work can be broken down into three sections, the preliminary case studies, systematic investigation of the effects of alternative airflow segmentation on RCREC and day time neurobehavioral correlates of RCREC. The preliminary case studies include the replication of the original work in addition to two other small sample studies, one on the relationship between RCREC and apnoea-hypopnoea index (the measure used in diagnosis of OSA) and slow wave sleep (SWS), and the other on sensitivity of RCREC to slight changes in airflow segmentation. The last case study in particular, led us to investigate the influence of airflow segmentation on RCREC further. Systematic investigation of the effects of alternative airflow segmentations on RCREC include a large sample study on 7 – 17 year old children (mostly normal) in which different airflow segmentation routines were shown to dramatically affect the significance of RCREC. This section also looks at how different nasal airflow measurement instruments can influence RCREC and finally mathematically assesses how an alternative segmentation can increase RCREC significance. The last section, day time neurobehavioral correlates of RCREC, looks at how RCREC parameters can be used to predict day time neurocognitive functions in normal children. The neurocognitive measures are those obtained from a CDR (cognitive drug research) test in addition to the WISC processing speed index and the Ravens progressive matrices.

In the preliminary case studies Chervin's original work was successfully replicated (and improved) as a first step and in the first case study. In the second study, comparison of the RCREC parameters with the AHI revealed no particular pattern between frequency band specific RCREC magnitude and AHI. Two interesting correlation however emerged from the analysis of SWS. Alpha RCREC was found to negatively correlate with percentage of SWS, and beta RCREC correlated positively with SWS absolute duration. Whilst these correlations appear interesting at first it should be noted that the correlations found were marginal and the number of samples used in the study was only seven, therefore, drawing out any solid conclusion would not have been feasible. The third case study showed for the first time that RCREC can be sensitive to small changes in airflow segmentation. By filtering the airflow signal using two different filters (a standard 5^{th} order low pass Butterworth against a Savitzky-Golay filter) it was shown that

small variations in airflow signal peak/trough position estimates imposed by different filters can notably change the significance of RCREC. The Savitzky-Golay filter was found to accentuate RCREC related parameters. Furthermore, the complexity of EEG signal was calcualted in each respiratory cycle segment throughout the first three hours of the night and for each subject. Complexity of the EEG signal as calculated using sample entropy (SE) was not found to be different between respiratory cycle segments (i.e. early expiration, late expiration, etc.). Note that findings in the third case study inspired further investigation of the effects of alternative airflow signal segmentation on RCREC in a larger cohort.

In systematic investigation of the effects of airflow segmentation on RCREC it was aimed to solidly address whether changes in segmentation of airflow signal can affect RCREC and if so, why? In the first study, effect of alternative airflow segmentation on RCREC was explored in a large cohort of children (47 subjects). Statistical significance of RCREC was quantified in all frequency bands using a number of different segmentation routines, namely, transition segmentation, small shift forward and backward, and long shift forward and backward. Transition segmentation emphasises the transitions from expiration to inspiration and vice versa. Small shift forward and backward look at how application of a small (≈200 msec) but consistent phase shift to the conventional segmentation points can affect RCREC, and long shift forward and backward can assess the sensitivity of RCREC to synchronisation between the airflow and the EEG signals. It was concluded that transition and small shift backward segmentations dramatically increase the significance of RCREC whilst small shift forward and long shift forward and backward considerably decreased the significance of RCREC. The small shift forward and backward segmentations suggest once again that RCREC is sensitive to small changes in airflow segmentation and long shift (≈ 1 min) forward and backward show that the underlying synchronisation between the airflow and the EEG channels is key in quantification of RCREC. The fact that small shift backward and the transition segmentation increase the significance of RCREC may be related to the inherit delay in the thermistor flow measurement instruments. By shifting the conventional segmentation points backward, a portion of that delay is being accounted for automatically. It may also provide a better alignment with the physiology driving the RCREC and potentiate the RCREC parameters to better relate to day time neurobehavioral measures.

In the second study, to understand the delays imposed by the flow measurement instrument, a pilot study was carried out to compare two nasal airflow measurement devices, a thermistor and a pressure transducer nasal cannula. Based on 111 respiratory cycles acquired simultaneously with both devices, it was found that on average the thermistor generated peaks (start of expiration) are delayed by approximately one second, and the troughs are delayed by

approximately two seconds when compared to the pressure transducer nasal cannula. This result in addition to those previously published in the literature suggest that although delays of this magnitude are generally negligible in most sleep scoring and staging applications, it has been shown that they can significantly affect RCREC and should hence be accounted for in future RCREC related experimental designs.

In the third study of this section, given that delays in airflow data acquisition are almost impossible to avoid, and that a small shift backward increases the significance of RCREC, it was attempted to mathematically address the question of why a small backward shift increases the significance of RCREC? It was first inferred that an increment in significance of RCREC is likely to be an effect caused directly by an increment (or decrement) of the mean relative EEG power (MREP) in one of the respiratory cycle segment. The condition under which a backward shift of conventional segmentation points results in an increased MREP in one of the respiratory cycle segments was then derived. Finally, it was concluded that if the energy of the new samples added to a respiratory cycle segment after applying the shift is on average greater than the average energy of the samples removed from the same respiratory cycle segment, MREP in that respiratory cycle segment is likely to increase.

The final section of the work on RCREC is dedicated to identifying daytime neurocognitive correlates of RCREC and assessing whether RCREC calculated with alternative segmentations (transition, shifted) improves these correlations. Using the magnitude and significance of RCREC as independent variables and neurocognitive measures as dependent variables in a multiple regression model, having controlled for common confounding factors (age, gender and altitude) found three significant relations between day time neurocognition and RCREC were found. It was concluded that the quality of episodic memory was predicted by RCREC magnitude in the theta band. This result is partially supported by the literature as EEG signal power in the theta band is known to increase in response to episodic memory related tasks in awake human subjects. We speculate that theta RCREC magnitude reflects sleep and maybe respiratory related strengthening of recently established memory traces in the episodic memory. Power of attention was strongly predicted by the significance of RCREC (as measured using Fisher's F value generated from one way ANOVA) in the alpha band. Various aspects of attention are known to affect EEG signal power in the alpha band. It is therefore sensible to assume that the relationship between RCREC significance in the alpha band and power of attention is a genuine one. It was speculate that RCREC alpha significance reflects breath-to-breath stability of the EEG signal power in the alpha band and it appears that subjects with more stable alpha EEG activity during sleep score better (faster response time) in day time power of attention tests. Transition RCREC significance in the delta band was found to predict the WISC processing speed index.

Given that delta band EEG activity is related to some of the components of processing speed (working memory load and internal attention) we suggest a sleep related regulation of processing speed in the brain. Whilst transition and shifted segmentation were not found to improve the existing correlations, use of transition segmentation revealed an additional relation between RCREC and neurocognition and it may hence be worthwhile to keep transition segmented RCREC as predictive measures.

7.1 Future work

The field of RCREC research is a recently established one and therefore there is much work to be done in the area. Some of these are addressed below.

7.1.1 Major physiological driver of RCREC

The major driver of RCREC remains unknown, whilst the working hypothesis suggests that numerous micro-arousals throughout the sleep are responsible for the effect, this is in fact not proven. Further experimental and analytical work is required to understand the underlying physiological driver of RCREC. Since RCREC can be identified in as few as 101 respiratory cycles [15], miniaturised versions of the experiments could be repeated in awake subjects to clarify whether RCREC is at all a sleep specific phenomenon and gain deeper insight into its physiology. Moreover, and as mentioned, the method for calculation of RCREC bears a striking resemblance to the well established field of event related EEG synchronisation and de-synchronisation (ERS/D) [73] yet no links have so far been made between the two fields. Hence, event related synchronisation/de-synchronisation analysis of RCREC may also be of value in identifying the underlying mechanisms that generate RCREC. It was also speculated that intracranial pressure (ICP) changes may play a role in RCREC, it was intended to run a set of experiments to measure simultaneous EEG, airflow (with/without resistance) and tympanic membrane displacement (TMD) to learn more about this, but the time did not allow. This remains as a future work. Mayer waves (blood pressure related) may also be a factor in RCREC. They occur at a similar frequency as breathing and are used as a surrogate marker of sympathetic nervous system (SNS) activation. SNS activation is related to frequent micro-arousals and if the original hypothesis is true then these waves may help us prove that.

7.1.2 Potential shortcomings in RCREC quantification

There are a few points to be made on how RCREC is calculated. Although the nasal flow signal provides a relatively good indicate of where expiratory peaks and inspiratory troughs are located, it does not give their exact positions. In order to take full advantage of the physiological information embedded within the airflow signal, one needs to produce better estimates of the actual peak and trough positions. Estimating the true location of inspiration from the conventional flow signals (nasal cannula and thermistor) may therefore be beneficial in RCREC quantification. It is speculated that simultaneous use of abdominal and thoracic excursions may help in shedding more light on this matter.

Another issue is the arbitrary division of a respiratory cycle into four segments based on mid points. In alveolar pressure simulations, each respiratory cycle is divided into three segments, one for inspiration, one for a hold time and one for expiration. Therefore, as a future work, each respiratory cycle may be divided into three segments each representing a distinct physiology. Another suggestion may be to mathematically estimate the position of the segmentation points to maximise RCREC significance. If then there is consistency between the estimated segmentation points throughout sleep and in different subjects, it would provide a very valuable clue as to what the driver of RCREC is.

A rather different issue is that RCREC quantification only benefits from a single EEG lead. Whilst it is very convenient to perform multichannel RCREC analysis, so far, this has not been done in large samples. It is noted specifically that neurocognitive functions are brain region dependent, and therefore, use of multiple EEG channels is advantageous in uncovering relations between RCREC and neurocognition.

7.1.3 Individually adjusted frequency bands

As mentioned in the last chapter of the thesis, a few of the studies on event related synchronisation analysis employ an experimental method to individually adjust the frequency bands used in EEG analysis. EEG power changes in the individually adjusted bands are shown to better relate to neurocognivie functions such as attention or memory processes. This may be included in experimental designs for RCREC analysis and may reveal further information about the sleep and respiratory related regulation of neurocognition.

7.1.4 Respiratory related evoked potential (RREP) and RCREC

The relationship between RCREC and RREP was briefly assessed in the thesis. However, the study was done on a single subject. It may be worthwhile to repeat the analysis in a larger population with an objective measure to quantify the degree of similarity between RCREC and RREP (respiratory related evoked potential).

References

1. Chervin, R.D., et al., *Correlates of respiratory cycle-related EEG changes in children with sleep-disordered breathing.* Sleep, 2004. **27**(1): p. 116-121.
2. Hill, C.M., A.M. Hogan, and A. Karmiloff-Smith, *To sleep, perchance to enrich learning?* Archives of Disease in Childhood, 2007. **92**(7): p. 637-643.
3. Marcus, C.L., *Sleep-disordered breathing in children.* American Journal of Respiratory and Critical Care Medicine, 2001. **164**(1): p. 16-30.
4. Grigg-Damberger, M., et al., *The visual scoring of sleep and arousal in infants and children.* J Clin Sleep Med, 2007. **3**(2): p. 201-40.
5. Touchette, E., et al., *Associations between sleep duration patterns and behavioral/cognitive functioning at school entry.* Sleep, 2007. **30**(9): p. 1213-1219.
6. Walker, M.P. and R. Stickgold, *Sleep, Memory, and Plasticity.* Annual Review of Psychology, 2006. **57**(1): p. 139-166.
7. Krueger, J.M., et al., *Sleep as a fundamental property of neuronal assemblies.* Nature Reviews Neuroscience, 2008. **9**(12): p. 910-919.
8. Stickgold, R., *Sleep-dependent memory consolidation.* Nature, 2005. **437**(7063): p. 1272-1278.
9. Van Dongen, H.P.A., et al., *The cumulative cost of additional wakefulness: Dose-response effects on neurobehavioral functions and sleep physiology from chronic sleep restriction and total sleep deprivation.* Sleep, 2003. **26**(2): p. 117-126.
10. Cohen, A., *Time and Frequency Domains Analysis*. 1986, Florida: CRC Press, Inc.
11. Rangayyan, R.M., *Biomedical Signal Analysis, A case study approach*. 2002: Wiley Inter-Science.
12. Klem, G.H., et al., *The ten-twenty electrode system of the International Federation. The International Federation of Clinical Neurophysiology.* Electroencephalogr Clin Neurophysiol Suppl, 1999. **52**: p. 3-6.
13. Rechtschaffen, A. and A. Kales, *A manual of standardized terminology, techniques and scoring system for sleep stages of human subjects.* . National Institutes of Health (U.S.) ; no. 204. 1968: U. S. National Institute of Neurological Diseases and Blindness, Neurological Information Network.
14. Grigg-Damberger, M.M., *The AASM Scoring Manual Four Years Later.* Journal of Clinical Sleep Medicine. **8**(3): p. 323-332.
15. Chervin, R.D., et al., *Method for detection of respiratory cycle-related EEG changes in sleep-disordered breathing.* Sleep, 2004. **27**(1): p. 110-115.
16. Chervin, R.D., J.W. Burns, and D.L. Ruzicka, *Electroencephalographic Changes during Respiratory Cycles Predict Sleepiness in Sleep Apnea.* Am. J. Respir. Crit. Care Med., 2005. **171**(6): p. 652-658.
17. Bandla, H.P.R. and D. Gozal, *Dynamic changes in EEG spectra during obstructive apnea in children.* Pediatric Pulmonology, 2000. **29**(5): p. 359-365.
18. Terzano, M.G., et al., *Atlas, rules, and recording techniques for the scoring of cyclic alternating pattern (CAP) in human sleep.* Sleep Med, 2002. **3**(2): p. 187-99.
19. Rechtschaffen, A. and A. Kales, *A Manual of standardized terminology, techniques and scoring system for sleep stages of human subjects*. 1973, Los Angeles, Calif.: Brain Information Service etc.
20. Mograss, M.A., F.M. Ducharme, and R.T. Brouillette, *MOVEMENT AROUSALS - DESCRIPTION, CLASSIFICATION, AND RELATIONSHIP TO SLEEP-APNEA IN CHILDREN.* American Journal of Respiratory and Critical Care Medicine, 1994. **150**(6): p. 1690-1696.
21. Tat-Kong Wong, M., and Carole L. Marcus, MBChB, *Pediatric Scoring Challenge*, in *Sleep Review*. 2006.

22. Castronovo, V., et al., *Prevalence of habitual snoring and sleep-disordered breathing in preschool-aged children in an Italian community.* Journal of Pediatrics, 2003. **142**(4): p. 377-382.
23. O'Brien, L.M., et al., *Neurobehavioral implications of habitual snoring in children.* Pediatrics, 2004. **114**(1): p. 44-49.
24. Kaditis, A.G., et al., *Sleep-disordered breathing in 3,680 Greek children.* Pediatric Pulmonology, 2004. **37**(6): p. 499-509.
25. Carole L. Marcus, A.H., Gerald M. Loughlin,, *Natural history of primary snoring in children.* Pediatric Pulmonology, 1998. **26**(1): p. 6-11.
26. Urschitz, M.S., et al., *Habitual snoring, intermittent hypoxia, and impaired behavior in primary school children.* Pediatrics, 2004. **114**(4): p. 1041-1048.
27. Cao, M. and C. Guilleminault, *Sleep difficulties and behavioral outcomes in children.* Archives of Pediatrics & Adolescent Medicine, 2008. **162**(4): p. 385-389.
28. Kheirandish-Gozal, L., et al., *Reduced NREM sleep instability in children with sleep disordered breathing.* Sleep, 2007. **30**(4): p. 450-457.
29. Punjabi, N.M., *The Epidemiology of Adult Obstructive Sleep Apnea.* Proceedings of the American Thoracic Society, 2008. **5**(2): p. 136-143.
30. Dorland, N.W., *Dorland's Medical Dictionary for Healthcare Consumers*. 2007, Elsevier publication.
31. Fauroux, B., *What's new in paediatric sleep?* Paediatric Respiratory Reviews, 2007. **8**(1): p. 85-89.
32. Kwok, K.L., D.K. Ng, and C.H. Chan, *Cardiovascular changes in children with snoring and obstructive sleep apnoea.* Annals Academy of Medicine Singapore, 2008. **37**(8): p. 715-721.
33. O'Brien, L.M. and D. Gozal, *Autonomic dysfunction in children with sleep-disordered breathing.* Sleep, 2005. **28**(6): p. 747-752.
34. Baharav, A., et al., *Autonomic cardiovascular control in children with obstructive sleep apnea.* Clinical Autonomic Research, 1999. **9**(6): p. 345-351.
35. Schlaug, G., et al., *Training-induced Neuroplasticity in Young Children.* Neurosciences and Music Iii: Disorders and Plasticity, 2009. **1169**: p. 205-208.
36. American-Thoracic-Society, *Standards and indications for cardiopulmonary sleep studies in children.* American Journal of Respiratory and Critical Care Medicine, 1996. **153**(2): p. 866-78.
37. Iber, C., *The AASM manual for the scoring of sleep and associated events: rules, terminology and technical specifications*. 2007: American Academy of Sleep Medicine.
38. Chervin, R.D., R.K. Malhotra, and J.W. Burns, *Respiratory Cycle-Related EEG Changes during Sleep Reflect Esophageal Pressures.* Sleep, 2008. **31**(12): p. 1713-1720.
39. Chervin, R.D., et al., *System and method for analysis of respiratory cycle-related EEG changes in sleep-disordered breathing*. 2007, The Regents of the University of Michigan; Altarum Institute.
40. Chervin, R.D., A.V. Shelgikar, and J.W. Burns, *Respiratory Cycle-Related EEG Changes: Response to CPAP.* Sleep, 2012. **35**(2): p. 203-209.
41. Paruthi, S. and R.D. Chervin, *Approaches to the assessment of arousals and sleep disturbance in children.* Sleep Medicine, 2010. **11**(7): p. 622-627.
42. Howell, D., *Statistical Methods for Psychology*. 8th ed. 2011.
43. Schmider, E., et al., *Is It Really Robust? Reinvestigating the Robustness of ANOVA Against Violations of the Normal Distribution Assumption.* Methodology-European Journal of Research Methods for the Behavioral and Social Sciences, 2010. **6**(4): p. 147-151.
44. Krzanowski, W.J., *Principles of Multivariate Analysis: A user's Perspective*. Oxford Statstical Science Series. 2000: Oxford University Press.
45. Hogg, R.V., *Engineering Statistics*. 1987: Macmillan 442.
46. Gibbons, J.D., *Nonparametric Statistical Inference*. Fifth ed. Statistics: Textbooks and Monographs. 2010: Chapman and Hall.

47. Shapiro, S.S. and M.B. Wilk, *An analysis of variance test for normality (complete samples).* Biometrika, 1965. **52**(3-4): p. 591-611.
48. Dijk, D.J., D.P. Brunner, and A.A. Borbely, *Time course of EEG power density during long sleep in humans.* Am J Physiol Regul Integr Comp Physiol, 1990. **258**(3): p. R650-661.
49. Richman, J.S. and J.R. Moorman, *Physiological time-series analysis using approximate entropy and sample entropy.* Am J Physiol Heart Circ Physiol, 2000. **278**(6): p. H2039-2049.
50. Aboy, M., et al., *Characterization of sample entropy in the context of biomedical signal analysis.* 2007 Annual International Conference of the IEEE Engineering in Medicine and Biology Society, Vols 1-16, 2007: p. 5943-5946.
51. Vidaurre, C., T.H. Sander, and A. Schlögl, *BioSig: The Free and Open Source Software Library for Biomedical Signal Processing.* Computational Intelligence and Neuroscience. **2011**.
52. IEEE Acoustics, S. and D.S.P.c. Signal Processing Society, *Programs for digital signal processing*. 1979, New York: IEEE Press.
53. Marcus, C.L., et al., *Normal polysomnographic values for children and adolescents.* American Review of Respiratory Disease, 1992. **146**(5): p. 1235-1239.
54. Cohen, J., *Statistical Power Analysis for the Behavioral Sciences*. 1969, NY: Academic Press.
55. Pan, J. and W.J. Tompkins, *A Real-Time QRS Detection Algorithm.* Biomedical Engineering, IEEE Transactions on, 1985. **BME-32**(3): p. 230-236.
56. Castiglioni, P., et al., *Modulation of pulmonary arterial input impedance during transition from inspiration to expiration.* Journal of Applied Physiology, 1997. **83**(6): p. 2123-2130.
57. Murgo, J. and N. Westerhof, *Input impedance of the pulmonary arterial system in normal man. Effects of respiration and comparison to systemic impedance.* Circulation Research, 1984. **54**(6): p. 666-673.
58. Ezure, K., I. Tanaka, and Y. Saito, *Activity of Brainstem Respiratory Neurones just before the Expiration-Inspiration Transition in the Rat.* The Journal of Physiology, 2003. **547**(2): p. 629-640.
59. Xiong, C., et al., *Problems in timing of respiration with the nasal thermistor technique.* Journal of the American Society of Echocardiography : official publication of the American Society of Echocardiography, 1993. **6**(2): p. 210-6.
60. Melendres, M.C., et al., *Respiratory-related evoked potentials during sleep in children.* Sleep, 2008. **31**(1): p. 55-61.
61. Lv, J., D.A. Simpson, and S.L. Bell, *Objective detection of evoked potentials using a bootstrap technique.* Medical Engineering & Physics, 2007. **29**(2): p. 191-198.
62. Trang, H., V. Leske, and C. Gaultier, *Use of Nasal Cannula for Detecting Sleep Apneas and Hypopneas in Infants and Children.* American Journal of Respiratory and Critical Care Medicine, 2002. **166**(4): p. 464-468.
63. Budhiraja, R., et al., *Comparison of nasal pressure transducer and thermistor for detection of respiratory events during polysomnography in children.* Sleep, 2005. **28**(9): p. 1117-1121.
64. Kerl, J., D. Kohler, and B. Schonhofer, *The application of nasal and oronasal cannulas in the detection of respiratory disturbances during sleep: A review.* Somnologie - Schlafforschung und Schlafmedizin, 2002. **6**(4): p. 169-172.
65. MacIntyre, N.R., *Mechanical ventilation strategies for lung protection*. Anaesthesia, Pain, Intensive Care and Emergency Medicine - Apice 19, ed. A. Gullo. 2005, Milan: Springer-Verlag Italia. 323-330.
66. Plambeck, A. *Adult Ventilation Management*. Available from: http://www.corexcel.com/courses/vent.htm.
67. Lilliefors, H.W., *On the Kolmogorov-Smirnov Test for Normality with Mean and Variance Unknown.* Journal of the American Statistical Association, 1967. **62**(318): p. 399-402.

68. Wesnes, K.A., et al., *The memory enhancing effects of a Ginkgo biloba/Panax ginseng combination in healthy middle-aged volunteers.* Psychopharmacology, 2000. **152**(4): p. 353-361.
69. Wechsler, D., *wechsler intelligence scale for children - Forth edition*. 2003, San Antonio: Harcourt Assessment Inc. .
70. Robert M. Kaplan, D.P.S., *Psychological Testing Principles, Applications, & Issues*. 2012: Wadsworth Publishing Co Inc.
71. Tulving, E., *Precis Elements of Episodic Memory* Behavioral and Brain Sciences, 1984. **7**(2): p. 223-238.
72. Klimesch, W., *EEG alpha and theta oscillations reflect cognitive and memory performance: a review and analysis.* Brain Research Reviews, 1999. **29**(2â€“3): p. 169-195.
73. Pfurtscheller, G. and F.H. Lopes da Silva, *Event-related EEG/MEG synchronization and desynchronization: basic principles.* Clinical Neurophysiology, 1999. **110**(11): p. 1842-1857.
74. Fisher, R.S., et al., *Epileptic Seizures and Epilepsy: Definitions Proposed by the International League Against Epilepsy (ILAE) and the International Bureau for Epilepsy (IBE).* Epilepsia, 2005. **46**(4): p. 470-472.
75. Yuen, A.W.C. and J.W. Sander, *Can slow breathing exercises improve seizure control in people with refractory epilepsy? A hypothesis.* Epilepsy & Behavior, 2010. **18**(4): p. 331-334.
76. Fried, R., M.C. Fox, and R.M. Carlton, *Effect of Diaphragmatic Respiration with End-Tidal CO2 Biofeedback on Respiration, EEG, and Seizure Frequency in Idiopathic Epilepsyab.* Annals of the New York Academy of Sciences, 1990. **602**(1): p. 67-96.
77. Rauchs, G.r., et al., *Consolidation of Strictly Episodic Memories Mainly Requires Rapid Eye Movement Sleep.* Sleep: Journal of Sleep and Sleep Disorders Research, 2004. **27**(3): p. 395-401.
78. Fosse, M.J., et al., *Dreaming and Episodic Memory: A Functional Dissociation?* Journal of Cognitive Neuroscience, 2003. **15**(1): p. 1-9.
79. Damodar Gujarati, D.P., *"Multicollinearity: what happens if the regressors are correlated?" Basic Econometrics*. 4th ed. 2003: McGraw Hill.
80. Klimesch, W., et al., *Induced alpha band power changes in the human EEG and attention.* Neuroscience Letters, 1998. **244**(2): p. 73-76.
81. Ray, W.J. and H.W. Cole, *EEG alpha activity reflects attentional demands, and beta activity reflects emotional and cognitive processes.* Science, 1985. **228**(4700): p. 750-752.
82. Aftanas, L.I. and S.A. Golocheikine, *Human anterior and frontal midline theta and lower alpha reflect emotionally positive state and internalized attention: high-resolution EEG investigation of meditation.* Neuroscience Letters, 2001. **310**(1): p. 57-60.
83. Kelly, S.P., et al., *Increases in Alpha Oscillatory Power Reflect an Active Retinotopic Mechanism for Distracter Suppression During Sustained Visuospatial Attention.* Journal of Neurophysiology, 2006. **95**(6): p. 3844-3851.
84. Butnik, S.M. *Working Memory and Processing Speed in the Classroom*. Available from: http://vbida.org/PDFs/WorkingMemoryProcessingSpeedClassroom.pdf.
85. Harmony, T.a., et al., *EEG delta activity: an indicator of attention to internal processing during performance of mental tasks.* International Journal of Psychophysiology, 1996. **24**(1â€“2): p. 161-171.
86. Zarjam, P., J. Epps, and F. Chen. *Characterizing working memory load using EEG delta activity*. 2011.
87. Kubicki, S. and W.M. Herrmann, *The future of computer-assisted investigation of the polysomnogram: Sleep microstructure.* Journal of Clinical Neurophysiology, 1996. **13**(4): p. 285-294.
88. Anderer, P., et al., *Artifact processing in computerized analysis of sleep EEG - A review.* Neuropsychobiology, 1999. **40**(3): p. 150-157.

89. Walls-Esquivel, E., et al., *Electroencephalography (EEG) recording techniques and artefact detection in early premature babies.* Neurophysiologie Clinique-Clinical Neurophysiology, 2007. **37**(5): p. 299-309.
90. Brunner, D.P., et al., *Muscle artifacts in the sleep EEG: Automated detection and effect on all-night EEG power spectra.* Journal of Sleep Research, 1996. **5**(3): p. 155-164.
91. A. Hyvarinen, J.K., E. Oja, *Independent Component Analysis*. 2001: John Wiley&Sons.
92. Crespo-Garcia, M., M. Atienza, and J.L. Cantero, *Muscle artifact removal from human sleep EEG by using independent component analysis.* Annals of Biomedical Engineering, 2008. **36**(3): p. 467-475.
93. Devuyst, S., et al., *Removal of ECG artifacts from EEG using a modified independent component analysis approach.* Conf Proc IEEE Eng Med Biol Soc, 2008. **2008**: p. 5204-7.
94. Tzyy-Ping Jung, S.M., Colin Humphries, Te-Won Lee, Martin J. McKeown, Vicente Iragui Terrence J. Sejnowski, *Removing electroencephalographic artifacts by blind source separation.* Psychophysiology, 2000. **37**(2): p. 163-178.
95. Romero, S., et al. *Reduction of EEG artifacts by ICA in different sleep stages*. 2003. Cancun, Mexico: IEEE.
96. Anderer, P., et al., *Artifact processing in topographic mapping of electroencephalographic activity in neuropsychopharmacology.* Psychiatry Research-Neuroimaging, 1992. **45**(2): p. 79-93.
97. Woestenburg, J.C., M.N. Verbaten, and J.L. Slangen, *The removal of the eye-movement artifact from the EEG by regression-analysis in the frequency-domain.* Biological Psychology, 1983. **16**(1-2): p. 127-147.
98. Boxtel, A., P. Goudswaard, and L.R.B. Schomaker, *Amplitude and Bandwidth of the Frontalis Surface EMG: Effects of Electrode Parameters.* Psychophysiology, 1984. **21**(6): p. 699-707.
99. Davidson, R.J., *EEG measures of cerebral asymmetry-conceptual and methodological issues.* International Journal of Neuroscience, 1988. **39**(1-2): p. 71-89.
100. Pivik, R.T., et al., *Guidelines for the recording and quantitative-analysis of electroencephalographic activity in research contexts.* Psychophysiology, 1993. **30**(6): p. 547-558.
101. Rohalova, M., et al. *Detection of the EEG artifacts by the means of the (extended) Kalman filter*. 2001. Smolenice, Slovakia: Inst. Meas. Sci.
102. Hae-Jeong, P., J. Do-Un, and P. Kwang-Suk, *Automated detection and elimination of periodic ECG artifacts in EEG using the energy interval histogram method.* IEEE Transactions on Biomedical Engineering, 2002. **49**(12): p. 1526-1533.
103. Klekowicz, H., et al., *On the Robust Parametric Detection of EEG Artifacts in Polysomnographic Recordings.* Neuroinformatics, 2009. **7**(2): p. 147-160.
104. Paul, K., et al., *Comparison of quantitative EEG characteristics of quiet and active sleep in newborns.* Sleep Medicine, 2003. **4**(6): p. 543-552.
105. Bodenstein, G. and H.M. Praetorius, *Feature extraction from the electroencephalogram by adaptive segmentation.* Proceedings of the IEEE, 1977. **65**(5): p. 642-652.
106. Amir, N. and I. Gath, *Segmentation of EEG during sleep using time-varying autoregressive modeling.* Biological Cybernetics, 1989. **61**(6): p. 447-455.
107. Barlow, J.S., et al., *Automatic adaptive segmentation of clinical EEGs.* Electroencephalography and Clinical Neurophysiology, 1981. **51**(5): p. 512-525.
108. Barlow, J.S., *Computer characterization of trace alternant and REM-sleep patterns in the neonatal EEG by adaptive segmentation - an exploratory-study.* Electroencephalography and Clinical Neurophysiology, 1985. **60**(2): p. 163-173.
109. Krajca, V., et al., *Automatic identification of significant graphoelements in multichannel EEG recordings by adaptive segmentation and fuzzy clustering.* International Journal of Bio-Medical Computing, 1991. **28**(1-2): p. 71-89.
110. Agarwal, R. and J. Gotman, *Adaptive segmentation of electroencephalographic data using a nonlinear energy operator.* Iscas '99: Proceedings of the 1999 IEEE International Symposium on Circuits and Systems, Vol 4, 1999: p. 199-202.

111. Agarwal, R. and J. Gotman, *Computer-assisted sleep staging.* IEEE Transactions on Biomedical Engineering, 2001. **48**(12): p. 1412-1423.
112. Arnold, M., et al., *Use of adaptive Hilbert transformation for EEG segmentation and calculation of instantaneous respiration rate in neonates.* Journal of Clinical Monitoring, 1996. **12**(1): p. 43-60.
113. Barlow, J.S., *Methods of analysis of nonstationary EEGs, with emphasis on segmentation techniques - a comparative review.* Journal of Clinical Neurophysiology, 1985. **2**(3): p. 267-304.
114. Aapo Hyvärinen, E.O. *Independent Component Analysis: Algorithms and Applications*. 2000; Available from: **http://www.cs.helsinki.fi/u/ahyvarin/papers/NN00new.pdf**.
115. Lanquart, J.P., M. Dumont, and P. Linkowski, *QRS artifact elimination on full night sleep EEG.* Medical Engineering & Physics, 2006. **28**(2): p. 156-165.
116. Lee, J.H., et al., *Application of independent component analysis for the data mining of simultaneous EEG-fMRI: preliminary experience on sleep onset.* International Journal of Neuroscience, 2009. **119**(8): p. 1118-1136.
117. Park, H.J., et al., *Automated sleep stage scoring using hybrid rule- and case-based reasoning.* Computers and Biomedical Research, 2000. **33**(5): p. 330-349.
118. Hae-Jeong, P., et al. *A study on the elimination of the ECG artifact in the polysomnographic EEG and EOG using AR model*. 1998. Hong Kong, China: IEEE.
119. Kalman, R.E., *A New Approach to Linear Filtering and Prediction Problems.* Transactions of the ASME--Journal of Basic Engineering, 1960. **82**(Series D): p. 35--45.
120. Maragos, P. and R.W. Schafer, *Morphological filters .1. Their set-theoretic analysis and relations to linear shift-invariant filters.* IEEE Transactions on Acoustics Speech and Signal Processing, 1987. **35**(8): p. 1153-1169.
121. Lima, P., J. Leitao, and T. Paiva. *Artifact detection in sleep EEG recording*. 1989. Lisbon, Portugal: IEEE.
122. Schetinin, V., et al., *Comparison of the Bayesian and Randomised Decision Tree Ensembles within an Uncertainty Envelope Technique.* Journal of Mathematical Modelling and Algorithms, 2006. **5**(4): p. 397-416.
123. Schetinin, V. and C. Maple. *A Bayesian model averaging methodology for detecting EEG artifacts*. 2007. Cardiff, UK: IEEE.
124. Kaiser, J.F. *Some useful properties of Teager's energy operators*. 1993. Minneapolis, MN,: IEEE.
125. Chui, C.K., *An Introduction to Wavelets*. 1992: Academic Press, Inc.
126. Gao, J.B., et al., *Denoising Nonlinear Time Series by Adaptive Filtering and Wavelet Shrinkage: A Comparison.* IEEE Signal Processing Letters. **17**(3): p. 237-240.
127. Paul, K., et al., *Quantitative topographic differentiation of the neonatal EEG.* Clinical Neurophysiology, 2006. **117**(9): p. 2050-2058.
128. Piryatinska, A., et al., *Automated detection of neonate EEG sleep stages.* Computer Methods and Programs in Biomedicine, 2009. **95**(1): p. 31-46.
129. Krajca, V., et al. *Automatic detection of sleep stages in neonatal EEG using the structural time profiles*. 2006. Shanghai, China: IEEE.
130. Gerla, V., et al., *System Approach to Complex Signal Processing Task*, in *Computer Aided Systems Theory - Eurocast 2009*, R. MorenoDiaz, F. Pichler, and A. QuesadaArencibia, Editors. 2009, Springer-Verlag Berlin: Berlin. p. 579-586.
131. Krajca, V., et al., *Modeling the Microstructure of Neonatal EEG Sleep Stages by Temporal Profiles*, in *13th International Conference on Biomedical Engineering, Vols 1-3*, C.T. Lim and J.C.H. Goh, Editors. 2009, Springer: New York. p. 133-137.
132. Gath, I. and E. Baron, *Computerized method for scoring of polygraphic sleep recordings.* Computer Programs in Biomedicine, 1980. **11**(3): p. 217-223.
133. Gath, I., C. Feuerstein, and A. Geva, *Unsupervised classification and adaptive definition of sleep patterns.* Pattern Recognition Letters, 1994. **15**(10): p. 977-984.
134. Djordjevic, V., et al. *Feature extraction and classification of EEG sleep recordings in newborns*. 2009. Larnaca, Cyprus: IEEE.

135. Gath, I. and E. Bar-on, *Classical Sleep Stages and the Spectral Content of the EEG Signal.* International Journal of Neuroscience, 1983. **22**(1-2): p. 147-155.
136. Glavinovitch, A., M.N.S. Swamy, and E.I. Plotkin. *Wavelet-based segmentation techniques in the detection of microarousals in the sleep EEG*. 2005. Covington, KY,: IEEE.
137. Kaplan, A., et al., *Macrostructural EEG characterization based on nonparametric change point segmentation: application to sleep analysis.* Journal of Neuroscience Methods, 2001. **106**(1): p. 81-90.
138. Geering, B.A., et al., *Period-amplitude analysis and power spectral analysis: a comparison based on all-night sleep EEG recordings.* Journal of Sleep Research, 1993. **2**(3): p. 121-129.
139. Isaksson, A., A. Wennberg, and L.H. Zetterberg, *Computer-analysis of EEG signals with parametric models.* Proceedings of the IEEE, 1981. **69**(4): p. 451-461.
140. Armitage, R., et al., *A comparison of period amplitude and power spectral-analysis of sleep EEG in normal adults and depressed outpatients.* Psychiatry Research, 1995. **56**(3): p. 245-256.
141. Carrozzi, M., A. Accardo, and F. Bouquet, *Analysis of sleep-stage characteristics in full-term newborns by means of spectral and fractal parameters.* Sleep, 2004. **27**(7): p. 1384-1393.
142. Hjorth, B., *EEG analysis based on time domain properties.* Electroencephalography and Clinical Neurophysiology, 1970. **29**(3): p. 306-310.
143. Saastamoinen, A., et al., *Computer program for automated sleep depth estimation.* Computer Methods and Programs in Biomedicine, 2006. **82**(1): p. 58-66.
144. Gudmundsson, S., T.P. Runarsson, and S. Sigurdsson. *Automatic sleep staging using support vector machines with posterior probability estimates*. 2005. Vienna, Austria: IEEE.
145. Peng, C.K., et al., *Mosaic organization of DNA nucleotides.* Physical Review E, 1994. **49**(2): p. 1685-1689.
146. Jong-Min, L., et al. *Analysis of scaling exponents of waken and sleeping stage in EEG*. 2001. Granada, Spain: Springer-Verlag.
147. Shen, Y., et al., *Dimensional complexity and spectral properties of the human sleep EEG.* Clinical Neurophysiology, 2003. **114**(2): p. 199-209.
148. Jong-Min, L., et al., *Detrended fluctuation analysis of EEG in sleep apnea using MIT/BIH polysomnography data.* Computers in Biology and Medicine, 2002. **32**(1): p. 37-47.
149. Leistedt, S., et al., *Characterization of the sleep EEG in acutely depressed men using detrended fluctuation analysis.* Clinical Neurophysiology, 2007. **118**(4): p. 940-950.
150. Fell, J., et al., *Discrimination of sleep stages: A comparison between spectral and nonlinear EEG measures.* Electroencephalography and Clinical Neurophysiology, 1996. **98**(5): p. 401-410.
151. Grozinger, M., J. Fell, and J. Roschke, *Neural net classification of REM sleep based on spectral measures as compared to nonlinear measures.* Biological Cybernetics, 2001. **85**(5): p. 335-341.
152. Welch, P., *The use of fast Fourier transform for the estimation of power spectra: A method based on time averaging over short, modified periodograms.* Audio and Electroacoustics, IEEE Transactions on, 1967. **15**(2): p. 70-73.
153. Campbell, I.G., *EEG recording and analysis for sleep research.* Curr Protoc Neurosci, 2009. **Chapter 10**: p. Unit10.2.
154. Haykin, S., *Adaptive Filter Theory*. 1996: Prentice Hall.
155. Akaike, H., *New look at statistical-model identification.* IEEE Transactions on Automatic Control, 1974. **AC19**(6): p. 716-723.
156. Herrera, R.E., et al., *Vector autoregressive model selection in multichannel EEG*, in *Proceedings of the 19th Annual International Conference of the IEEE Engineering in Medicine and Biology Society, Vol 19, Pts 1-6 - Magnificent Milestones and Emerging Opportunities in Medical Engineering*. 1997, IEEE: New York. p. 1211-1214.
157. Pardey, J., S. Roberts, and L. Tarassenko, *A review of parametric modelling techniques for EEG analysis.* Medical Engineering & Physics, 1996. **18**(1): p. 2-11.

158. MathWorks, T. *Spectral Estimation Method*. Available from: http://www.mathworks.com/access/helpdesk/help/toolbox/signal/f12-6587.html#bqit7yy.
159. Subasi, A., et al., *Comparison of subspace-based methods with AR parametric methods in epileptic seizure detection.* Computers in Biology and Medicine, 2006. **36**(2): p. 195-208.
160. A. Swami, J.M.M., C.L. Nikias (1998) *Higher-Order Spectral Analysis Toolbox*.
161. Schwab, K., et al., *Time-variant parametric estimation of transient quadratic phase couplings during electroencephalographic burst activity.* Methods of Information in Medicine, 2005. **44**(3): p. 374-383.
162. Sleigh, J.W., et al., *The bispectral index: A measure of depth of sleep?* Anesthesia and Analgesia, 1999. **88**(3): p. 659-661.
163. McPherson, C., et al. *Characterization of sleep using bispectral analysis*. 2001. Istanbul, Turkey: IEEE.
164. Nieuwenhuijs, D., et al., *Bispectral index values and spectral edge frequency at different stages of physiologic sleep.* Anesthesia and Analgesia, 2002. **94**(1): p. 125-129.
165. Schwilden, H., *Concepts of EEG processing: from power spectrum to bispectrum, fractals, entropies and all that.* Best Practice & Research Clinical Anaesthesiology, 2006. **20**(1): p. 31-48.
166. G. M. Jenkins, D.G.W., *Spectral analysis and its applications*. 1968.
167. Duckrow, R.B. and H.P. Zaveri, *Coherence of the electroencephalogram during the first sleep cycle.* Clinical Neurophysiology, 2005. **116**(5): p. 1088-1095.
168. Kaminski, M., K. Blinowska, and W. Szelenberger, *Topographic analysis of coherence and propagation of EEG activity during sleep and wakefulness.* Electroencephalography and Clinical Neurophysiology, 1997. **102**(3): p. 216-227.
169. Achermann, P. and A.A. Borbely, *Coherence analysis of the human sleep electroencephalogram.* Neuroscience, 1998. **85**(4): p. 1195-1208.
170. Achermann, P. and A.A. Borbely, *Temporal evolution of coherence and power in the human sleep electroencephalogram.* Journal of Sleep Research, 1998. **7**: p. 36-41.
171. Kaminski, M.J. and K.J. Blinowska, *A new method of the description of the information-flow in the brain structures.* Biological Cybernetics, 1991. **65**(3): p. 203-210.
172. Inouye, T., et al., *Quantification of EEG irregularity by use of the entropy of the power spectrum.* Electroencephalography and Clinical Neurophysiology, 1991. **79**(3): p. 204-210.
173. Cohen, L., *Time-Frequency Analysis*. 1995, New Jersey: Prentice-Hall. 299.
174. Jobert, M., et al., *Wavelets - a new tool in sleep biosignal analysis.* Journal of Sleep Research, 1994. **3**(4): p. 223-232.
175. Durka, P.J., *From wavelets to adaptive approximations: time-frequency parametrization of EEG.* Biomed Eng Online, 2003. **2**: p. 1.
176. Zoubek, L., et al., *Feature selection for sleep/wake stages classification using data driven methods.* Biomedical Signal Processing and Control, 2007. **2**(3): p. 171-179.
177. Zygierewicz, J., et al., *High resolution study of sleep spindles.* Clinical Neurophysiology, 1999. **110**(12): p. 2136-2147.
178. Mallat, S.G. and Z.F. Zhang, *Matching pursuits with time-frequency dictionaries.* IEEE Transactions on Signal Processing, 1993. **41**(12): p. 3397-3415.
179. Durka, P.J., D.Ircha, and K.J. Blinowska, *Stochastic time-frequency dictionaries for matching pursuit.* IEEE Transactions on Signal Processing, 2001. **49**(3): p. 507-510.
180. Blinowska, K.J. and P.J. Durka, *Unbiased high resolution method of EEG analysis in time-frequency space.* Acta Neurobiologiae Experimentalis, 2001. **61**(3): p. 157-174.
181. Huupponen, E., et al., *Determination of dominant simulated spindle frequency with different methods.* Journal of Neuroscience Methods, 2006. **156**(1-2): p. 275-283.
182. Huang, N.E., et al., *The Empirical Mode Decomposition and the Hilbert Spectrum for Nonlinear and Non-Stationary Time Series Analysis.* Proceedings: Mathematical, Physical and Engineering Sciences, 1998. **454**(1971): p. 903-995.

183. Jansen, B.H., *Quantitative-analysis of electroencephalograms - is there chaos in the future.* International Journal of Bio-Medical Computing, 1991. **27**(2): p. 95-123.
184. Gallez, D. and A. Babloyantz, *Predictability of human EEG - a dynamic approach.* Biological Cybernetics, 1991. **64**(5): p. 381-391.
185. Fell, J., J. Roschke, and C. Schaffner, *Surrogate data analysis of sleep electroencephalograms reveals evidence for nonlinearity.* Biological Cybernetics, 1996. **75**(1): p. 85-92.
186. Milnor, J.W. *Attractor*. 2006; Available from: http://www.scholarpedia.org/article/Attractor.
187. Stam, C.J., *Nonlinear dynamical analysis of EEG and MEG: Review of an emerging field.* Clinical Neurophysiology, 2005. **116**(10): p. 2266-2301.
188. Bruce Henry , N.L., O Camacho, *Nonlinear Dynamics Time Series Analysis*, in *Nonlinear Biomedical Signal Processing volume 2*, M. Akay, Editor. 2001.
189. Palus, M., *Nonlinearity in normal human EEG: Cycles, temporal asymmetry, nonstationarity and randomness, not chaos.* Biological Cybernetics, 1996. **75**(5): p. 389-396.
190. Ferri, R., et al., *Non-linear EEG measures during sleep: effects of the different sleep stages and cyclic alternating pattern.* International Journal of Psychophysiology, 2002. **43**(3): p. 273-286.
191. Grassberger, P. and I. Procaccia, *Characterization of Strange Attractors.* Physical Review Letters, 1983. **50**(5): p. 346.
192. Janjarasjitt, S., M.S. Scher, and K.A. Loparo, *Nonlinear dynamical analysis of the neonatal EEG time series: The relationship between sleep state and complexity.* Clinical Neurophysiology, 2008. **119**(8): p. 1812-1823.
193. Scher, M.S., et al., *Prediction of neonatal state and maturational change using dimensional analysis.* Journal of Clinical Neurophysiology, 2005. **22**(3): p. 159-165.
194. Roeschke, J. and J. Aldenhoff, *The dimensionality of human's electroencephalogram during sleep.* Biological Cybernetics, 1991. **64**(4): p. 307-314.
195. Achermann, P., et al., *All-night sleep EEG and artificial stochastic-control signals have similar correlation dimensions.* Electroencephalography and Clinical Neurophysiology, 1994. **90**(5): p. 384-387.
196. Janjarasjitt, S., M.S. Scher, and K.A. Loparo, *Nonlinear dynamical analysis of the neonatal EEG time series: The relationship between neurodevelopment and complexity.* Clinical Neurophysiology, 2008. **119**(4): p. 822-836.
197. Kobayashi, T., et al., *Non-linear analysis of the sleep EEG.* Psychiatry and Clinical Neurosciences, 1999. **53**(2): p. 159-161.
198. Acharya, R., et al., *Non-linear analysis of EEG signals at various sleep stages.* Computer Methods and Programs in Biomedicine, 2005. **80**(1): p. 37-45.
199. Kobayashi, T., et al., *Human sleep EEG analysis using the correlation dimension.* Clinical Electroencephalography, 2001. **32**(3): p. 112-118.
200. Roschke, J. and J.B. Aldenhoff, *A nonlinear approach to brain-function - deterministic chaos and sleep EEG.* Sleep, 1992. **15**(2): p. 95-101.
201. Kobayashi, T., et al., *Analysis of the human sleep electroencephalogram by the correlation dimension.* Psychiatry and Clinical Neurosciences, 2000. **54**(3): p. 278-279.
202. Niestroj, E., I. Spieweg, and W.M. Herrmann, *On the dimensionality of sleep-EEG data - using chaos mathematics and a systematic variation of the parameters of the corex program to determine the correlation exponents of sleep EEG segments.* Neuropsychobiology, 1995. **31**(3): p. 166-172.
203. Pradhan, N. and P.K. Sadasivan, *The nature of dominant Lyapunov exponent and attractor dimension curves of EEG in sleep.* Computers in Biology and Medicine, 1996. **26**(5): p. 419-428.
204. Pradhan, N., et al., *Patterns of attractor dimensions of sleep EEG.* Computers in Biology and Medicine, 1995. **25**(5): p. 455-462.

205. Roeschke, J., *Strange attractors chaotic behavior and informational aspects of sleep EEG data.* Neuropsychobiology, 1992. **25**(3): p. 172-176.
206. Skinner, J., M. Molnar, and C. Tomberg, *The point correlation dimension: Performance with nonstationary surrogate data and noise.* Integrative Psychological and Behavioral Science, 1994. **29**(3): p. 217-234.
207. HG Schuster, W.J., *Deterministic Chaos, An introduction*. 2005: Wiley-VCH.
208. Roschke, J., J. Fell, and P. Beckmann, *The calculation of the 1st positive lyapunov exponent in sleep EEG data.* Electroencephalography and Clinical Neurophysiology, 1993. **86**(5): p. 348-352.
209. Fell, J., J. Roschke, and P. Beckmann, *Deterministic chaos and the 1st positive lyapunov exponent - a nonlinear-analysis of the human electroencephalogram during sleep.* Biological Cybernetics, 1993. **69**(2): p. 139-146.
210. Wang, X.Y., L. Chao, and M. Juan, *Nonlinear dynamic research on EEG signals in HAI experiment.* Applied Mathematics and Computation, 2009. **207**(1): p. 63-74.
211. Wolf, A., et al., *Determining lyapunov exponents from a time-series.* Physica D, 1985. **16**(3): p. 285-317.
212. Addison, P.S., *Fractals and Chaos: An illustrated course*. 1997: IOP publishing Ltd.
213. Accardo, A., et al., *Use of the fractal dimension for the analysis of electroencephalographic time series.* Biological Cybernetics, 1997. **77**(5): p. 339-350.
214. Higuchi, T., *Approach to an irregular time series on the basis of the fractal theory.* Phys. D, 1988. **31**(2): p. 277-283.
215. Katz, M.J., *Fractals and the analysis of waveforms.* Computers in Biology and Medicine, 1988. **18**(3): p. 145-156.
216. Arle, J.E. and R.H. Simon, *An application of fractal dimension to the detection of transients in the electroencephalogram.* Electroencephalography and Clinical Neurophysiology, 1990. **75**(4): p. 296-305.
217. Peiris, M.T.R., et al. *Fractal dimension of the EEG for detection of behavioural microsleeps*. 2006. Shanghai, China: IEEE.
218. Pincus, S.M., I.M. Gladstone, and R.A. Ehrenkranz, *A regularity statistic for medical data-analysis.* Journal of Clinical Monitoring, 1991. **7**(4): p. 335-345.
219. Pincus, S.M., *Approximate entropy as a measure of system-complexity.* Proceedings of the National Academy of Sciences of the United States of America, 1991. **88**(6): p. 2297-2301.
220. Pincus, S.M. and A.L. Goldberger, *Physiological time-series analysis - what does regularity quantify.* American Journal of Physiology, 1994. **266**(4): p. H1643-H1656.
221. Yang Fusheng, H.B., and Tang Qingyu, *Approximate entropy and its application in biosignal analysis*, in *Nonlinear Biomedical Signal Processing*, M. Akay, Editor. 2000, IEEE Press.
222. Ge, J., et al. *Sample entropy analysis of sleep EEG under different stages*. 2007. Beijing, China: IEEE.
223. Subha, D., et al., *EEG Signal Analysis: A Survey.* Journal of Medical Systems. **34**(2): p. 195-212.
224. Pritchard, W.S. and D.W. Duke, *Measuring chaos in the brain - a tutorial review of EEG dimension estimation.* Brain and Cognition, 1995. **27**(3): p. 353-397.
225. Darosa, A.C., et al., *A model-based detector of vertex waves and K-complexes in sleep electroencephalogram.* Electroencephalography and Clinical Neurophysiology, 1991. **78**(1): p. 71-79.
226. Pearson, K., *The problem of the Random Walk.* Nature, 1905. **72**: p. 294.
227. Cai, S.-M., et al., *Scale invariance of human electroencephalogram signals in sleep.* Phys Rev E Stat Nonlin Soft Matter Phys, 2007. **76**(6 Pt 1): p. 061903.
228. Thakor, N.V. and S.B. Tong, *Advances in quantitative electroencephalogram analysis methods.* Annual Review of Biomedical Engineering, 2004. **6**: p. 453-495.
229. Bashashati, A., et al., *A survey of signal processing algorithms in brain-computer interfaces based on electrical brain signals.* Journal of Neural Engineering, 2007. **4**(2): p. R32-R57.

230. Gerla, V., et al., *Multivariate Analysis of Full-Term Neonatal Polysomnographic Data.* IEEE Transactions on Information Technology in Biomedicine, 2009. **13**(1): p. 104-110.
231. Duffy, F.H., H. Als, and G.B. McAnulty, *Infant EEG spectral coherence data during quiet sleep: Unrestricted principal components analysis - Relation of factors to gestational age, medical risk, and neurobehavioral status.* Clinical Electroencephalography, 2003. **34**(2): p. 54-69.
232. Jobert, M., et al., *Automatic-analysis of sleep using 2 parameters based on principal component analysis of electroencephalography spectral data.* Biological Cybernetics, 1994. **71**(3): p. 197-207.
233. Jobert, M., et al., *A comparison between visual and computer assessment of sleep onset latency and their application in a pharmacological sleep study.* Sleep, 1993. **16**(3): p. 233-238.
234. Vural, C. and M. Yildiz, *Determination of Sleep Stage Separation Ability of Features Extracted from EEG Signals Using Principle Component Analysis.* Journal of Medical Systems. **34**(1): p. 83-89.
235. Goldberg, D.E., *Genetic Algorithms in Search, Optimization and Machine Learning*. 1989: Addison-Wesley Longman Publishing Co., Inc. 372.
236. Kim, B.Y. and K.S. Park. *Automatic sleep stage scoring system using genetic algorithms and neural network*. 2000. Chicago, IL,: IEEE.
237. Largo, R., et al., *CAP event detection by wavelets and GA tuning*. 2005 IEEE International Workshop on Intelligent Signal Processing. 2005, New York: IEEE. 44-48.
238. Mitra, S.K. and S.N. Sarbadhikari, *Iterative function system and genetic algorithm-based EEG compression.* Medical Engineering & Physics, 1997. **19**(7): p. 605-617.
239. Lofhede, J., et al., *Automatic classification of background EEG activity in healthy and sick neonates.* Journal of Neural Engineering. **7**(1).
240. Saccomandi, F., et al., *Automatic detection of transient EEG events during sleep can be improved using a multi-channel approach.* Clinical Neurophysiology, 2008. **119**(4): p. 959-967.
241. Figueroa Helland, V.C., et al., *Comparison of different methods for the evaluation of treatment effects from the sleep EEG of patients with major depression.* J Biol Phys, 2008. **34**(3-4): p. 393-404.
242. Mann, K., P. Backer, and J. Roschke, *Dynamical properties of the sleep EEG in different frequency bands.* International Journal of Neuroscience, 1993. **73**(3-4): p. 161-169.
243. Millan, J., O. Ozdamar, and J. Bohorquez. *Acquisition and analysis of high rate deconvolved auditory evoked potentials during sleep*. 2006. New York, NY,: IEEE.
244. Navona, C., et al., *An automatic method for the recognition and classification of the A-phases of the cyclic alternating pattern.* Clinical Neurophysiology, 2002. **113**(11): p. 1826-1831.
245. Shmiel, O., et al., *Data mining techniques for detection of sleep arousals.* Journal of Neuroscience Methods, 2009. **179**(2): p. 331-337.
246. Yu-Hsun, L., C. Yong-Sheng, and C. Li-Fen. *Automated sleep staging using single EEG channel for REM sleep deprivation*. 2009. Taichung, Taiwan: IEEE.
247. Hoffmann, R.F., et al., *Conceptual and methodological considerations towards the development of computer-controlled research on the electro-physiology of sleep.* Waking Sleeping, 1979. **3**(1): p. 1-16.
248. Uchida, S., et al., *A comparison of period amplitude analysis and FFT power spectral analysis of all-night human sleep EEG.* Physiology & Behavior, 1999. **67**(1): p. 121-131.
249. Armitage, R., et al., *Comparison of the delta-EEG in the 1st and 2nd non-REM periods in depressed adults and normal controls.* Psychiatry Research, 1992. **41**(1): p. 65-72.
250. Armitage, R., R.F. Hoffmann, and A.J. Rush, *Biological rhythm disturbance in depression: temporal coherence of ultradian sleep EEG rhythms.* Psychological Medicine, 1999. **29**(6): p. 1435-1448.
251. Armitage, R., et al., *Sex-differences in the distribution of EEG frequencies during sleep - unipolar depressed outpatients.* Journal of Affective Disorders, 1995. **34**(2): p. 121-129.

252. Armitage, R. and H.P. Roffwarg, *Distribution of period-analyzed delta activity during sleep.* Sleep, 1992. **15**(6): p. 556-561.
253. Sekimoto, M., et al., *Asymmetric interhemispheric delta waves during all-night sleep in humans.* Clinical Neurophysiology, 2000. **111**(5): p. 924-928.
254. Tan, X., I.G. Campbell, and I. Feinberg, *Internight reliability and benchmark values for computer analyses of non-rapid eye movement (NREM) and REM EEG in normal young adult and elderly subjects.* Clinical Neurophysiology, 2001. **112**(8): p. 1540-1552.
255. Kedem, B., *Spectral-analysis and discrimination by zero-crossings.* Proceedings of the IEEE, 1986. **74**(11): p. 1477-1493.
256. Holzmann, C.A., et al., *Expert-system classification of sleep/waking states in infants.* Medical & Biological Engineering & Computing, 1999. **37**(4): p. 466-476.
257. Doman, J., et al., *Automating the sleep laboratory - implementation and validation of digital recording and analysis.* International Journal of Bio-Medical Computing, 1995. **38**(3): p. 277-290.
258. Estevez, P.A., et al., *Polysomnographic pattern recognition for automated classification of sleep-waking states in infants.* Medical & Biological Engineering & Computing, 2002. **40**(1): p. 105-113.
259. Scher, M.S., et al., *Computer analyses of EEG-sleep in the neonate - methodological considerations.* Journal of Clinical Neurophysiology, 1990. **7**(3): p. 417-441.
260. Pfurtscheller, G., D. Flotzinger, and K. Matuschik, *Sleep classification in infants based on artificial neural networks.* Biomedizinische Technik, 1992. **37**(6): p. 122-130.
261. Estrada, E.F., H. Nazeran, and H. Ochoa. *HRV and EEG Signal Features for Computer-Aided Detection of Sleep Apnea*. 2009. Miami, FL,: Springer-Verlag.
262. Novak, D., et al. *Speech recognition methods applied to biomedical signals processing*. 2004. San Francisco, CA,: IEEE.
263. Pacheco, O.R. and F. Vaz. *Integrated system for analysis and automatic classification of sleep EEG*. 1998. Hong Kong, China: IEEE.
264. Redmond, S.J. and C. Heneghan, *Cardiorespiratory-based sleep staging in subjects with obstructive sleep apnea.* IEEE Transactions on Biomedical Engineering, 2006. **53**(3): p. 485-496.
265. Dumont, M., et al., *Scale-free dynamics of the synchronization between sleep EEG power bands and the high frequency component of heart rate variability in normal men and patients with sleep apnea-hypopnea syndrome.* Clinical Neurophysiology, 2007. **118**(12): p. 2752-2764.
266. Rosa, A.C., L. Parrino, and M.G. Terzano, *Automatic detection of cyclic alternating pattern (CAP) sequences in sleep: preliminary results.* Clinical Neurophysiology, 1999. **110**(4): p. 585-592.
267. Jobert, M., et al., *Pattern-recognition by matched filtering - an analysis of sleep spindle and K-complex density under the influence of lormetazepam and zopiclone.* Neuropsychobiology, 1992. **26**(1-2): p. 100-107.
268. Jobert, M., et al., *Topographical analysis of sleep spindle activity.* Neuropsychobiology, 1992. **26**(4): p. 210-&.
269. Marsalek, K. and J. Rozman, *Recognition of transient phenomena in a biosignal.* Radioengineering, 2000. **9**(1): p. 1-3.
270. Ahmed, B., A. Redissi, and R. Tafreshi, *An automatic sleep spindle detector based on wavelets and the Teager energy operator.* Conf Proc IEEE Eng Med Biol Soc, 2009. **2009**: p. 2596-9.
271. Duman, F., et al., *Efficient sleep spindle detection algorithm with decision tree.* Expert Systems with Applications, 2009. **36**(6): p. 9980-9985.
272. Athanasios Papoulis, S.U.P., *Probability, Random Variales and Stochastic Processes*. 4 ed. 2002.
273. Beauseroy, P. and E. Grall-Maes. *Data driven feature extraction based on parameterized transformations of representation space*. 2002. Yasmine Hammamet, Tunisia: IEEE.

274. Grall-Maes, E., P. Beauseroy, and S.P.S.I.S.P.S. Ieee, *Features extraction for signal classification based on Wigner-Ville distribution and mutual information criterion*. Proceedings of the IEEE-Sp International Symposium on Time-Frequency and Time-Scale Analysis. 1998, New York: IEEE. 589-592.
275. Tsallis, C., *Possible generalization of Boltzmann-Gibbs statistics.* Journal of Statistical Physics, 1988. **52**(1): p. 479-487.
276. Korotchikova, I., et al., *EEG in the healthy term newborn within 12 hours of birth.* Clinical Neurophysiology, 2009. **120**(6): p. 1046-1053.
277. De Gennaro, L., et al., *Slow eye movements and EEG power spectra during wake-sleep transition.* Clinical Neurophysiology, 2000. **111**(12): p. 2107-2115.
278. Michel, C.J., *A computer method for identifying patterns in electroencephalogram signals.* Journal of Medical Engineering & Technology, 2003. **27**(6): p. 267-275.
279. Piarulli, A., et al., *Likeness-Based Detection of Sleep Slow Oscillations in Normal and Altered Sleep Conditions: Application on Low-Density EEG Recordings.* IEEE Transactions on Biomedical Engineering. **57**(2): p. 363-372.
280. Uchida, S., et al., *Computerization of Fujimori's method of waveform recognition - A review and methodological considerations for its application to all-night sleep EEG.* Journal of Neuroscience Methods, 1996. **64**(1): p. 1-12.
281. Scher, M.S., et al., *Functional brain maturation in neonates as measured by EEG-sleep analyses.* Clinical Neurophysiology, 2003. **114**(5): p. 875-882.
282. Scher, M.S., et al., *Comparisons of EEG spectral and correlation measures between healthy term and preterm infants.* Pediatric Neurology, 1994. **10**(2): p. 104-108.
283. Huupponen, E., et al., *Development and comparison of four sleep spindle detection methods.* Artificial Intelligence in Medicine, 2007. **40**(3): p. 157-170.
284. Huupponen, E., et al., *Automatic analysis of electro-encephalogram sleep spindle frequency throughout the night.* Medical & Biological Engineering & Computing, 2003. **41**(6): p. 727-732.
285. Huupponen, E., et al. *Comparison of fuzzy reasoning and autoassociative MLP in sleep spindle detection*. 2000. Tampere, Finland: Tampere Univ. Technology.
286. Huupponen, E., et al., *Autoassociative MLP in sleep spindle detection.* J Med Syst, 2000. **24**(3): p. 183-93.
287. Huupponen, E., et al., *Optimization of sigma amplitude threshold in sleep spindle detection.* Journal of Sleep Research, 2000. **9**(4): p. 327-334.
288. Myers, M.M., et al., *A novel quantitative measure of Trace-alternant EEG activity and its association with sleep states of preterm infants.* Developmental Psychobiology, 1997. **31**(3): p. 167-174.
289. Okumura, A., et al., *Amplitude spectral analysis of maturational changes of delta waves in preterm infants.* Brain & Development, 2003. **25**(6): p. 406-410.
290. Baraglia, D.P., et al., *Automated sleep scoring and sleep apnea detection in children*, in *Complex Systems*, A. Bender, Editor. 2006, SPIE- Soc Photo-Optical Instumentation Engineering: Bellingham. p. T390-T390.
291. Scher, M.S., et al., *Computer classification of sleep in preterm and full-term neonates at similar postconceptional term ages.* Sleep, 1996. **19**(1): p. 18-25.
292. Baumgart-Schmitt, R., *Device and method for determining sleep profiles*. 2001, 2RCW GmbH, Berlin, Germany.
293. Haejeong, P., P. Kwangsuk, and J. Do-Un. *Hybrid neural-network and rule-based expert system for automatic sleep stage scoring*. 2000. Chicago, IL,: IEEE.
294. Tian, J.Y. and J.Q. Liu, *Automated sleep staging by a hybrid system comprising neural network and fuzzy rule-based reasoning*, in *2005 27th Annual International Conference of the IEEE Engineering in Medicine and Biology Society, Vols 1-7*. 2005, IEEE: New York. p. 4115-4118.
295. Van Hese, P., et al. *Automatic detection of sleep stages using the EEG*. 2001. Istanbul, Turkey: IEEE.

296. Bruni, O., et al., *All-night EEG power spectral analysis of the cyclic alternating pattern at different ages.* Clinical Neurophysiology, 2009. **120**(2): p. 248-256.
297. Accardo, A.P., et al. *Comparison between spectral and fractal EEG analyses of sleeping newborns*. 1998. Hong Kong, China: IEEE.
298. Werth, E., et al., *Spindle frequency activity in the sleep EEG: individual differences and topographic distribution.* Electroencephalography and Clinical Neurophysiology, 1997. **103**(5): p. 535-542.
299. Alvarez, D., et al., *Spectral analysis of electroencephalogram and oximetric signals in obstructive sleep apnea diagnosis.* Conf Proc IEEE Eng Med Biol Soc, 2009. **2009**: p. 400-3.
300. Liu, D.R., Z.Y. Pang, and S.R. Lloyd, *A neural network method for detection of obstructive sleep apnea and narcolepsy based on pupil size and EEG.* IEEE Transactions on Neural Networks, 2008. **19**(2): p. 308-318.
301. Xavier, P., et al. *Detecting electroencephalography variations due to sleep disordered breathing events*. 2007. Lyon, France: IEEE.
302. Alvarez-Estevez, D. and V. Moret-Bonillo, *Model comparison for the detection of EEG arousals in sleep apnea patients.* Bio-Inspired Systems: Computational and Ambient Intelligence. Proceedings 10th International Work-Conference on Artificial Neural Networks, IWANN 2009, 2009: p. 997-1004|xlix+1356.
303. Bertini, M., et al., *Directional information flows between brain hemispheres during presleep wake and early sleep stages.* Cerebral Cortex, 2007. **17**(8): p. 1970-1978.
304. Bodizs, R., et al., *The individual adjustment method of sleep spindle analysis: Methodological improvements and roots in the fingerprint paradigm.* Journal of Neuroscience Methods, 2009. **178**(1): p. 205-213.
305. Buysse, D.J., et al., *EEG Spectral Analysis in Primary Insomnia: NREM Period Effects and Sex Differences.* Sleep, 2008. **31**(12): p. 1673-1682.
306. Corsi-Cabrera, M., M.A. Guevara, and Y. del Rio-Portilla, *Brain activity and temporal coupling related to eye movements during REM sleep: EEG and MEG results.* Brain Research, 2008. **1235**: p. 82-91.
307. Crainiceanu, C.M., et al., *Nonparametric Signal Extraction and Measurement Error in the Analysis of Electroencephalographic Activity During Sleep.* Journal of the American Statistical Association, 2009. **104**(486): p. 541-555.
308. Dumont, M., et al., *Interdependency between heart rate variability and sleep EEG: linear/non-linear?* Clinical Neurophysiology, 2004. **115**(9): p. 2031-2040.
309. Ferri, R., et al., *The time course of high-frequency bands (15-45 Hz) in all-night spectral analysis of sleep EEG.* Clinical Neurophysiology, 2000. **111**(7): p. 1258-1265.
310. Grozinger, M., et al., *Online detection of REM sleep based on the comprehensive evaluation of short adjacent EEG segments by artificial neural networks.* Progress in Neuro-Psychopharmacology & Biological Psychiatry, 1997. **21**(6): p. 951-963.
311. Grozinger, M., J. Roschke, and B. Kloppel, *Automatic recognition of rapid eye-movement (REM) sleep by artificial neural networks.* Journal of Sleep Research, 1995. **4**(2): p. 86-91.
312. Huupponen, E., et al., *Fuzzy detection of EEG alpha without amplitude thresholding.* Artificial Intelligence in Medicine, 2002. **24**(2): p. 133-147.
313. Ktonas, P.Y., I. Fagioli, and P. Salzarulo, *Delta (0.5-1.5 hz) and sigma (11.5-15.5 hz) EEG power dynamics throughout quiet sleep in infants.* Electroencephalography and Clinical Neurophysiology, 1995. **95**(2): p. 90-96.
314. Morikawa, T., M. Hayashi, and T. Hori, *Auto power and coherence analysis of delta-theta band EEG during the waking-sleeping transition period.* Electroencephalography and Clinical Neurophysiology, 1997. **103**(6): p. 633-641.
315. Morikawa, T., M. Hayashi, and T. Hori, *Spatiotemporal variations of alpha and sigma band EEG in the waking-sleeping transition period.* Perceptual and Motor Skills, 2002. **95**(1): p. 131-154.

316. Schramm, D., et al., *Spectral analysis of electroencephalogram during sleep-related apneas in pre-term and term born infants in the first weeks of life.* Clinical Neurophysiology, 2000. **111**(10): p. 1788-1791.
317. Thordstein, M., et al., *Spectral analysis of burst periods in EEG from healthy and post-asphyctic full-term neonates.* Clinical Neurophysiology, 2004. **115**(11): p. 2461-2466.
318. Estrada, E., et al., *EEG feature extraction for classification of sleep stages*, in *Proceedings of the 26th Annual International Conference of the Ieee Engineering in Medicine and Biology Society, Vols 1-7*. 2004, IEEE: New York. p. 196-199.
319. Zhovna, I. and I.D. Shallom, *Automatic detection and classification of sleep stages by multichannel EEG signal modeling*, in *2008 30th Annual International Conference of the IEEE Engineering in Medicine and Biology Society, Vols 1-8*. 2008, IEEE: New York. p. 2665-2668.
320. Pan, X.L. and T. Ogawa, *Microstructure of longitudinal 24 hour electroencephalograms in healthy preterm infants.* Pediatrics International, 1999. **41**(1): p. 18-27.
321. Acir, N. and C. Guzelis, *Automatic recognition of sleep spindles in EEG by using artificial neural networks.* Expert Systems with Applications, 2004. **27**(3): p. 451-458.
322. Asyali, M.H., et al., *Determining a continuous marker for sleep depth.* Computers in Biology and Medicine, 2007. **37**(11): p. 1600-1609.
323. Benoit, O., A. Daurat, and J. Prado, *Slow (0.7-2 Hz) and fast (2-4 Hz) delta components are differently correlated to theta, alpha and beta frequency bands during NREM sleep.* Clinical Neurophysiology, 2000. **111**(12): p. 2103-2106.
324. Tufts, D.W. and R. Kumaresan, *Estimation of frequencies of multiple sinusoids: Making linear prediction perform like maximum likelihood.* Proceedings of the IEEE, 1982. **70**(9): p. 975-989.
325. Fortunato, E., et al. *Combining time frequency representation and parametric analysis for the enhancement of transients in sleep EEG signal*. 2001. Istanbul, Turkey: IEEE.
326. Olbrich, E. and P. Achermann, *Analysis of the Temporal Organization of Sleep Spindles in the Human Sleep EEG Using a Phenomenological Modeling Approach.* Journal of Biological Physics, 2008. **34**(3-4): p. 341-349.
327. Olbrich, E. and T. Wennekers, *Dynamics of parameters of neurophysiological models from phenomenological EEG modeling.* Neurocomputing, 2007. **70**(10-12): p. 1848-1852.
328. Roberts, S. and L. Tarassenko. *Analysis of the human EEG using self-organising neural nets*. 1992. London, UK: IEE.
329. Roberts, S. and L. Tarassenko, *Analysis of the sleep eeg using a multilayer network with spatial-organization.* IEE Proceedings-F Radar and Signal Processing, 1992. **139**(6): p. 420-425.
330. Roberts, S. and L. Tarassenko, *New method of automated sleep quantification.* Medical & Biological Engineering & Computing, 1992. **30**(5): p. 509-517.
331. Zamora, M., L. Tarassenko, and I.E.E. Iee, *The study of micro-arousals using neural network analysis of the EEG*, in *Ninth International Conference on Artificial Neural Networks*. 1999, Inst Electrical Engineers Inspec Inc: Edison. p. 625-630.
332. Caspary, O., et al., *Enhanced high resolution spectral analysis of sleep spindles*. Proceedings of the 16th Annual International Conference of the IEEE Engineering in Medicine and Biology Society - Engineering Advances: New Opportunities for Biomedical Engineers, Pts 1&2, ed. N.F. Sheppard, M. Eden, and G. Kantor. 1994, New York: IEEE. 1232-1233.
333. Caspary, O. and P. Nus, *Adaptive spectral analysis of Sleep Spindles based on subspace tracking*, in *Proceedings of the 18th Annual International Conference of the IEEE Engineering in Medicine and Biology Society, Vol 18, Pts 1-5*, H. Boom, et al., Editors. 1997, IEEE: New York. p. 976-977.
334. Schwab, K., et al., *On the rhythmicity of quadratic phase coupling in the trace alternant EEG in healthy neonates.* Neuroscience Letters, 2004. **369**(3): p. 179-182.
335. Akgul, T., et al., *Characterization of sleep spindles using higher order statistics and spectra.* IEEE Transactions on Biomedical Engineering, 2000. **47**(8): p. 997-1009.

336. Romero, S., et al. *Analysis of sleep spindles in different NREM-REM cycles by means of bispectra*. 2002. Houston, TX,: IEEE.
337. Hayashi, K., et al., *Ketamine increases the frequency of electroencephalographic bicoherence peak on the alpha spindle area induced with propofol.* British Journal of Anaesthesia, 2007. **99**(3): p. 389-395.
338. Ning, T.K. and J.D. Bronzino, *Autoregressive and bispectral analysis techniques - EEG applications.* IEEE Engineering in Medicine and Biology Magazine, 1990. **9**(1): p. 47-50.
339. Witte, H., et al., *Analysis of the interrelations between a low-frequency and a high-frequency signal component in human neonatal EEG during quiet sleep.* Neuroscience Letters, 1997. **236**(3): p. 175-179.
340. Nunez, P.L., et al., *EEC coherency II: experimental comparisons of multiple measures.* Clinical Neurophysiology, 1999. **110**(3): p. 469-486.
341. Cvetkovic, D., I. Cosic, and Ieee, *Sleep Onset Estimator: Evaluation of Parameters*, in *2008 30th Annual International Conference of the IEEE Engineering in Medicine and Biology Society, Vols 1-8*. 2008, IEEE: New York. p. 3860-3863.
342. Grieve, P.G., et al., *EEG functional connectivity in term age extremely low birth weight infants.* Clinical Neurophysiology, 2008. **119**(12): p. 2712-2720.
343. Khandoker, A.H., C.K. Karmakar, and M. Palaniswami. *Interaction between sleep EEG and ECG signals during and after obstructive sleep apnea events with or without arousals*. 2008. Bologna, Italy: IEEE.
344. Rezek, I.A. and S.J. Roberts, *Stochastic complexity measures for physiological signal analysis.* IEEE Transactions on Biomedical Engineering, 1998. **45**(9): p. 1186-1191.
345. Wei-Xing, H., et al. *Nonlinear feature extraction of sleeping EEG signals*. 2006. Shanghai, China: IEEE.
346. Ferenets, R., et al., *Comparison of the properties of EEG spindles in sleep and propofol anesthesia.* Conf Proc IEEE Eng Med Biol Soc, 2006. **1**: p. 6356-9.
347. Huupponen, E., et al., *Anteroposterior difference in EEG sleep depth measure is reduced in apnea patients.* J Med Syst, 2005. **29**(5): p. 527-38.
348. Huupponen, E., et al., *Improved computational fronto-central sleep depth parameters show differences between apnea patients and control subjects.* Medical & Biological Engineering & Computing, 2009. **47**(1): p. 3-10.
349. Eiselt, M., et al., *Quantitative analysis of discontinuous EEG in premature and full-term newborns during quiet sleep.* Electroencephalography and Clinical Neurophysiology, 1997. **103**(5): p. 528-534.
350. Smith, J.O., *Mathematics of the Discrete Fourier Transform (DFT) with audio applicationn*. 2007.
351. Melges, D.B., et al., *Using the Discrete Hilbert Transform for the comparison between Trace Alternant and High Voltage Slow patterns extracted from full-term neonatal EEG*, in *World Congress on Medical Physics and Biomedical Engineering 2006, Vol 14, Pts 1-6*, S.I. Kim and T.S. Suh, Editors. 2007, Springer-Verlag Berlin: Berlin. p. 1111-1114.
352. Xanthopoulos, P., et al. *Modeling the time-varying micro structure of simulated sleep EEG spindles using time-frequency analysis methods*. 2006. New York, NY,: IEEE.
353. Kong, X., N. Thakor, and V. Goel. *Characterization of EEG signal changes via Itakura distance*. in *Engineering in Medicine and Biology Society, 1995., IEEE 17th Annual Conference*. 1995.
354. Ebrahimi, F., et al., *Assessment of Itakura Distance as a valuable feature for computer-aided classification of sleep stages.* Conf Proc IEEE Eng Med Biol Soc, 2007. **2007**: p. 3300-3.
355. Estrada, E., et al. *Itakura distance: a useful similarity measure between EEG and EOG signals in computer-aided classification of sleep stages*. 2006. Shanghai, China: IEEE.
356. Held, C.M., et al. *Dual approach for automated sleep spindles detection within EEG background activity in infant polysomnograms*. 2004. San Francisco, CA,: IEEE.
357. Aijun, H., et al. *Phase synchronization in sleep electroencephalogram*. 2007. Beijing, China: IEEE.

358. Berthomier, C., J. Prado, and O. Benoit, *EEG analysis using non-uniform oversampled filter banks.* Biomed Sci Instrum, 1997. **34**: p. 119-24.
359. Doering, A., et al., *Adaptable preprocessing units and neural classification for the segmentation of EEG signals.* Methods of Information in Medicine, 1999. **38**(3): p. 214-224.
360. Tang, W.C., et al., *Harmonic Parameters with HHT and Wavelet Transform for Automatic Sleep Stages Scoring*, in *Proceedings of World Academy of Science, Engineering and Technology, Vol 22*, C. Ardil, Editor. 2007, World Acad Sci, Eng & Tech-Waset: Canakkale. p. 414-417.
361. Gharieb, R.R. and A. Cichocki. *On-line EEG classification and sleep spindles detection using an adaptive recursive bandpass filter*. 2001. Salt Lake City, UT,: IEEE.
362. Gharieb, R.R. and A. Cichocki, *Segmentation and tracking of the electro-encephalogram signal using an adaptive recursive bandpass filter.* Medical & Biological Engineering & Computing, 2001. **39**(2): p. 237-248.
363. Hao, Y.L., Y. Ueda, and N. Ishii, *Improved procedure of complex demodulation and an application to frequency-analysis of sleep spindles in EEG.* Medical & Biological Engineering & Computing, 1992. **30**(4): p. 406-412.
364. Ktonas, P.Y., et al., *Potential dementia biomarkers based on the time-varying microstructure of sleep EEG spindles.* 2007 Annual International Conference of the Ieee Engineering in Medicine and Biology Society, Vols 1-16, 2007: p. 2464-2467.
365. Ishii, N., et al., *Computer classification of the EEG time-series by Kullback information measure.* International Journal of Systems Science, 1980. **11**(6): p. 677-687.
366. Negin, M. and J. Nicholas. *Phase locked loop detection of sigma spindles from the electroencephalogram*. 1971. Las Vegas, NV: Alliance for Engineering in Medicine and Biology.
367. Swarnkar, V., U.R. Abeyratne, and A.S. Karunajeewa. *Left-right information flow in the brain during EEG arousals*. 2006. New York, NY,: Ieee.
368. Takizawa, Y., et al., *Electroencephalogram analysis based on the instantaneous maximum entropy method*, in *Isie '97 - Proceedings of the IEEE International Symposium on Industrial Electronics, Vols 1-3*. 1997, IEEE: New York. p. 978-982.
369. Uchida, S., et al., *Human sleep electroencephalogram analysis based on the instantaneous maximum entropy method.* Ieice Transactions on Fundamentals of Electronics Communications and Computer Sciences, 1997. **E80A**(6): p. 965-970.
370. De Carli, F., et al., *A method for the automatic detection of arousals during sleep.* Sleep, 1999. **22**(5): p. 561-572.
371. Akin, A. and T. Akgul, *Detection of sleep spindles by discrete wavelet transform*, in *Proceedings of the IEEE 24th Annual Northeast Bioengineering Conference*, S. Wolpert, W.J. Weiss, and R.P. Gaumond, Editors. 1998, IEEE: New York. p. 15-17.
372. Ebrahimi, F., et al., *Automatic Sleep Stage Classification Based on EEG Signals by Using Neural Networks and Wavelet Packet Coefficients*, in *2008 30th Annual International Conference of the Ieee Engineering in Medicine and Biology Society, Vols 1-8*. 2008, IEEE: New York. p. 1151-1154.
373. Maeda, M., et al., *Time-frequency analysis of human sleep EEG and its application to feature extraction about biological rhythm*. Proceedings of Sice Annual Conference, Vols 1-8. 2007, New York: IEEE. 1934-1939.
374. Lin, R., et al., *A new approach for identifying sleep apnea syndrome using wavelet transform and neural networks.* Biomedical Engineering, Applications Basis Communications, 2006. **18**(3): p. 138-143.
375. Sezgin, N. and M.E. Tagluk, *Energy based feature extraction for classification of sleep apnea syndrome.* Computers in Biology and Medicine, 2009. **39**(11): p. 1043-1050.
376. Tagluk, M.E., M. Akin, and N. Sezgin, *Classification of sleep apnea by using wavelet transform and artificial neural networks.* Expert Systems with Applications, 2009. **37**(2): p. 1600-1607.

377. Mikaili, M. and S. Golpayegani, *Assessment of the complexity/regularity of transient brain waves (EEG) during sleep, based on wavelet theory and the concept of entropy.* Iranian Journal of Science and Technology, 2002. **26**(B4): p. 639-646.
378. Sinha, R.K., *Artificial neural network and wavelet based automated detection of sleep spindles, REM sleep and wake states.* Journal of Medical Systems, 2008. **32**(4): p. 291-299.
379. Tang, Z.W. and N. Ishii, *Detection of the K-complex using a new method of recognizing wave-form based on the discrete wavelet transform.* Ieice Transactions on Information and Systems, 1995. **E78D**(1): p. 77-85.
380. Durka, P.J., et al., *Multichannel matching pursuit and EEG inverse solutions.* Journal of Neuroscience Methods, 2005. **148**(1): p. 49-59.
381. Durka, P.J., et al., *Explicit parameterization of sleep EEG transients.* Computers in Biology and Medicine, 2007. **37**(4): p. 534-541.
382. Durka, P.J., et al., *Adaptive time-frequency parametrization in pharmaco EEG.* Journal of Neuroscience Methods, 2002. **117**(1): p. 65-71.
383. Durka, P.J. and K.J. Blinowska, *Analysis of eeg transients by means of Matching Pursuit* Annals of Biomedical Engineering, 1995. **23**(5): p. 608-611.
384. Durka, P.J., et al., *High resolution parametric description of slow wave sleep.* Journal of Neuroscience Methods, 2005. **147**(1): p. 15-21.
385. Durka, P.J. and K.J. Blinowska, *A unified time-frequency parametrization of EEGs.* IEEE Engineering in Medicine and Biology Magazine, 2001. **20**(5): p. 47-53.
386. Malinowska, U., et al., *Micro- and macrostructure of sleep EEG - A universal, adoptive time-frequency parameterization.* IEEE Engineering in Medicine and Biology Magazine, 2006. **25**(4): p. 26-31.
387. Malinowska, U., et al., *Fully Parametric Sleep Staging Compatible with the Classical Criteria.* Neuroinformatics, 2009. **7**(4): p. 245-253.
388. Schonwald, S.V., et al., *Benchmarking matching pursuit to find sleep spindles.* Journal of Neuroscience Methods, 2006. **156**(1-2): p. 314-321.
389. Cho, S.P., et al. *Detection of arousals in patients with respiratory sleep disorders using a single channel EEG*. 2006. Shanghai, China: IEEE.
390. Kokkinos, V., et al., *The hypnospectrogram: An EEG power spectrum based means to concurrently overview the macroscopic and microscopic architecture of human sleep.* Journal of Neuroscience Methods, 2009. **185**(1): p. 29-38.
391. Vivaldi, E.A. and A. Bassi. *Frequency domain analysis of sleep EEG for visualization and automated state detection*. 2006. New York, NY: IEEE.
392. Zygierewicz, J., et al., *Event-related desynchronization and synchronization in evoked K-complexes.* Acta Neurobiologiae Experimentalis, 2009. **69**(2): p. 254-261.
393. Yang, Z.H., L.H. Yang, and D.X. Qi, *Detection of spindles in sleep EEGs using a novel algorithm based on the Hilbert-Huang transform*, in *Wavelet Analysis and Applications*, Q. Tao, V. Mang, and Y. Xu, Editors. 2007, Birkhauser Boston: Cambridge. p. 543-559.
394. Yi, L., et al., *Sleep stage classification based on EEG Hilbert-Huang transform.* 2009 4th IEEE Conference on Industrial Electronics and Applications, 2009: p. 3676-81.
395. Mingui, S., et al., *Localizing functional activity in the brain through time-frequency analysis and synthesis of the EEG.* Proceedings of the IEEE, 1996. **84**(9): p. 1302-1311.
396. Martens, W.L.J., *The Fast Time-Frequency Transform (FTFT) - a novel online approach to the instantaneous spectrum.* Proceedings of the Annual International Conference of the IEEE Engineering in Medicine and Biology Society, Vol 14, Pts 1-7, 1992. **14**: p. 2594-2595.
397. Martens, W.L.J. *Segmentation of `rhythmic' and `noisy' components of sleep EEG, heart rate and respiratory signals based on instantaneous amplitude, frequency, bandwidth and phase*. 1999. Atlanta, GA,: Ieee.
398. Choi, H.I. and W.J. Williams, *Improved time-frequency representation of multicomponent signals using exponential kernels.* IEEE Transactions on Acoustics Speech and Signal Processing, 1989. **37**(6): p. 862-871.

399. Richard, C. and R. Lengelle, *Joint time and time-frequency optimal detection of K-complexes in sleep EEG.* Computers and Biomedical Research, 1998. **31**(3): p. 209-229.
400. Takens, F., *Detecting strange attractors in turbulence*, in *Dynamical Systems and Turbulence, Warwick 1980*. 1981. p. 366-381.
401. Ferri, R., et al., *Correlation dimension of EEG slow-wave activity during sleep in children and young adults.* Electroencephalography and Clinical Neurophysiology, 1998. **106**(5): p. 424-428.
402. Achermann, P., et al., *CORRELATION DIMENSION OF THE HUMAN SLEEP ELECTROENCEPHALOGRAM - CYCLIC CHANGES IN THE COURSE OF THE NIGHT.* European Journal of Neuroscience, 1994. **6**(3): p. 497-500.
403. Burioka, N., et al., *Relationship between correlation dimension and indices of linear analysis in both respiratory movement and electroencephalogram.* Clinical Neurophysiology, 2001. **112**(7): p. 1147-1153.
404. Cerf, R., et al., *Boublet-split-scaling of correlation integrals in nonlinear dynamics and in neurobiology.* Biological Cybernetics, 1992. **68**(2): p. 115-124.
405. Pradhan, N., et al. *Analysis of the chaotic characteristics of sleep EEG patterns from dominant Lyapunov exponents*. 1995. New Delhi, India: Ieee.
406. Akay, M., *Nonlinear Biomedical Signal Processing, Volume 2, Dynamic Analysis and Modeling*, ed. M. Akay. 2001: Wiley-IEEE Press.
407. Raghavendra, B.S., D.N. Dutt, and Ieee, *Multiresolution Area-based Fractal Dimension Estimation of Signals Applied to EEG Data*, in *2008 IEEE Region 10 Conference: Tencon 2008, Vols 1-4*. 2008, Ieee: New York. p. 661-665.
408. In-Ho, S., et al. *Multiscale characteristics of human sleep EEG time series*. 2006. Reading, UK: Springer-Veralg.
409. Ma, Q.L., et al., *Sleep-stage characterization by nonlinear EEG analysis using wavelet-based multifractal formalism*, in *2005 27th Annual International Conference of the IEEE Engineering in Medicine and Biology Society, Vols 1-7*. 2005, IEEE: New York. p. 4526-4529.
410. Song, I.H., et al. *Multifractal analysis of sleep EEG dynamics in humans*. 2007. Kohala Coast, HI,: IEEE.
411. Bruce, E.N., M.C. Bruce, and S. Vennelaganti, *Sample Entropy Tracks Changes in Electroencephalogram Power Spectrum With Sleep State and Aging.* Journal of Clinical Neurophysiology, 2009. **26**(4): p. 257-266.
412. Stam, C.J. and B.W. van Dijk, *Synchronization likelihood: an unbiased measure of generalized synchronization in multivariate data sets.* Physica D-Nonlinear Phenomena, 2002. **163**(3-4): p. 236-251.
413. Eckmann, J.P., S.O. Kamphorst, and D. Ruelle, *Recurrence plots of dynamic-systems.* Europhysics Letters, 1987. **4**(9): p. 973-977.
414. Gautama, T., D.P. Mandic, and M.M. Van Hulle, *The delay vector variance method for detecting determinism and nonlinearity in time series.* Physica D: Nonlinear Phenomena, 2004. **190**(3-4): p. 167-176.
415. Mo, C., et al. *A novel tool for sequential fusion of nonlinear features: a sleep psychology application*. 2006. Heidelberg, Germany: IEEE.
416. Kosanovic, B.R., L.F. Chaparro, and R.J. Sclabassi. *Signal modeling with dynamic fuzzy sets*. 1996. Atlanta, GA,: IEEE.
417. Mukesh, D. and R.Y. Nadkar, *Neural network modelling of human electroencephalogram patterns.* Current Science, 1997. **72**(4): p. 261-265.
418. Pereda, E. and J.J. Gonzalez, *Nonlinear Dynamical Analysis of the Interdependence Between Central and Autonomic Nervous Systems in Neonates During Sleep.* Journal of Biological Physics, 2008. **34**(3-4): p. 405-412.
419. Titchener, M.R. *T-entropy of EEG/EOG sensitive to sleep state*. 2006. Bologna, Italy: Research Society of Nonlinear Theory and its Applications.
420. Poree, F., et al., *Blind source separation for ambulatory sleep recording.* IEEE Transactions on Information Technology in Biomedicine, 2006. **10**(2): p. 293-301.

421. Barros, A.K., et al., *Extraction of sleep-spindles from the electroencephalogram (EEG)*, in *Artificial Neural Networks in Medicine and Biology*, H. Malmgren, M. Borga, and L. Niklasson, Editors. 2000, Springer-Verlag London Ltd: Godalming. p. 125-130.
422. Ventouras, E.M., et al., *Independent components of sleep spindles*, in *2007 Annual International Conference of the IEEE Engineering in Medicine and Biology Society, Vols 1-16*. 2007, IEEE: New York. p. 4002-4005.
423. Ventouras, E.M., et al. *Slow and fast EEG sleep spindle component extraction using Independent Component Analysis*. 2008. Athens, Greece: IEEE.
424. Pascual-Marqui, R.D., C.M. Michel, and D. Lehmann, *Low resolution electromagnetic tomography: a new method for localizing electrical activity in the brain.* International Journal of Psychophysiology, 1994. **18**(1): p. 49-65.
425. HervÃ, A. and J.W. Lynne, *(in press, 2010). Wiley Interdisciplinary Reviews: Computational Statistics, 2 Principal Component Analysis*. 2009.
426. Lopes da Silva, F.H., et al., *Model of brain rhythmic activity.* Biological Cybernetics, 1974. **15**(1): p. 27-37.
427. Rosa, A.C. and L.J. Allen. *Fuzzy classification of microstructural dynamics of human sleep*. 1996. Beijing, China: IEEE.
428. Kemp, B. and H.A.P. Blom, *Optimal detection of the alpha state in a model of the human electroencephalogram.* Electroencephalography and Clinical Neurophysiology, 1981. **52**(2): p. 222-225.
429. Darosa, A.C. and T. Paiva, *Automatic detection of K-complexes - validation in normals and dysthymic patients.* Sleep, 1993. **16**(3): p. 239-248.
430. Kemp, B., et al., *An optimal monitor of the electroencephalographic sigma-sleep state.* Biological Cybernetics, 1985. **51**(4): p. 263-270.
431. Kemp, B., et al., *Analysis of a sleep-dependent neuronal feedback loop: The slow-wave microcontinuity of the EEG.* IEEE Transactions on Biomedical Engineering, 2000. **47**(9): p. 1185-1194.
432. Martins, N. and A.C. Rosa. *EEG non-stationary spectrum analysis and feature extraction*. 1996. Beijing, China: IEEE.
433. Wang, D.L., *Object selection based on oscillatory correlation.* Neural Networks, 1999. **12**(4-5): p. 579-592.
434. Leistritz, L., et al., *Coupled oscillators for modeling and analysis of EEG/MEG oscillations.* Biomedizinische Technik, 2007. **52**(1): p. 83-89.
435. Haykin, S., *Neural Networks: A Comprehensive Foundation*. 1994: Prentice Hall PTR. 768.
436. Shimada, T., T. Shiina, and Y. Saito. *Sleep stage diagnosis system with neural network analysis*. 1998. Hong Kong, China: Ieee.
437. Robert, C., J.F. Gaudy, and A. Limoge, *Electroencephalogram processing using neural networks.* Clinical Neurophysiology, 2002. **113**(5): p. 694-701.
438. Bishop, C.M., *Neural Networks for Pattern Recognition*. 1995: Oxford University Press, Inc. 482.
439. Mitchell, T.M., *Machine learning and data mining.* Commun. ACM, 1999. **42**(11): p. 30-36.
440. Cybenko, G., *Approximation by superpositions of a sigmoidal function.* Mathematics of Control, Signals, and Systems (MCSS), 1989. **2**(4): p. 303-314.
441. Balakrishnan, D. and S. Puthusserypady. *Multilayer perceptrons for the classification of brain computer interface data*. in *Bioengineering Conference, 2005. Proceedings of the IEEE 31st Annual Northeast*. 2005.
442. Teuvo Kohonen, T.H. *Kohonen network*. 2007; Available from: http://www.scholarpedia.org/article/Kohonen_network.
443. Kohonen, T., *Self-organized formation of topologically correct feature maps.* Biological Cybernetics, 1982. **43**(1): p. 59-69.
444. Kohonen, T., *The self-organizing map.* Proceedings of the IEEE, 1990. **78**(9): p. 1464-1480.
445. Kohonen, T., *Self-organizing maps*. 2001: Springer.

446. Fisher, R., *The use of multiple measurements in taxonomic problems.* Annals Eugen., 1936. **7**: p. 179-188.
447. D. Michie, D.J.S., C.C. Taylor, ed. *Machine learning, neural and statistical classification*. 1994, Ellis Horwood. 289.
448. Devroye, L., L. G, and G. Lugosi, *A Probabilistic Theory of Pattern Recognition (Stochastic Modelling and Applied Probability)*. 1996: Springer.
449. Vapnik, V.N., *Statistical Learning Theory*, ed. S. Haykin. 1998: Wiley Inter-Science.
450. Lotte, F., et al., *A review of classification algorithms for EEG-based brain-computer interfaces.* Journal of Neural Engineering, 2007. **4**(2): p. R1-R13.
451. Cho, S.P., et al., *Detection of EEG Arousals in Patients with Respiratory Sleep Disorder*, in *World Congress on Medical Physics and Biomedical Engineering 2006, Vol 14, Pts 1-6*, S.I. Kim and T.S. Suh, Editors. 2007, Springer-Verlag Berlin: Berlin. p. 1131-1134.
452. Burges, C.J.C., *A Tutorial on Support Vector Machines for Pattern Recognition.* Data Min. Knowl. Discov., 1998. **2**(2): p. 121-167.
453. Rabiner, L.R., *A tutorial on hidden Markov models and selected applications in speech recognition.* Proceedings of the IEEE, 1989. **77**(2): p. 257-286.
454. Rabiner, L. and B. Juang, *An introduction to hidden Markov models.* ASSP Magazine, IEEE, 1986. **3**(1): p. 4-16.
455. Flexer, A., et al., *An automatic, continuous and probabilistic sleep stager based on a hidden Markov model.* Applied Artificial Intelligence, 2002. **16**(3): p. 199-207.
456. Zadeh, L.A., *Fuzzy sets.* Information and Control, 1965. **8**: p. 338-353.
457. Gath, I. and A.B. Geva, *Unsupervised optimal fuzzy clustering.* IEEE Transactions on Pattern Analysis and Machine Intelligence, 1989. **11**(7): p. 773-781.
458. JC Bezdek, S.P., ed. *Fuzzy Models for Pattern Recognition: Background, Significance, and key points*. Fuzzy Models for Pattern Recognition 1992, IEEE Press.
459. Jain, A.K., M.N. Murty, and P.J. Flynn, *Data clustering: a review.* ACM Comput. Surv., 1999. **31**(3): p. 264-323.
460. Held, C.M., et al., *Extracting fuzzy rules from polysomnographic recordings for infant sleep classification.* IEEE Transactions on Biomedical Engineering, 2006. **53**(10): p. 1954-1962.
461. Bankman, I.N., et al., *Feature-based detection of the K-complex wave in the human electroencephalogram using neural networks.* IEEE Transactions on Biomedical Engineering, 1992. **39**(12): p. 1305-1310.
462. Strungaru, C. and M.S. Popescu, *Neural network for sleep EEG K-complex detection.* Biomed Tech (Berl), 1998. **43 Suppl 3**: p. 113-6.
463. Gevins, A.S., R.K. Stone, and S.D. Ragsdale, *Differentiating the effects of 3 benzodiazepines on non-REM sleep EEG spectra - a neural-network pattern-classification analysis.* Neuropsychobiology, 1988. **19**(2): p. 108-115.
464. Siegwart, D.K., et al. *Sleep apnoea analysis from neural network post-processing*. 1995. Cambridge, UK: IEE.
465. McGrogan, N., E. Braithwaite, and L. Tarassenko. *BioSleep: a comprehensive sleep analysis system*. 2001. Istanbul, Turkey: IEEE.
466. Sykacek, P., et al., *Improving biosignal processing through modeling uncertainty: Bayes vs, non-Bayes in sleep staging.* Applied Artificial Intelligence, 2002. **16**(5): p. 395-421.
467. Ventouras, E., et al. *Detection of EEG sleep spindles using backpropagation multilayer perceptrons*. 2001. Pula, Croatia: Univ. Zagreb.
468. Ventouras, E.M., et al., *Sleep spindle detection using artificial neural networks trained with filtered time-domain EEG: A feasibility study.* Computer Methods and Programs in Biomedicine, 2005. **78**(3): p. 191-207.
469. Schwaibold, M.H., et al. *Combination of AI components for biosignal processing application to sleep stage recognition*. 2001. Istanbul, Turkey: IEEE.
470. Berger, A., D.P.F. Moller, and M. Renter. *Detection of sleep with new preprocessing methods for EEG analysing*. 1997. Dortmund, Germany: Springer-Verlag.

471. Golz, M., et al. *Classification of pre-stimulus EEG of K-complexes using competitive learning networks*. 1998. Aachen, Germany: Verlag Mainz.
472. Shimada, T., T. Shiina, and Y. Saito, *Detection of characteristic waves of sleep EEG by neural network analysis.* IEEE Transactions on Biomedical Engineering, 2000. **47**(3): p. 369-379.
473. Shimada, T. and T. Shiina, *Detection of characteristic waves of sleep EEG by neural network analysis.* 1995 IEEE Engineering in Medicine and Biology 17th Annual Conference and 21 Canadian Medical and Biological Engineering Conference, 1997.
474. Anderer, P., et al., *An E-health solution for automatic sleep classification according to Rechtschaffen and Kales: Validation study of the Somnolyzer 24 x 7 utilizing the Siesta database.* Neuropsychobiology, 2005. **51**(3): p. 115-133.
475. Galhanone, P.R., et al. *Multivariate analysis of neonatal EEG in different sleep stages: methods and preliminary results*. 1997. Montreal, Que., Canada: IEEE.
476. Merica, H. and J.M. Gaillard, *The EEG of the sleep onset period in insomnia - a discriminant-analysis.* Physiology & Behavior, 1992. **52**(2): p. 199-204.
477. Flexer, A., G. Gruber, and G. Dorffner, *A reliable probabilistic sleep stager based on a single EEG signal.* Artificial Intelligence in Medicine, 2005. **33**(3): p. 199-207.
478. Kam, A., et al. *Detection of K-complexes in sleep EEG using CD-HMM*. 2004. San Francisco, CA,: IEEE.
479. Kosanovic, B.R., L.F. Chaparro, and R.J. Sclabassi. *Hidden process modeling*. 1995. Detroit, MI,: IEEE.
480. Navarro-Mesa, J.L., et al., *On the determination of differences between good and bad sleepers by means of a hidden Markov model.* WSEAS Transactions on Computers Research, 2006. **1**(2): p. 321-324.
481. Hanaoka, M., M. Kobayashi, and H. Yamazaki, *Automatic sleep stage scoring based on waveform recognition method and decision-tree learning.* Systems and Computers in Japan, 2002. **33**(11): p. 1-13.
482. Huupponen, E., et al. *Improving reliability in sleep spindle detection*. 2001. Rhodes, Greece: ACTA Press.
483. Principe, J.C., S.K. Gala, and T.G. Chang, *Sleep staging automaton based on the theory of evidence.* IEEE Transactions on Biomedical Engineering, 1989. **36**(5): p. 503-509.
484. Barcaro, U., et al., *A general automatic method for the analysis of NREM sleep microstructure.* Sleep Medicine, 2004. **5**(6): p. 567-576.
485. Heiss, J.E., et al., *Classification of sleep stages in infants: A neuro fuzzy approach.* IEEE Engineering in Medicine and Biology Magazine, 2002. **21**(5): p. 147-151.
486. Pohl, V. and E. Fahr. *Neuro-fuzzy recognition of K-complexes in sleep EEG signals*. 1997. Montreal, Que., Canada: IEEE.
487. Shafer, G., *A Mathematical Theory of Evidence*. 1976: Princeton University Press.
488. Lafferty, J.D., A. McCallum, and F.C.N. Pereira, *Conditional Random Fields: Probabilistic Models for Segmenting and Labeling Sequence Data*, in *Proceedings of the Eighteenth International Conference on Machine Learning*. 2001, Morgan Kaufmann Publishers Inc.
489. Luo, G. and W. Min, *Subject-adaptive real-time sleep stage classification based on conditional random field.* AMIA Annu Symp Proc, 2007: p. 488-92.
490. Alan V. Oppenheim, A.S.W., with S. Hamid, *Signals and Systems*. 1997: Prentice Hall. 957 pages.
491. Feuerstein, D., K.H. Parker, and M.G. Boutelle, *Practical Methods for Noise Removal: Applications to Spikes, Nonstationary Quasi-Periodic Noise, and Baseline Drift.* Analytical Chemistry, 2009. **81**(12): p. 4987-4994.
492. Tukey, J.W., *Exploratory Data Analysis*. 1976. 688.
493. Widrow, B., et al., *Adaptive Noise Cancelling - Principles and Applications.* Proceedings of the IEEE, 1975. **63**(12): p. 1692-1716.
494. Aapo Hyvärinen, J.K., Erkki Oja, *Independent Component Analysis*. 2001: John Wiley & Sons.

495. James, C.J., O. Gibson, and M. Davies, *On the analysis of single versus multiple channels of electromagnetic brain signals.* Artificial Intelligence in Medicine, 2006. **37**(2): p. 131-143.
496. James, C.J. and C.W. Hesse, *Independent component analysis for biomedical signals.* Physiological Measurement, 2005. **26**(1): p. R15-R39.
497. James, C.J. and O.J. Gibson, *Temporally constrained ICA: An application to artifact rejection in electromagnetic brain signal analysis.* IEEE Transactions on Biomedical Engineering, 2003. **50**(9): p. 1108-1116.
498. James, C.J. and D. Lowe, *Extracting multisource brain activity from a single electromagnetic channel.* Artificial Intelligence in Medicine, 2003. **28**(1): p. 89-104.
499. Mathworks, T. *Periodogram*. 2009; Available from: http://www.mathworks.com/access/helpdesk/help/toolbox/signal/periodogram.html.
500. Alan V. Oppenheim, R.W.S., John R. Buck, *Discrete-Time Signal Processing*. 2nd ed. 1999: Prentice Hall.
501. Papoulis, A., *Probability, Random Variables and Stochastic Processes*. 4th edition ed. 2001: McGraw-Hill.
502. Akay, M., *Time frequency and wavelets in biomedical signal processing*. IEEE press series in Biomedical Engineering. 1998: IEEE Press.
503. Bruce, E.N., *Biomedical Signal Processing and Signal Modelling*. Wiley series in Telecommunication and Signal Processing. 2001.

Appendix

Appendix A

Application of signal processing to human sleep EEG- A review

Sleep EEG signals have been a valuable source of information for decades. Much of the information inferred from these signals to date, are acquired through visual inspection. Signal processing techniques are mathematical tools which unveil further information about signals which may be hidden otherwise. However, choosing an appropriate method for a particular application can often be difficult. This section aims to provide a thorough overview of signal processing techniques applied to the analysis of sleep EEG signals.

Introduction

Understanding and measuring brain activity in sleep is an exciting frontier of neuroscience and polysomnography (PSG) provides a data-rich source for understanding sleep in both health and disease. Signal processing allows extraction of detailed information from such signals. Applications of these methods in relation to sleep EEG range from simple time and frequency domain analysis to implementation of sophisticated nonlinear pattern recognition and classification algorithms. Kubicki *et al.* [87] emphasize that going beyond the well-known and commonly used Rechtschaffen and Kales scoring criteria [13] will not be possible without the use of signal processing techniques and computer aided analysis to unveil further information on microstructure of sleep. The body of literature developed for the analysis of sleep EEG is huge and therefore this review provides a synthesis of a selection of this literature to generate an overview of signal processing techniques applied to human sleep EEG analysis and their relative merits. Signal processing techniques will be considered under three main sections, namely: pre-processing, feature extraction and feature classification. Each section describes the most frequently addressed methods related to its topic followed by a full Taxonomy table which contains the relevant signal processing techniques, their brief descriptions (and their pros and cons where appropriate), their specific applications in sleep EEG analysis and the corresponding references. In order to further increase the readability, an additional table is provided which categorises the signal processing techniques based on their applications in intensively researched sleep areas such as sleep staging, transient pattern (e.g. sleep spindles, K-complexes) detection and OSA diagnosis. The Taxonomy tables are designed to be self contained

so that each can be used like a dictionary. Studies included in this survey are limited to surface EEG signals in sleeping humans (including the paediatric population).

Pre-processing

In biomedical signal analysis it is essential to understand the data, and differentiate between signal and artefact. Having successfully understood the difference between artefact and data, it is then important to understand the features of interest in the data (e.g. a certain oscillation frequency, some peaks or notches or general trend of data). EEG recordings and in particular sleep EEG recordings typically suffer from various types of artefacts. In biomedical signal processing, artefacts are unwanted patterns not caused by the underlying physiological event of interest. Thus, depending on the purpose of the analysis, judgement must be made as to what is, and what is not, an artefact. For successful analysis and to obtain reliable results it is essential to give special care and attention to identifying artefacts as ignoring them may dramatically influence the results and the consequent conclusions. In PSG sleep EEGs are often recorded in conjunction with other physiological signals. Hence many artefacts in sleep EEGs are caused by interference. Such artefacts include, but are not limited to:

- ocular artefacts that can occur due to eye movements (slow or fast) which affects the electrical field of the corneal-retinal dipole
- muscle artefacts (i.e. EMG interference) which occupy a broad frequency range and can appear in the form of spikes or continuous interference
- electrical field changes induced by the cardiac muscle depolarisation which interfere with EEG signals

Other types of artefacts include:

- head, body and chest movements
- changes in electrolyte concentration at electrodes (e.g. sweat artefacts)
- mains (power-line) interference at 50 or 60 Hz depending on local standards

These can all distort the EEG signals and result in misinterpretation (see Anderer *et al.* [88] for a review on sleep EEG artefact processing). Examples of such artefacts are shown in Figure A1.

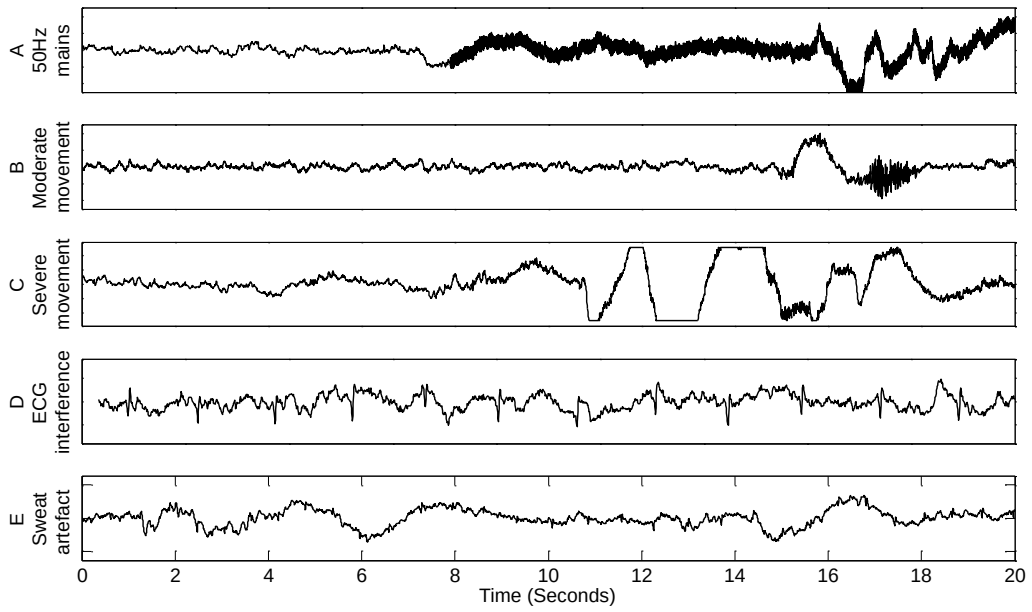

Figure A1. Common EEG artefacts. A) 50 Hz mains interference appears as a thickened signal caused by superposition of 50 Hz mains waves on the EEGs. B) Movement causes a sudden and significant deviation from the background EEG and C) severe movement can clip the EEG. D) ECG interference appears as a pulsed EEG, it occurs when the pulses on the ECG are superimposed on the EEG. E) Sweat artefact is a slow drift of the baseline EEG.

The EEGs of infants and newborns also suffer from similar artefacts (for a detailed illustration of EEG artefacts in newborns see Walls-Esquivel *et al*. [89]).

Even though a major part of pre-processing deals with artefact handling it is not limited to that. Segmentation of the EEG signal is also a step which is commonly taken prior to the analysis of sleep EEG. This section highlights some of the most frequently used signal processing techniques for dealing with artefacts and touches on segmentation techniques and their application in sleep EEG signal analysis.

Artefact processing:

Successful analysis of sleep EEGs requires appropriate artefact handling. This involves detection of the artefacts, and depending on their type, may require the exclusion of the whole epoch which contains the artefacts, removal of small contaminated portions of signal or artefact reduction (i.e. recovering the EEG as best as we can using signal processing techniques). Methods that have been frequently used for processing sleep EEG artefacts include, but are not limited to, frequency selective filtering, independent component analysis (ICA) and regression and correlation based methods. Note that mathematical details of artefact processing are not given here, instead, an overview of applications of signal processing techniques in the analysis of contaminated sleep EEGs is provided. See Taxonomy Table A1 for the complete list of signal processing techniques employed in sleep EEG artefact handling.

Frequency selective filters (low-pass, high-pass, band-pass, band-stop) have been almost universally used in artefact processing (e.g. see [90] for application of simple and effective filtering methods to muscle artefact detection).

ICA is a statistical signal processing technique which aims to linearly decompose a set of random variables into new sets of maximally independent variables [91]. It has been frequently applied to sleep EEG signal for source isolation or artefact reduction. There are several algorithms (e.g. AMUSE, SOBI, JADE, Infoamx) which can be employed to achieve ICA. AMUSE (Algorithm for Multiple Unknown Source Extraction) and SOBI (Second Order Blind Identification) are based on second order statistics which makes them computationally more efficient than JADE (Joint Diagonalization of Eigen Matrices) and Infomax which are based on higher order statistics. Each of these algorithms uses a fundamentally different assumption to achieve ICA and this affects the performance and applicability of these techniques in different situations. Crespo-Garcia *et al.* [92] have recently compared the performance of these four algorithms for EMG interference reduction and found that AMUSE not only shows the best performance but also requires the lowest computation time. Devuyst *et al.* [93] have reported that the use of conventional ICA techniques does not result in efficient ECG artefact reduction due to lack of synchrony (phase shift) between interference peaks and R peaks of the ECG and thus proposed a modified ICA method. ICA has been frequently and successfully used for sleep EEG artefact reduction and it has been particularly useful in high resolution studies where the number of EEG electrodes exceeds the usual 4-8 channels conventionally used in PSG. For more details on the application of ICA to EEG artefact processing (not limited to sleep), see Jung *et al*. [94].

Regression based methods commonly assume that that an artefact induced in the EEG signal is correlated with the source of that artefact (e.g. EOG interference in EEG is correlated with the EOG signal itself). This class of methods has the advantage of simplicity but may suffer from bidirectional contamination (i.e. removing a portion of the EEG activity as well as the artefact) [94, 95]. Regression based de-noising has been commonly used to remove ocular artefacts by subtraction of an attenuated version of the EOG from the EEG signal [96]. For more details on EOG artefact removal by regression see Woestenburg *et al*. [97]. Whilst, conventional frequency selective filtering cannot eliminate EMG artefacts due to their broad spectrum (10 to 200 Hz [98]) it is reported that in high resolution studies they can be removed using linear regression and spectral estimation [99, 100]. This is particularly important in sleep studies which aim to analyse alpha (8-12 Hz), sigma (13-15 Hz) or beta (16-30 Hz) band since their analysis may be undesirably affected by the muscle artefact due to their overlapping spectra.

Not all artefact processing methods focus on eliminating a single type of artefact. Artefacts can often be thought of as any significant deviation from normal (e.g. a sudden change in sleep EEG

amplitude which lasts for 2 seconds). These changes manifest themselves as non-stationarities and therefore, techniques which can detect dynamic changes in a signal can then be used to identify potential artefacts. For example, embedding an autoregressive (AR) model into a Kalman filter can form such an artefact detection method used in pre-processing of sleep EEGs [101]. Energy operators are also useful markers of sudden changes (e.g. spikes) as they are operators sensitive to instantaneous fluctuations of frequency dependent energy [102].

In a more recent work, Klekowicz *et al.* [103] proposed a computerised system which can parametrically detect most polysomnographic artefacts including EMG, ECG, EOG interference in addition to sweat and high frequency artefacts. Depending on the state of the sleep EEG signal the program can be tuned (manually by an expert or automatically by self-learning) to be more or less sensitive towards different artefact types.

Sleep EEG segmentation:

Segmentation of the sleep EEG signal before the analysis (i.e. feature extraction and classification) is the other crucial pre-processing step. There are almost no studies in which some form of segmentation is not done prior to the analysis. Segmentation can be performed uniformly or non-uniformly (adaptively). Uniform segmentation is the most widely used segmentation routine carried out in sleep EEG pre-processing. Dividing the signal into constant 30 or 20 or even 1 second epochs are examples of uniform segmentation. Depending on the analysis which is to be carried out, use of this method of segmentation may be sufficient. However, in some applications, for instance when a large number of data samples are required (such as high resolution spectral analysis, or nonlinear analysis of signal complexity), one second portions may not contain sufficient number of samples. Uniform segmentation offers simplicity but may lack flexibility.

Adaptive segmentation on the other hand is the more sophisticated approach to segmentation. It aims to detect sudden dynamical changes or non-stationarities in the signal and separates or classifies them. This divides the EEG signal into quasi-stationary portions of variable length. One advantage is that feature extraction after adaptive segmentation will be more reliable since features are extracted from homogenous epochs rather than constant length ones [104]. Adaptive segmentation of EEG signals was first proposed by Bodenstein and Praetorius in 1977 [105]. Their method was based on detection of sudden spectral changes driven from a linear prediction autoregressive (AR) model using a single sliding window. Amir and Gath [106] extended this work by employing time varying autoregressive (TV-AR) modelling for adaptive segmentation of EEG signals. Barlow *et al.* [107] reported the use of mean amplitude and mean frequency for adaptive segmentation of EEG signals. This work was later extended and modified to be also applicable to infant EEGs [108]. Krajca *et al.* [109] proposed another method based on

spectral estimation and use of statistical measures and shape parameters. They used two connected sliding windows rather than one. Agarwal *et al.* [110, 111] exploited the use of nonlinear energy operators, and Arnold *et al.* [112] applied Hilbert Transform Filters (HTF) to achieve adaptive segmentation.

All of the above methods have been successfully used in segmentation of sleep EEGs in different studies and for different applications (see Taxonomy Table A1). Segmentation techniques are not limited to those highlighted above; and in fact any technique which can capture and follow the dynamics of a signal can be potentially used for segmentation. For an early clear review on segmentation of EEG signals see Barlow [113]. The next section is dedicated to the extraction of features from sleep EEGs and techniques used for this purpose.

Taxonomy Table A1. Artefact Processing and segmentation of sleep EEG signals.

Technique	Technique variations	Technique brief description	Applications and references
Artefact removal			
	Independent component analysis (ICA)	Linear decomposition of signals into maximally independent components [114]	Comparison of four ICA algorithms (AMUSE, SOBI, JADE, Informax) for muscle artefact removal [92], artefact reduction (ocular, myogenic and cardiac) [95], ECG interference cancelation [93, 115], ballistocardiogram artefact removal [116], general artefact removal [94]
	Regression-correlation	Assumes that contaminated and contaminating signals are correlated and uses this to detect artefacts, see [97] for an example	EOG artefact removal [96, 97], EMG artefact removal [99], ECG interference removal [117]
	Interpolation	Approximating an unknown data value from future and past samples	ECG artefact removal (assumes missing data and then interpolates) [118]
	Kalman filtering	Famous predictive de-noising filter in fields of communication and control [119]	Detect discrete dynamic changes, general artefact detection (combined with AR model and RBFNN which stands for Radial Basis Function-Neural Network) [101]
	Morphological filtering	Non linear filters which alter the geometrical features of signals [115, 120]	ECG interference elimination [115], ocular artefact removal [121]
	Bayseian model averaging	Uncertainty based classification method [122]	Application of technique in sleep EEG artefact removal [123]
	Energy operators	Analyses the energy of a single component signals[124]	Smoothed non-linear Teager-Kaiser energy operator for detection of R peaks in EEG (ECG interference reduction) [102]
	Ensemble averaging	Simple point by point averaging of several parallel time series	ECG artefact reduction [102]
	Wavelet transform	Signal decomposition into a set of fast decaying functions (wavelets) [125]	Wavelet shrinkage combined with non linear adaptive filtering for ECG interference cancelation [126]
Segmentation			
	Adaptive segmentation	Signal division into variable length epochs which enforce quasi-stationarity, done prior to feature extraction for improved performance. Can also be used for artefact detection	Topographic analysis of neonatal EEG [127], neonatal sleep state discrimination [104, 108], automatic sleep staging (infants [128-131], adults [111, 130, 132, 133]), application of TV-AR in segmentation [106], burst and spike detection in neonates (based on Hilbert transform) [112], neonatal state discrimination [134], spectral analysis [135], microarousal detection [136], application of change point detection in segmentation [137]

Feature extraction

Analyses of time series are often carried out by extracting features from the signal of interest. Features can be defined as parameters which provide information about underlying structures of our data such as mean amplitude, median frequency or number of zero crossings. There have been numerous techniques applied to sleep EEG signals for the purpose of feature extraction. These techniques range from simple averaging to computationally intensive complexity measures. Names, descriptions and applications of these techniques to sleep EEG processing are given in Taxonomy Table A2. Note that studies often employ more than one feature in their analyses and hence more often than not, features are complementary. The rest of this section provides additional information on some of the most frequently used techniques and features found in the table.

Temporal features:

Temporal features are characteristics obtained from the signal of interest primarily in the time domain. Amplitude values, standard deviation of the time series, and number of zero crossings are examples of such features. Some of the more widely used temporal features and their associated signal processing techniques are described below.

Standard statistics which are measures of the basic properties of a time series are the most frequently used temporal features in sleep EEG analysis. These statistics can include absolute amplitude values, mean amplitude values over an interval, mode, median, standard deviation, variance, skewness, and kurtosis. These parameters are easy to derive and often provide essential basic information about the signal.

Period-Amplitude Analysis (PAA) and zero-crossings are closely related methods based on parameterisation of a given signal using the zero crossing points. PAA generally extracts parameters such as amplitude, period, or area underneath the curve from half-waves (curves between two successive zero crossings) and uses these to characterise a signal [138]. For instance, the distribution of intervals between consecutive zero crossings provides a measure of rhythmic activity - the smaller the intervals, the faster the activity [139]. Geering *et al.* [138] state that the method is very sensitive to noise and more importantly, for reliable use of the technique, the signal should not contain superimposed components. This limits the use of this technique in practical situations existence of superimposed components is almost inevitable when dealing with biomedical signals and particularly the sleep EEG. They further suggest the use of band-pass filtering to avoid some of the superimposed components and hence obtain

more reliable results. Armitage *et al*. [140] carried out a study to compare PAA and Power Spectral Analysis (PSA). They argue that PAA and PSA are comparable even without pre-filtering and hence disagree with the conclusion reached by Geering *et al.* [138]. They further promote the method by stating that it performs better than PSA in quantifying low amplitude activities. Insensitivity to non-stationarities and general variability (not noise) are other properties of PAA which can be beneficial or detrimental depending on the application [140]. *Zero crossing* can be thought of as a subset of PAA which generally aims to measure central frequency fluctuations of the dominant band by counting the number of zero (baseline) crossings [141]. Both methods can easily be implemented and used in practice; however, for the purpose of rhythmic activity quantification, more suitable frequency domain signal processing techniques (high resolution spectral analysis, wavelet transform, matching pursuits, etc.) may be used.

Hjorth parameters were developed in 1970 by Bo Hjorth [142] for the purpose of EEG time domain analysis. Hjorth parameters are designed to describe activity, mobility (shape) and complexity of EEG signals using simple time domain operators such as amplitude, variance and time derivatives [142, 143]. They have been used as complementary features in a variety applications related to sleep EEG analysis. One shortcoming is that Hjorth parameters are sensitive to noise and hence the signal of interest is commonly filtered prior to calculation of these parameters [144].

Detrended Fluctuation Analysis (DFA) proposed by Peng *et al.* [145] is a relatively new technique which allows accurate detection of long range temporal correlations in a time series [146]. It can also be used as a linear measure of self-similarity [147]. It is theoretically suitable for the analysis of non-stationary, noisy signals such as the sleep EEGs [148, 149]. Since its development, the method has received considerable attention in various fields of science and engineering. It has been used in a variety of applications in sleep EEG analysis.

Entropy of amplitudes (ENA) is a non-conventional temporal feature used in a number of sleep EEG related studies [150]. It is a measure of disorder (regularity, complexity) in the amplitude distribution of a time series. It is simply defined as:

$$ENA = -\sum x_i \times \log(x_i) \tag{A1}$$

Where x_i is the amplitude distribution (histogram) of the signal in a given interval [151]. As can be seen, ENA can be simply calculated and thus has been used as a complementary feature in a few studies.

There have been other less commonly used temporal feature extraction techniques applied to the analysis of sleep EEG signals, these are not discussed in the text but are included in Taxonomy table A2.

Spectral features:

Arguably the most commonly extracted features from sleep EEGs are the spectral features. They are essentially parameters which characterize the signal in the frequency domain. Sleep EEGs are traditionally divided into five frequency bands namely delta (0-4 Hz), theta (5-7 Hz), alpha (8-12 Hz), sigma (13-15 Hz) and beta (16-30 Hz). Many of the visual scoring criteria for sleep EEG signals are based on these frequency bands, which may explain in part the widespread use of spectral features in the analysis of these signals. This section describes some of the most frequently employed spectral features and their associated signal processing techniques, and highlights the important properties of each technique where appropriate.

Non parametric, parametric and subspace spectral estimation methods are different techniques for approximating the power spectrum of a given signal. As can be seen in Taxonomy Table A2, these spectral estimators have numerous applications in sleep EEG analysis. *Non-parametric spectral estimators* are based on direct use of the Fourier transform (FT) which is commonly calculated using the Fast Fourier transform (FFT) algorithm. The Welch method is, for instance, a well known non-parametric power spectral density (PSD) estimator [152]. Non-parametric spectral estimators have been by far the most frequently used techniques in sleep EEG analysis. They are simple to implement and interpret but can only be applied to a small portion (e.g. 1 second window) of the sleep EEG signal at a time or they may violate the stationarity assumption. Instructions on how to use FFT for sleep EEG analysis are given by Campbell [153]. *Parametric spectral estimation* is a model-based approach in which the spectrum of the signal is approximated by fitting a mathematical model to it. Upon calculation of the parameters of such a model one can obtain a spectral estimate which is often more accurate than those obtained by non-parametric counterparts. In addition, close spectral peaks in the spectrum are more likely to be resolved using a parametric estimator than a non-parametric one. Autoregressive (AR) modelling, adaptive AR modelling [154] and Kalman filtering are all considered as parametric modelling methods. A very important issue which rises in parametric modelling is the choice of the model order (number of parameters in the AR model). The Akaike information criterion (AIC) [155] has often been used to determine the model order for reliable spectral analysis [139]. Herrera *et al.* [156] have more specifically discussed the model order selection issue for sleep EEG signals. For a review of parametric modelling techniques applied to EEG analysis see Pardey *et al*. [157]. *Subspace methods* (also referred to as high resolution or super resolution techniques) are spectral estimation methods based on Eigen analysis. They are particularly

good at capturing the spectral characteristics of single component signals (which may be hidden by noise). Multiple Signal Classification (MUSIC) or Eigenvector (EV) methods are examples of subspace spectral estimators [158, 159].
All the above spectral estimation methods, when employed appropriately, that is taking into account possible non-stationarities and optimal model order selection, can provide useful information about the underlying structure of the signal and can consequently be used as features for further analysis.

Higher-order spectral analysis (HOSA) is the extension of power (second order) spectral analysis. A reasonable motivation for the use of higher order statistics is that the power spectrum does not contain any information about the phase of the signal. This issue can be overcome by use of higher order spectra as under certain circumstances, they can provide a means for the phase information to be recovered [160]. This additional phase information has made HOSA a major investigative tool in analysis of phase coupling in sleep EEG [161]. Bispectral analysis is a well established branch of HOSA which has been widely used in estimating the depth of anaesthesia (and sleep) by calculating the Bispectral index (BIS) from the EEG signals [162-164]. Various other instances in which bispectral analysis or HOSA in a more general sense have been applied to sleep EEGs are shown in Taxonomy Table2. It should be noted that quantities such as bispectrum, bicoherence, trispectrum, and tricoherence, are all related to the more general higher order spectral analysis; they are in fact the Fourier transform of different moments of the signal [160, 165]. To summarise, HOSA provides complementary information to that which can be obtained by power spectral analysis and is especially suitable to analyses where phase information is of particular importance.

Coherence analysis is very closely related to the spectral analysis methods previously mentioned. It is in fact, the normalised cross-spectrum and can be thought of as frequency domain correlation [166, 167]. Coherence is a parameter which reflects the degree of synchrony between frequency components of two signals and can provide estimates of functional connectivity in the brain. It has hence, often been used in investigation of cortical interactions [100, 168]. For instance, existence of sleep spindles in two separate channels can be shown by a high coherence value at about 13 Hz, that is, a higher degree of synchrony at 13 Hz. Coherence analysis can theoretically only be applied to stationary signals and hence sleep EEG signals have to be segmented to quasi-stationary portions prior to the analysis. Coherence analysis is most suitable in high resolution studies when the number of derivations is not limited to 4 or 8. For a detailed discussion on application of coherence analysis to sleep EEGs see Achermann [169]. In short, coherence analysis is simple to implement and interpret, and has been shown to be a

powerful tool in unveiling new information about functional cortical connections [170]. It is worth mentioning that *Directed Transfer Function (DTF)* method (previously called directed coherence) is a more recently developed method for the purpose of investigating functional connectivity in different brain regions. As the name suggests, it not only reveals a possible link between two channels, but also specifies a direction for the information flow [171]. DTF is sensitive to phase shifts between signals but robust in presence of noise [168].

Spectral entropy (SEN), similar to amplitude entropy, is a measure of irregularity of EEG signals [172]. It reflects the degree of disorder in the spectrum of the signal. For instance, if the spectral power is accumulated on a single frequency, SEN is minimised (i.e. there is little irregularity) and if it is uniformly distributed over a broad spectrum it is maximised [150]. Spectral entropy is given as:

$$SEN = -\sum P_i \times \log(P_i) \tag{2}$$

where P_i are amplitude values of the discrete power spectrum. SEN has been used in the analysis of sleep EEGs usually as a complementary feature. It is simple to calculate and can provide useful information about the complexity of a time series.

The spectral features listed above are by no means inclusive of all methods proposed in the literature, but they provide an overview of the frequency domain techniques used in the analysis of sleep EEG. Taxonomy Table A2 provides further details on the application of these techniques in human sleep EEG analysis.

Time-frequency features:

Time-frequency analysis is a powerful tool which allows decomposition of signals into both time and frequency. It thus provides a means for frequency tracking in time [173].

Sleep EEGs are non-stationary signals, i.e. their amplitude, frequency and phase vary rapidly with time. In the analysis of such signals one is often interested in the evolution of the frequency content with time. This is particularly important in analysis of sleep EEGs where many of the events such as arousals, sleep spindles and alpha intrusions are manifested by sudden changes in amplitude and frequency characteristics. Some of the more widely used time-frequency methods in the analysis of sleep EEGs are highlighted below.

The wavelet transform is one of the major mathematical tools in time-frequency analysis. It is analogous to Fourier series. In Fourier series a signal is broken down into its basic sinusoidal components of different amplitudes and frequencies; in wavelet analysis however, the signal is

decomposed into several wavelets (fast decaying waves) with different scaling factors and time shifts. The scaling factor and time shifts can then be translated to frequency and time parameters respectively [125]. Wavelet transform uses variable size windows to achieve time-frequency decomposition; this essentially means that the sizes of the windows can be adopted to suit the characteristics of a signal and achieve optimal time-frequency resolution. This optimal resolution, in addition to the capability to deal with non-stationary signals are significant advantages of wavelet transform [174]. On the other hand, an orthogonal discrete wavelet transform is not generally time shift invariant, that is, different time shifts in the input do not result in time shifted version of the decomposition but a different decomposition; this may limit the use of wavelet transform in certain applications [175]. Although wavelet transform has often been successfully applied to analysis of sleep EEGs, there have been few studies which have employed but not benefited greatly from this technique (see Zoubek [176] for an example). Hence depending on the nature of the analysis one may choose simpler techniques which can be easier to implement and interpret. Applications of wavelet analysis in the processing of sleep EEGs are shown in Taxonomy Table A2.

Matching pursuits (MP) is a more recently developed time-frequency method. It is based on signal description via a collection of mathematical functions (commonly Gaussian modulated sinusoids) called dictionaries. An advantage of MP is the large dictionary size which is not limited to a certain form of function (as opposed to the Fourier transform which uses only sinusoids or the wavelet transform which employs a mother wavelet function) [177]. MP achieves time-frequency decomposition by finding the best matches that fit the structure of the signal from the dictionary. Parameterisation of the identified matches in time, frequency, amplitude and energy results in a complete decomposition [178]. Analyses which employ MP benefit from high time-frequency resolution, accurate transient event description and appropriate characterisation of non-stationarities. Furthermore, parameterisation of sleep EEGs using MP is compatible with the conventional visual scoring criteria. An addressed issue of MP algorithm in analysing sleep EEGs is the statistical bias which is caused by the structure of the employed dictionary and can be alleviated by use of stochastic dictionaries [179, 180]. However, a possible shortcoming of the method is its high computational cost which may limit its use in real-time applications. In short, since its introduction, MP has been widely used in the analysis of sleep EEGs; its high time-frequency resolution makes MP an ideal candidate for estimating the dominant frequency of transient patterns [181]. More details on applications of MP to sleep EEG analysis can be found in Taxonomy Table A2.

Short Time Fourier Transform (STFT) is a simple, powerful tool in time-frequency analysis. In STFT the signal of interest is uniformly segmented into many short duration portions. The Fourier transform of overlapping segments of the signal is then calculated. This method can therefore capture the spectral characteristics of each segment. Thus one can see how these spectral properties change from one segment to another. The time-frequency resolution of STFT is directly determined by the segment size: the smaller the segment, the higher the time resolution and, the lower the frequency resolution. By increasing the size of segments one can increase the frequency resolution at the cost of time resolution. Also note that longer segments may violate the quasi-stationarity assumption required for appropriate application of the Fourier transform. Hence one should take into account issues about time and frequency resolution in addition to stationarity of the signal prior to analysis. STFT has been widely used in the analysis of sleep EEG mainly due to its simplicity and ease of implementation. For details on the techniques see Cohen [173].

Empirical mode decomposition (EMD) is a decomposition technique which aims to analyse non-stationary and nonlinear processes. In this method, the signal is broken down into several functions, called the intrinsic mode functions (IMF) which have distinct oscillatory modes. Instantaneous frequencies of each oscillatory mode are then computed using the Hilbert transform. Using the calculated frequency values one can produce an energy-time-frequency representation of the signal. This time-frequency plot is known as *Hilbert spectrum* [182]. Use of EMD in sleep EEG analysis has not been very wide, even though the method offers certain advantages such as capability of appropriately dealing with non-stationary and non linear processes. This could be partly due to the fact that the method has been developed relatively recently compared to most other time-frequency methods. It seems likely that the application of EMD to the analysis of sleep EEG signals will increase in the future.

Nonlinear features/complexity measures:

It is traditionally assumed that EEG signals are generated from stochastic processes and hence statistical methods should be employed to characterise them. A more recent view suggests that EEG signals may be generated from a deterministic nonlinear process [183]. Since nerve cells are highly nonlinear in nature, this recent view is intuitively more realistic [184]. In fact, Fell *et al.* [185] have shown that EEG signals are highly unlikely to be fully characterised by linear stochastic models.

A nonlinear dynamical system is typically described by its states (the system variables) and its dynamics. The space which these variables span is known as the phase space (or the state

space) and this contains all the possible states that the system can produce. The dynamics of the system can be defined as the rules by which the system changes in time i.e. the governing equations. An important concept in nonlinear dynamical systems is the attractor. An attractor is a subset of the phase space which, given enough time, the system tends to evolve to [186]. In systems with multiple attractors, the initial conditions determine which attractor the system will evolve to. Attractors have properties which can be estimated and be used as descriptive features. See Stam [187] for a very comprehensive review on nonlinear dynamical analysis of EEG signals.

Parameters which describe the nonlinear system can also be used as features in time series analysis. These features often incorporate information about the degree of nonlinearity of the system. Based on the assumption that more complex systems generate more complex time series, nonlinear features have also often been used as complexity measures (see Taxonomy Table A2). Nonlinear features have been widely applied to the analysis of sleep EEGs. They can provide complementary information to characterise specific waveforms as well as different stages of sleep. An important issue in nonlinear analysis of time series is the reliability and interpretability of the potential results. Successful application and interpretation of these techniques requires a good understating of the method and the application [184, 188]. However, careful analysis of nonlinearities can reveal useful information which is otherwise hidden [189]. The rest of this section briefly describes some of the nonlinear features/techniques which have been more frequently employed in the analysis of sleep EEGs.

Correlation dimension is by far the most frequent complexity measure used in the analysis of sleep EEGs [190]. In a one dimensional time series, it estimates the complexity of the nonlinear system which is capable of generating that time series. Correlation dimension is a property of an attractor and often exhibits a fractal (non-integer) dimension in practice. Correlation dimension is most commonly calculated using the numerical algorithm of Grassberger and Procaccia [191]. It has been applied to the analysis of both neonatal [192, 193] and adult [194, 195] sleep EEGs.

Correlation dimension has often been used in characterisation of different stages of sleep by monitoring the complexity of the EEG signal during different sleep stages. It is reported that correlation dimension can reflect statistically significant differences between most sleep stages. More specifically, studies suggest that the deeper the sleep the lower the complexity measure (see [192, 193, 196] for relevant paediatric complexity studies, and see [150, 197-205] for relevant adult studies). Accurate estimation of correlation dimension requires a large sample size and therefore, it is generally not suitable for parameterization of short transient events such as sleep spindles or arousals. The standard algorithm also requires the signal to be stationary. For a variant of the technique which can be applied to non-stationary signals see

Skinner *et al.* [206]. Taxonomy Table A2 highlights different applications of correlation dimension in the analysis of sleep EEGs.

Lyapunov exponents estimate the average convergence or divergence rate of trajectories in phase space. These exponents can be positive, zero or negative and their interpretation changes depending on their signs [187, 207, 208]. Most literature on sleep EEG analysis report the use of Largest Lyapunov Exponent (LLE) or first and second positive Lyapunov exponents as markers of chaotic source behaviour, and their high sensitivity to initial conditions [209]. Whether or not sleep EEGs are generated from a chaotic source remains unclear; Gallez *et al.* [184] argue that existence of at least two positive Lyapunov exponents is the footprint of chaos whereas Acherman *et al.* [195] and Palus [189] believe that their findings do not support the idea of a chaotic source for EEG signals.
Furthermore, Lyapunov exponents are used to characterize the attractors in dynamical systems. Assuming that sleep EEGs are generated from a nonlinear dynamical process, Lyapunov exponents can be used to parameterise an attractor of such a generator. This parameterisation can be used as a discriminative feature [150] or a diagnostic feature [210] in the analysis of sleep EEGs. The main algorithm for calculation of non-negative Lyapunov exponents from a one dimensional time series was proposed by Wolf *et al.* [211] in 1985 and is still in use to date. Taxonomy Table A2 shows several instances where Lyapunov exponents have been used for analysis of sleep EEGs.

Fractal dimension (FD) is also a complexity measure. The basic idea comes from quantification of dimensionalities of fractals. Fractals are geometries which are self-similar on different scales, see Koch snowflake in [212] as an example. That is to say for instance, one fractal is more "space-filling" than the other and hence has a higher dimension. This concept has been expanded to the analysis of time series highlighting the point that different signals may also be looked at as fractals and may differ in their space-filling property. For the one-dimensional sleep EEG signal, FD can range from 1 to 2 (its dimension is at least one and cannot be greater than two, FD=2 means the whole one dimensional space is filled by the signal) [213]. There are several algorithms for calculation of FD from a time series, but the algorithm proposed by Higuchi [214] and Katz [215] has been reported most frequently in sleep EEG analysis. FDs are suitable for transient detection (such as sleep spindles) in EEG signals [198, 216] but require the signal to be stationary. FDs can be applied to short segments of data and are relatively stable measures of complexity [217]. Taxonomy Table A2 shows applications of FD in the analysis of sleep EEGs.

Approximate entropy (ApEn) & Sample entropy (SampEn) are two closely related regularity measures. ApEn is a technique which is capable of quantifying the complexity of a system. The method was first introduced by Pincus [218] in 1990, and has become an attractive signal processing technique for researchers ever since. Generally speaking, ApEn reflects the conditional probability that two time series remain similar to each other for the next *m* samples, given that they have previously been similar; if the signals have high degree of regularity (low degree of complexity) it is more likely for them to stay similar for the next few samples and hence they produce a low ApEn value [219, 220]. According to Fusheng *et al.* [221] ApEn is:

1) robust in the analysis of short data segments (100 to 5000 samples),
2) resilient to outliers and strong transients,
3) capable of dealing with noise by appropriate estimation of its parameters and
4) can be applied to both stochastic and deterministically chaotic signals.

However, Pincus [219] states that ApEn requires at least 1000 samples to classify a complex system, hence for reliable and more interpretable results it is advisable to use at least 1000 data points in calculation of ApEn. In spite of being a practical technique, ApEn is a biased estimator of complexity and its measures may be inconsistent; this is the main motivation for introduction of *sample entropy (SampEn)* [49]. Theoretically SampEn and ApEn are very similar. SampEn is in fact an improved version of ApEn; its results are reported to be consistent, less biased and largely independent of sample sizes [49]. Both methods have been used in the analysis of sleep EEGs for instance, it has been reported that SampEn can capture and reflect the distinctive characteristics of sleep in different stages [222] (see Taxonomy Table A2 for more applications of these techniques). SampEn appears to be an appropriate method for the analysis of sleep EEGs and can be applied to characterise transient events with short durations.

The nonlinear methods highlighted above are the most frequently used techniques in the analysis of sleep EEGs. Sleep EEG specific applications of these methods in addition to several other methods are provided in Taxonomy table A2. For a review on some of these nonlinear methods see Subha [223] and for a tutorial see Pritchard & Duke [224].

Spatial features and ***Model based features*** are also features extracted for the analysis of sleep EEGs; however, their use has not been as wide as the four main categories mentioned above (i.e. temporal features, spectral features, time-frequency features and complexity measures).

Spatial features are very popular in high resolution brain studies where the number of EEG derivations exceeds those of usual PSGs (e.g. epilepsy research, brain computer interface applications, etc.). Spatial features are often extracted for source localization and techniques such as independent component analysis (ICA), principle component analysis (PCA) and low

resolution electro-magnetic tomography (LORETA) serve this purpose (see Taxonomy Table A2 for further details).

Model based features attempt to model the sleep EEG signal based on the observed signal (empirical) or some physiological assumption (e.g. neuronal interaction via feedback loops [225]). Parameters of these models can then be used as informative features which can be employed for further analysis (see Taxonomy Table A2 for the list of applications).

The application of ***random walk theory*** to sleep EEG analysis is included here due to the unusual nature of the method. The concept was first introduced by Karl Pearson in 1905 [226] and the theory has been applied to numerous fields of science and technology since then. The method has not been frequently used in sleep EEG analysis, but Cai *et al.* [227] have applied a modified version of the random walk theory to produce a stationary time series from the non-stationary sleep EEG signal. The resulting time series has been shown to be capable of characterising different sleep stages.

Features mentioned above, in addition to those highlighted in the Taxonomy Table A2 provide an overview of the features and feature extraction techniques used in the analysis of sleep EEGs (for further information also see Thakor [228] for a review of quantitative analysis techniques applied to EEG signal). It can be seen that the number of different features which can be obtained from a single time series can be enormous. Even though one may need to explore different aspects of the signal by looking at many different features, it may not be computationally possible, and hence there is often a need for feature space reduction by feature selection.

Feature selection is a procedure by which the preliminary feature space is reduced to a smaller space which preserves most of the information in the original space. There are numerous methods and algorithms which can be used for optimal and sub-optimal selection of features (See for example Bashashati [229] for a list of potential feature selection algorithms) out of which principle component analysis (PCA), genetic algorithm (GA) and factor analysis have been more frequently used in human sleep EEG analysis. PCA has been applied for feature reduction in analysis of both infant [230, 231] and adult [232, 233] sleep EEGs. It has also been recently used to study features which best capture the differences between sleep stages [234]. GA is a heuristic search algorithm which is often used in optimisation problems [235]. In sleep EEG analysis, GA has been employed in feature selection procedure for automatic sleep staging [236], cyclic alternating pattern (CAP) detection [237] and EEG signal compression [238]. Factor analysis, which is theoretically very similar to PCA has also been used for feature space reduction in neonatal sleep EEG analysis [127].

Taxonomy Table A2. Features and feature extraction techniques in sleep EEG signal processing.

Feature	Techniques	Technique/feature description	Applications and references
Temporal features			
	Standard statistics (amplitude, mean, median, mode, standard deviation, variance, skewness, kurtosis)	Features extracted by applying standard statistical operators to a time series.	Automatic sleep staging (in neonates [129, 239], adults [111]), topographic analysis of neonatal EEG [127], neonatal sleep state discrimination [104, 134, 176], automatic transient event detection [240], assessment of treating effects in patients with depression [241], RMS values used for characterization of sleep stages [242], analysis of auditory evoked potential in sleep [243], Automatic CAP detection [244], automatic arousal detection [245], study of sleep stage separability [234], automatic REM detection [246]
	Period-amplitude analysis	Parameterizing half-waves (curves between 2 adjacent zero crossings) by period, amplitude, area, etc [138, 247]	Comparison with spectral analysis [138, 140, 248], sleep study of depressed patients [249-251], analysis of delta activity [252], inter-hemispheric study of delta waves [253], comparison with spectral analysis in elderly vs. young [254]
	Zero crossings	Number of baseline (zero) crossings in a finite time series [141, 255]	Complementary feature for automatic state classification in neonates [239, 256], characterization of neonatal states [141], delta wave (0.5-2Hz) detection [257], delta wave detection for automatic sleep staging in infants [258],automatic transient event detection [240], REM detection in neonates [259]
	Hjorth parameters	Time domain parameters to describe activity, shape and complexity of EEG signals [142]	Neonatal state discrimination [134, 260], OSA diagnosis [261], automatic sleep staging [144, 262-264], study of sleep stage separability [234]
	Detrended fluctuation analysis (DFA)	Allows accurate detection of long-range correlations. Also a linear measure for self-similarity (or persistence) in a time series. Suitable for non-stationary signals [145, 147]	Investigation of linearity/nonlinearity of different sleep stages [147], characterization of sleep stages [148], Investigation of interdependencies between heart rate and sleep EEG [265], OSA diagnosis [261], analysis of sleep EEG scaling exponent (calculated from DFA) [146], characterization of sleep EEG in depressed men [149]
	Entropy of amplitudes (ENA)	Measures the degree of disorder in the amplitude distribution of a signal [150]	Discriminating sleep stages [150, 176], automatic state classification in neonates [128, 239], automatic REM detection [151]
	Matched filtering	Linear filtering based on template matching. Simple but not very flexible.	Automatic CAP detection [266], automatic spindle and K complex detection [267], topographic analysis of spindles [268], 3 types of matched filters used in K complex detection [269]
	Teager energy operator	Analyses the energy of a single component signals[124]	Automatic spindle detection [270, 271]
	Mutual information measure	Measures the amount of shared information between two random variables [272, 273]	Discriminating features in transient event detection [273], K complex/delta wave discrimination [274]
	Tsallis entproy	Generalization of Boltzmann-Gibbs entropy [275]	Characterization sleep stages [227]
	Other time related features		Cross correlation has been used to quantify the degree of synchrony in newborns [276] and Investigate the slow eye movement (SEM) and sleep EEG relationship [277], sleep event duration for automatic sleep staging [117], symbolic correlation function for EEG pattern recognition [278], likeness method-based on calculation of instantaneous phase- for Sleep Slow Oscillation detection (SSO) [279], application of Fujimori's method (a waveform recognition technique) [280]
Spectral features		Features obtained by analyzing the signal in frequency domain.	Characterization of brain maturation in infants [281], spectral analysis of pre vs. full term infants [282]
	Non-parametric spectral analysis	Frequency component calculation by direct use of	Sleep spindle detection [283-287], sleep stage discrimination (paediatrics [104, 230, 260, 288], adults [176]), study of delta

	(Periodogram, Welch, etc)	Fourier transforms.	waves in preterm infants [289], automatic sleep staging (paediatrics [128, 129, 256, 258, 290, 291], adults [144, 264, 292-295]), CAP analysis at different ages [296], characterization of neonatal states [141, 297], comparison with PAA [138, 140, 248], study of spindles [298], investigation of temporal evolution in sleep EEG [170], OSA diagnosis [299-301], arousal detection [245, 302], study of cortical interactions [303], study of fast and slow spindles [304], study of primary insomnia [305], study of temporal coupling in REM [306], combined with penalized spline smoothing for spectral analysis of EEG [307], Investigation of interdependencies between heart rate and sleep EEG [265, 308], delta wave detection in infants [258], analysis of high frequency bands (15-45 Hz) [309], automatic REM detection [151, 310, 311], dominant spindle frequency estimation [181], alpha activity detection [312], sleep onset estimation [233], parameterization of sleep EEG [232], spectral analysis of delta and sigma bands in infants [313], artefact detection [121], analysis of auditory evoked potential in sleep [243], analysis of wake-sleep transition [314, 315] (marikowa), spectral analysis of pre vs. full term infants [316], spectral analysis of young vs. elderly [254], spectral analysis of healthy vs. sick newborns [317]
	Parametric spectral analysis (AR, AAR , TV-AR modeling, Kalman filtering)	Power spectral estimation by fitting a mathematical model to the signal [157].	Complementary feature for automated sleep staging [111, 117, 262, 293, 318, 319], Investigation of linearity/nonlinearity of different sleep stages [147], neonatal state characterization [320], automatic spindle detection [321], continuous sleep depth monitoring [322], study of SWA [323], sleep stage discrimination [318], Tufts-Kumaresan (for method detail see [324]) for transient enhancement [325], spectral analysis of sleep EEG [135], artefact detection [121], phenomenological spindle analysis[326], phenomenological EEG modelling [327], analysis of sleep dynamics [328-330], study of sleep stage separability (feature selection) [234], automatic arousal detection [331]
	Subspace methods (MUSIC and EV)	Spectral estimation based on Eigen decomposition of the covariance matrix [158]	Multiple Signal classification (MUSIC) used in high resolution spindle study [332], subspace tracking for spectral analysis of spindles [333], MUSIC used in automatic spindle detection [271], Hankel total least square method used in dominant spindle frequency estimation [181]
	Higher order spectral analysis (bispecrum, bicoherence, etc)	Fourier transform of different moments (greater than 2) of the signal [160].	Adaptive quadratic phase coupling analysis in infant sleep EEG [161, 334], bispectral index (BIS) used as a measure of sleep depth [162, 164], characterization of sleep spindles [335, 336], drug effect study [337], BIS used for sleep staging [163], exploratory study of HOS techniques [338], phase coupling analysis in neonates [339]
	Coherence analysis	Normalized cross spectral density (CSD). Extracts linearly correlated rhythms between multiple signals [11].	Investigation of sleep related oscillations (SWS, spindle) in human EEG (spindles found highly coherent) [169], investigation of neurobehavioral status of infants [231], investigation of cortical interaction [167, 168, 340], investigation of temporal evolution in sleep EEG [170], study of depressed patients [250], sleep onset estimation [341], functional connectivity in low birth weight infants [342], investigation of heart rate-EEG interaction in OSA patients [343], analysis of wake-sleep transition [314, 315]
	Spectral entropy	Shannon entropy of frequencies. power spectrum of the signal is used instead of the probability distribution function in calculation of entropy [172]	Investigation of the practical aspect of the method in sleep EEG [344], discriminating sleep stages [150], characterization of sleep states in (newborns [276], adults [345], automatic sleep staging (infants [128, 130], adults [130, 144, 262]), OSA diagnosis [299], comparison of spindles in sleep and anaesthesia [346], automatic REM detection [151]
	Spectral edge frequency (SEF)	Evaluating the frequency, up to which X% (usually 85-95) of total power is accumulated [150].	Discriminating sleep stages [150], measure of sleep depth [162, 164], characterization of sleep states in newborns [276], automatic sleep staging in infants [128], drug effect study [337], spectral analysis of healthy vs. sick newborns [317], study of sleep stage separability [234]
	Spectral mean frequency	Mean frequency value calculated from spectral estimates	sleep depth measure [143, 347, 348], analysis of quiet sleep in premature and full term infants [349], study of sleep stage separability [234]
	Hilbert transform	Filters out all negative	Adaptive Hilbert transform in burst and spike detection in neonates

	filter	frequency components of a signal [350], also used for envelope detection	[112], analysis of quiet sleep in premature and full term infants [349, 351], Hilbert transform for spindle parameterisation [352]
	Itakura distance (ID)	Distance measure between coefficients of two AR models [353]	Sleep stage discrimination [318, 354], assessment of similarity between EEG and EOG [355], OSA diagnosis [261]
	Directed transfer function (DTF)	Describes direction and spectral characteristics of propagation between channels [168, 171]	Investigation of cortical interactions [168, 303]
	Frequency selective filtering	Extracting a frequency band of interest from the spectrum of the signal.	Spindle feature extraction (in infants [356], in adults [283]), neonatal state discrimination [288]
	Delta power	Evaluates Sum of spectral densities in delta band [150]	Discriminating sleep stages [150], characterization of sleep states in newborns [276]
	Other spectral parameters		Spectral centroid, spectral flux, spectral flatness, cepstral coefficients and 3 Hz power were used as complementary features for automatic state classification in neonates [239], brain symmetry index (BSI) used to quantify symmetry in newborns [276], first spectral moment was used in automatic sleep staging in infants [128], evolution map approach (EMA) was used to assess phase synchronization [357], median frequency for OSA diagnosis [299], cross spectral power used in sleep study of depressed patients [250], cosine modulated filter banks used for sleep spindle study [358], quadrature filter in burst pattern recognition in neonates [359], harmonic parameters for sleep stage discrimination [295, 318, 360] and OSA diagnosis [261], adaptive recursive filter for centre frequency tracking and spindle detection [361, 362], brain rate (weighted mean frequency) used in sleep onset estimation [341], complex demodulation used in study of spindles [352, 363, 364], Kullback information measure used as a distance metric for sleep staging [365], phase lock loops for spindle detection [366], spectral correlation for information flow calculation in arousals [367], maximum entropy method for spectral analysis [368, 369]
Time-Frequency decomposition		Tracking the evolution of frequencies in time.	
	Wavelet transform (wavelet coefficients)	Signal decomposition into a set of fast decaying functions (wavelets). Dilation and translation of wavelets can provide a time-frequency representation [125]	Complementary feature for automatic arousal detection [370], sleep stage discrimination [176], automatic spindle detection [270, 271], spindle identification [371], neonatal state discrimination [134], automatic sleep staging (infants [130], adults [130, 372]), microarousal detection (the same as arousal detection) [136], dominant spindle frequency estimation [181], applicability of wavelets in sleep EEG analysis [174, 373], CAP detection [237], OSA diagnosis [374-376], feature extraction-application of wavelet entropy to sleep EEG [377], automatic REM and spindle scoring [378], automatic K complex detection [379], spindle parameterization [352]
	Matching Pursuits (MP)	High resolution time-frequency method, decomposes a signal into a large set of functions with known parameters (frequency, amplitude, phase, etc) [177].	Study of sleep spindles [175, 177, 179, 180, 380-383], study of delta waves [381, 384], study of Slow Wave activity (SWA) [382], investigation of drug effects on sleep [385], dominant spindle frequency estimation [181], spindle parameterization [352, 364], parameterization of sleep EEG (micro and macro structures) [386], automatic sleep staging [387], automatic spindle detection [388]
	Short Time Fourier Transform (STFT)	Time-frequency decomposition by evaluation of Fourier transform for successive overlapping windows.	Analysis of respiratory cycle related EEG changes (RCREC) [15, 39], spectrogram ($\|STFT\|^2$) used for automatic arousal detection [389],sleep onset estimation [341], automatic spindle detection [271], visualization of sleep micro and macro structure [390], sleep stage characterization [391], phenomenological analysis of K complexes [392]
	Empirical mode decomposition (Hilbert-Haung tranform)	Signal decomposition into single oscillatory mode functions and extraction of instantaneous frequencies	Automatic spindle detection [393], automatic sleep staging [394]

		using Hilbert transform [182]	
	Wigner-Ville distribution	High resolution time-frequency method, suffers from cross-terms due to bilinear structure [173]	K complex/delta wave discrimination [274], sleep spindle localization [395]
	Fast time frequency transform (FTFT)	High resolution time-frequency method, based on instantaneous frequency estimation [396]	Sleep EEG segmentation [397]
	Choi-Williams distribution	Improved time-frequency method by control of cross terms through use of exponential kernels [398]	comparison of spindles in sleep and anaesthesia [346]
	Joint time and time-frequency (T-TF)	Optimal transient event detection, combines time and time-frequency features to minimize the error probability [399]	Automatic K-complex and delta wave detection [399]
Complexity measures/nonlinear parameters		Quantifies irregularity (variability or randomness) in a signal, often based on nonlinear dynamical analysis.	
	Correlation dimension (or its estimate: dimensional complexity)	Property of an attractor which can be used as a complexity (irregularity) measure of time series [184]. Based on the work of Takens [400]. Most often calculated using Grassberger-Procaccia's algorithm [191].	Feature to characterize different sleep stages (in infants [192, 193, 196], in adults [194, 197-205]), used for discriminating sleep stages [150], Investigation of linearity/nonlinearity/chaos in different sleep stages [147, 195], characterization of SWA [401], investigation of SWA [402], investigation of possible relationships with respiration [403], variation of correlation dimension in delta sleep investigation [404] , OSA diagnosis[261], assessment of non-linearity of sleep EEG [185], automatic REM detection [151]
	Lyapunov exponents	Assess the degree of nonlinearity in a signal, (e.g. existence of two positive Lyapunov exponents is a marker of chaos) [184, 211].	Assessing the predictability of human EEG in different states e.g. deep sleep vs. wake [184], characterization of EEG signals at different sleep stages [203, 209, 405], discriminating sleep stages [150], assessment of sleep EEG non-linearity [185], automatic REM detection [151]
	Fractal dimension	Measure of how "space filling" an object is. Allows non-integer dimension values. Powerful in transient event detection [198, 406].	Characterization of EEG signals at different sleep stages (infants [297], children [290], adults [198, 407]), characterization of neonatal states [141], automatic sleep staging (infants [128]), comparison of spindles in sleep and anaesthesia [346], wavelet based multifractal analysis in sleep stage characterization [408-410]
	Approximate entropy (ApEn)	Signal complexity (or regularity) measured by evaluating conditional entropy [219].	Investigation of the practical aspect of the method [344], characterization of EEG signals at different sleep stages [198, 345], comparison of spindles in sleep and anaesthesia [346]
	Sample entropy (SampEn)	Improved ApEn. More consistent, unbiased and suitable for short data segments [49]	Characterization of sleep stages [222], characterization of sleep stages in different age groups [411]
	Synchronization likelihood	Unbiased measure of dynamical (non-linear) interdependencies between time series, can deal with non-stationarities and non-linearities [412]	Investigation of interdependencies between heart rate and sleep EEG [265, 308]
	Recurrence plot	Visual aid for diagnosis of dynamical systems. Describes natural time correlation. information [413]. Reveals non-stationarities of time series [223]	Used to characterize EEG signals at different sleep stages [198], assessment of treating effects in patients with depression [241]
	Autoregressive model order	Number of past samples (AR model order) used in	Investigation of the practical aspect of the method in [344], neonatal state characterization [320]

		prediction of a future sample is a complexity measure, not robust [344].	
	Kolmogorov-Sinai entropy (also known as metric entropy or KS entropy)	Rate of information loss in a system. Measure of average time interval in which the signal remains similar to itself [184].	Assessing the predictability of EEGs in different states e.g. deep sleep vs. wake [184], discriminating sleep stages [150]
	Phase space plot	Plotting a signal against its time delayed version. Requires a mean for time delay estimation [198].	Characterization of EEG signals at different sleep stages [198]
	Hurst exponent	Evaluates the extent of long range dependencies and roughness in a time series [147, 198].	Feature to characterize EEG signals at different sleep stages [198]
	Delay vector variance	Method for detection of non-linearity and determinism in a time series [414]	Automated sleep staging [415]
	Embedding space Eigen spectrum	Uses the rank of the embedding matrix as a measure of complexity [344].	Investigation of the practical aspect of the method [344]
	Other non-linear techniques		Green-Savit measure used to assess non-linearity of sleep EEG [185], fuzzy sets used for modelling sleep dynamics [416], neural networks used for measuring complexity of sleep EEG [417], correlation exponent in sleep stage characterization [202], a non linear index was used to investigate interdependencies between heart rate in infants (similar to synchoronisation method) [418], T-entropy used for sleep staging [419], Lampel-Ziv complexity for characterization of sleep stages [345]
Spatial features/ source localization			
	Independent component analysis (ICA)	Linear decomposition of signals into maximally independent components [114]	Separating different physiological signals in ambulatory sleep recording [420], spindle identification [421], Spindle source localization [422, 423]
	Low resolution electro-magnetic tomography (LORETA)	Brain activity localization through direct calculation of it current distribution. Assumes simultaneous firing of adjacent neurons [424]	Spindle source localization [422, 423]
	Principle component analysis (PCA)	Multivariate method which transforms a high number of inter-correlated variables into a smaller number of uncorrelated variables [425].	Study of temporal coupling in REM [306]
Model based features			
	EEG generation model (rhythmic activity modeling)	Reproducing EEG by filtering and parameterising white noise [225, 426]	Automatic CAP detection [266, 427], optimal detection of alpha rhythm [428], automatic K complex and vertex wave detection [225, 429], sleep staging by sigma rhythm monitoring [430], SWS analysis [431], non-stationary model for spectral analysis [432]
	Coupled oscillators model	Modelling the inter-relation between signals by degree of coupling between differential equations [433]	Analysis of signal coupling in neonates [434]
Random walk theory		Theory based on the problem of estimating the distance of an object from its origin after taking "n" random steps [226]	Characterization of sleep stages [227]

Feature classification

Features are individual measurable characteristics of a time series. Once features are extracted from the signal we often attempt to group them; that is to divide the feature space into a discrete number of categories. For instance, in sleep staging we may have five possible classes (wake, stage1, stage2, slow wave sleep and REM) or in automatic spindle detection, we may have two (i.e. spindle vs. non-spindle). Classification can improve the automation process and enhances our understanding and interpretation of the underlying system.

In classification, features within each category (or class) share some form of similarity and are classified based on that similarity. In sleep EEG analysis we commonly have to deal with sleep micro and macro structural classification problems. Classification can be undertaken for a diagnostic purpose, e.g. classifying patients with obstructive sleep apnoea vs. controls, or can aid automation (classification of transient events in sleep or classifying sleep stages). Numerous techniques have been proposed and used for sleep EEG signal classification. Taxonomy Table A3 is dedicated to these methods and their applications in the analysis of sleep EEGs. As with previous sections, we explore the more frequently used techniques and comment on them where appropriate.

Neural network (NN) classification:

Neural networks or artificial neural networks (ANN) are the outcomes of early attempts to understand how the human brain works. They are mathematical models inspired by neuronal interactions in the brain and can be used to model a wide range of complex systems. An ANN commonly consists of an input layer, an output layer and a number of hidden layers. Layers are composed of artificial neurons (or nodes). Neurons linearly combine their weighted inputs and produce an output based on their nonlinear output function. Using several neurons in conjunction, ANNs become capable of modelling very complex nonlinear systems [435]. Similarly, they can be used to define nonlinear boundaries between sets of features in the feature space.

Parameters of ANNs are generally the weights by which the inputs are scaled. These weights are obtained through training (or learning), for instance, for classification of sleep stages, one can use a previously scored polysomnogram with known sleep stages to train an ANN (i.e. adjust the weights for each sleep stage) and then employ the trained ANN to classify new polysomnograms (see Shimada [436] as an example).

ANNs are adaptive and can deal with nonlinearities in classification. In other words, decision boundaries generated by ANNs can be nonlinear. Decision boundaries are hyper-planes (or

hyper-surfaces) which partition the feature space into several classes. ANNs have been very frequently used in the analysis of sleep EEGs and have been generally successful. They are often not computationally efficient and their performance is directly dependent on their training. There are many different types of ANNs with different architectures and training algorithms, some of which are included in Taxonomy Table A3. Note that more details about different structures and training algorithms of ANNs are outside the scope of this thesis (see Haykin [435] for more details on ANNs and Robert [437] for a review of applications of ANNs to EEG analysis).

Multilayer perceptron (MLP) is the most commonly reported ANN in the literature. It consists of an input layer, one or more hidden layers and an output layer [438]. The nonlinear output (or activation) function of neurons in the hidden layer(s) usually follows a sigmoid function (a smooth "s" shaped graph which is differentiable everywhere) [435, 439]. Given enough neurons in the hidden layers, MLPs can be used to approximate any continuous function arbitrarily well [440]. Thus, MLP (and ANN in general) benefit from considerable flexibility in classification. However, this flexibility may also result in sensitivity to overtraining [441]. MLPs are widely used in the analysis of sleep EEGs for in a variety of applications such as sleep staging, event detection and obstructive sleep apnoea (OSA) diagnosis. Providing that there is enough data available for reliable training, MLPs are effective classifiers. For more information on use of MLPs in the analysis of sleep EEGs refer to Taxonomy Table A3.

Self-organizing maps (SOM) or Kohonen maps are neural network based mapping methods the for analysis and visualisation of high dimensional data [442]. When classifying, SOMs do not need prior knowledge about the number of classes and they can achieve classification through maximal separation of input features [443, 444] (see Roberts & Tarassenko [328, 329] for an examples of this).

SOMs can yield satisfactory results with a small number of training data sets and can also be significantly faster than conventional ANNs by employing computationally efficient algorithms [442].

The advantages mentioned above in addition to the general benefits of ANNs (such as the capability to produce nonlinear decision boundaries and flexibility) make SOMs a competitive candidate in classification problems (for more details on SOM see Kohonen [445]).

Its use in sleep EEG analysis has been moderate but diverse which highlights the flexibility of this technique. Taxonomy Table A3 shows the applications of SOMs in sleep EEG analysis.

Two other types of ANNs (learning vector quantizer and sleep EEG recognition neural network) and their use in the analysis of sleep EEGs are also shown in Taxonomy Table A3.

Statistical classification:

Statistical classification is another popular routine for classifying the feature spaces. In this section, the term statistical classification accommodates a range of diverse methods, from classical Fisher's discriminant analysis [446] to more modern hidden Markov models to statistical learning theory based support vector machines (SVM).

Statistical classifiers usually separate the feature space into different classes by calculating the probability that a certain feature belongs to a certain class, in other words, they are based on probabilistic models [447] (note that SVMs are exempt from this, they are not based on explicit probabilistic models).

The rest of this subsection briefly describes some of the more frequently used statistical classifiers in the analysis of sleep EEG signals, for more details on the actual applications see Taxonomy Table A3.

Linear discriminant analysis (LDA)/ Fisher's linear discriminant (FLD) are linear classification methods which attempt to divide the feature space into several classes by hyperplanes (planes which exist in one lower dimension than the feature space, for instance, a two dimensional feature space can be separated into two by a line and a three dimensional feature space by a plane) [446, 447]. Both methods are very similar in principles and the terms have been used interchangeably. LDA is simple to implement (particularly when separating only two classes), easy to interpret and generally works well in classifying linearly separable data; however, there exist distributions for which the error probability of LDA is close to one even when the data are linearly separable [448]. Also note that LDA, as the name suggests, is a linear classifier and is unable to produce nonlinear decision boundaries, thus it is not suitable for classification of features which are nonlinearly separated. Note that a simple variation of LDA, namely *Fisher's quadratic discriminant analysis* may be useful in dealing with nonlinearly separated data if the classes of interest can be separated by a quadratic curve.

LDA and its variations have been used relatively frequently in the analysis of sleep EEGs, Taxonomy Table A3 shows the areas for which LDA has been found useful.

Support vector machines (SVM) are linear learning machines used for pattern classification through use of optimal separating hyperplanes [435, 449]. SVMs map the current input vector into a higher dimensional feature space through some nonlinear mapping and then exploit the use of optimal hyperplanes for separating the features [449].

SVMs are conventionally categorised as linear classifiers, however, they can also be easily integrated with neural networks to create nonlinear decision boundaries. They are flexible (i.e. can be generalised to suit different needs), robust and not sensitive to overtraining; they may however, suffer from high computational expense [450].
Use of SVMs in sleep EEG analysis has been moderate but inclusive of a relatively wide range of applications. They have been frequently successful in classification problems and can work well even in situations where the training data set is small [451]. Taxonomy Table A3 shows the instances where SVMs have been employed for the analysis of sleep EEGs (for a thorough tutorial on SVMs see Burges [452]).

Hidden Markov models (HMM) are an extension of Markov models (or Markov chain models). A Markov process is a stochastic model which attempts to characterise a system by its possible states (outputs) and transition probabilities between those states at any one time. If the states of the system are deterministic, i.e. each transition leads to a certain outcome, we have a Markov model, however, if the states (outcomes) are themselves probabilistic (i.e. at the end of each transition, all states can possibly occur) we have a Hidden Markov model (HMM) [453, 454]. HMMs can be applied to the analysis of non-stationary signals by dividing the signal into locally stationary segments and calculating the probabilities for transitions and states. For instance, in the analysis of sleep EEGs, locally stationary states can be thought of as the sleep stages and can be further analysed with HMMs [455].
HMMs are promising tools for classification of time series; they achieve classification by calculating the likelihood that a feature belongs to a certain class. They are also capable of dealing with nonlinearly separated data [450].
They have been moderately used in sleep EEG analysis and their use has been relatively focused on sleep staging related applications. Taxonomy Table A3 provides the details on these applications.

The three above methods conclude most of the statistical classifiers used in analysis of sleep EEGs. Bayesian classifiers have also been employed but their use has not been very wide, see Taxonomy Table A3 for the details.

Fuzzy classification:
Fuzzy sets were introduced by Zadeh in 1965 as an attempt to mathematically describe ambiguous classes, those are classes which do not have a well defined boundary such as “the class of beautiful women” or “the class of tall men” [456]. Ever since its introduction, the

concept of fuzziness has become a practical and widely used tool in pattern recognition and classification.

Fuzzy classifiers do not assume absolute membership of feature to a single class and hence they are more applicable to real data where boundaries between subgroups might not be well defined [457].

Fuzzy classifiers are versatile; they have very good generalization capabilities and can be effectively integrated with other classification routines for better performance (e.g. neuro-fuzzy classifiers, fuzzy decision trees, fuzzy k-nearest neighbour algorithm, etc.). For details and fundamental concepts of fuzzy classification, see Bezdek [458].

Use of fuzzy classifiers and their simple variations have been frequent and successful in the analysis of sleep EEGs. Taxonomy Table A3 shows the instances where fuzzy classification or fuzzy based reasoning has been employed to analyse sleep EEGs.

Cluster analysis, or clustering, is the process of dividing a set into natural homogenous subgroups where elements within each subgroup are similar to each other and different from those within other subgroups [458]. Although there are subtle theoretical differences between clustering and classification, in practice, the terms are often used interchangeably. The simplest and the most widely employed clustering algorithm is the *k-means*. This algorithm assumes that the feature space consists of *k* clusters (this can be decided beforehand based on possible knowledge of the data) whose centres are randomly distributed. It then iteratively adjusts those random centre points to get closer to the centre of the actual clusters. This adjustment is done by minimizing a simple squared error function.

The algorithm is computationally efficient and simple to implement. Its downside however, is that due to random initialization of the centroids, clustering may result in error, that is , the algorithm may fail to detect the true clusters. Hence, in practice, clustering is done with a number of sets of random initial points rather than a single set. For the exact description of the algorithm and more details, see Jain [459].

Due to its simple implementation, use of k-means algorithm in the analysis of sleep EEGs has been relatively frequent; Taxonomy Table A3 shows its specific applications.

Rule based classification is simply classification based on pre-defined rules. In practice, it is very similar to the "if" and "else" statements used in programming: *if event X occurred, then perform act Y, else, perform Z*. In the context of sleep EEG analysis one may notice that Rechtschaffen and Kales [13] have proposed a set of rules for scoring sleep PSGs. Those rules can be exactly implemented in a computerized system for classification of stages and events using a rule based classifier [117].

Rule based classifiers are simple, can be implemented as soon as the pre-defined rules are available, and are as flexible as the rules that they are based on. By convention, they solely rely on human knowledge which maybe limited and hence, their use in the analysis of sleep EEGs has been sparse, Taxonomy Table A3 shows the details.
For more information on rule based classification see Michie *et al.* [447].

Last but not least, ***combined classifiers*** are, as the name suggests, classifiers which are based on two or more conventional classifiers. Although these are generally bound to be slower in execution, they tend to achieve more accurate classification, hence they can be used for offline analysis where execution speed is not the main concern. A widely used combined classifier is the *Neuro-fuzzy classifier (NFC)*. NFCs are particularly good at approximating nonlinearities; however, their complexity grows exponentially with additional inputs, this is referred to as the "curse of dimensionality" [460]. See Taxonomy Table A3 for applications of NFCs in sleep EEG analysis. More detailed information on the classifiers described above can be found in Lotte *et al.* [450] and Jain *et al.* [459].

Taxonomy Table A3. Feature classification techniques applied to sleep EEG signals.

Technique	Technique variations	Technique brief description	Applications and references
Neural network classification		Mathematical models inspired by human brain neuronal interactions. Used to model nonlinear and complex systems. They are adaptive and capable of producing nonlinear decision boundaries. Need training [435]	Automatic K-complex detection [461, 462], feature based classification of sleep stages (paediatrics [290], adults [292]), arousal identification [302], transient event classification [273], burst and spike detection in neonates [112], study of drug effects [463], automatic REM detection [151, 311], OSA diagnosis [300, 374, 376, 464], micro and macro structure analysis [465], automatic REM and spindle scoring [378], Bayesian inference based NN for sleep staging [466]
	Multilayer perceptron (MLP)	Basic ANNs. Given enough neurons in the hidden layer, they can approximate any continues function. Flexible but sensitive to overtraining [435]	Sleep stage discrimination [176], automatic spindle detection [285, 286, 321, 467, 468], neonatal state classification [260], burst-suppression and burst-interburst pattern recognition [359],automatic sleep staging [263, 372, 469], automatic REM detection [310], OSA diagnosis [375]
	Self-organizing maps (SOM, Kohonen networks)	ANN based mapping method for analysis and visualization of high dimensional data. Flexible. Can be initialized with small training set [442]	Characterization of sleep stages for classification [470], study of evoked K complexes [471], analysis of sleep dynamics [328-330], automatic sleep staging [294]
	Learning Vector Quantizer (LVQ)	Predecessor of SOM (Kohohen networks). Based on competitive supervised learning [445]	Neonatal state classification [260], study of evoked K complexes [471]
	Sleep EEG recognition NN (SRNN)	NN for sleep EEG transient detection, recognition based on time-frequency patterns [472, 473]	Transient event detection (spindles, alpha waves, humps and background activity) [472], automatic sleep staging [436]
	Other neural networks		Radial basis function NN (RBFNN) combined with Kalman filtering for artefact removal [101], RBFNN has been used in

			automatic arousal detection [331]
Statistical classification			
	Linear discriminant analysis (LDA)/Fisher's linear discriminant (FLD)	Separation of classes by hyperplanes, optimized by least squares or maximum likelihood. Simple, generally good for linearly separable data, cannot produce nonlinear boundaries [446, 447]	FLD for artefact detection [121], neurobehavioral and risk assessment of infants [231], FLD for classification of neonatal brain states as well as classification of burst suppression patterns [239], automatic sleep staging [474], automatic state recognition in infants [291], stepwise LDA for automatic arousal detection [370] , high voltage, low voltage discrimination in neonates [475], classification of insomniacs vs. controls [476]
	Support vector machines (SVM)	Linear learning machines which achieve classification by exploiting optimal separating hyperplanes [435, 449]. Robust and flexible	Radial basis SVM for automatic spindle detection [321], automatic arousal detection [302, 389, 451], neonatal state discrimination [134], automatic sleep staging [144, 360], automatic REM detection [246]
	Hidden Markov model (HMM)	Stochastic model that evaluates the future state of a process by its present state. Both states and transitions are probabilistic. Can deal with nonlinear data [453]	Development of a new sleep staging scheme (not based on RKR) [455, 477], automatic sleep staging in infants and adults [130], continuous density HMM used for K complex detection [478], hidden process modeling (generalization of HMM) used for modelling sleep EEG dynamics [479], automated sleep staging [262, 480]
	Bayesian classifier	Probabilistic classification through calculation of *a posteriori* probabilities using Bayes rule	Sleep stage discrimination [176], naïve Bayes classifier for neonatal state discrimination [134]
	Other statistical/machine learning classifiers		Fisher's quadratic discriminant analysis for Arousal identification [302], decision trees (a machine learning classifier) for transient event detection [481], k-nearest neighbours algorithm for automatic sleep staging [144, 394]
Fuzzy classification		Classification by evaluating the membership degree of each feature vector to each class [458].	Used in a sleep spindle detector (classifying spindle vs. non-spindle [283, 482], classifying spindle amplitude profile in infant PSGs [356]), spindle detection [284, 285, 287], sleep stage classification [132, 294], sleep EEG segmentation [133, 135], fuzzy ganglionar lattice for automatic neonatal state classification [256], alpha activity classification [312], fuzzification of features prior to sleep staging [483], automatic CAP detection [427]
	UFP-ONC (unsupervised fuzzy partition-optimum number of clusters)	Fuzzy K-means + fuzzy MLE. Uses no *a priori* information. Works well even with variable cluster shapes and densities [457].	Combination of fuzzy K-means and fuzzy Maximum Likelihood estimation results in optimal partitioning of sleep EEG signals (sleep staging) [457],
Cluster analysis			Automatic arousal detection [245],
	K-means algorithm	Simple iterative algorithm which finds the clusters by minimizing the distance of the points in a class from their centre point. Sensitive to initial condition [459]	Classification of time structure of neonatal sleep [129], automatic sleep stage classification (infants [128, 130], adults [111, 130, 263, 295]), clustering of similar EEG segments (EEG segmentation) [137], artefact detection [121]
Rule based classification		Similar to "if" and "else" statements in programming: *if X then do Y, else do Z*	Simple rule based classification of sleep microstructure (e.g. arousals, spindles, A phase of CAPs) [484], minimum distance classification for automatic K complex detection [379], sleep stage characterization [391]
	Rule based case based (RBCB)	Improved rule based classification through by further post-processing	Automatic sleep stage classification [117, 293]

	hybrid	[117]	
Combined classification		Classification by merging (or simultaneously applying) two or more classifiers	
	Neuro-fuzzy classifiers (NFC)	Combination of neural networks (NN) and fuzzy inference system. Works well with no *a priori* information but suffers from the curse of dimensionality [460]	Sleep stage classification in infants [460, 485], K complex detection [486], automatic sleep staging [469]
Other classification routines			Theory of evidence (for details of the method see [487]) for sleep stage classification [483], conditional random field (for details on CRF see Lafferty [488]) for sleep stage classification [489]

The categorisation of techniques from a sleep perspective

The previous two tables in this review (Tables A2 and A3) are technique oriented, that is they are organised by techniques and further information about application to sleep EEG is then given. Some readers may be more interested in quickly identifying an area of sleep analysis (e.g. automatic sleep staging, sleep spindle analysis or K-complex detection) in which particular signal processing techniques have been useful. Table A4 has been designed to achieve such identification. All the references cited in Taxonomy tables A2 and A3 are cross-referenced in Table A4. The columns of the table represent the more frequently addressed topics in sleep EEG analysis and the rows are the signal processing techniques in the same order as they appear in Taxonomy Tables A2 and A3. Thus, tracking down techniques of interest becomes straight-forward. For instance, if one is interested in finding the signal processing techniques employed for sleep staging, one can look into the sleep staging column of Table A4. If one further wishes to find techniques which are applied to paediatric sleep staging, within the same column, it will be noted that some of the references are marked with capital "P", denoting "paediatric". Transient events are also clearly addressed in Table A4. There are two separate columns for sleep spindle and arousal events. Other commonly discussed transients appear under the "other transient detection/analysis" column. Detection applications are marked with a small "d" and analysis applications with a small "a". For example, "Dwa" stand for Delta wave analysis and "Kcd" stands for K-complex detection. The guide at the bottom of Table A4 provides the necessary information for interpreting the table. Having found the event of interest, one can then go back to Taxonomy Tables A2 or A3 for a brief description of the technique and a slightly more detailed explanation on the application, and ultimately refer to the related references.

Table A

Table A4. Categorization of signal processing techniques from sleep perspective

Technique	Technique variations	Sleep staging*	Sleep stage characterisation**	OSA diagnosis	CAP detection, analysis	Spindle detection, analysis	Arousal detection, analysis	Other transient detection, analysis***	Cortical interaction	Exploratory study
Temporal features										
	Standard statistics	P[129, 239], [111], Rd[246]	P[104, 134, 176], [234, 242]		d[244]		d[245]	Gd[240]	[127]	[241, 243]
	PAA		Da[252]						[253]	[138, 140, 248-251, 254]
	Zero-crossings	P[239, 256],P-Rd [259]	P[141]					Gd[240], Dwd[257], PDwd[258]		
	Hjorth parameters	[144, 262-264]	P[134, 260], [234]	[261]						
	DFA		[147-149]	[261]						[146, 265]
	ENA	P[128, 239], Rd[151]	[150, 176]							
	Matched filtering				d[266]	d[267], a[268]		Kcd[267, 269]		
	Teager operator					d[270, 271]				
	Mutual information							Gd[273], Kcd[274]		
	Tsallis entropy		[227]							
Spectral feature extraction										
	Non-parametric spectral estimators	P[128, 129, 256, 258, 290, 291], [144, 264, 292-295], Rd[151, 310, 311], S_1d[233]	P[104, 141, 230, 260, 288, 297], [176], Ba[309], P-DSa[313]	[299-301]	a[296]	d[283-287], a[181, 298, 304]	d[245, 302]	P-Dwa[289], P-Dwd[258], Ad[312],	[303]	P[316, 317],[121, 138, 140, 170, 232, 243, 248, 254, 265, 305-308, 314, 315]
	Parametric spectral analysis	[111, 117, 262, 293, 318, 319]	P[320], [147, 234, 318], Da[323],			d[321], a[326],	d[331]	Ga[325]		[121, 135, 322, 327-330],
	Technique variations	**Sleep staging***	**Sleep stage characterisation****	**OSA diagnosis**	**CAP detection, analysis**	**Spindle detection, analysis**	**Arousal detection, analysis**	**Other transient detection, analysis*****	**Cortical interaction**	**Exploratory study**
	Subspace					a[181, 332,				

	methods					333], d[271],				
	HOS	[163]				a[335, 336]			[161, 334, 339]	[162, 164, 337, 338]
	Coherence analysis	S_1d[341],						Ga[169]	[167, 168, 340, 342]	[170, 231, 250, 314, 315, 343]
	Spectral entropy	P[128, 130], [130, 144, 262], Rd[151]	P[276], [150, 345]	[299]		a[346]				[344]
	Spectral edge frequency	P[128]	P[276], [150, 234]							P[317],[162, 164, 337],
	Spectral mean frequency		P[349], [234]							[143, 347, 348],
	Hilbert filters		P[349, 351]			a[352]				[112]
	Itakura distance		[318, 354]	[261]						[355]
	DTF								[168, 303]	
	Spectral Filtering					Pd[356], d[283]				
	Delta power		P[276], [150]							
Time-frequency features										
	Wavelet transform	P[130],[130, 176, 372], Rd[378]	[134]	[374-376]	d[237]	d[270, 271, 371, 378], a[181, 352]	d[136, 370]	Kcd[379]		[174, 373, 377]
	Matching pursuit	[387]	[386], Da[382]			a[175, 177, 179-181, 352, 364, 380-383], d[388]		Dwa[381, 384]		[385]
	STFT	S_1d[341]	[391]			d[271]	d[389]	Kca[392]		[15, 39, 390]
	EMD	[394]				d[393]				
	Wigner-Ville					d[395]		Kcd[274]		
	FTFT									[397]
	Choi-williams					a[346]				
	T-TF							Kcd+Dwd [399]		
Technique	**Technique variations**	**Sleep staging***	**Sleep stage character-isation****	**OSA diag-nosis**	**CAP detection, analysis**	**Spindle detection, analysis**	**Arousal detection, analysis**	**Other transient detection, analysis*****	**Cortical interact-tion**	**Explora-tory study**

Complexity measures/ nonlinear parameters										
	Correlation dimension	Rd[151]	P[192, 193, 196], [150, 194, 197-205], D[401, 402, 404]	[261]						[147, 185, 195, 403],
	Lyapunov exponents	Rd[151]	[150, 203, 209, 405]							[184, 185]
	Fractal dimension	[128]	P[141, 290, 297], [198, 407-410]			a[346],				
	Approximate Entropy		[198, 345]			a[346]				[344]
	Sample Entropy	[222, 411]								
	Synchroniza-tion likelihood									[265, 308]
	Recurrence plot		[198]							[241]
	AR model order		P[320]							[344]
	Kolmogorov entropy		[150]							[184]
	Phase space plot		[198]							
	Hurst exponent		[198]							
	Delay vector variance	[415]								
	Embedding space Eigen spectrum									[344]
Spatial features										
	ICA					d[421], a[422, 423]				[420]
	LORETA					a[422, 423]				
	PCA								[306]	
Model based features										
	EEG generation model	[430]	Da[431]		d[266, 427]			Awd[428], Kcd+Vwd[225, 429]		[432]
	Coupled oscillators model								P[434]	
Random walk theory			[227]							
Technique	**Technique variations**	**Sleep staging***	**Sleep stage character-isation****	**OSA diag-nosis**	**CAP detection, analysis**	**Spindle detection, analysis**	**Arousal detection, analysis**	**Other transient detection, analysis*****	**Cortical interact-tion**	**Explora-tory study**

Neural network classifiers		P[290], [292, 466], Rd[151, 311, 378]	[465]	[300, 374, 376, 464]		d[378],	d[302]	Kcd[461, 462], Gd[273], PGd[112]		[463]
	MLP	P[260], [263, 372, 469],Rd [310]	[176]	[375]		d[285, 286, 321, 467, 468]		Gd[359]		
	SOM	[294]	[470]					Kca[471]		[328-330]
	LVQ	P[260]						Kca[471]		
	SRNN	[436]						Gd[472]		
Statistical classifiers										
	LDA/FLD	[291, 474]	P[239]				d[370]	PGd[475],		[121, 231, 476]
	SVM	[144, 360], Rd[246]	P[134]			d[321]	d[302, 389, 451]			
	HMM	[130, 262, 480]						Kcd[478],		[455, 477, 479]
	Bayesian classifier		P[134],[176]							
Fuzzy classifiers		P[256], [132, 294, 483]	[133, 135],		d[427]	d[283-285, 287, 482], Pa[356]		Awd[312]		
	UFP-ONC	[457]								
Cluster analysis							d[245]			
	K-means	P[128, 130], [111, 130, 263, 295])								P[129], [121, 137]
Rule based classifiers			[391]					Gd[484], Kcd[379]		
	RBCB	[117, 293]								
Combined classifiers										
	NFC	P[460, 485], [469]						Kcd[486]		

*P stands for paediatrics, R for REM, S_1 for stage 1 (sleep onset), "d" stands for detection, "a" for analysis

** D,T,A,S,B stand for delta (slow wave), theta, alpha, sigma and beta activities respectively

*** G stands for general, Dw, Aw, Vw stand for delta wave, alpha wave and vertex sharp wave respectively, Kc stands for K complex

Examples: "PDwd" stands for paediatric delta wave detection, "Pa" stands for paediatric analysis, "Ga" stands for general analysis

Summary and conclusion

An overview of signal processing techniques applied to the analysis of sleep EEG signals in both paediatric subjects and adult population was given. The analysis was broken down into three main parts: pre-processing, feature extraction and feature classification.

- *Taxonomy table 1* provided further details of pre-processing techniques,
- *Taxonomy table 2* served as a guide to aid sleep researchers choose the appropriate signal processing techniques for their application of interest and provided brief descriptions of signal processing techniques in addition to their existing applications in the analysis of sleep EEG signals,
- *Taxonomy table 3* provided an overview of classification techniques as an aid to researchers in selecting appropriate algorithms, and
- *Table 4* summarised the more frequently addressed topics of sleep EEG analysis, splitting them into nine main categories (sleep staging, sleep stage characterisation, OSA diagnosis, cyclic alternating pattern detection, spindle detection/analysis, arousal detection/analysis, other transient detection/analysis, cortical interactions in sleep and other exploratory analyses) and providing details of signal processing techniques which have been employed in their analyses. Utilising this table, one can conveniently navigate and quickly identify the topic of interest (e.g. paediatric sleep stage characterisation or sleep spindle analysis)

An important aspect of this review is that it can show us potential gaps in the field of sleep research; that is where quantitative analysis of sleep is lacking. Such cases have been identified from Table Four and are highlighted here. According to Table Four (categorisation of signal processing techniques from a sleep perspective), analysis of cortical interactions in the sleeping brain is an area not touched upon by many researchers. Given that signal processing techniques such as the directed transfer function (DTF) and synchronisation likelihood exist and are very well suited to applications such as functional connectivity analysis, it seems logical and interesting to explore this field further. The table also points out that OSA diagnosis is still very much a manual process with sleep technicians going through hours of PSG data to diagnose OSA. This is certainly an area which can benefit from the advances of signal processing however, what may be an apparent lack of communication between the two fields might have limited this. Finally, it reveals that certain well defined cortical patterns seem to be less attended to than others (e.g. vertex sharp waves vs. sleep spindles) which may mask their true importance. The review also drew our attention to RCREC and helped us develop it further.

Appendix B

Objective detection of evoked potentials in RCREC

Given that the physiology driving RCREC is not yet identified, a valid speculation is that it may be originated from respiratory related evoked potentials (RREP). To assess this hypothesis we selected a single control subject with very significant RCREC in all bands. Table below shows the RCREC significance as denoted with Fisher's F value in this subject.

Table B1. RCREC significance in all frequency bands in a single subject

	All bands	***Delta***	***Theta***	***Alpha***	***Sigma***	***Beta***
P69 F-values	*77.57*	*83.03*	*24.97*	*45.41*	*43.94*	*72.22*

The data was automatically segmented into large chunks with reasonable quality for RCREC quantification. Eight chunks each having at least 250 respiratory cycles were selected for objective evoked potential detection. Each of the eight chunks had a significant RCREC when looking at the whole spectrum. First, for every chunk, the EEG signal was segmented according to the conventional airflow segmentation points. The segmented EEG signals were then coherently averaged across early expirations, late expirations, early inspirations and late inspirations to produce evoked potentials. Since respiratory cycle stages vary in length, for each segment, we looked at 210 samples (approximately 0.8 seconds) including and after each of the conventional segmentation point. Here we are assuming that the conventional segmentation points are analogous stimuli in evoked potential studies. To assess whether the produced evoked potentials were significant, each of the produced results was compared with 500 other randomly generated evoked potentials, random in the sense that the starting point for each segment was selected at random. Figure below shows an example of the produced evoked potentials plotted together with five and then 500 randomly generated evoked potentials.

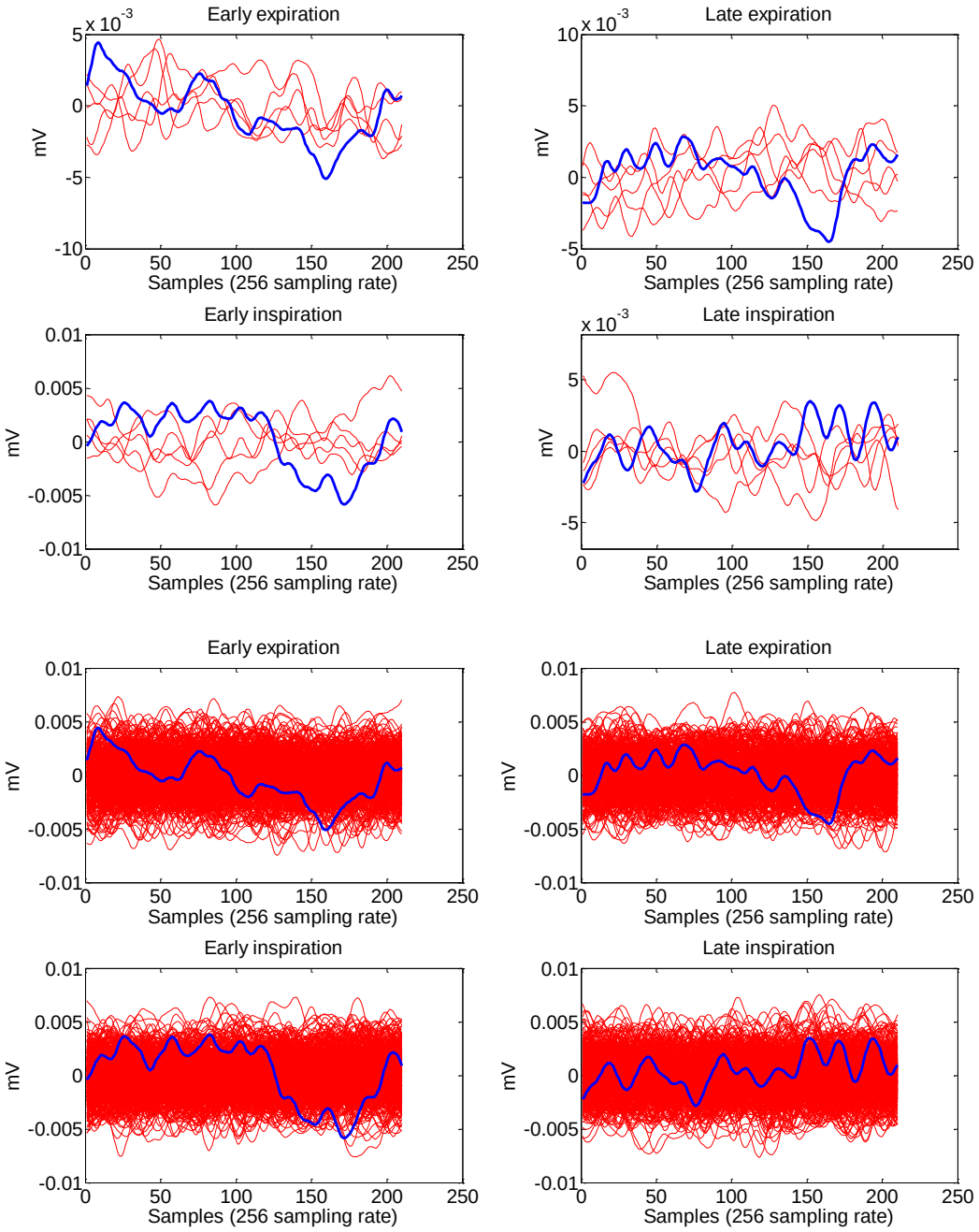

Figure B1. Evoked potentials generated based on respiratory signal landmarks (blue) vs. randomly generated potentials (red). The blue trends are often not significantly different from red ones.

If the produced potentials based on the physiological segmentation (i.e. segmentation based on respiratory signal land marks) are significantly different from those produced randomly, we may be able to safely state that RCREC is related to and may be a manifest of RREP. Minimum, maximum and peak to peak amplitude values were used to compare patterns.

In our pilot study, in seven out of eight chunks analysed; the generated patterns were not significantly different than randomly generated patterns. Moreover, the produced patterns themselves were not similar in morphology. These evidence suggest that RCREC and RREP are at least not immediately related however, a solid conclusion requires dedicated research and is hence recommended as a future work.

Appendix C

Examples of other investigations

This section of the thesis highlights some of the techniques previously mentioned in chapter 4 in more details; some of the techniques are implemented in Matlab and tested in practice for further understanding of the method.

Conventional Pre-Processing techniques

As mentioned, pre-processing techniques are not unique and indeed there are many techniques which can be employed for pre-processing purposes. Some of the techniques which have been extensively used in practice are briefly discussed here.

Filtering

In many practical cases, it is desirable to attenuate some frequency components of a signal, and/or completely eliminate them. This process of changing the frequency spectrum of a signal by attenuating some of its frequency components and not attenuating others is referred to as filtering [490].

Wiener filtering:

Parameters of common digital frequency selective filters (i.e. lowpass, bandpass and highpass) are sometimes obtained empirically (i.e. the cut off frequencies for instance are chosen partially based on trial and error). Hence, it is clear that those filters do not have a mean to remove the superimposed noise optimally (unless there is further information regarding the underlying sources of errors). Wiener filtering (also referred to as optimal filtering), assumes that signal and noise are generated from independent sources and that they are both stationary random processes [11]. Based on these assumptions, Wiener filter then finds filter coefficients in a way to minimise the difference between the estimated output and the desired output in a Least Mean Square (LMS) sense. Figure C1 further clarifies how a Wiener filters works.

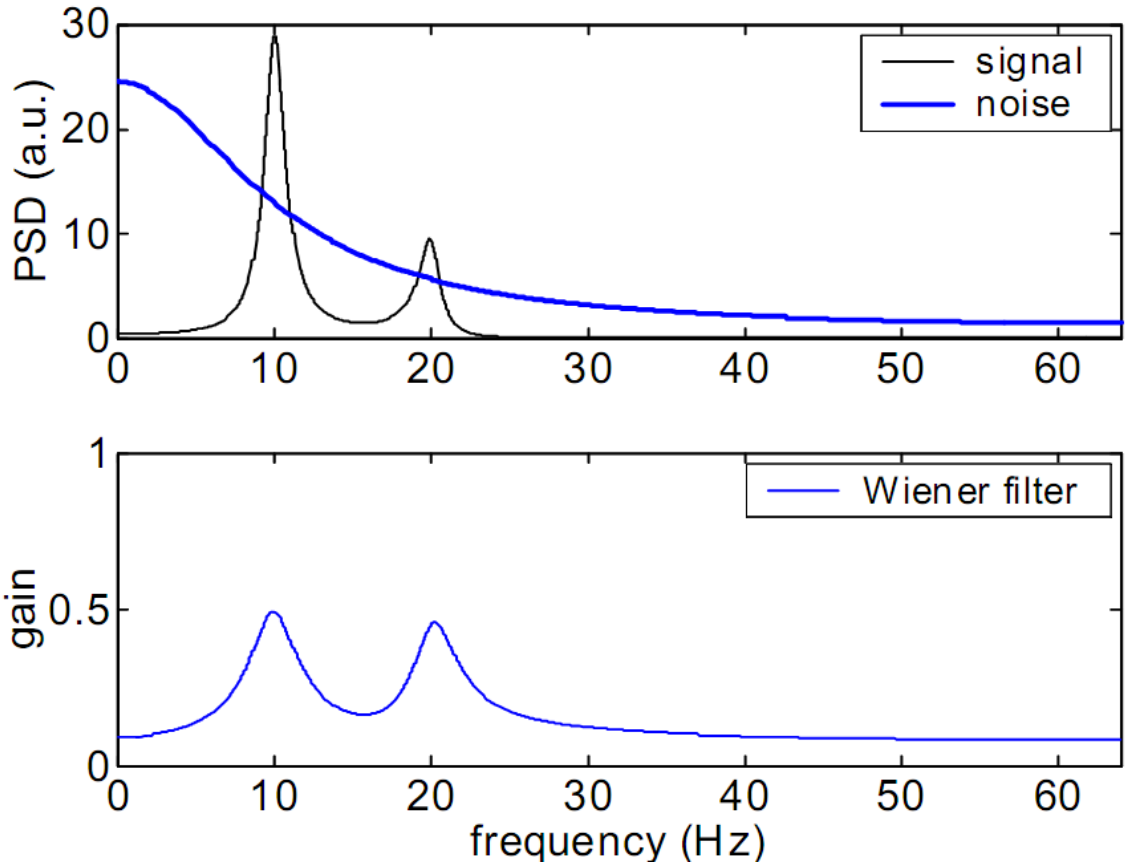

Figure C1. Wiener filter principle. As can be seen above, Wiener filter improves the Signal to Noise Ratio (SNR) of the output signal by amplifying the signal at frequencies which most power is concentrated in.

Another interesting fact about Wiener filter is that filter coefficients are calculated using an elegant closed form solution (i.e. no iterative algorithm needs to be employed) and this could significantly simplify practical implementation issues.

Wiener filters could be useful in situations where one signal is contaminated with another, (e.g. ECG signal contaminated by EMG or EEG signal with interference from ECG) as by defining the contaminated signal as the input to the filter and the uncontaminated signal as the output of the filter, noise spectrum can be estimated and removed from the signal.

Median Filtering:

Another type of digital filter which can be used for pre-processing is the median filter. This non-linear filter (as opposed to the filters mentioned above) has been often used to remove unwanted and spurious spikes in a given signal [491]. In short, this non linear technique, defines a sliding window on a sequence, sorts the values of that sequence (in ascending of descending order to find the median) and then replaces the central value of the window with the median, and then slides the window by one sample. Smoothing by running medians was

first introduced by John Tukey in 1976 [492] where he mentioned that outliers (e.g. spikes in our case) whether or not they are errors, disturb a smooth curve and we do not want that. That was the principle idea behind the median filter. Figure C2 shows an example of stereotypical spike removal using a 5 point median filter (i.e. the window length is 5 samples). Note that the signal shown in Figure C2 is a smoothed EEG signal with synthetic spikes generated for demonstration only.

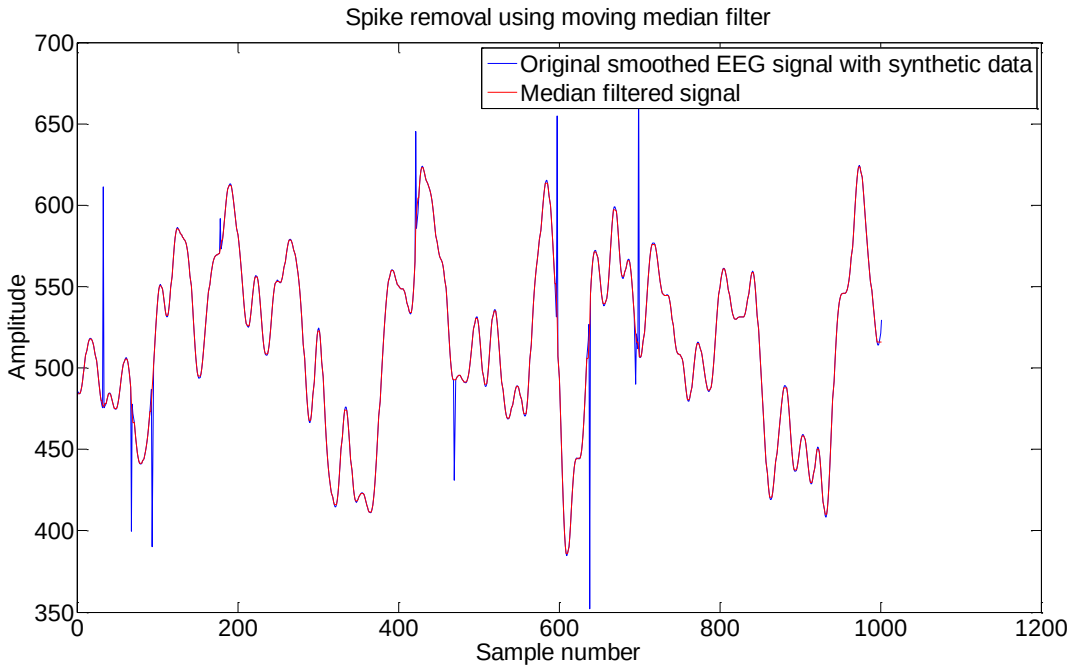

Figure C2. Spike removal using one dimensional median filter. As can be seen all the spikes are successfully removed from the original signal after median filtering. Note that the spikes are synthetically generated and the graph above is shown for illustration purpose only. Although, median filter works generally well for spike removal, it does alter the trend of the original signal (the higher the window length, the more significant the changes). Peak amplitude reduction and peak flattening are the main distortions which are mediated by median filtering.

As can be seen in the graph above, median filtering can be considered a good candidate for pre-processing of a signal with numerous erroneous spikes. However, in a signal where the fine trends are of critical importance, median filtering could potentially ruin the data as it brings about significant distortions to the curves and results in flat-topped truncated peaks [491]. The magnitude of this distortion depends on the window length of the median filter and in general, the higher the window length the more considerable the distortion. Another less important disadvantage associated with median filtering is its relatively high computational expense. This is due to the sorting process which needs to be done before identifying the median, however, as far as data analysis is concerned this is not an issue. Hence, it is again clear that median filtering

is another pre-processing tool which its performance is completely dependent on the application it is used for.

Adaptive filtering (or Adaptive Noise Cancellation):

Another pre-processing method used for additive noise (i.e. interference, stochastic or deterministic noise) removal is the adaptive noise cancelling approach. In short, adaptive noise cancelling is a variation of optimal filtering (analogous to Wiener filtering) that can be very advantageous in many applications (e.g. it can be applied to non-stationary signals to remove non-stationary interference). It makes use of a reference signal which is acquired in the noise field (i.e. containing little to no signal) and filters it to produce an estimate of the noise which is present in the primary input (i.e. signal AND noise). It then subtracts the estimated noise from the primary input to reduce or eliminate the noise [11, 493]. Figure C3 shows a schematic of an adaptive noise canceller (the figure is directly taken from [493]).

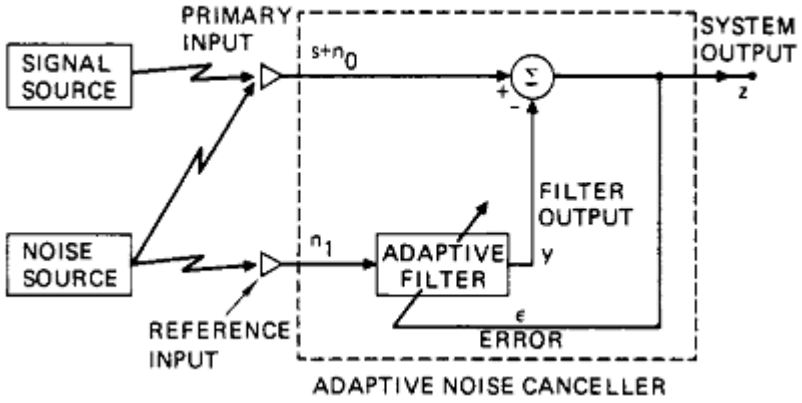

Figure C3. A Schematic of an adaptive noise canceller. As can be seen the reference input is filtered optimally to produce an estimate of the noise present in the primary input [493].

A very interesting biomedical application which Adaptive Noise Cancellers (ANC) have been successfully used for, is the extraction of fetal heart beat (an ideally its waveform) from maternal ECG and abdominal signals. It is known that the waveform measured from mother's abdomen using normal electrodes contains both fetal and maternal heart beat signals. Hence, using the maternal ECG signal as the reference input (i.e. noise with no signal, as we are interested in fetal heart beat) and abdominal signal as the primary input, the employed adaptive noise canceller successfully extracted the fetal heart beat. Note that, the obtained results from this adaptive filtering yielded a significantly better result compared to the previous attempt made to extract fetal heart beat from maternal ECG [493]. Figure C4 (taken directly from [493]) clarifies this further.

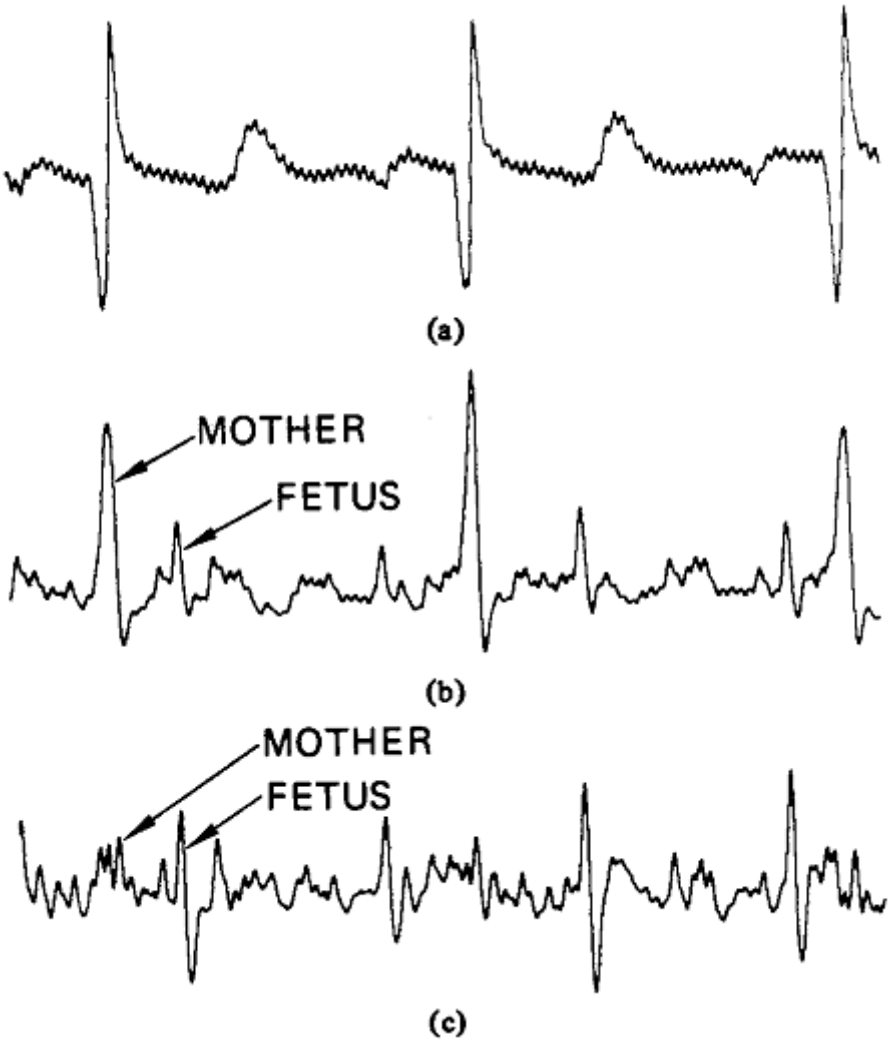

Figure C4. a. Reference input (chest lead), b. primary input (abdominal lead), c. fetal heart signal after adaptive filtering [493]

As can be seen in the graph above, use of adaptive noise cancellers can be very beneficial in applications where a reference input signals is available.

Two of the popular adaptive filters which have been extensively used for noise cancelling are the Least Mean Squares adaptive filter (LMS) and the Recursive Least Squares (RLS) adaptive filter. In the LMS method, filter coefficients which minimise the mean squared error (MSE) are determined using a gradient based approach. LMS is particularly advantageous because of its simplicity and ease of implementation. However, it is not suitable for rapidly varying signals (i.e. very non-stationary signals) as its convergence is relatively slow. RLS on the other hand, has been used in real time system identification and noise cancellation due to its fast convergence and it works by minimising the exact Least Squares. An interesting fact about RLS algorithm is

its built-in forgetting factor which gives more weight to more recent error values. This is particularly useful in dealing with non-stationary signals as varying characteristics of those signals make the exclusion of the past data very appropriate [11]. Hence, adaptive noise cancellers are potentially very useful tools in pre-processing of biomedical signals with additive noise or interference (because of the non-stationary nature of those signals).

Independent Component Analysis (ICA)

In the vast majority of scientific investigations where there is a need for data acquisition through experiments, the acquired data is not a direct measure of the activity of interest but a correlate (in general sense) of that. For instance, EEG signals are indeed not indicative of deep brain activities but superposition of scalp synaptic discharges. Nevertheless, the assumption is that these synaptic discharges in the cortex provide valuable information about deep brain activities. Similarly, in many applications, the measured signal is a combination of several activities emerged from different sources. Microphone recording in an orchestra is a good example of that. Although there are many instruments (i.e. sources) producing different sounds, the signal measured by the microphone contains only the linear combination of all the sounds (produced by all the instruments). The contribution that each instrument makes to the measured signal is dependent on many factors such as the total number of instruments in the room, the distance of each instrument from the microphone, the loudness of each instrument, and possibly factors which we are not aware of yet. If one knew all these factors, it would be possible to perfectly reconstruct the music played by each instrument; however that is very difficult in practice. Finding the underlying sources in a set of measurements is potentially very beneficial as it can reveal significantly more information about the nature of data which is being investigated. Figure C5 clarifies this with a synthetic example (the graph is taken directly from [494]).

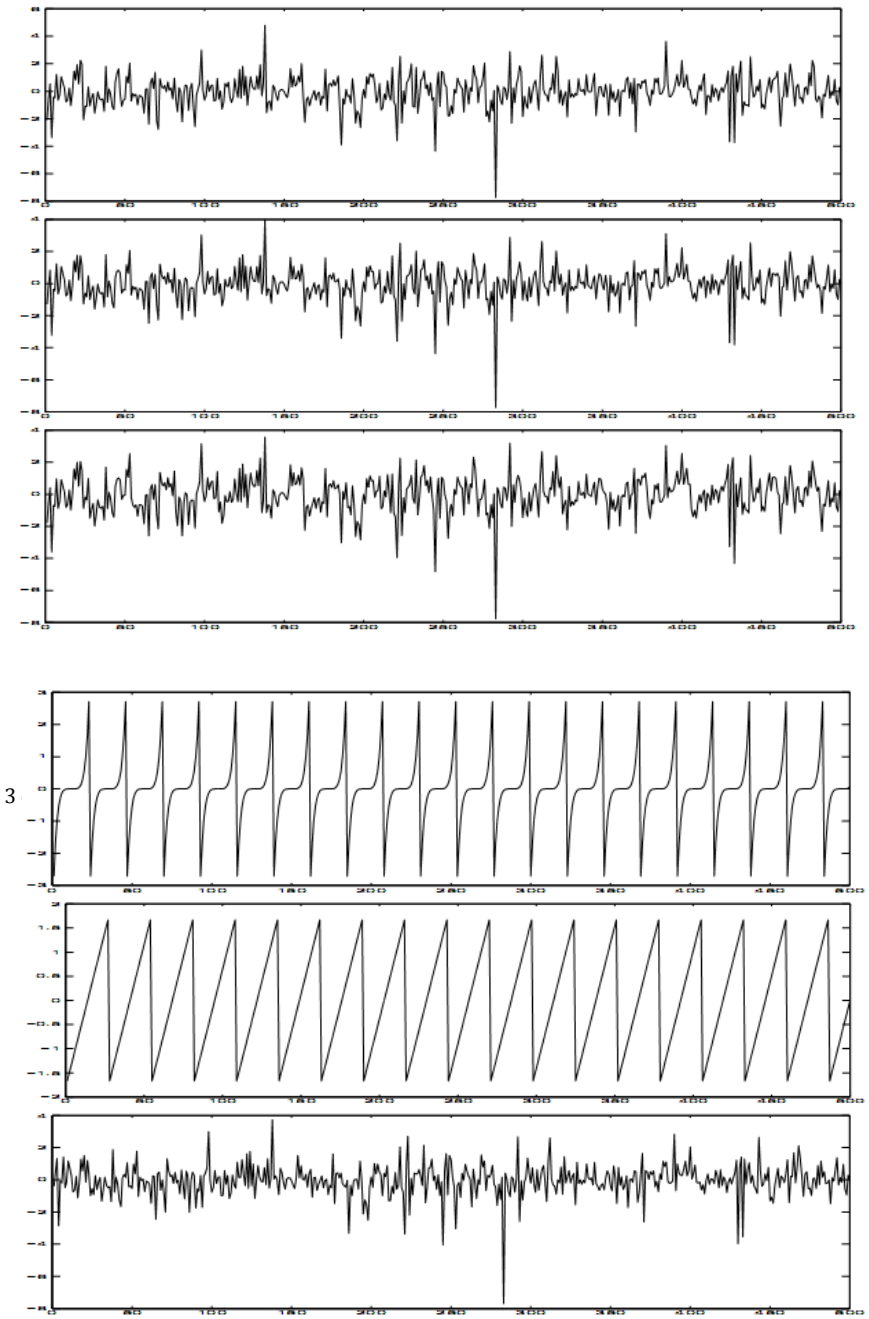

Figure C5. 3 different sources which generated the signals shown in figure 38. As can be seen, knowing the underlying sources which generated the observed signals can greatly improve our understanding of the nature of observed data [494].

As can be seen in the above two figures, the underlying sources of the observed data shown in Figure C5 provide more information about the observed data. For instance, it is now clear that waveforms produced by two of the sources are deterministic and only one seems to be random. In practice, such observations can be very important for analysis (or diagnosis).

In biomedical signal processing where it is rarely feasible to work with direct measures of the parameters of interest, it would be extremely advantageous to have a processing technique which can provide an estimate of the signals produced by their underlying sources (based on any assumption). If those estimates have physical interpretations, the processing technique used in the procedure can be very important. This problem of transforming a set of measurements into their original form created by their sources without having specific prior knowledge about the process is referred to as Blind Source Separation (BSS).

Independent Component Analysis (ICA) is a promising method used in Blind Source Separation problems. The only assumption in the method is that the signals generated by each source are maximally independent from signals generated by other sources (e.g. assuming that instruments play independently) and that the observed data are linear superposition of the signals generated from the sources. The statistical independence assumption has been shown to be particularly meaningful in Neurophysiology and hence very useful in multi channel EEG analysis [495]. In short, an ICA problem can be formulated as follows: we assume that any observed measurement is driven from a linear combination of n (number of sources) signals. For n observed signals that is:

$$\begin{pmatrix} x_1(t) \\ x_2(t) \\ . \\ . \\ x_n(t) \end{pmatrix} = A \begin{pmatrix} s_1(t) \\ s_2(t) \\ . \\ . \\ s_n(t) \end{pmatrix}$$

Where $x_i(t)$ is the ith observed signal and $s_i(t)$ is the ith original signal (i.e. signal generated by ith source) and A is an $n \times n$ mixing matrix (i.e. linear mixing coefficients). ICA aims at calculating the signals generated by the sources. If matrix A has an inverse, the equation above can be re-written as:

$$\begin{pmatrix} s_1(t) \\ s_2(t) \\ . \\ . \\ s_n(t) \end{pmatrix} = A^{-1} \begin{pmatrix} x_1(t) \\ x_2(t) \\ . \\ . \\ x_n(t) \end{pmatrix}$$

Where A^{-1} is the inverse of the mixing matrix or the de-mixing matrix. Based on the initial assumptions made to find the de-mixing matrix, there have been numerous methods proposed

in the literature (for more information see [496]). There have also been software packages (FastICA) which allow the decomposition of a set of signals into their independent components.
ICA is a technique which can be used in a wide range of applications; it has for instance been used in digital imaging, economic and financial markets and psychometric tests along with the analysis of biomedical signals such as neurophysiological and cardiac signals. It has also been used for the analysis of biomedical images such as in fMRI (functional Magnetic Resonance Imaging), and for feature extraction [496]. With some modifications, ICA can also be used for efficient artefact removal. This variation of ICA which is used for artefact removal is known as "constrained ICA". In this method, extracted independent components are also constrained to resemble a reference signal [497].
Hence, ICA is a technique which can be used in analysis of multichannel (or single channel, see [495, 498]) EEG signals for both artefact removal and feature extraction.

Feature extraction techniques

In general, any alterations made to a signal which helps us gain more information and understand the signal (or its physical interpretation) better, is useful. Feature extraction techniques are methods which can be applied to signals to reveal information which can not be readily seen. This section is dedicated to some of those feature extraction techniques which have been used in biomedical applications.

Spectral analysis

We often deal with signals in the time domain, meaning that we look at the time variations of a signal. This is because time is a fundamental parameter. However, it is often useful to look at a signal in another representation. This is usually done by decomposing the signal into a set of functions. Mathematically, there are infinitely many ways for doing this. What separates these representations from each other and makes some distinct, is the physical interpretation of those representations [173]. The idea behind one of these expansions which was founded by Fourier in 1807 was to decompose a signal on sinusoids (Fourier's original idea was to express a discontinuous function with a sum of many continuous functions). Expanding a signal using its underlying sinusoidal components is very advantageous for two main reasons. 1) Sinusoids of different frequencies (oscillation rates) are orthogonal and 2) sinusoids are common in nature and they can therefore be physically interpreted very well. Hence, Fourier's work resulted in a fundamental, orthogonal and physically interpretable decomposition and provided a powerful tool for scientists to learn more about the nature by looking at the frequency components of signals rather than their time variations. Note that frequency components of a signal can not be readily seen in the time domain signal and there is a need for the Fourier decomposition. This

process of analysing a signal in frequency domain or simply looking at the frequency components of a given signal is referred to as spectral analysis or frequency domain analysis. Spectral analysis is one of the most useful techniques for understanding the nature of a signal. It can be also thought of as a feature extraction technique as it reveals the spectral features of a signal. In spectral analysis we are often interested in power of the signal in different frequency bands or the Power Spectral Density (PSD). There has been abundant literature on how to estimate the PSD of a given signal from its time domain representation. They range from Fourier transform (FFT) of the signal to more complex statistical modelling (e.g. Auto-Regressive modelling). The rest of this section briefly introduces three of those PSD estimation methods namely Periodogram, Welch method and Auto-Regressive modelling and complements them by including the practical use of those methods in sleep related spectral analysis.

Periodogram:

Possibly, the simplest way to estimate the PSD of a given signal is to use the Periodogram method, which in discrete time and amplitude is practically calculated by using the Discrete Fourier Transform (DFT). Formula below shows the details:

$$S(e^{jw}) = \frac{\frac{1}{2\pi N}\left|\sum_{n=1}^{N} t[n].x[n].e^{-jwn}\right|^2}{\frac{1}{N}\sum_{n=1}^{N}\left|t[n]\right|^2}$$

Where *t[n]* is a window (for weighting the signal) of length *N, x[n]* is the discrete time signal and $S(e^{jw})$ is the continues and periodic estimate of the PSD of the signal [499]. Sampling $S(e^{jw})$ at $w=2\pi k/N$ for *k=0,1,..., N-1* results in the discrete frequency PSD which is more appropriate for efficient computation and storage in computers. Alternatively, if *V(k)* is the *N* point DFT of the windowed signal *v[n]=t[n].x[n]* then the discrete frequency PSD can be defined as:

$$S(k) = \frac{\frac{1}{2\pi N}\left|V[k]\right|^2}{\frac{1}{N}\sum_{n=1}^{N}\left|t[n]\right|^2}$$

Further, note that if *t[n]* is a rectangular window the denominator of the equation above will be equal to one and hence the PSD calculations become further simplified. It is worth mentioning that this method is called Periodogram only when the window used is rectangular. In cases where other windows (e.g. Hamming, Hanning, etc) are used, this method will be referred to as modified Periodogram [500].

As an example to illustrate the PSD estimation by Periodogram, 128 seconds of EEG (C3A2) was taken from a paediatric OSA patient whilst in sleep stage 2 (sampling frequency of 100 Hz). Figure C6 shows the acquired EEG signal after removing the DC component (i.e. the mean value).

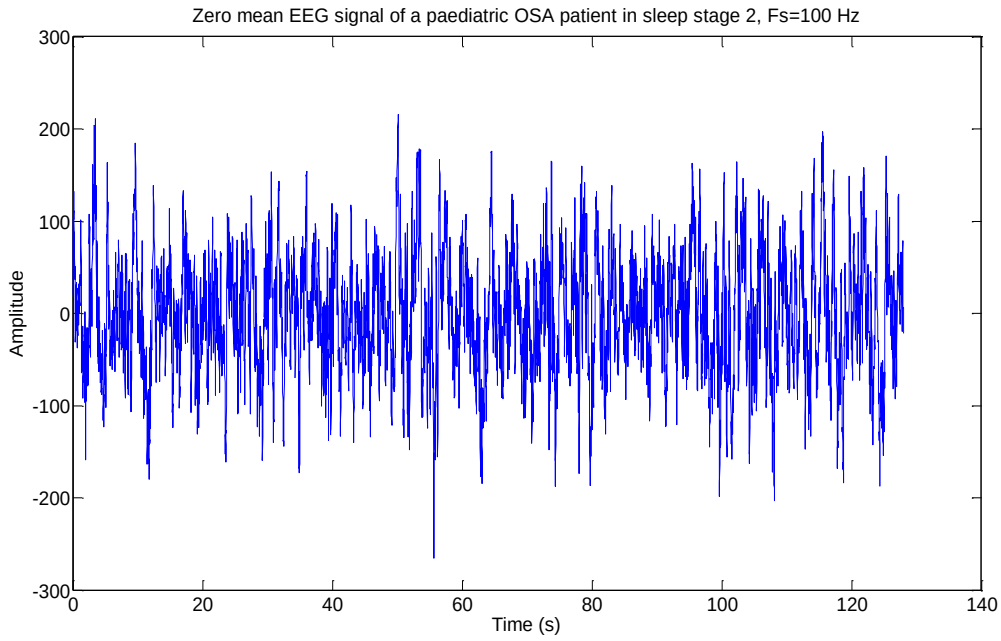

Figure C6. The EEG signal acquired from the C3/A2 lead from a paediatric OSA patient in second stage of sleep.

The estimated PSD (using the standard Periodogram method) of the EEG signal shown above is depicted in Figure C7.

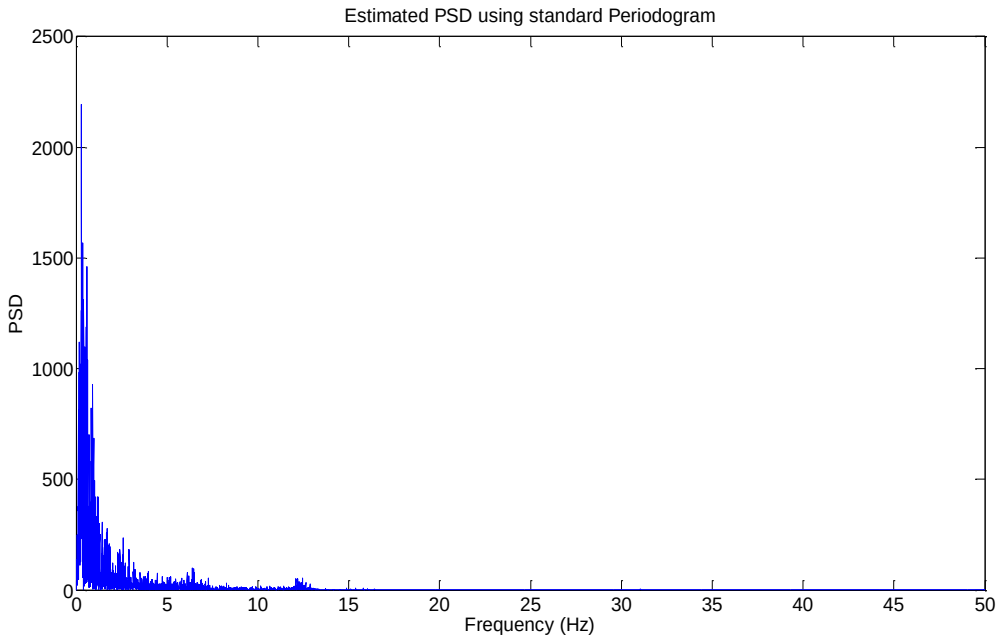

Figure C7. Power Spectral Density (PSD) of the EEG signal shown figure C6. The small peak on the 12-13 Hz shows multiple occurrences of sleep spindles which are expected in sleep stage 2. As can be seen the PSD estimation is not smooth and has a relatively large variance (i.e. the signal seems to be noisy).

Note that even though the results may seem sufficiently meaningful, it is not appropriate to apply the Periodogram to a non-stationary signal (Stationarity is not a very good assumption when dealing with 128 seconds of EEG signal, however, at the same time, the assumption is not too bad as the whole EEG chunk is taken from a single sleep stage and is bound to have similar characteristics throughout the whole chunk). The next section describes a new method based on the windowing principle which is capable of producing smooth PSDs.

Welch PSD estimation method:

As it was briefly mentioned above, standard or modified Periodograms are not likely to give a smooth PSD estimate in real applications where considerable noise and artefacts are present. Hence there is a need for better estimators of PSDs, those which yield smaller variances.

A conventional method to reduce the variance in an estimate is time averaging (also referred to as synchronised or coherent averaging), that is averaging over a number of statistically independent estimates. However, in many cases it is not feasible to use this method as there is only a single signal available and not an ensemble of signals. Therefore, a procedure was developed (this is attributed to Bartlett) in order to reduce the variance of PSD estimate from a single signal. The idea was to divide the original data into N segments, calculate the Periodogram of each segment and finally, coherently average all N PSD estimates (that is if segments can be assumed to be independent). Bartlett's method yields a smoother PSD

estimate. In 1967 Welch showed that the by dividing a time series into *N* segments, the variance of the estimated PSD (at best) will be reduced by factor of *1/N* (i.e. number of segments is inversely proportional to the variance if the segments are not overlapping) [11, 152]. However, note that by segmenting a signal, we also reduce the frequency resolution and consequently, for a time limited signal, we can not make the variance arbitrarily small. Welch's method suggests that by overlapping the segments we achieve a better reduction in variance with the same frequency resolution (i.e. the same segment length). Figure C8 shows the PSD of the EEG signal shown in Figure C6, estimated by the Welch method.

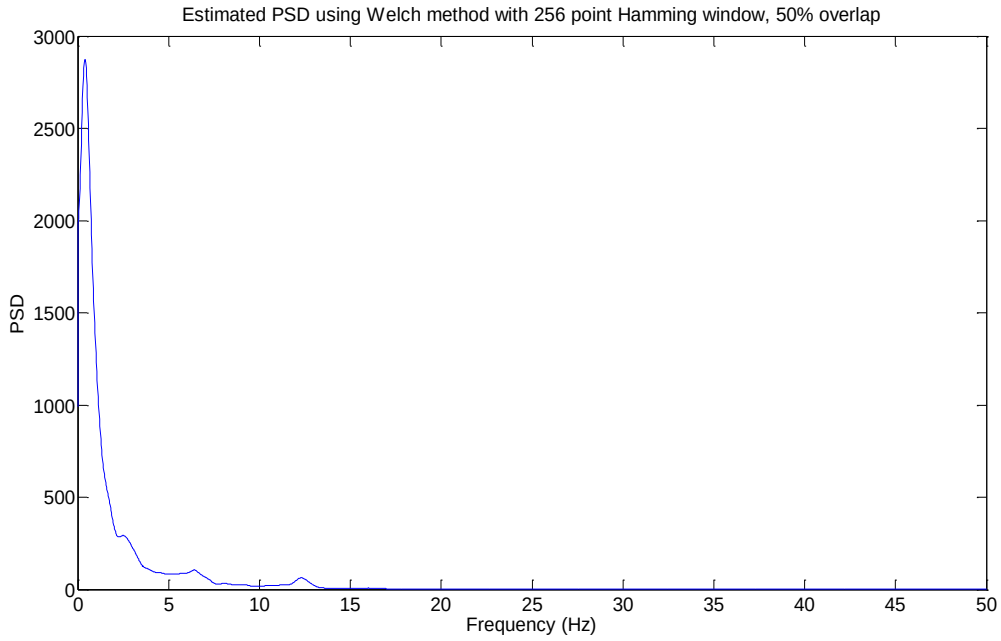

Figure C8. Power Spectral Density (PSD) of the EEG signal shown figure C6 calculated using the Welch method. The bump on the 12-13 Hz shows multiple occurrences of sleep spindles which are expected in sleep stage 2. As can be seen the PSD estimate is significantly smoother than the estimate made by the standard Periodogram and it is also meaningful. Note that a 256 points window results in frequency resolution of 1/2.56 which is about 0.4 Hz.

Note that the above graph was obtained by using a 256 points Hamming window with 50% (i.e. 128 samples) overlap and 4096 points FFT. Hence, it is clear that in terms of smoothness and lower variance in the estimate, Welch method is a better estimator of PSD when compared to standard Periodogram. Furthermore, it is worth pointing out that stationarity assumption is stronger when we are dealing with 2.56 seconds of EEG rather than 128. Also note that decreasing the number of windows results in a higher frequency resolution but a less smooth curve (i.e. higher variance). The frequency resolution in the graph above is $1/(2.56)\approx 0.4$ Hz which is sufficiently high.

Next section describes a different PSD estimation method based on Auto-Regressive modelling.

Auto-Regressive (AR) modelling:

Process *y[n]* is autoregressive if:

$$y[n] + a_1 y[n-1] + a_2 y[n-2] + \ldots + a_p y[n-N] = b_0 x[n]$$

That is when the current output value depends only on the current input value and past output values. The equation above can be equivalently written as follows:

$$\frac{Y(z)}{X(z)} = \frac{b_0}{1 + a_1 z^{-1} + a_2 z^{-2} + \ldots + a_p z^{-p}}$$

Where *X(z)* and *Y(z)* are the z transforms of the input and output signals respectively, a_ks are the model parameters and b_0 is a constant [501]. Note that the equation above is in fact an all pole FIR linear filter of order *p*. One interesting property of AR models is their capability in directly estimating the PSD from coefficient estimation (that is assuming white noise as the input signal). The following formula clarifies how PSD is estimated from an AR model.

$$S(w) = \frac{\sigma^2}{\left| 1 + \sum_{k=1}^{p} a_k . e^{-jwk} \right|^2}$$

Where σ^2 is the variance of the white noise at the input, *p* is the model order, and a_ks are model parameters [502]. AR modelling can be applied to both stationary and non-stationery signals (with some modifications) and it also results in a smooth PSD estimate, hence it can often be a useful estimator of PSD. Figure C9 shows the PSD estimate of the signal shown in Figure C6, using the AR modelling approach.

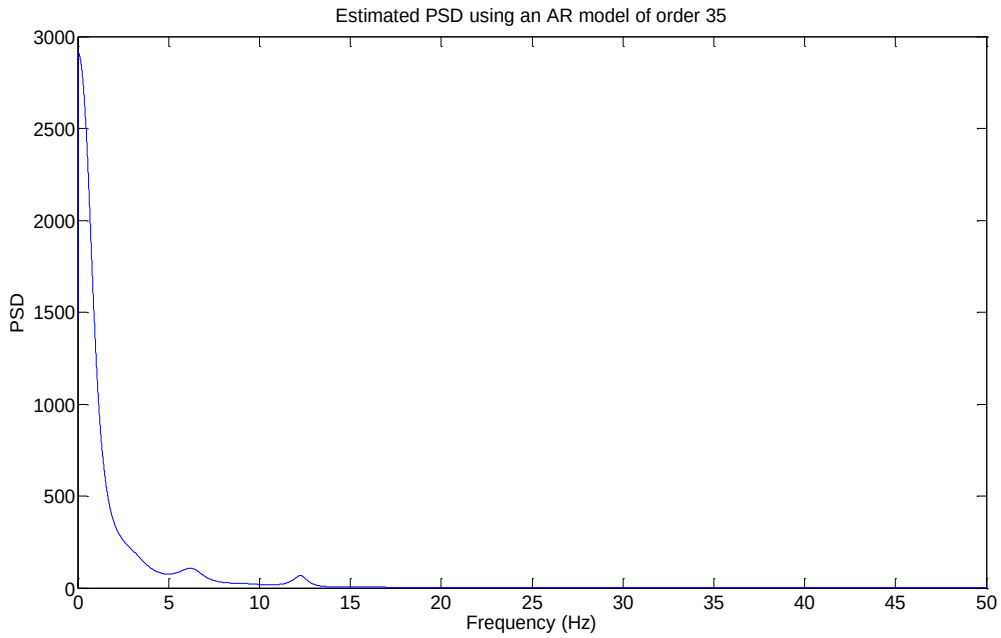

Figure C9. Power Spectral Density (PSD) of the EEG signal shown in figure C6 calculated using the AR modelling approach. The small peak on the 12-13 Hz shows multiple occurrences of sleep spindles which are expected in sleep stage 2. As can be seen the PSD estimate is even smoother than the estimate made by the Welch method and it is also meaningful. Note that by increasing the model order the variance of estimate increases (the curve becomes less smooth) hence choosing a good model order has to be taken care of.

As can be seen in the figure above, AR modelling results in a smooth and meaningful PSD estimation. Hence it can be a good candidate for spectral analysis of biomedical signals. Various ways for estimation of AR model parameters have been suggested in literature (see [501-503] for more details).

The methods mentioned above are by no means the only ways for spectral analysis and there are numerous methods suggested in the literature for achieving the goal of analysing a signal in frequency domain, however, the above methods give practical examples of how spectral analysis can be used and for further detail one can refer to references provided.

Time-Frequency analysis

In many applications it is not the power spectrum of the signal that we are looking for but the evolution of frequencies with time. That is the frequency content of a signal in a given time instance (or a given time interval). With PSDs we know that certain frequencies exist in a signal however, what we do not know is when those frequencies have actually occurred. Taking the EEG signal shown in figure 54 as an example, it is clear from the PSD estimates that sleep spindles have been occurring in that 128 seconds of EEG (shown by the small peak between 12-13 Hz in PSD estimates shown in figures 33-35). However, the time of occurrence and duration of those spindles are not present in the PSD estimates. Time-frequency analysis is a tool which

enables us to look at the frequency components of a signal in different time instances and has indeed been very useful in elevating our understanding of the underlying system. The rest of this section is dedicated to two of the Time-Frequency methods namely, the Wavelet Transform and the Empirical Mode Decomposition (EMD).

Wavelet transform:

As mentioned above, the need for time-frequency methods to unveil more information about the nature of signals is undeniable and the simple Fourier transform does not satisfy that need. As it was pointed out in the Spectral Analysis section, mathematically, there are infinite ways to decompose a signal into several underlying components. What makes a decomposition method distinct is its physical interpretation or its mathematical content. One way of decomposing a signal is to find its constituting sinusoidal components; that is what Fourier method achieves (i.e. breaking down a signal into sinusoidal basis functions). Fourier Transform is well suited only to the study of stationary signals and cannot properly deal with discontinuities and sharp spikes. Wavelets, on the other hand, are mathematical functions that divide the data into different frequency components and analyse them with resolutions matching their scales.

Wavelet Transform (WT) provides a time-frequency representation of the signal and has been developed to overcome the short comings of the Short FFT (also used to analyse non-stationary signals). More specifically, while SFFT gives a constant resolution at all frequencies, WT uses multi-resolution technique by which different frequencies are analyzed with different resolutions.

A wavelet, is a small wave which decays to zero at $\pm\infty$ and for practical reasons, this decay should be very fast [125]. Figure C10 shows an example of a wavelet function (known as the Mexican Hat wavelet).

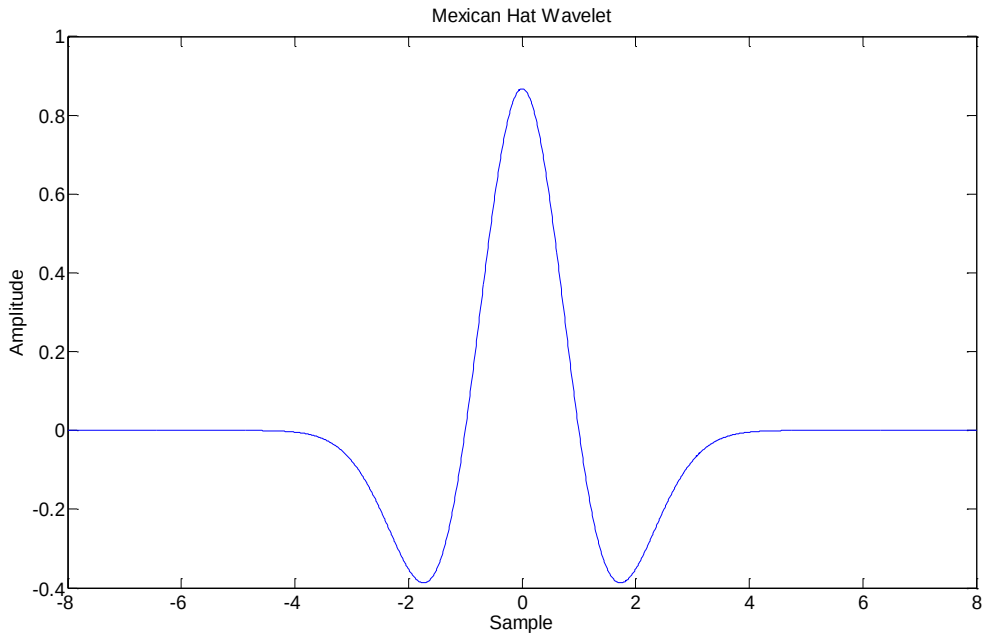

Figure C10. An example of a wavelet function known as the Mexican Hat wavelet. The fast decay to zero is clear in the above graph

Note that there have been numerous wavelet functions introduced in the literature (based on application needs) and the Mexican Hat is only a simple example of those.

As can be seen in figure 58, it is not possible to reconstruct a whole signal using only a single wavelet, just as it is not possible to reconstruct a signal from a single sinusoid in Fourier decomposition. Analogous to Fourier methods in which we use a sum of sinusoids with different amplitudes and frequencies to reconstruct a signal, in wavelet analysis, we use a sum of scaled and time shifted wavelet functions to achieve this goal (i.e. a wavelet series). A generalisation of the wavelet series results in a more practical tool of the wavelet transform which can then be used in time-frequency analysis as one of its many applications.

The wavelet transform uses scaled and time shifted wavelet functions to decompose a signal. It is more formally defined as:

$$W(a,b;x,\psi) = \frac{1}{\sqrt{|a|}} \int_{-\infty}^{\infty} x(t).\psi(\frac{t-b}{a})dt$$

Where $\Psi(t)$ is the basic wavelet function which has to satisfy some general conditions, a is the scaling factor and b is the time shift factor. Although Frequency and time do not directly appear in the equation above, parameter $1/a$ gives the frequency scaling and parameter b gives the local occurrence time of an event [182]. In short, Wavelet analysis can be thought of as an

adjustable window Fourier Spectral analysis [182] where window sizes can be adjusted by the scaling factor and hence time-frequency decomposition using the wavelet approach can adapt to the nature of the data in a more efficient manner.

Wavelets have had a wide range of applications since their introduction. They have been particularly effective in image and data processing (for de-noising and compression). As mentioned above, wavelets have also been extensively used for time-frequency analysis and feature extraction (for instance, see [502] for details on feature extraction from neurophysiologic signals using wavelets).

Last but not least, it is essential to emphasize that similar to all time-frequency methods, interpretation of the analysis is of significant importance and special care and attention should be given to understanding the chosen basic wavelet function and the result of the analysis.

Empirical Mode Decomposition (EMD):

A recent time frequency analysis method which is applicable to both non-linear processes and non-stationary signals is briefly explained in this section. As mentioned at the beginning of the section, time-frequency analysis is a tool which enables us to estimate the energy (or power) of a signal at a given time and frequency and hence understand the underlying mechanism of natural (or artificial) phenomena better. Numerous methods have been proposed in the literature for time-frequency decomposition out of which approaches such as Short Time Fourier Transform (STFT), wavelet analysis, and Wigner-Ville distribution have attracted significant attention. Each of the mentioned methods has its strengths and weaknesses but none of them is able to successfully deal with non-stationary signals and non-linear processes. Use of instantaneous frequencies as oppose to a variation of Fourier transform enables the EMD method to cope with non-stationary and non-linear processes [182]. Empirical Mode decomposition is an adaptive method (i.e. it is data driven) which looks at the local characteristics of a signal. The main part of the technique focuses on decomposing a signal into a set of few Intrinsic Mode Functions (IMFs). An IMF is a function that satisfies the following two criteria:

1) The number of zero crossings and extremas should be equal (or differ by one)

2) The envelope mean of the signal should at any time be equal to zero (this enforces symmetry on the signal)

It is shown that any function which satisfies the above two conditions (i.e. an IMF) has a well defined Hilbert transform and it can hence be represented as an analytic signal with no ambiguities. The method then uses the derivative of the phase of the analytic signal as the instantaneous frequency, that is if $z(t)$ is an analytic signal:

$$z(t) = a(t).e^{j\theta(t)}$$

Then instantaneous frequency is given by:

$$\omega = \frac{d\theta(t)}{dt}$$

Huang *et al* [182] admit that there has been controversy over the concept and definition of instantaneous frequency however, they believe that this definition is better than other existing ones as it matches our intuition better.

The process of obtaining IMFs from a given signal is somewhat simple. Let *x[n]* denote the original signal and $m_{x1}[n]$ denote the envelope mean of *x[n]*, we then have:

$$x[n] - m_{x1}[n] = r_1[n]$$

Where $r_1[n]$ is the signal which results from subtraction of the envelope mean of the signal from the signal itself. We then treat $r_1[n]$ as the original signal, that is:

$$r_1[n] - m_{r1}[n] = r_2[n]$$
.
.
.
$$r_{k-1}[n] - m_{r(k-1)}[n] = r_k[n]$$

Where $m_{rk}[n]$ is the envelope mean of $r_k[n]$. This iterative process continues till the difference between $r_k[n]$ and $r_{k-1}[n]$ becomes negligible (this is practically done by setting a threshold on the standard deviation calculated using $r_k[n]$ and $r_{k-1}[n]$). If the mentioned condition is met, $r_k[n]$ is chosen as the first IMF. The first IMF is then subtracted from the original signal to produce $x_2[n]$. The procedure explained above is then repeated on $x_2[n]$ to get the second IMF. This procedure continues till there are no more IMFs, that is $x_m[n]$ is a constant or a monotonic

function. Note that the first IMF contains the highest oscillations (shortest period components) of the signal and last IMF contains lowest oscillations (longest period components) of the signal. The process of obtaining IMFs is referred to as the “sifting process”. Figure C11 shows the IMFs calculated from the EEG signal shown in figure C6.

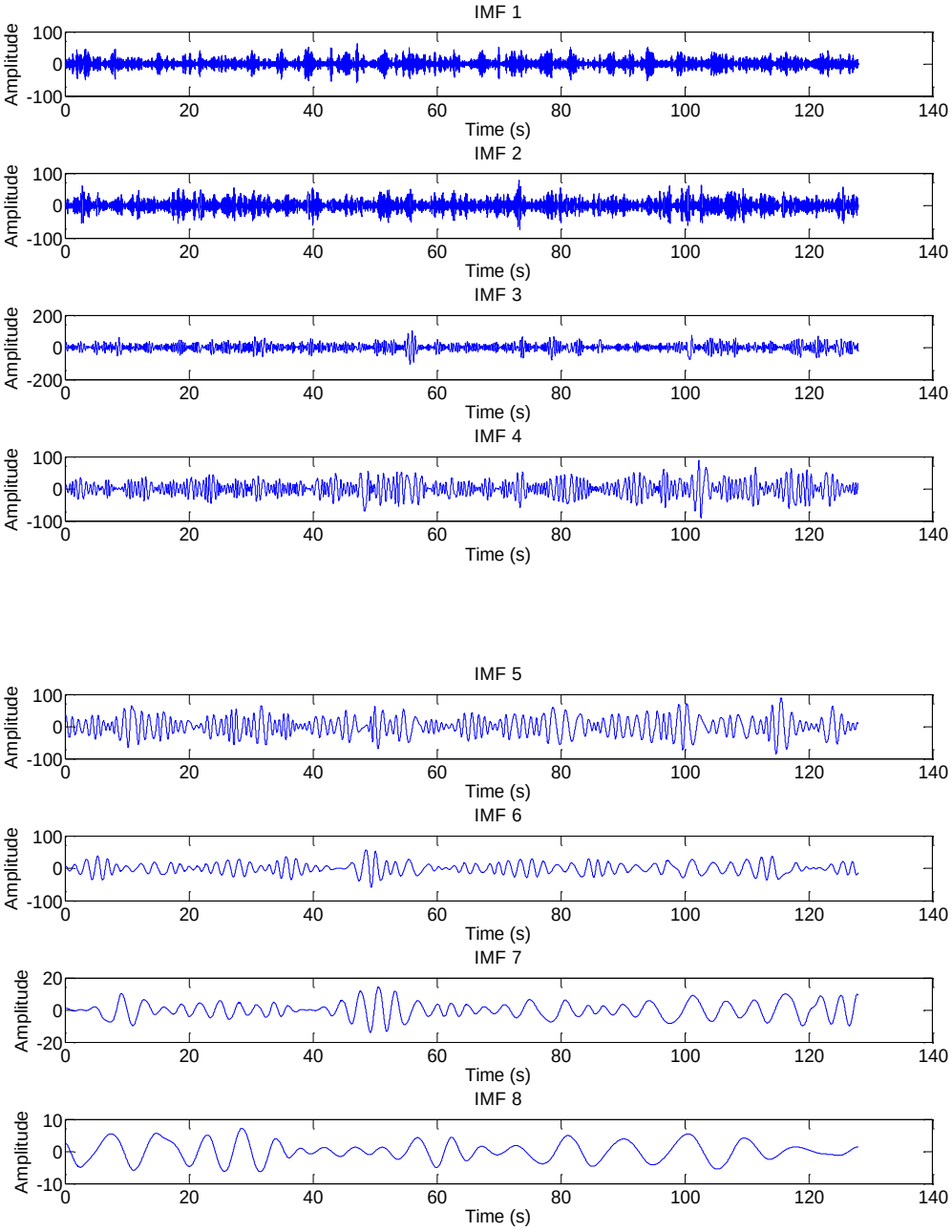

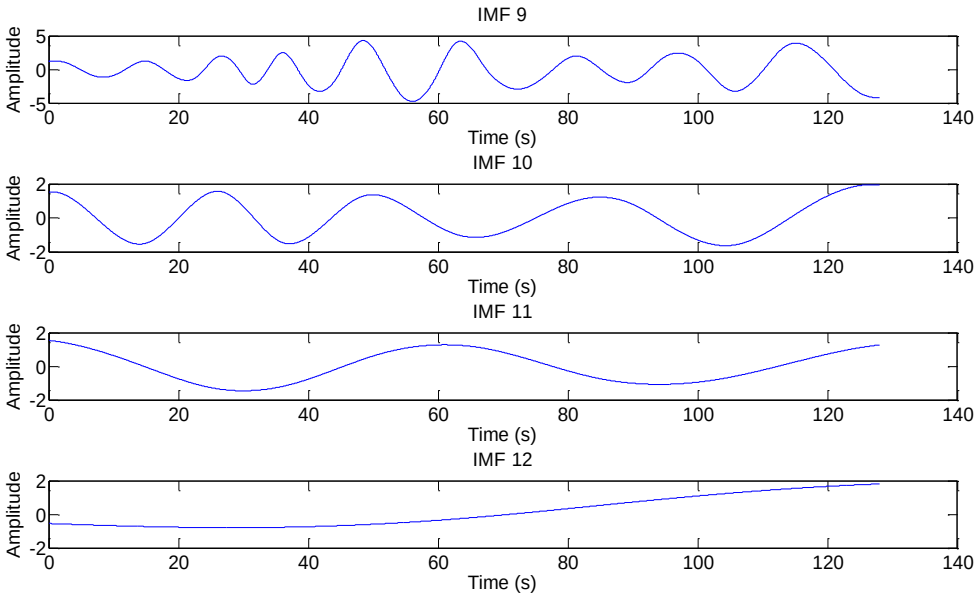

Figure C11. Intrinsic Mode Function (IMFs) calculated from 128 seconds of sleep stage 2 EEG signal. Note that addition of all the IMFs shown above results in perfect reconstruction of the original signal and hence the words "complete decomposition". As can be seen each IMF has a different oscillation rate when compared to the rest of the IMFs.

As can be seen in the figure above, 12 IMFs have been resulted from the EEG data, each having a different oscillation rate. Note that the input signal in the above case was band pass filtered from 0.4 to 25 Hz in order to remove spurious higher frequency components.

Having calculated the IMFs, we can produce an energy-frequency-time spectrum (Hilbert-Huang spectrum) which shows the energy of the signal at any given time and frequency. Frequency components were obtained by differentiating the phase of the analytic signals which were derived from IMFs. Figure C12 shows the smoothed (convolved with a 5x5 Gaussian mask) Hilbert-Huang spectrum of the EEG signal shown in Figure 62.

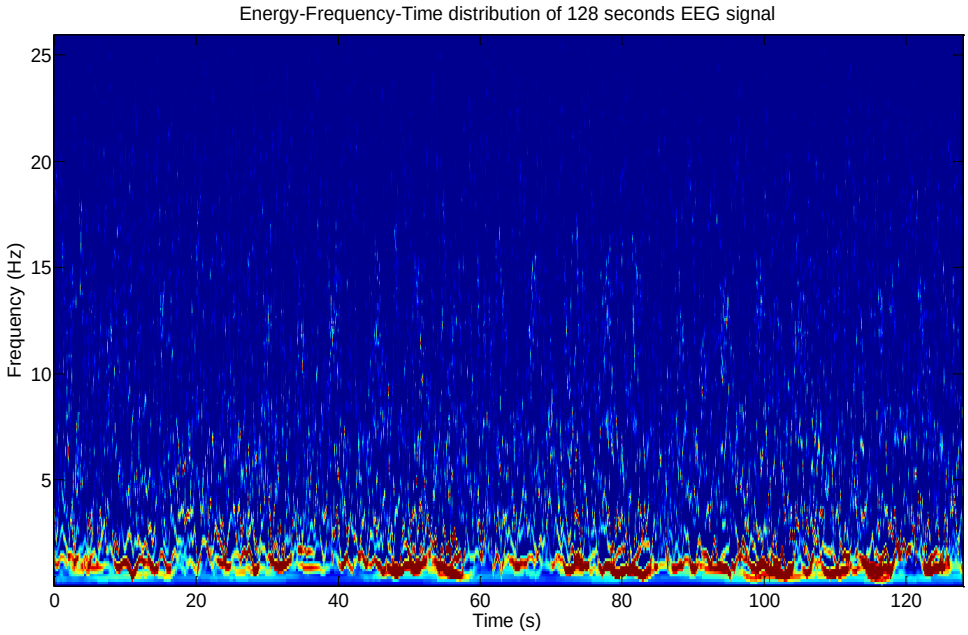

Figure C12. Smooth Hilbert-Huang spectrum. The energy distribution of the EEG data in time and frequency can be seen. As with all time-frequency analysis methods, interpretation of the analysis and how well it fits our intuition is of essence.

As can be seen in the above figure, low frequency dominance is clear. Lack of low frequency components and presence of 12-14 Hz activity can probably be interpreted as sleep spindles, however for rigorous event detection in sleep, complimentary algorithms may be needed (see [393] for details on automatic sleep spindle detection using Hilbert-Huang spectrum).

To summarise, EMD is a useful way of decomposing signals which are not stationary or are generated by non-linear processes. This decomposition enables us to obtain a rich Energy-Time-Frequency distribution which increases our understanding of the nature of the signal we are dealing with.

Appendix D

List of seminars, conferences and publications

[1] Motamedi Fakhr, S., Moshrefi-Torbati, M., Hill, M. and Hill, C.M. (2010) Processing of Biomedical signals – an example in paediatric sleep. In, Clinical Neurosciences Division 15th Academic Meeting,Southampton, GB, 17pp.

[2] Motamedi-Fakhr, S., Moshrefi-Torbati, M., Hill, C.M., Paul, A. and Hill, M. (2010) On respiratory cycle related EEG changes (RCREC). At Congress of the International Pediatric Sleep Association joint meeting with Pediatric Sleep Medicine Conference, Rome, IT, 1pp.

[3] Motamedi Fakhr, S., Moshrefi-Torbati, M., Hill, C.M. and Hill, M. (2011). Sleep research: Respiratory Cycle Related EEG Changes (RCREC). In Electromechanical Engineering research group seminar series, Southampton, GB, 40pp.

[4] Motamedi-Fakhr, S., Hill, C.M., Moshrefi-Torbati, M., Bucks, R. and Hill, M. (2012) Respiratory cycle related EEG spectral changes in sleep as a predictor of cognitive function in the De-SAt study. In Clinical and Experimental Sciences division seminar series, Southampton, GB, 23pp.

[5] Motamedi Fakhr, S., Moshrefi-Torbati, M., Hill, C.M., Simpson, D., Paul, A., Bucks, R. and Hill, M. (2013) Respiratory Cycle Related EEG Changes: Modified respiratory cycle segmentation. Published in Biomedical Signal Processing and Control.

[6] Motamedi Fakhr, S., Moshrefi-Torbati, M., Hill, C.M. and Hill, M. (2013) Signal processing techniques applied to human sleep EEG – a review. Accepted for publication in Biomedical Signal Processing and Control.